sierra research

Report No. SR92-10-06

Development of Vehicle Emissions Computer Simulation Model

prepared for:

U.S. Environmental Protection Agency

October 16, 1992

prepared by:

Sierra Research, Inc.
1801 J Street
Sacramento, California 95814
(916) 444-6666

DEVELOPMENT OF VEHICLE EMISSIONS COMPUTER SIMULATION MODEL

EPA Contract No. 68-C1-0079
Work Assignment No. 06

prepared for:

U.S. Environmental Protection Agency

October 16, 1992

principal author:

Larry Caretto

Sierra Research, Inc.
1521 I Street
Sacramento, CA 95814
(916) 444-6666

DEVELOPMENT OF VEHICLE EMISSIONS COMPUTER SIMULATION MODEL

Table of Contents

DEVELOPMENT OF VEHICLE EMISSIONS COMPUTER SIMULATION MODEL

1. SUMMARY

EPA is currently developing a new motor vehicle emissions simulation model called VEMISS (for Vehicle EMISSions). This study was intended to provide critical evaluation of concepts and methods to be used in supporting EPA's development of VEMISS. The model requires input engine maps giving fuel consumption and emission at several engine operating points. The independent variables for these operating points are engine speed and engine load. This study examined methods for taking data obtained at a smaller number of speed and load points and constructing an engine map for a wider range of speed and load points.

The first task was an examination of the approach in the dissertation by Feng An which showed that fuel consumption at low speeds and loads could be correlated for a wide variety of engines by the simple equation

$$P_{fuel} = a' \; V_d \; N + b \; P_{engine} \qquad [1.1]$$

In this equaion are P_{fuel} is the fuel energy rate, V_d is the engine displacement, N is the engine speed, and P_{engine} is the brake power output of the engine; a' and b are empirical constants.

This equation has produced good results for low speed and power outputs, but is not applicable for off-cycle operations at high engine speeds. In addition, the data used to fit the constants a' and b did not consider the normal engine idle point. The equation had an average error of -42% in predicting the idle fuel flow rates for the EPA engine data.

The relation between emissions rates and engine operating parameters was studied. No simple quantitative relation was found that could be used as a "magic bullet" to fill in missing data point in the engine maps. Two significant problems were noted for missing data points. The first was a need to determine the fuel flow rates and emissions at zero and negative loads to obtain a complete engine map. The second problem was for the interpolation of missing data. The observed engine maps showed sharp transitions, particularly in hydrocarbon (HC) and carbon monoxide (CO) emissions. An important step in the development of good engine maps is the accurate determination of these transition points for conditions where the exact location cound not be found from the experimental data.

Several procedures were evaluated for providing answers to these missing data points. A final procedure was developed to provide fuel and emissions rates at zero and negative loads which could be used in a straightforward manner. This procedure examined two analytical approaches and used the best combination of the two that was consistent with the experimental data.

A protocol was developed to estimate the location of the transition points in the emissions map. This was based on the observation that these transitions were typically associated with enrichment of the fuel/air mixture. Some analysis of the behavior of these transition points was done, but no automated system could be developed for filling in these data points as was done for the fuel and emissions rates at zero and negative loads.

A second task was the investigation of a possible correlation between manifold vacuum and engine load expressed as brake-mean effective pressure. This task consisted of two parts: (1) an examination of the mapping data for these parameters and (2) a theoretical analysis of their relationship. The experimental data showed a linear behavior with extremely high correlation coefficients. This experimental relationship was supported by the theoretical analysis which showed that the BMEP should be related to the manifold intake pressure, p_{in}, at a given engine speed, by a linear equation,

$$BMEP = \alpha(N) + \beta(N)\ p_{in} \qquad [1.2]$$

From the theoretical analysis an estimate could be made of typical values for α and β; these estimates agreed with the values found in the empirical correlations of BMEP and p_{in}.

2. EVALUATION AND DEVELOPMENT OF AN ALTERNATIVE EMISSION MAPPING PROCEDURE

Introduction

This task was intended to provide EPA with a way to fill holes in the engine mapping data that EPA obtained for use in their VEMISS program. The initial subtask was a critical review of the dissertation by Feng An on vehicle fuel economy. The results of this work were evaluated for potential application to filling fuel flow rates in the EPA engine mapping data and for extending this work to filling in emisions data. Based on this work and a literature review Sierra was to develop a technique for interpolating and/or extrapolating data in the EPA engine maps. The goal was the development of a procedure for determining fuel consumption and emissions as a function of engine speed and load (expressed as brake mean effective pressure, BMEP). EPA provided Sierra with preliminary copies of their engine mapping data for use in this task.

Review of An Dissertation

The work reviewed for this subtask was the doctoral dissertation of Feng An[1] and a related paper by An and his dissertation chair, Marc Ross.[2] In addition to reviewing these documents we contacted Dr. An and Prof. Ross to clarify some points of their work.

Description of An's Results – The dissertation appears to provide a good engineering analysis of vehicle fuel economy for use in transportation studies. It results in a simple analytical expression for the fuel economy of various vehicles in various driving cycles. This analysis consists of two parts. The first part defines a relationship for engine fuel consumption as a function of engine speed, and load; the second part determines the engine power required for various driving cycles in terms of a few basic driving cycle parameters.

In the first step, An has determined regression coefficients that relate engine fuel energy rate, P_{fuel}, which is simply the the mass flow rate of fuel times its heat of combustion, engine speed, N, engine displacement, V_d, and engine power, P_{engine} by the following equation:

$$P_{fuel} = a' \; V_d \; N + b \; P_{engine} \qquad [2.1]$$

The engine displacement, V_d, is the only parameter that characterizes a particular engine. The values of the constants a' and b that An recommends for "1990 vehicle models" are:[3]

$a' = .271$ kJ/rev-liter* $b = 2.5$ (dimensionless)

An used values of $a' = 0.286$ kJ/rev-liter and $b = 2.5$ for the data examined in his dissertation. The actual regression fits for fuel economy data were for an equation of the form

$$P_{fuel} = a\ N + b\ P_{engine} \qquad [2.2]$$

After the regression coefficients a and b were determined the simple dependence of a on engine displacement, $a = a'\ V_d$, was found.

Ross and An note a wider range for a' values in newer engines and state that it is "premature to draw detailled conclusions about the values of a for modern engines."[4]

Equation [2.1] or [2.2] is intended to apply in the low speed and load regions in which the engine spends almost all of its time during typical driving cycles.[5] The specific regions that were used in a regression analysis to determine the coefficients a and b are given below.[6]

1500–2500 RPM for four cylinder engines
1300–2100 RPM for six cylinder engines
1200–2000 RPM for eight cylinder engines

This speed range starts above the normal idle range for most engines; all the engines considered by An in his dissertation have idle speeds between 600 and 800 RPM.[7]

In addition to a limited speed range, the data used at each engine speed were limited to the points for which the engine power was less than some fraction of the wide-open-throttle power at that speed. (I.e. only points for which $P_{engine} < f\ P_{engine,\ WOT}$) were considered. Three different methods were used to select the value of f; these were shown to provide consistent results. For the final regression analysis the fraction, f, was chosen to produce the best fit. The restriction to the low speed-load points was justified by an examination of typical emissions test and fuel economy driving cycles which have a majority of their operation in the low speed–load region used for the regression analysis.

The second step is based on the conventional equation for the vehicle power required to overcome rolling friction and aerodynamic friction and the power required for acceleration that is ultimately absorbed in braking losses.[8] The major thrust of the dissertation is the combination of the equation for fuel energy rate and the equation for the vehicle power requirements, along with some models for the resulting terms, to arrive at a single equation which gives a general equation for the energy consumption of a vehicle over a driving cycle. This final

---

* The units of kJ/rev-liter are equivalent MPa/rev. Thus the fuel equation could be written in terms of the brake mean effective pressure (BMEP) as follows (for four-stroke engines)

$$P_{fuel} = [\ a' + (b/2)\ (BMEP)\ ]\ N\ V_d$$

equation uses only a few simple parameters for the vehicle and the driving cycle.[9] These are:

v_r The average running speed = cycle distance/(total time - idle time)

v_p The mean square peak speed. Most cycles consist of subcycles. The peak speed in each cycle is noted and averaged in an root mean square manner to obtain this quantity.

t_c The proportion of the time that the brakes are applied.

t_{pwr} The proportion of time that the engine is powering the vehicle (as opposed to braking and idling).

n The average number of stops per unit distance.

In addition to these driving cycle parameters, An's analysis requires the following vehicle parameters to compute the fuel consumption for a cycle:

N/v The engine speed/vehicle velocity ratio at the highest gear.

N_{idle} The idle speed of the engine.

M The vehicle mass.

V_d The engine displacement used in the equation for P_{fuel}.

C_r The coefficient of rolling friction.

C_d The aerodynamic drag coefficient.

A The frontal area of the vehicle for aerodynamic drag.

The fuel economy from the model equation was compared with actual data on the fuel economy of nine cars For the composite Urban/Highway EPA cycle; the agreement was within 5%.[10]

The fuel economy model was further refined to consider variables more appropriate to transportation analysis. In this refinement the cycle speed parameters given above are replaced by the average speed, v_{avg}, the "free-flow" speed (defined as $v_{ff} = (v_p)^2/v_{avg}$), and the average time per stop, T_s.

The use of these results in conjunction with the EPA engine mapping data is discussed below.

Implications of Ross/An Work for Fuel Consumption Calculations in Engine Simulation Programs - The most significant part of the An disseration for the application to the EPA mapping data is the basic relation between fuel rate, engine speed, and engine power given by equation [2.1] or [2.2]. There are two aspects to this equation. The first is the qualitative notation that there is a linear relation between these variables over a limited range of engine operating conditions. The

second is the use of specific empirical constants a' and b which could be applied to estimate the fuel energy rate for an engine at a given speed and brake power output knowing only its displacement.

The qualitative results provide important support to the bilinear interpolation process typically used in engine simulation programs such as VEHSIM. The equation of the form $P_{fuel} = a\ N + b\ P_{engine}$ is consistent with bilinear interpolation. The discussion on interpolation below shows that this is true even if torque or BMEP is used in place of brake power to represent the load on the engine. The quantitative results can be used to provide a check on interpolated data, but they should not be used blindly because of the limited range over which the empirical constants were derived.

This limited range for quantitative applicability is perhaps the most important aspect of this work for application to engine mapping. Although excellent agreement has been demonstrated for some cycle data the authors point out that the empirical constants used previous may not be applicable to modern engines.

Some of the reasons for the limitations of this equation can be seen by examining the physics of engine friction. Setting the engine brake power to zero in equation [2.1] gives the fuel energy rate as $P_{fuel}(P_{engine}=0) = a\ N$. This fuel rate is that required to overcome engine friction at the given engine speed. One reason for the limitation of the An equation to lower speeds is that this linear representation of engine friction is only valid at such speeds. This is discussed further below.

Heywood[11] divides engine friction forces into three components:

> Boundary friction between two solid surfaces without sufficient lubricant. This is independent of engine speed.
>
> Hydrodynamic friction force between surfaces separated by a sufficiently thick lubricant film. This force is proportional to the engine speed.
>
> Fluid friction. This is proportional to the fluid velocity squared which is roughly proportional to the engine speed squared.

Thus, the friction force (or the friction mean effective pressure) is expected to follow an equation of the form

$$(mep)_{friction} = C_1 + C_2\ N + C_3\ N^2 \qquad [2.3]$$

For example, friction mep data for six engines at wide open throttle have been correlated by this equation with the following constants:

$C_1 = 0.97$ bar $\qquad C_2 = 0.00015$ bar/RPM $\qquad C_3 = 5 \times 10^{-8}$ bar/(RPM)^2

The increasing importance of the non-linear terms at higher engine speeds is shown in the table below:

RPM	C_1	C_2 N	C_3 N^2	Total	Increment
0	.97	0	0	0.97	
1000	.97	.15	.05	1.17	0.20
2000	.97	.30	.20	1.47	0.30
3000	.97	.45	.45	1.87	0.40
4000	.97	.60	.80	2.37	0.50

Because these data were obtained at wide open throttle they will not include throttling friction.

From the usual relation between power and mean effective pressure, the friction power will proportional to the friction mep (or force) times the engine speed. Thus the friction power is expected to follow an equation of the form

$$P_{friction} = (C_1 N + C_2 N^2 + C_3 N^3) (V_d/2) \quad [2.4]$$

This represents the actual energy required to overcome mechanical friction. The fuel rate required for this friction power will equal the friction power divided by the "efficiency" for converting fuel energy into the mechanical power required to overcome this friction. This "efficinecy" is not commonly reported, but it would be expected to be low because low power operation is the least efficient engine operating condition.

This efficiency can be be roughly compared with the An equation at low speeds where the quadratic and higher terms can be neglected. The value of a' = 0.271 MPa/rev. The fuel energy rate for zero brake power, P_{fuel} = a' N V_d. The friction power (neglecting quadratic and higher terms) is $P_{friction} = C_1/2$. The "efficiency" of coverting fuel into mechanical motion required to overcome engine friction is then [$C_1/2$] / [a' N V_d] = $C_1/(2a')$. C_1 = 0.97 bar = 0.097 MPa and a' = 0.271 MPa giving a value of 16% for the conversion of fuel energy into mechanical power to overcome friction. This seems like a reasonable value confirming the magnitude of the a' factor in the An equation.

Interpolation of Fuel Flow in Vehicle Simulation Codes - An is critical of the process of using brake specific fuel consumption (bsfc) data from an engine map and interpolating to find the actual fuel consumption.[12] He points out that a linear interpolation on an engine map, particularly at low engine power, is not accurate. This has already been recognized by the original authors of the VEHSIM program[13] who required the basic engine map data to be entered as mass per unit time of fuel. It is *not* given in terms of brake specific fuel consumption (bsfc). This avoids the errors created by interpolating brake specific quantities in low load regions where the brake-specific quantities approach infinity.

The analysis below shows how the double interpolation in VEHSIM, which is used to find the fuel flow rate as a function of engine speed and engine load is entirely consistent with the equations in An's dissertation. The fuel data in VEHSIM as in terms of fuel rate (mass per unit time) which is simply P_{fuel} divided by the heat of combustion of the fuel. Thus the same procedure would be used to interpolate the fuel mass flow rate, m_{fuel}, or $P_{fuel} = m_{fuel} Q_c$. The basic relation between fuel

energy rate, P_{fuel}, engine speed, N, and engine power output, P_{engine}, that An uses as the starting point in his analysis[14] is a mathematical representation of a chart in the Bosch handbook:

$$P_{fuel} = f(N) + g(N)\ P_{engine} \qquad [2.5]$$

In this equation f(N) and g(N) represent arbitrary functions of engine speed. Equation [2.2] is obtained by assuming that f(N) = a N, and g(N) = b. The more general f(N) and g(N) notation can be used to describe the VEHSIM interpolation used to find P_{fuel} at a given engine speed, N, and engine power, P_{engine}, between tabulated data such that

$$N_i < N < N_{i+1} \qquad \text{and} \qquad P_{engine\,j} < P_{engine} < P_{engine\,j+1}$$

At any (speed, power) point in the engine map, $(N_i, P_{engine\,j})$, the value of the fuel rate is $P_{fuel\,i,j}$. The double interpolation starts with an interpolation over engine power points which is equivalent to computing the following terms:

$$g(N_i) = [P_{fuel\,i,j+1} - P_{fuel\,i,j}] \ / \ [P_{engine\,j+1} - P_{engine\,j}] \qquad [2.6]$$

$$f(N_i) = P_{fuel\,i,j} - g(N_i)\ P_{engine\,j} \qquad [2.7]$$

$$g(N_{i+1}) = [P_{fuel\,i+1,j+1} - P_{fuel\,i+1,j}] \ / \ [P_{engine\,j+1} - P_{engine\,j}] \qquad [2.8]$$

$$f(N_{i+1}) = P_{fuel\,i+1,j} - g(N_{i+1})\ P_{engine\,j} \qquad [2.9]$$

Thus the first steps of the usual linear interpolation in the VEHSIM program may be regarded as an evaluation of f(N) and g(N) in An's basic equation. From these values we can compute the fuel rate at the two tabulated engine speeds in the map data and the given engine load. This computation gives:

$$P_{fuel}(N_i, P_{engine}) = f(N_i) + g(N_i)\ P_{engine} \qquad [2.10]$$

$$P_{fuel}(N_{i+1}, P_{engine}) = f(N_{i+1}) + g(N_{i+1})\ P_{engine} \qquad [2.11]$$

The desired fuel rate is given by a final linear interpolation between these two fuel rate values:

$$P_{fuel} = f(N_i) + g(N_i)\ P_{engine} + [P_{fuel}(N_{i+1}, P_{engine}) - P_{fuel}(N_i, P_{engine})]\ [\ N - N_i\ ] / [\ N_{i+1} - N_i\ ] \qquad [2.12]$$

Combining equations [2.10], [2.11], and [2.12] gives

$$P_{fuel} = f(N_i) + g(N_i)\ P_{engine} + [f(N_{i+1}) + g(N_{i+1})\ P_{engine} - f(N_i) - g(N_i)\ P_{engine}]\ [\ N - N_i\ ] / [\ N_{i+1} - N_i\ ] \qquad [2.13]$$

In order for this to be consistent with the basic result of equation [2.5] that $P_{fuel} = f(N) + g(N)\ P_{engine}$ the values of f(N) and g(N) implied by equation [2.13] are:

$$f(N) = f(N_i) + [f(N_{i+1}) - f(N_i)] * [\ N - N_i\ ] / [\ N_{i+1} - N_i\ ] \qquad [2.14]$$

and

$$g(N) = g(N_i) + [g(N_{i+1}) - g(N_i)] * [\ N - N_i\ ] / [\ N_{i+1} - N_i\ ] \qquad [2.15]$$

Substitution of An's assumptions that $f(N) = a\ N$ and $g(N) = b$ is consistent with equations [2.14] and [2.15]. Torque is often used, instead of power is used as the interpolation variable for engine load. Since $P_{engine} = 2\ \pi\ N\ T$, equation [2.5] may be writtten as

$$P_{fuel} = f(N) + h(N)\ T \qquad [2.16]$$

where

$$h(N) = 2\ \pi\ N\ g(N) \qquad [2.17]$$

It the above derivation were repeated using this interpolation equation, equation [2.14] would be unchanged and equation [2.15] would be replaced by a similar equation in h(N) instead of g(N):

$$h(N) = h(N_i) + [h(N_{i+1}) - h(N_i)] * [\ N - N_i\ ] / [\ N_{i+1} - N_i\ ] \qquad [2.18]$$

Under the assumption that $g(N) = b$ equation [2.17] gives $h(N) = 2\ \pi\ N\ b$. Equation [2.17] is consistent with this expression for h(N).

Thus, the linear interpolation for the fuel rate as a function of engine speed is consistent with An's results that g(N) can be regarded as a constant and f(N) is proportional to N. This is true if engine power or if engine torque is used as the load variable. Since the interpolation process is consistent if torque is used as the interpolation variable it will also be consistent if BMEP is used as the interpolation variable to represent load.

Extension of An Model to Emissions - An states that additional applications can be made "to supplement transportation and highway planning models with simple but accurate modeling of fuel consumption and NO_x emissions."[15] He further states that it should be possible to "analyze the dependance of NO_x emissions on engine and vehicle parameters and driving characteristics."

We contacted both Professor Ross and Dr. An to discuss their ideas for modelling emissions. Both of them told us that they intended their remarks to be limited to NO_x emissions and expected that the results of applying a similar model to NO_x emission would yield less accurate results than they obtained for fuel economy. The expected that the initial approximation would be to assume that the NO_x emissions were directly proportional to the engine power, over the range that they expected their model to be valid. This would be equivalent to assuming that the brake-specific NO_x emissions are constant over the region in which the approximate model is to be applied.

An is interested in exploring models of CO and HC emissions which he believes are linked mainly to cold starts. He believes that a model which uses the number of starts and stops as the main parameter can be

used to obtain results for CO and HC emissions that will be useful in transportation analysis.

Literature Search - The literature search for this part of the project started with presonal references of Sierra personnel. Additional literature searches were made using a) Sierra's in-house computerized SAE literature data base, b) a computerized literature search of the National Technical Information Service (NTIS) data base, c) a computerized literature search of the Engineering Index, and d) follow-up on references found by these preliminary searches.

There is a wide range of spark-ignition engine models available. Heywood,[16] Ramos,[17] and various Society of Automotive Engineers (SAE) publications[18] provide overviews of the range of available engine models. The use of detailled computational fluid dynamic models (e.g. KIVA-II)[19] is a current research topic, but these models are not ready for direct application of these models to the determination of emissions data for engine maps.

A key classification of fuel economy/emission models is their need for input data. Most of the models discussed below have significant requirements for input engine mapping data. These data represent both emissions and vehicle performance. An alternative to such data-intensive models are those which attempt to compute the emissions from some model of the in-cylinder combustion process. Such models typically require other assumptions or data (e.g. a model for the heat release rate or data on cylinder pressure rise) and are not capable of treating the behavior of multicylinder engines. The most frutiful path for improved emissions modeling, in the short term, is with data-intensive models.

Most of the recent work on engine modeling that had applicability to the engine mapping data dealt with emissions. The previous work on fuel economy modeling was reviewed by An in his disseratation. Much of that work was done in the 1970s and 1980s in reponse to concerns over energy shortages. The papers by Watson and his co-workers,[20,21] cited in An's dissertation, provide a good background to the modeling of emissions and fuel economy. These papers look at emissions and fuel economy for various driving cycles in use throughout the world and point out the need for consideration of transient, warm-up operation to obtain better agreement between theory and experiment.

The work that is most applicable to EPA's engine mapping work has been published by Nissan. Hori, *et al.*[22] discuss the Total Automotive Performance (TAP) program which models fuel economy, emissions, performance, acceleration, and exterior noise. This model is similar to the VEHSIM code in that it requires a large amount of input data about the vehicle being modeled. In a later work Matsumoto *et al.*,[23] developed a similar model that was able to account for transient behavior in the intake system. This is potentially an important source of emissions. This model also required extensive data inputs for each engine and vehicle. The road load was translated into an engine speed and load in a manner similar to that used in the VEHSIM program. In addition to having a data base for engine speed, engine load, throttle

opening, and intake mainfold pressure, additional data was available on the air volume entering the cylinders and the volumetric efficiency.

The feedback behavior of the oxygen sensor and the response of the air/fuel ratio to this sensor was modeled to compute the fuel flow rate and the air/fuel ratio. The engine-out exhaust emissions were determined from engine maps which determined the composition at various air/fuel ratios for a given speed/load combination. The tail pipe emissions were computed from a model for the three-way catalytic converter which included a term for adsorption of pollutant species on the catalyst. Again, the specific empirical constants were required for use in this catalyst model. The authors developed the model to evaluate the effects of changes in the feedback control system on emissions from the vehicle. For the one data comparison shown the discrpeancy between experimental data and the model was as large as 25% for engine out emissions and 20% for tail pipe emissions. This model appears to have the greatest promise in terms of its ability to handle engine trasnients, however, it requires a large amount of data on a specific vehicle/engine/catalyst combination in order to work.

Previous work by Sierra Research for EPA has examined the use of simulation programs for cold start.[24,25] This work used the VEHSIM code and an emissions simulation model which required engine mapping data for performance and emissions. The cold start was handled by using an adjustment factor for engine out emissions and for catalysts light-off time. The authors considered these adjustment factors to be a "first-order approximation" requiring additional work prior to any widespread application. However, their use of a light-off time for catalyst warm-up is consistent with the work of Chen *et al.*,[26] who developed a detailled model of catalyst performance. Their detailled model showed a shart rise in converter efficiency over a very brief time. It appears that the concept of a catalyst light-off time is a good starting point for extension of models to transient operation.

The current status of engine modeling can be divided into two groups. The first is a research area, which does a fundamental analysis of engine combustion using computational fluid dynamics approaches and supercomputers. Simplifications of these models, which require some empirical input on a fundamental level such as a correlation equation for the flame speed, are available, but are mostly useful for predicting trends. The second group, discussed here, are data-intensive models which require certain data for various engine operating conditions and use various analysis tools to determine how combinations of vehicle and engine operations will affect emissions and vehicle performance. This second class of models requires a large amount of data input, but can provide the most accurate results in the short term.

Correlations for Filling Holes in Engine Emission Maps

An initial exploration of the fundamental relationships between emissions rates and engine operating variables was done to determine the basic relatiionships between these variables that should be reflected in any interpolation or extrapolation procedure. With this basic

understanding in mind the EPA mapping data was examined to determine possible correlations.

Theoretical Background - The exhaust emissions rate can be related to engine variables through the exhaust flow rate. To do this, the mass flow rate (mass/time) of the i^{th} pollutant species, m_i, is written as its mass fraction, w_i, times the mass flow rate of exhaust. The latter is given by the mass of air plus the mass of fuel which equals the mass flow rate of fuel, m_{fuel}, times one plus the air fuel ratio. We thus have,

$$m_i = w_i \, m_{fuel} \, (\, 1 + A/F \,) \qquad [2.19]$$

The pollutant mass fraction is used here as a measure of "concentration" because it provides a simpler analysis of the mass rate data on emissions and fuel consumption that are used in the engine mapping data. The mass fraction is related to the usual parts per million measurement--on a mole fraction (volume) basis--as follows:

$$w_i = 10^6 \, (ppm)_i \, M_i \, / \, M_{exhaust} \qquad [2.20]$$

where M_i is the molecular weight of the pollutant species and $M_{exhaust}$ is the molecular weight of the exhaust. Although equation [2.19] gives a basic relationship between emissions rate and other engine parameters it reatains the unknown mass fraction as a variable.

Sierra was asked to investigate the use of emissions per engine revolution as a possible fitting variable. This can be done by writing the fuel mass rate, m_{fuel}, in equation [2.19] as P_{fuel}/Q_c and using equation [2.2] for P_{fuel} to give

$$m_i = w_i \, [\, a \, N + b \, P_{engine} \,] \, (\, 1 + A/F \,) \qquad [2.21]$$

Dividing by N and using the usual relation between engine power, speed and torque, $P_{engine} = 2 \, \pi \, N \, T$, gives

$$m_i/N = w_i \, [\, a + 2 \, \pi \, b \, T \,] \, (\, 1 + A/F \,) \qquad [2.22]$$

This shows that the relation between emissions per revolution and torque is not a simple one, but depends on the pollutant mass fraction.

For a catalyst-equipped engine the pollutant concentrations, w_i, depend on the engine-out emissions and the catalyst efficiency. The engine-out concentrations are a function of engine parameters. The catalyst efficiency depends on the catalyst temperature, exhaust flow rate, and air/fuel ratio over the catalyst.

The behavior of engine-out emissions has been studied for many years.[27] Engine-out concentrations of CO concentration depend only on the air/fuel ratio. The NO concentration is governed by the peak temperatures in the engine. Hydrocarbons in the fuel may be trapped in engine crevices or absorbed in the oil layer on the cylinder wall and remain unburned during the combustion process. During the power and exhuast strokes these unburned hydrocarbons may be entrained in the hot combustion products and undergo some oxidation. Increased turbulent

mixing, usually produced by higher engine speeds, can enhance this oxidation and reduce unburned hydrocarbons; a rich air/fuel ratio will reduce this oxidation rate and increased exhaust hydrocarbons. These qualitative observations have been established by many quantitative studies, but there is no simple mathematical relationship between engine variables and emissions.

Although there is no simple relationship for the concentration of pollutant species in the exhaust, equation [2.19] can be used to interpolate or extrapolate emissions data over small regions if no data are available. If the pollutant concentration and the air/fuel ratio are assumed to be constant constant over this small region, equation [2.19] states that m_i/m_{fuel} will be a constant. Thus pollutant emissions rates at an unknown point, 2, can be found by knowing the fuel rate at that point and the emissions and fuel rates at some known point, 1, by the simple ratio:

$$m_{i\,2} = m_{fuel\,2}\ (m_{i\,1} \ / \ m_{fuel\,1}) \qquad [2.23]$$

This would be expected to apply only over a very narrow range and only at lower loads. At higher loads where enrichment occurs the air fuel ratio is expected to change and pollutant concentrations will also show sharp changes.

Empirical Approaches - Another possible approach is the direct interpolation or extrapolation of emissions from two load points (0 and 1) at a given engine speed. This would result in the following equation for the emissions rate at point 2 if torque, T, is used as the extrapolation variable.

$$m_{i,2} = m_{i,1} + \frac{m_{i,1} - m_{i,0}}{T_1 - T_0}\ [T_2 - T_1] \qquad [2.24]$$

If the exhaust mass flow rate is significantly different between these interpolation points, equation [2.21] can be used to compute the mass fraction and the intrepolation of equation [2.24] can be replaced by the following interpolation on mass fractions:

$$w_{i,2} = w_{i,1} + \frac{w_{i,1} - w_{i,0}}{T_1 - T_0}\ [T_2 - T_1] \qquad [2.25]$$

This would require an interpolation/extrapolation procedure for fuel rate and air/fuel ratio to compute the emissions rate at point 2. It could account for differences in these variables beween different interpolation points. This procedure is expected to produe more accurate results provided that a satisfactory interpolation/-extrapolation for the fuel rate and the air/fuel ratio can be found.

The interpolation/extrapolation equation for the fuel flow rate at point 2 is similar to the previous equations:

$$m_{fuel,2} = m_{fuel,1} + \frac{m_{fuel,1} - m_{fuel,0}}{T_1 - T_0}\ [T_2 - T_1] \qquad [2.26]$$

It is possible to use the interpolation/extrapolation of equation [2.26] to find the fuel rate and the scaling of equation [2.23] to find the emissions. Combining these two equations gives:

$$m_{i,2} = m_{i,1} + \frac{m_{i,1} - m_{i,1} \frac{m_{fuel,0}}{m_{fuel,1}}}{T_1 - T_0} [T_2 - T_1] \qquad [2.27]$$

The choice of which extrapolation procedure to use will be determined by an examination of the actual mapping data.

Examination of Initial EPA Mapping Data – Engine mapping data were provided to Sierra by EPA in the form of Lotus spreadsheets. Sample copies of the spreadsheets for two test vehicles were delivered to Sierra at the start of the projet. These were used to learn the basic structure of the mapping data and to determine subsequent analysis procedures. Subsequently Sierra obtained preliminary data for twenty-nine vehicles; these data were used for the main part of the analysis on this project. A final set of corrected data were used in the later stages of the work.

The initial analysis used a spreadsheet template which could be combined with the EPA spreadsheets to perform the following computations for all data points:

Carbon balance across the catalyst

Computation of mass fractions and emission per revolution for both engine out and tail pipe gas streams.

Computation of fuel rate by An equation and comparison with measured data.

Linear regression of all data points to obtain the best straight line fit of fuel consumption per revolution to torque.

A check on the reported air/fuel ratio as described below.

The mapping data were given in terms of mass emissions, not concentration. The check of the air/fuel ratio started with the computation of the exhaust mole fractions from the equation:

$$y_i = m_i M_{exhaust} / [M_i m_{fuel} (1 + A/F)] \qquad [2.28]$$

where the exhaust molecular weight was assumed to be that of air. The use of this assumed molecular weight and the reported air/fuel ratio in a procedure to check the air/fuel ratio are obvious weak points in this check, but it was the only alternative for computing mole fractions from the available data. Once the mole fractions for HC, CO, CO_2, and NO_x were known the air/fuel ratio was computed by simple element balance equations.

The fuel energy rate predicted by the equation $P_{fuel} = a' V_d N + b P_{engine}$ was computed for each data point. As expected, the agreement was much better for lower engine speeds and loads than it was at higher ones. An

attempt to do a correlation of fuel rate per revolution versus torque using all data points did not produce a good result. This was not considered a serious problem since the fuel rate data in the engine maps is well behaved and closely spaced so that linear interpolation should provide an effective tool for filling any missing data. The correlation could have been improved by using a limited data set, but this did not seem to be an important task for this study.

The equation underpredicted the idle fuel rate for all vehicles. The errors ranged from -18% to -72% with an average value of -42% for the 29 vehicles in the EPA mapping study. This was not unexpected since idle points were not used in determining the empirical coefficients. However, it did point out concerns with using this approach for estimating fuel rates at zero torque.

Except for the idle point, the errors in the predicted fuel rates usually ranged from 5% at low speeds and loads to 50% at higher speeds and loads. Points with larger errors usually had some error in the fuel rate. Thus, the An equation provided a useful tool for flagging potential errors in fuel rate measurements.

All data were reviewed for probable errors. A partial, but not exclusive, list of problems found is shown below:

a. Brake-specific fuel consumption below 0.4 lb/HP-hr.

b. Fuel rates that do not increase with load at constant RPM.

c. Air-fuel ratios greater than 16.

d. Negative catalyst efficiencies or catalyst efficiencies greater than 100%.

e. Inconsistent emissions results (e.g., CO/CO_2 ratios greater than one at stoichiometric or lean air/fuel ratios).

These points wre eliminated the points identified above from further consideration unless there was some independent confirmation of their validity. Points with "irregular" behavior were not eliminated unless there was some reason to suspect an error. These points were assumed to be valid data points representing irregular behavior in the emissions map.

The problems identified were communicated to EPA during the performance of this project. At the same time EPA was reviewing the correctness of their data. Following the completion of this initial task EPA delivered a revised set of mapping data which was used for the second part of this work assignment.

Computer graphics of the emissions data were produced to provide a visual evaluation of potential data relations. These were done as surface plots and topographical plots. Emissions data were examined on four bases: (1) emissions rates (grams/second), (2) brake-specific emissions (grams/HP-hr), (3) mass fractions, and (4) emissions rate

divided by engine speed (grams/revolution). Figure 2.1 shows surface plots of the emissions data on a brake-specific basis for the Mercedes 300E. Although there is variation in the emissions maps for various vehicles, the samples shown here are typical of all the engines observed. Additional surface plots of emissions are shown in Appendix A.

The most significant observation from the surface plots is the division of each emissions map into two regions: the first has very low emisions; the second has very high emissions and the transition between the two regions is fairly sharp. This is especially true for HC and CO where the transition is associated with enrichment. The effect is less noticeable, but still substantial for NOx emissions.

The same data are shown as a contour plot in Figure 2.2. These plots use logarithmatic contour lines with values of $1x10^n$, $2x10^n$ and $5x10^n$ with values of the exponent n chosen to cover the entire range of data. (Some plots also include a contour for $7.5x10^n$.) These contour plots do not provide the clear picture of the overall emissions behavior shown in the surface plots. They do show large relative changes in emissions, even in regions where the surface plots show nearly constant emissions near zero. Of course, the absolute level of these emission changes is small compared to the maximum level.

Thus, the combined use of surface plots and contour plots gives the following picture of the emission maps.

- There are two distinct regions with sharp separation; one is a low emissions region, the other is a high emissions region.

- The low emissions region has changes which are large compared to the levels present.

These same observations hold regardless of the basis for the emissions maps. Figures 2.3 to 2.5 are contour plots of emissions maps for emission rates, mass fractions and emissions per revolution, respectively.

A clear feature of these maps is the lack of any regular behavior that can be used to determine simple relationships between emissions and engine operating conditions. Contour plots for throttle setting, manifold vacuum, and fuel consumption are shown in Figure 2.6. The regular behavior noted here is a marked contrast to that observed for emissions. These data confirm the results of the theoretical analysis that there is no simple relation between emissions and engine operating varibles that can apply to the entire range of engine operating conditions.

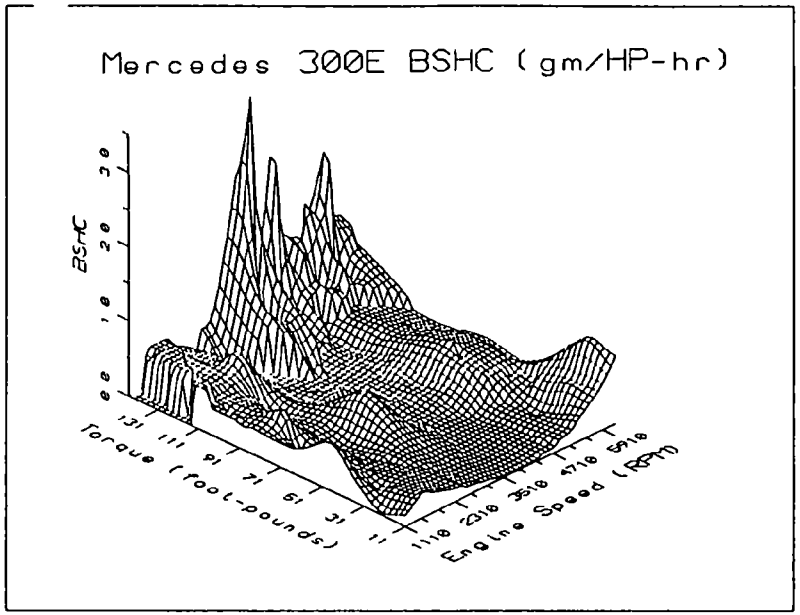

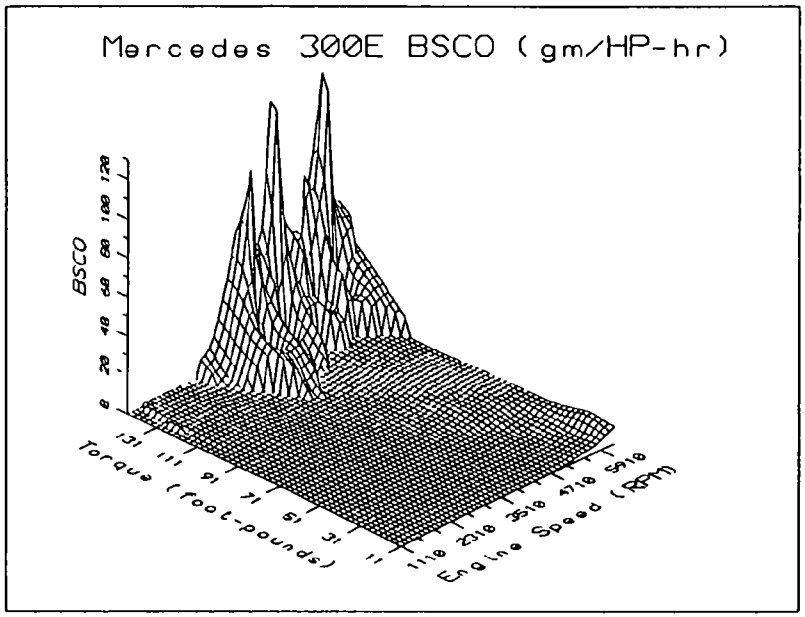

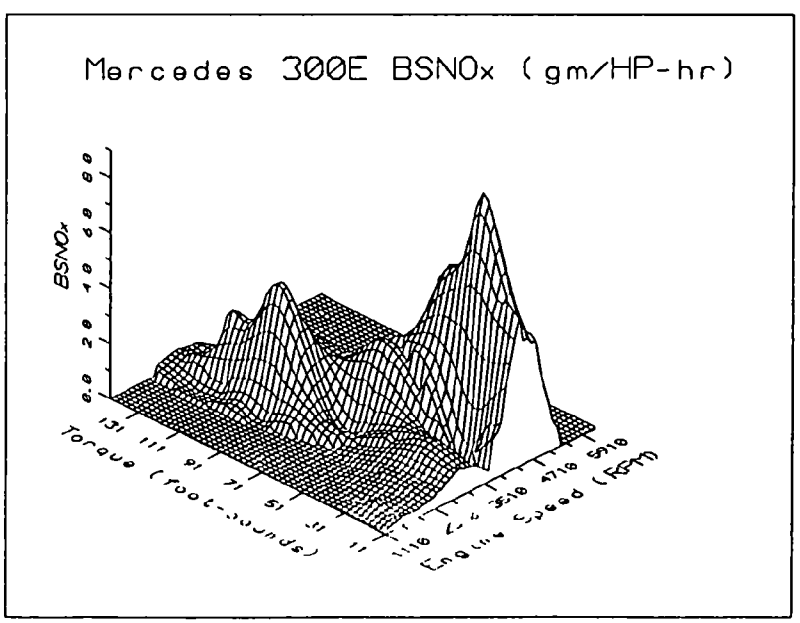

Figure 2.1

Surface Plots of Brake-Emissions for
1992 Mercedes Benz 300E
3.0L A4 4-Door Sedan

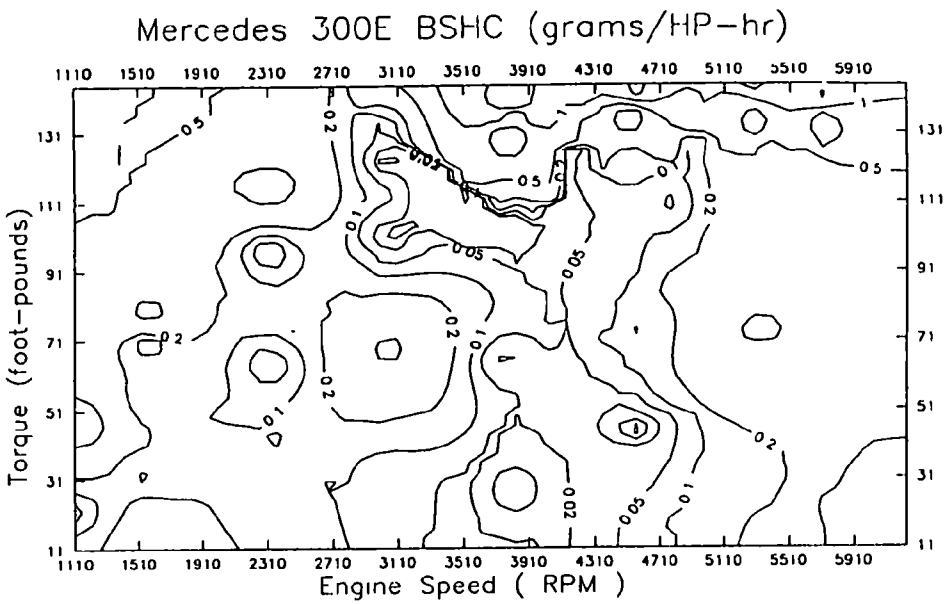

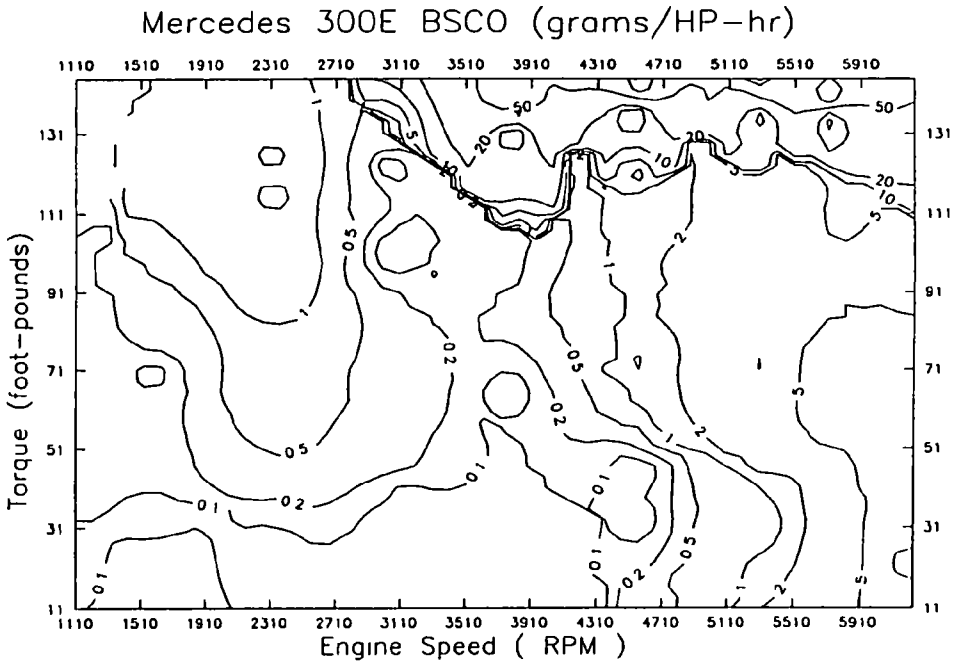

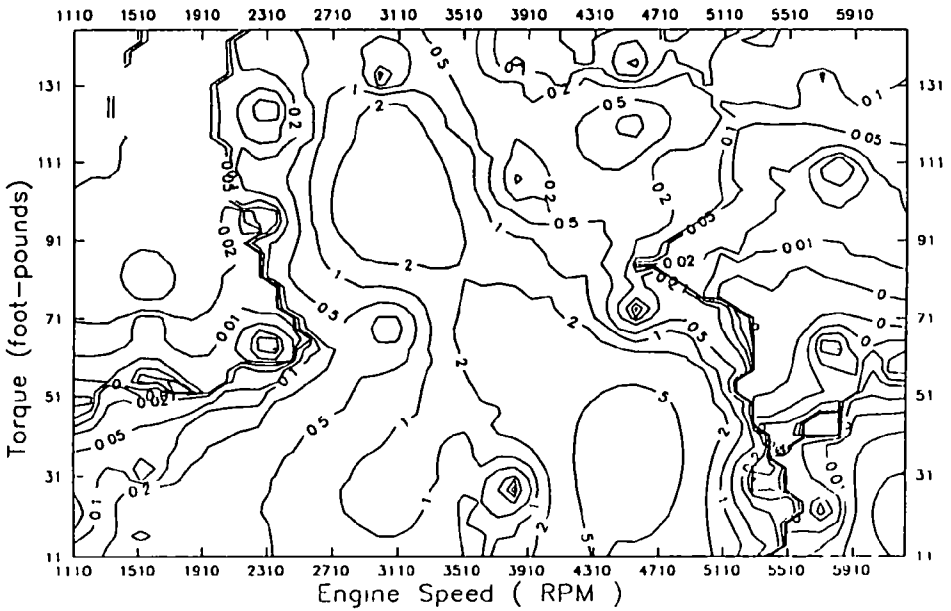

Figure 2.2

Contour Plots of Brake Specific Emissions for
1992 Mercedes Benz 300E
3.0L A4 4-Door Sedan

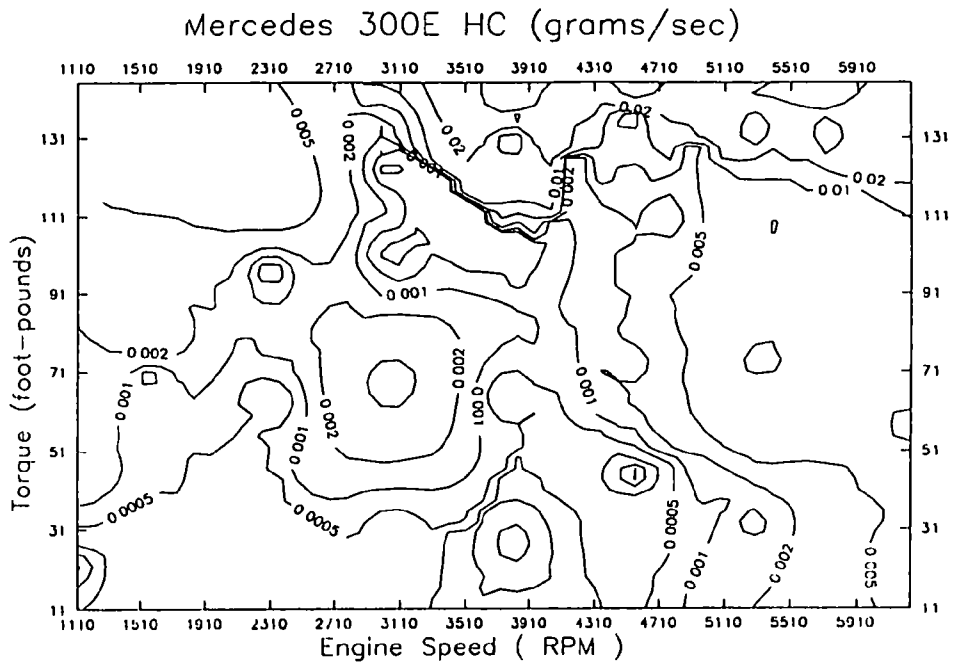

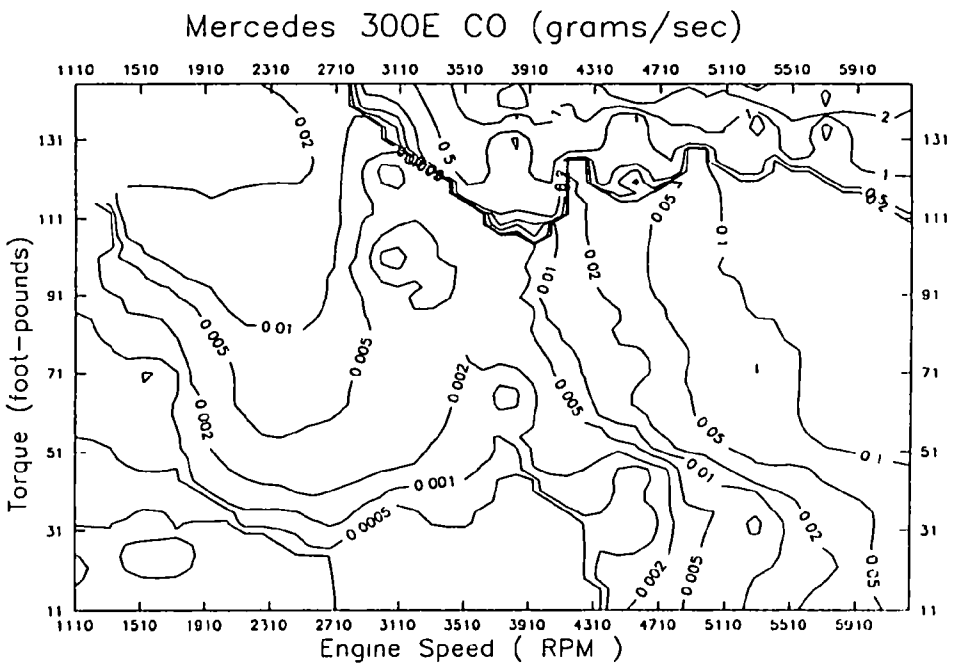

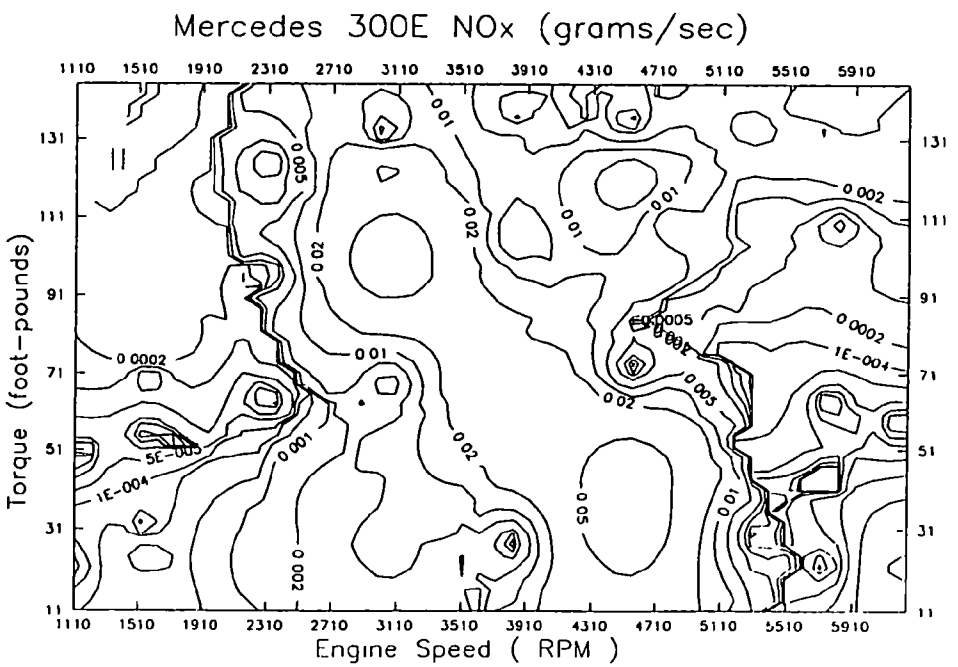

Figure 2.3

Contour Plots of Emission Rates for
1992 Mercedes Benz 300E
3.0L A4 4-Door Sedan

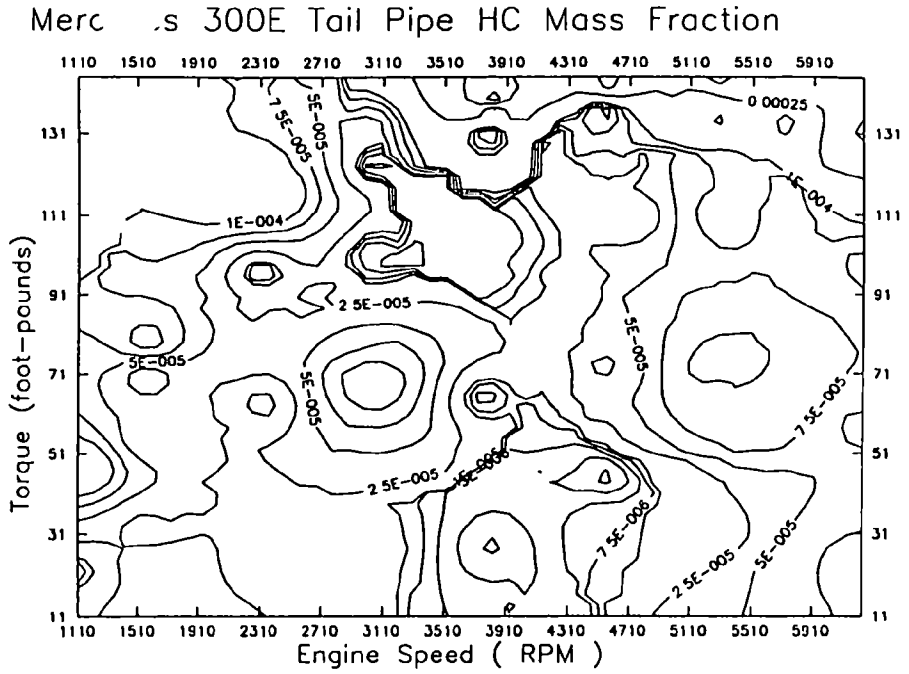

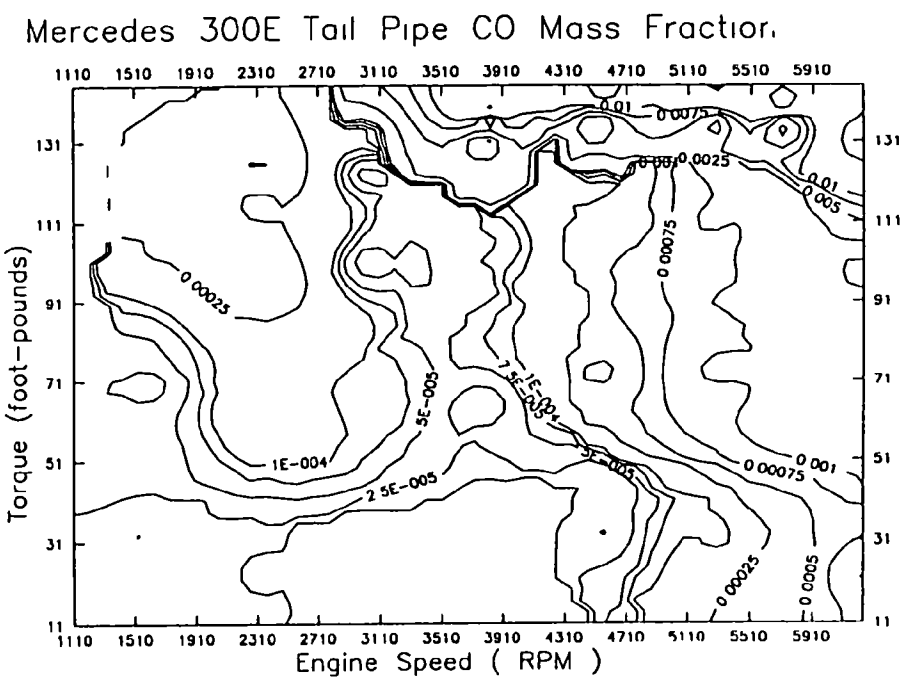

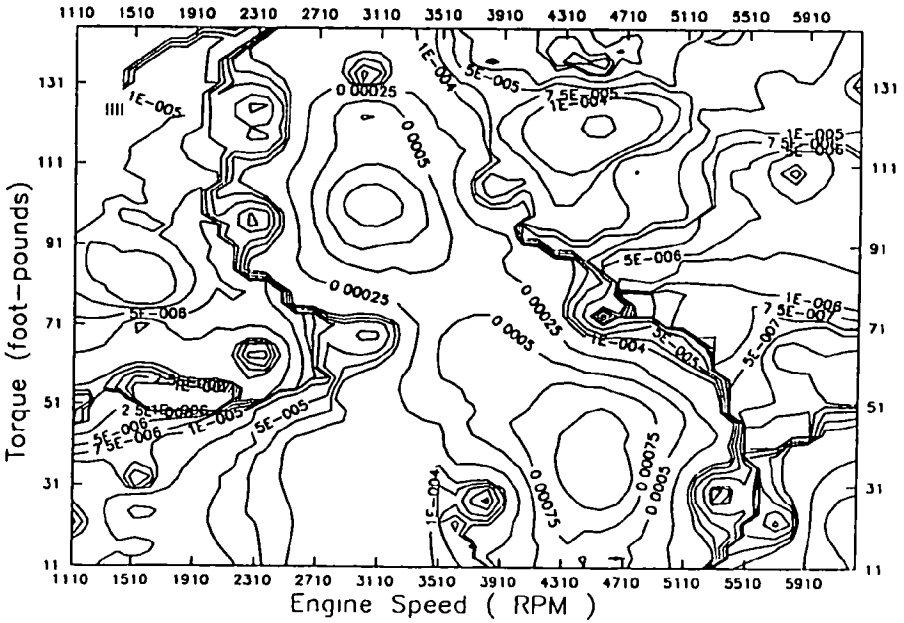

Figure 2.4

Contour Plots of Mass Fractions for
1992 Mercedes Benz 300E
3.0L A4 4-Door Sedan

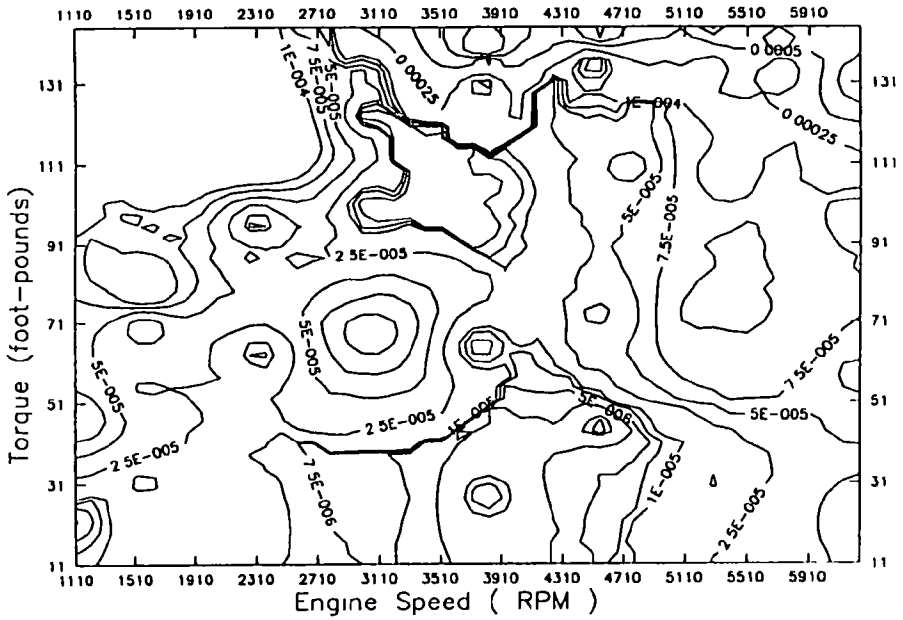

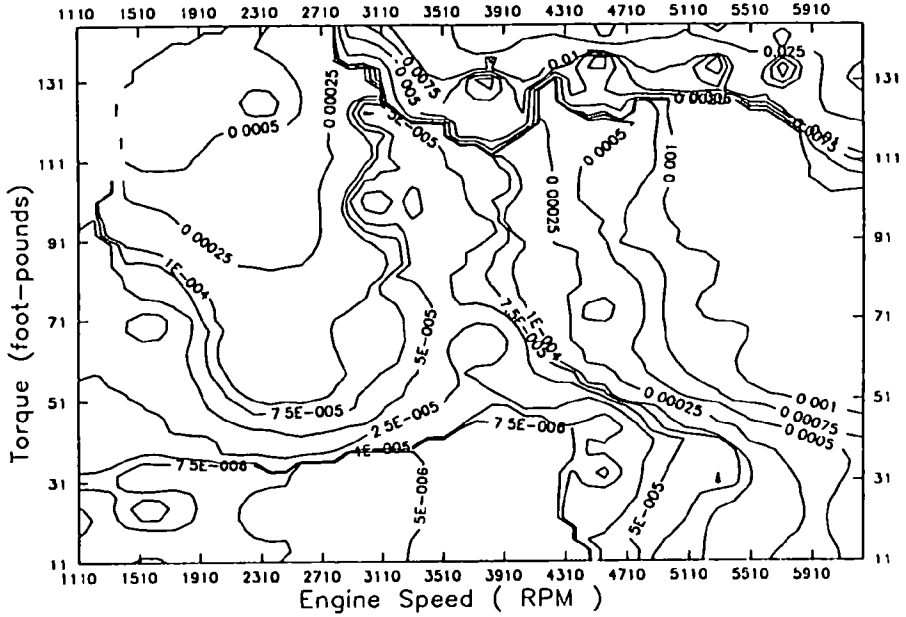

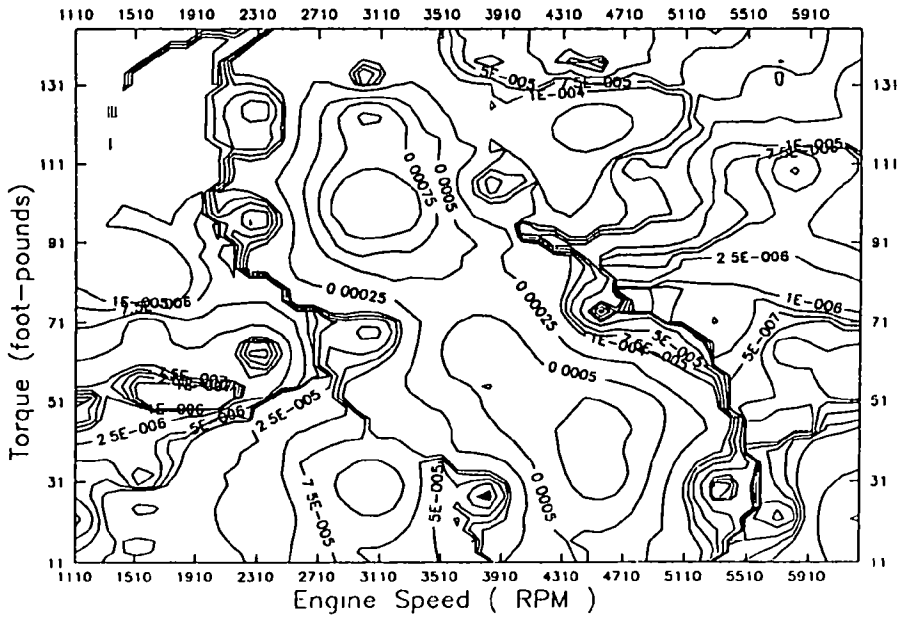

Figure 2.5

Contour Plots of Emissions Per Revolution for 1992 Mercedes Benz 300E 3.0L A4 4-Door Sedan

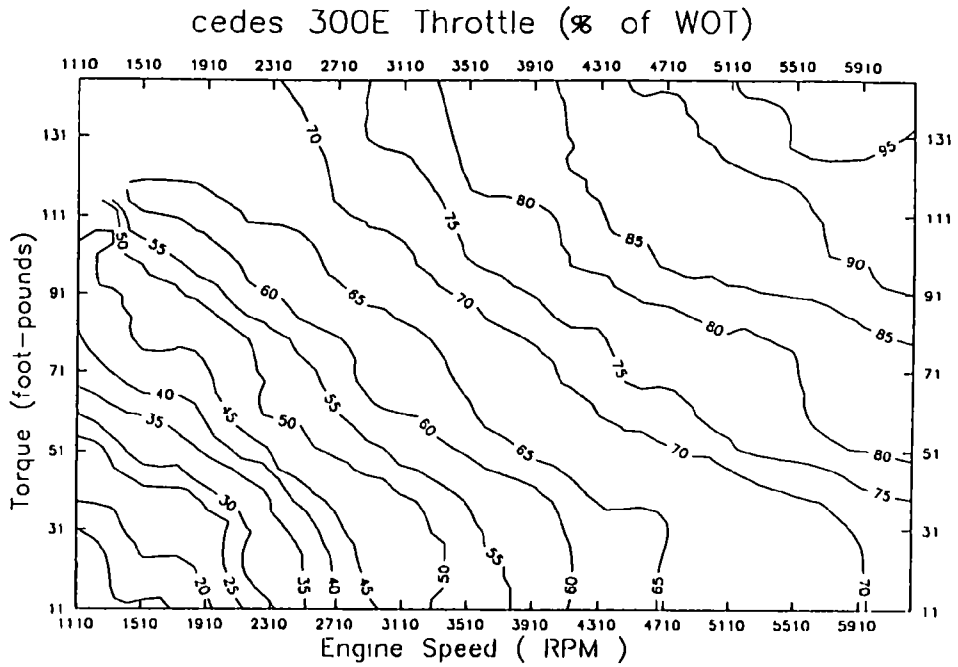

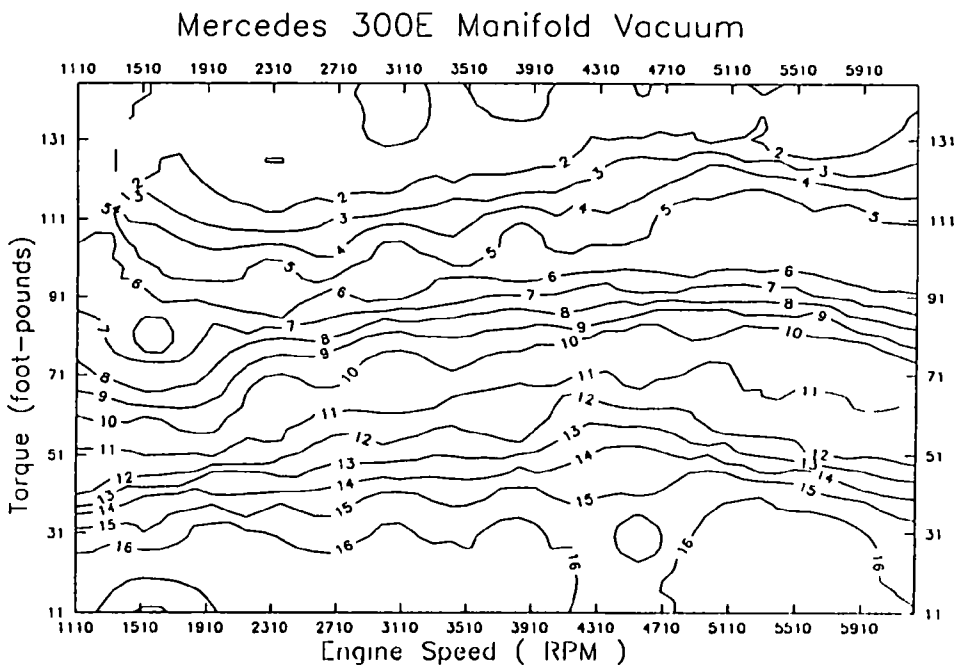

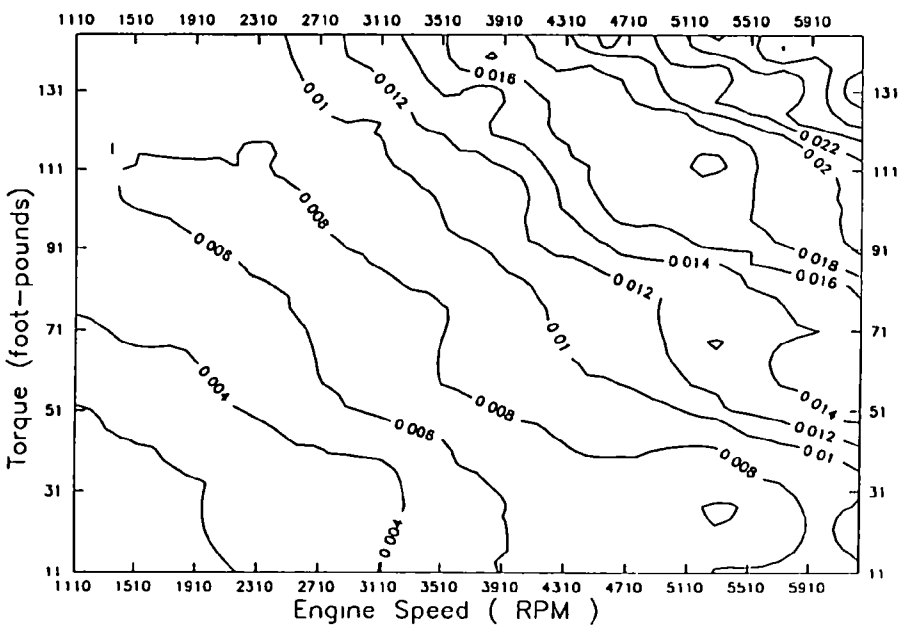

Figure 2.6

Contour Plots of Engine Performance Parameters for 1992 Mercedes Benz 300E 3.0L A4 4-Door Sedan

Computer Graphics Techniques for Generating Engine Maps

The algorithm that is used for gridding irregularly spaced data for computer graphics was investigated for possible use as an engine mapping tool. This algorithm proceeds by taking a set of input data points, e.g., a series of pollutant concentration data points, C_k, at measured speed, N_k, and torque, T_k. These data are used to construct a set of regularly spaced data points representing the initial data. If the grid values of speed and torque are denoted as $N_{grid,i}$ and $T_{grid,j}$, then the problem is to find the values of the variable at these grid points, $C(N_{grid,i}, T_{grid,j})$. There are a variety of ways for doing this. The most common uses an inverse distance weighting of the nearest neighbor points. The distance d_k between the measured data points and the desired grid point is defined as follows:

$$d_k^2 = \frac{(N_k - N_{grid,i})^2}{(N_{max} - N_{min})^2} + \frac{(T_k - T_{grid,j})^2}{(T_{max} - T_{min})^2} \qquad [2.29]$$

A set of n measured data points in the neighborhood of the desired grid point is selected and the value of C on the grid is computed by the following formula:

$$C(N_{grid,i}, T_{grid,j}) = \frac{\sum_{k=0}^{n} \frac{C_k}{d_k^2}}{\sum_{k=0}^{n} \frac{1}{d_k^2}} \qquad [2.30]$$

There are many alternatives for choosing which n data points to use in this equation. The simplest choice is to take the n nearest neighbors. Alternative choices limit the points used to those within a certain radius of the grid point. Another selection method requires that points come from each quadrant (or octant) surrounding the grid point. It is also possible to use alternative equations for fitting the experimental data to the regular grid. A technique known as kerning is based on fitting gradients at the boundaries of the region.

The methods for developing plotting techniques are taken from drafting and mapping where there is no difference in scale for the two independent variables. In cases where the physical variables are not the distance in a coordinate direction, it is important to define the distance to account for the difference in scale as is done in equation [2.29]. Actually, it is only necessary to use the single parameter, K, defined as the ratio of Speed to Torque ranges. This is defined by the following equation.

$$K^2 = \frac{(N_{max} - N_{min})^2}{(T_{max} - T_{min})^2} \qquad [2.31]$$

This definition of K can be used to obtain a modified distance, D_k, defined as

$$D_k^2 = (N_{max} - N_{min})^2 \, d_k^2 = (N_k - N_{grid,i})^2 + K^2 \, (T_k - T_{grid,j})^2 \qquad [2.32]$$

Equation [2.32] can be used to substitute D_k for d_k in equation [2.30]. When this is done the $(N_{max} - N_{min})^2$ terms cancel leaving

$$C(N_{grid,i}, T_{grid,j}) = \frac{\sum_{k=0}^{n} \frac{C_k}{D_k^2}}{\sum_{k=0}^{n} \frac{1}{D_k^2}} \qquad [2.33]$$

It was necessary to consider many of these ideas in order to obtain satisfactory plots of the EPA engine mapping data. The Surfer software package[28] used for generating surface and topographical plots allowed various user options for selecting the method used to distribute experimental data over the regular grid used in the plots. One of the poor features of this system was the use of a default value of K = 1. Since the difference in speed range was typically about 4000 RPM while the difference in torque was about 125 ft-lb_f, the typical K value was about 30. Plots obtained with a K value of 1 displayed an irregular pattern which was not observed when the actual K value based on the minimum and maximum torque and speed values was used.

The observation of several surface and contour plots of the mapping data suggested the use of this technique for the formation of a final engine map. This had the particular appeal of being able to handle the slight variation in the engine speed data and the ability of treating the occasional point which was available at only one engine speed. A Fortran program was written to take the intermediate file from the graphics program and use it to generate an engine map. This provided the values of engine speed, torque, intake manifold vacuum, throttle position, fuel flow rate, and emissions rates (both engine out and tail pipe) for HC, CO and NOx. These were obtained on a 50 by 50 grid of speed and load points.

In order to verify the utility of this procedure, a second Fortran program was written which used the engine map generated by the first program to compute the values corresponding to the speed and load points in the initial mapping data. Although good agreement was obtained for most points, some points had relative errors of 1000% or more in CO and HC emissions. This was due to the nature of equation [2.30] or [2.33] which tend to smooth the experimental data. The actual data does have sharp increases in emissions over a narrow region of engine load. The process used in generating the graph tends to smooth these out resulting in enormous errors for points where the sharp increase is occurring.

This effect was studied by varying the number of nearest neighbor points, n, used in equation [2.30]. The agreement improved as the value of n was decreased. However the resulting engine maps were very jagged. Figure 2.7 shows the hydrocarbon emissions rates as the number of points used in constructing the graph was decreased from the five poins used to generate the usual surface plots to two and one point. Although the map generated by equation [2.30] for one data point is very jagged, it provided the best agreement between the engine map and the experimental data. For this map, at a given location on the regularly spaced grid, the "interpolated" value was simply set equal to that of the nearest

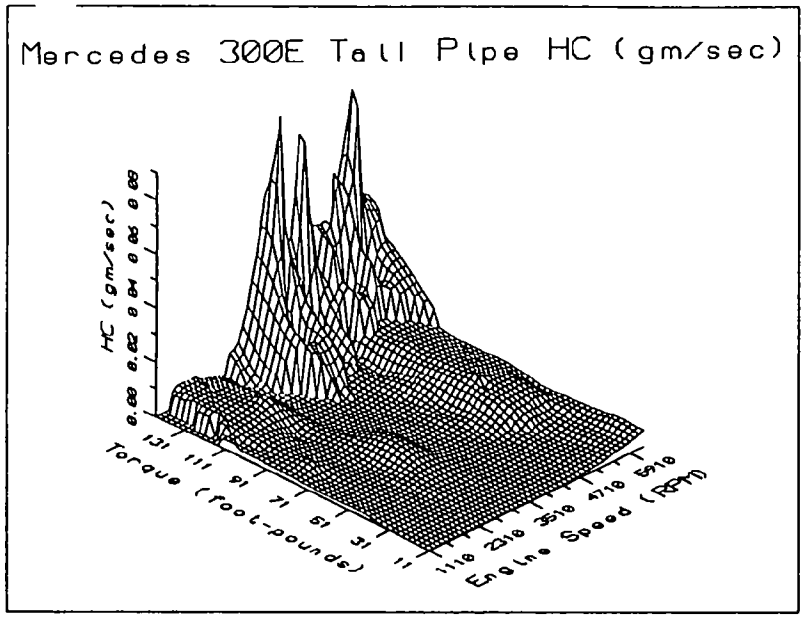

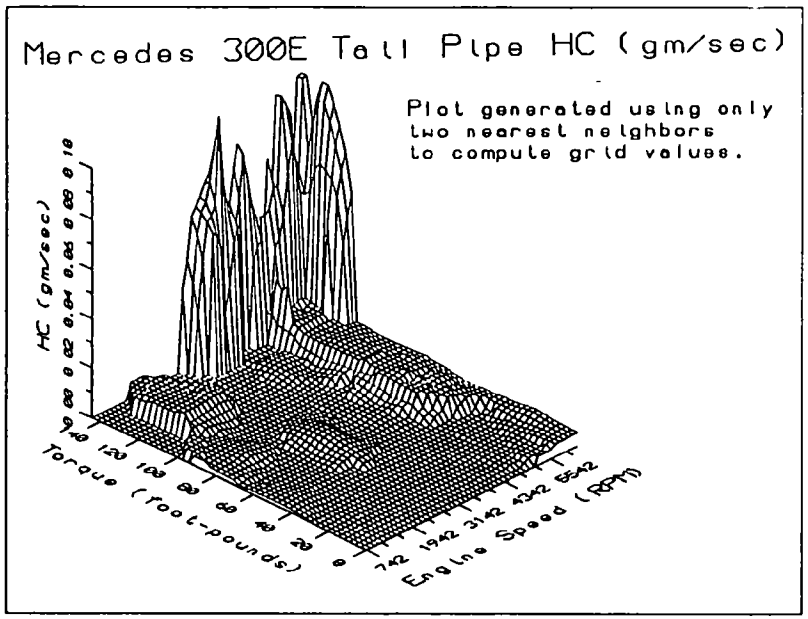

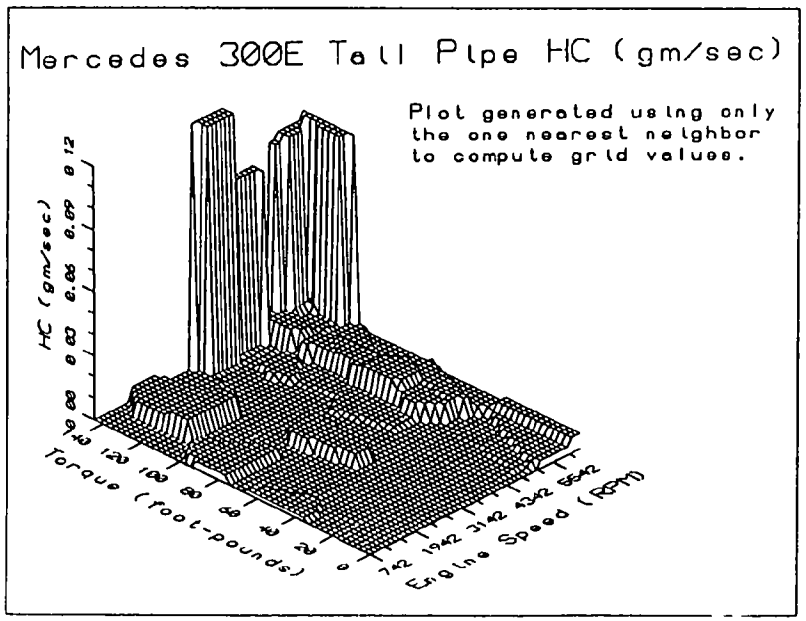

Figure 2.7

Effect of Number of Fitting Points on Emissions Map

experimental data point. This one-point scheme can be reduced to the following rules:

1. For a given grid point ($N_{grd,i}$, $T_{grd,j}$) use equation [2.29] to compute the "distance" to the nearest neighbors. Find the smallest value of d_k.

2. Set the value of C at $N_{grd,i}$, $T_{grd,j}$ equal to the value, C_k at the minimum distance d_k.

Although this approach gave a gridded engine map which matched the experimental points well in most cases, the result was essentially a step function which did not seem to provide a good representation of a real engine map. In addition, this approach did not provide any relation to the underlying engine operating parameters. Consequently, no further application of this method was explored. Although the results of this study were not used in the final procedure for preparing engine maps, the work in obtaining these results did point out the need to resolve properly the sharp increases in emissions that did occur in the actual engine maps.

Conclusions from this Task

The use of the equation $P_{fuel} = a' V_d N + b P_{engine}$ is limited to low speed and load points. It does represent a bilinear representation and is consistent with the usual interpolation procedures used in engine map codes such as VEHSIM.

The data used to determine the empirical coefficients a' and b did not include the normal idle points. Its use for estimating the fuel rate at zero torque is uncertain.

There is no simple relation between emissions rates and engine operating conditions which is valid over the entire range of engine operating conditions.

The emissions maps can be divided into low-emission and high-emission regions with a fairly sharp transition between them. An analyticla representation of these maps must have a careful definition of these regions.

3. PROTOCOLS FOR INTERPOLATION AND EXTRAPOLATION IN ENGINE MAPPING DATA

Introduction

As noted in the previous section, there is no simple correlation between emissions and engine operating parameters that can be applied in a simple fashion to all data to produce the desired predictions of emissions (and fuel rate) where such data are missing in the EPA mapping data. The theoretical background and the data analysis of the previous section can be used to develop a protocol for filling in the missing values to allow the mapping data to be used in a vehicle emissions simulation code.

Preliminary Protocol for Filling Emission Maps

This protocol was developed and submitted to EPA about midway through the work assignment. Following their comments, additional work was done to improve this protocol. An improved method was developed for filling fuel and emission rates at zero and negative torques, but the examination of improved methods for filling in transition points in the engine map did not yield a significant improvement.

Background and Rationale - The most significant feature of the emissions engine maps is the dramatic increase in CO and HC emissions in operating modes that have fuel-rich operation. This can increase these emissions rates by factors of 10 to 1,000 over very small changes in engine speed and/or load. This is the key feature that will need to be considered in any interpolation process. For all pollutant species, there are regions of the engine map where the emissions rates are dramatically higher than in all other regions. Any small time spent in these regions would probably result in failing an emissions test.

Emissions data show irregular trends. In some cases, there may be reason to suspect experimental error. In most cases, however, these "irregular" points are mutually consistent. For example, at a single engine speed the emissions of HC and CO may generally increase with torque, but there may be one torque point where there is a dip. If this occurred only in HC and not in CO, it might indicate a measurement error. Generally, such dips occur in both HC and CO indicating a consistent improvement in emissions reduction for that point. Such "irregular" data should be included in any final engine unless there is some other indication of experimental error.

There is no "magic bullet" that will automate the correlation of emissions with the usual engine mapping variables—engine speed and load, the latter usually expressed in terms of torque or brake mean effective pressure (BMEP). Instead, the holes on each engine map must be filled using good engineering judgement. The following procedure is recommended to provide the final vehicle simulation engine maps from the experimental data.

Rules for Preliminary Protocol -

1. Review all data for probable errors. A partial, but not exclusive, list of problems found is shown below:

   a. Brake-specific fuel consumption below 0.4 lb/HP-hr.

   b. Fuel rates that do not increase with load at constant RPM.

   c. Air-fuel ratios greater than 16.

   d. Negative catalyst efficiencies or catalyst efficiencies greater than 100%.

   e. Inconsistent emissions results (e.g., CO/CO_2 ratios greater than one at stoichiometric or lean air/fuel ratios).

2. Eliminate the points identified above from further consideration unless there is independent confirmation of their validity.

3. Do not eliminate "irregular" behavior data points unless there is some reason to suspect an error. Assume that these points are valid data points representing irregular behavior in the emissions map.

4. Form the engine map for a VEHSIM type code; this requires data at fixed speed points, but the load points can change from speed to speed. A procedure for filling in missing points is given below. This discussion assumes that the emissions map will be described in terms of a mass emissions rate (e.g., grams per second - g/s) rather than using brake-specific emissions rates to avoid problems as the load goes to zero.

   a. Use an average engine speed for all points in a series of runs with different torques provided that the measures engine speed is within ±70 RPM of the average speed.

   b. Examine the various runs at each average speed and determine the region where any sharp increases (or decreases) in emissions occur. Depending on the engine speed, there may or may not be such a point.

   c. Define a "sharp change" in emissions levels as 50% of the maximum emissions rate. Where the sharp change in emissions is contained in a torque interval which is less than 20% of the maximum measured torque, use the experimental data only.

d. Where the sharp change is found in a wider torque interval, use data at adjacent engine speeds to estimate the point at which a dramatic increase in emissions would occur. Place an interpolated point in the engine map that defines this transition more sharply.

Determine the torque value for this point from those at neighboring speed runs. Use linear interpolation to obtain the fuel rate, throttle setting and manifold vacuum for this point. Set the emissions rates at this point to a value determined from adjacent regions of the engine map. This determination should be based not only on the observed emission rates, but also on the corresponding operating conditions such as air/fuel ratios, operation as open or closed loop, and anticipated EGR operation.

This procedure is illustrated in the following hypothetical example.

Speed (RPM)	Torque (ft-lb)	Emissions (grams/second)
4500	50	.0012
4500	90	.12

Assume the experimental data shown above were for an engine whose maximum measured torque was 120 ft-lb and whose maximum emissions rate for the species shown was .2 g/s. The emissions increase shown is greater than the defined sharp change (50% of the maximum rate). This rise should be contained in a torque interval of (.2)(120 ft-lb) = 24 ft-lb. In order to sharpen the definition of the increase in emissions, a torque point would be "interpolated" between these two points.

Examine the data at neighboring speed points. If the data showed that the sharp increase in emissions rate took place closer to the higher (90 ft-lb) torque point—and if the expected operations in terms of air/fuel ratio were expected to be similar for this speed range—an interpolation point would be created with a low emissions rate. If a mean value of 70 ft-lb were picked for the interpolation point, the emissions increase between the observed value at 50 ft-lb and the interpolation point would be estimated from the change in emissions for a similar increase in torque in neighboring regions. For example, if such data showed a 25% increase in emissions might be expected between 50 and 70 ft-lb, the interpolated point at 70 ft-lb would be assigned an emissions value of .0015 g/s.

If data at neighboring speed points indicated that the transition took place closer to 50 ft-lb torque point, then a high emissions rate would be used for the interpolation point. If the mean value of 70 ft-lb is chosen for the interpolation point and data from nearby regions indicate a 10% decrease in emissions might be expected between 90 and 70 ft-lb, the

interpolated point at 70 ft-lb would be assigned an emissions value of .11 g/s.

In either case, the value used should be consistent with the engine operating conditions expected at the interpolation point. Note that this approach produces dramatically different results for the emissions at this interpolated point (.0015 vs. .11 g/s); if simple linear interpolation were used with the experimental data, this point would have an interpolated emissions rate of .06 g/s for both cases.

The approach above has been constructed as a first-order approximation using emission rates. An improved approximation technique would interpolate emission concentrations and obtain the emissions rate by multiplying the concentrations by the exhaust flow rate. This should provide a better approximation because the emission species concentrations are more nearly constant than the emission rates as the engine speed varies.

e. Vehicle emission simulation codes usually require a point at wide-open throttle (WOT) for each engine speed. The emissions at this point can usually be set to those of the highest measured torque at the same speed. If the highest load value is significantly below WOT operation, the WOT emissions rates can be determined from those at neighboring speed points.

f. Interpolations of fuel rate, engine vacuum, and throttle setting are generally regular and can be done by linear interpolation.

g. To get data at zero and negative torques, try the various estimation procedures outlined below. Choose the most "reasonable" results to provide physical reality and overall consistency in the engine map. (Negative fuel and/or emission rates and fuel rates at zero torque that are higher than fuel rates at the lowest measured torque point are examples of "unreal" results that may be obtained by these procedures.) The differences in these procedures should be checked by some preliminary runs with a VEHSIM-like code. Because the fuel rates and emissions rates are low at these conditions, the procedures used should not have a significant difference on the overall cycle results. The procedures to be used for fuel rate are the following:

    i. Assume that fuel rate at zero torque, at a given engine speed, is found by multiplying the fuel rate at idle by the ratio of the given engine speed to the idle speed. This may produce an zero-torque fuel rate which is greater than the fuel rate at the first measured torque point.

    ii. Extrapolate the fuel rate from the lowest two torque points. This may produce negative fuel rates.

iii. Extrapolate the computer-generated engine mapping data from the lowest torque points to zero torque.

iv. Use the Ross-An regression procedure to get an intercept which gives the fuel per revolution at zero torque. Multiply this value by a given engine speed to get the fuel rate at that speed.

The following procedures will be tried for estimating emissions rate at zero torque:

i. Use the value at the lowest torque point.

ii. Extrapolate from the two lowest torque points; this may produce a negative emissions rate.

iii. Multiply the emissions rate at the lowest torque point by the ratio of the fuel rate at zero torque divided by the fuel rate at the lowest torque point. This is equivalent to assuming that the mass fraction of the pollutant species and the air/fuel ratio do not change between these points.

iv. Multiply the emissions at the idle point by the ratio of the given engine speed to the idle speed.

For both the fuel rate and the emissions rate of the various species, engineering judgement will be used to reconcile the values obtained by these different approaches and select the most reasonable value.

h. Assume that the lowest possible operating RPM is the normal engine idle speed and that the emissions and fuel rate at this speed are the same, at each torque point, as those at the lowest measured engine speed. This is not a significant assumption as the lowest measured engine speed is usually the speed that would be encountered in normal engine operation.

i. Assume that the highest measured engine speed is the maximum speed so that no extrapolation is needed at this point.

j. Assume that emissions and fuel rate values for negative torque points (i.e., deceleration) will be the same as those for zero torque. This will not be correct if there is significant enrichment of the mixture for deceleration. However, this may not be a significant problem because the exhaust flow rates are low under these conditions.

k. The above discussion has focussed on emissions. As noted above, codes such as VEHSIM expect a wide open throttle load point at each speed. Values for the torque and fuel rate at these WOT points would be based on the observed relationship between these variables for similar engines.

Sample Application of Preliminary Protocol

Table 3.1 is an engine map for the Chrysler New Yorker which illustrates how this protocol would be applied to one engine. The points excluded from the original data and the added points are noted. The maximum measured torque is 178.8 ft-lb. Any sharp increase and/or decrease in emissions should be contained in a torque interval which is 20% of this maximum or 35.76 ft-lb. For this engine, the maximum measured HC, CO, and NOx emissions rates are .099, 9.8, and .11 g/s, respectively. Half of these emissions levels (.05, 4.8, and .055 g/s for HC, CO, and NOx) define a sharp change in emissions.

Examination of the data shows that it is necessary to add three interpolation points to the data in order to improve the definition of the sharp changes in the map.

(1) at 2765.85 RPM between 83.2 and 133.2 ft-lb to better define the increase in NOx a point is added at 100 ft-lb with an NOx emissions rate similar to the one at 3313.29 RPM and 96.8 ft-lb. All other data found by linear interpolation.

(2) at 4182.22 RPM between 56.1 and 96.9 ft-lb to better define the increase in HC and CO a point is added at 80 ft-lb. Emissions data are estimated based on data at neighboring speed points.

(3) at 4508.75 RPM between 89.3 and 134.4 ft-lb to better define the increase in HC and CO and the decrease in NOx. Emissions data are estimated based on data at the lower RPM.

Extrapolation points for zero and negative torque and for WOT operation are also added. The method used for obtaining these points is given in the "Description of Point" column.

Final Procedure for Determining Results at Zero and Negative Torques

The various methods for determining the emissions at zero and negative torques outlined in step 4.g of the preliminary protocol were examined for each engine in the data set. There was no one procedure that was most effective.

The best estimation of the emissions and fuel rates for negative torque was to set these equal to their values at zero torque, for each engine speed. The justification for this approach was that the fuel energy required to overcome engine friction would depend mainly on the engine speed. Although the air flow, and hence the fuel flow, would be expected to increase as the manifold pressure increased from the most negative torque to the zero torque value, these differences could be ignored for lack of any more reasonable approximation to use. Similarly, the emissions rates would be expected to be the same at both zero and negative torque. The problem that remained was the estimation of the values of emissions and fuel flow at zero torque.

1991 CHR. NEW YORK
4 DR SEDAN 3 8 L L4
VIN: 1C3X466R9MD260

Table 3.-

SAMPLE EXPANDED ENGINE MAP
July 14, 1992

RPM	Torque ft-#	BMEP psi	Man Vac in hg	Throttle %WOT	Fuel lbs/sec	TP HC gms/sec	TP CO gms/sec	TP NOx gms/sec	Description of Point
743 97 <--Average Speed for Data below									
693	0 0	0 0	29 9	0	0 000899	0 000306	0.000620	0.000151	Original Data In Final Map
795	16 2	10.5	17.6	0.7	0.000937	0 001984	0 004560	0 000165	Original Data In Final Map
						0 001984	0 004560	0 000165	Extrapolation point; last-torque emissions
1115 85 <--Average Speed for Data below									
	-50	-32 5	29 9	0	0 001031	0 000562	0 000231	0 000231	Extrapolation Point; Use zero torque entry.
	0	0 0	29 9	0	0.001031	0.000562	0 000231	0 000231	Extrapolation Point, Extrapolate Fuel; Scale Emissions by Fuel Rate
1114	11.2	7.3	18 8	3 0	0 001191	0 000649	0 000266	0 000267	Original Data In Final Map
1118	26 5	17.2	17.3	4 2	0 001409	0 003398	0 011484	0.002358	Original Data In Final Map
						0 003398	0 011484	0 002358	Extrapolation point; last-torque emissions
1666 57 <--Average Speed for Data below									
	-50	-32.5	29 9	0	0 001500	0 000229	0 000968	0 000000	Extrapolation Point, Use zero torque entry.
	0	0 0	29 9	0	0.001500	0 000229	0 000968	0.000000	Extrapolation Point; fuel rate by concensus; emissions scaled by fuel rate
1661	36 2	23 5	16 4	8 6	0 002252	0.000344	0 001453	0.000000	Original Data In Final Map
1672	82 8	53 9	11 0	13 9	0 003864	0 002482	0 020203	0 001021	Original Data In Final Map
						0 002482	0 020203	0 001021	Extrapolation point, last-torque emissions
2331.54 <--Average Speed for Data below									
	-50	-32 5	29 9	0	0 003303	0.001097	0 011012	0.000674	Extrapolation Point; Use zero torque entry.
	0	0 0	29 9	0	0 003303	0 001097	0 011012	0.000674	Extrapolation Point, fuel rate extrapolated, emissions scaled by fuel rate
2229	25 1	16 3	16 0	12 9	0 003700	0 001229	0 012335	0.000755	Original Data In Final Map
2222	80 0	52 0	11 6	17 2	0 005140	0 003632	0 008320	0 001159	Original Data In Final Map
2221	138 3	89 9	5 4	25 6	0 007011	0 001085	0 000871	0 061383	Original Data In Final Map
2220	150 2	97.7	1.9	39 2	0 007975	0 000957	0 000959	0.075298	Original Data In Final Map
	150 3	97.7	0	100	0 007975	0 000957	0 000959	0 075298	Use previous data for extrapolation point
2765.85 <--Average Speed for Data below									
	-50	-32 5	29 9	0	0.003600	0.001225	0 009890	0 000139	Extrapolation Point; Use zero torque entry.
	0	0 0	29 9	0	0 003600	0.001225	0 009890	0 000139	Extrapolation Point, Idle-scaled fuel rate; emissions scaled by fuel rate
2801	42 3	27.5	16 1	15.4	0 004607	0 001568	0 012656	0 000178	Original Data In Final Map
2773	83 2	54 1	11 1	20 3	0 006418	0 002758	0 018919	0 001091	Original Data In Final Map
	100	65 0	9 1	23 6	0 007991	0 002098	0 013584	0 001300	Interpolation point to localize NOx emissions rise
2772	133 2	86 6	5 3	30 2	0 011096	0 000796	0 003057	0 106257	Original Data In Final Map
2766	155 9	101 4	1.9	46 0	0 012792	0.000946	0 002404	0 083582	Original Data In Final Map
2717	165 1	107 4	0 4	96 8	0 019398	0 078899	6 507581	0 001571	Original Data In Final Map
	165 2	107.4	0	100	0 019398	0 078899	6 507581	0.001571	Extrapolation point to give highest measured values
3313.29 <--Average Speed for Data below									
	-50	-32 5	29 9	0	0 003800	0.000162	0 000288	0.013110	Extrapolation Point, Use zero torque entry.
	0	0 0	29.9	0	0.003800	0 000162	0 000288	0 013110	Extrapolation Point, fuel rate by concensus; emissions scaled by fuel rate
3313	14 9	9 7	19 3	14 0	0 004095	0 000175	0.000310	0 014126	Original Data In Final Map
3324	33 8	22 0	17 5	15.9	0 004990	0 000304	0 001525	0 000148	Original Data In Final Map
3309	43 0	27.9	16 3	17.8	0 005521	0 001462	0 022420	0 000311	Original Data In Final Map
3306	53 6	34 9	15.1	24 2	0.006141	0 001922	0 035396	0 000326	Original Data In Final Map
3297	85 3	55 5	11 1	29 3	0 007791	0 001074	0 016686	0 000421	Original Data In Final Map
3328	96 8	63 0	8 0	34 9	0 011970	0 001433	0 024995	0 001252	Original Data In Final Map
3323	134 3	87 3	5 6	36 8	0 013524	0 000612	0 001927	0 090989	Original Data In Final Map
3319	147 3	95 8	3 4	42 6	0 017264	0 036821	1 958976	0 008560	Original Data In Final Map
3288	173 9	113 1	2 0	54 2	0 017778	0 054263	2 498950	0 014817	Original Data In Final Map
3311	178 8	116 3	1 0	73 4	0 019020	0 048818	2 926357	0 008537	Original Data In Final Map
3328	177 6	115 5	0 7	97 9	0 024251	0 087890	8 669626	0 001792	Original Data Eliminated From Final Map Because of Torque Decrease
	179	116 4	0	100	0 024251	0 087890	8 669626	0 001792	Extrapolation Point

Table 3.1 (continued)

3812.15	<--Average Speed for Data below								
	−50	−32 5	29 9	0	0 006011	0 001173	0 035823	0 000476	Extrapolation Point, Use zero torque entry.
	0	0 0	29 9	0	0 006011	0 001173	0 035823	0.000476	Extrapolation Point; fuel rate extrapolated, emissions scaled by fuel rate
3844	44 6	29 0	16.1	20 1	0 003020	0 001760	0 053757	0 000714	Original Data In Final Map
3835	93 1	60 5	10 9	28 1	0 012287	0 003708	0 058764	0 003636	Original Data In Final Map
3853	142.4	92 6	5 4	41.1	0.016006	0 001550	0.008150	0.075068	Original Data In Final Map
3716	153 0	99 5	4 3	63 5	0 018680	0 013577	1.037994	0 065016	Original Data In Final Map
	179	116 4	0	100	0 027902	0 070000	8.500000	0.010000	Extrapolation Point Based on Neighboring Speed Data
3982	171 0	111.2	1 9	51.1	0 024760	0 070236	5 299946	0 010832	Excluded Data – Out of RPM Range
4182.22	<--Average Speed for Data below								
	−50	−32 5	29 9	0	0 006500	0 001294	0 036402	0 001243	Extrapolation Point; Use zero torque entry.
	0	0 0	29 9	0	0 006500	0 001294	0 036402	0.001243	Extrapolation; fuel from neighboring speeds; fuel−scaled emissions
4159	44 2	28.7	16 4	20 2	0 009441	0 001880	0 052875	0 001806	Original Data In Final Map
4182	56 1	36 5	14 8	23 0	0 010492	0 001085	0 042622	0 000607	Original Data In Final Map
	80	52 0	12 5	27 1	0.015356	0 002000	0.100000	0.003600	Interpolation point to localize CO/HC emissions rise
4190	96 9	63 0	10 8	30 0	0 018794	0 075311	6 028088	0.005716	Original Data In Final Map
4198	145 0	94 3	5.4	43 2	0 025795	0 099146	8.873959	0.005692	Original Data In Final Map
	179	116 4	0	100	0 030611	0 099146	8.873959	0.005692	Extrapolation: fuel/torque from previous speed; last−torque emissions
4508.75	<--Average Speed for Data below								
	−50	−32 5	29 9	0	0 007036	0 001241	0 030116	0.000834	Extrapolation Point; Use zero torque entry.
	0	0 0	29.9	0	0 007036	0 001241	0.030116	0 000834	Extrapolation Point, fuel rate extrapolated; emissions scaled by fuel rate
4520	38.7	25 2	16 3	21 7	0 009968	0 001758	0 042665	0 001181	Original Data In Final Map
4505	53 1	34 5	14 8	24 2	0 011055	0 002115	0 054925	0 001902	Original Data In Final Map
4506	89 3	58.1	10.8	31.5	0 015038	0 010494	0 654554	0 010692	Original Data In Final Map
	100	65.0	9 5	34 8	0 018042	0 070000	8.000000	0.005000	Interpolation point to localize CO/HC emissions rise
4504	134.4	87.4	5 4	45.7	0.027718	0 088631	9.765052	0.004418	Original Data In Final Map
	179	116.4	0	100	0.034665	0.088631	9.765052	0.004418	Extrapolation: fuel/torque from previous speed, last−torque emissions

The preliminary protocol recommended making estimates by all the various methods and to use "engineering judgement" to determine the best values of the fuel and emissions rates at each engine speed. Further examination of the various methods led to the development of the procedure outlined below. This procedure works in all cases studied and is capable of automation by a Lotus 1-2-3 macro for the data on the spreadsheets provided by EPA.

The first step was to use the scaling equation for emissions. This was done because extrapolation could lead to negative emissions rates whereas the scaling procedure would not. This provided a straightforward procedure for determining emissions rates with an understanding of its limitations. *I.e.* this procedure rests on the assumption that the pollutant species mass fraction and the air/fuel ratio are essentially constant over the region that this scaling is being done.

This reduces the problem of determining emissions and fuel flow at zero and negative torque to the single problem of finding, for each engine speed, the fuel flow at zero torque, $m_{fuel}(N,T=0)$. The two possible values considered are the value found by extrapolation from the two lowest torque points and the values found by scaling the fuel rate by the engine speed. For convenience these are called the "extrapolated" and "scaled" value in the discussion below. The exact definition of these values are:

$$m_{fuel,extrap}(N, T=0) = m_{fuel}(N, T_1) - T_1 \frac{m_{fuel}(N, T_2) - m_{fuel}(N, T_1)}{T_2 - T_1} \qquad [3.1]$$

$$m_{fuel,scaled}(N, T=0) = m_{fuel,idle} \frac{N}{N_{idle}} \qquad [3.2]$$

The automated procedure for doing this uses the following set of decision rules.

I. Determine the "best" value of the zero-torque fuel rate at each engine speed as follows:

   1. If the extrapolated value is positive and the scaled value is less than the value at the lowest torque point use the average of the extrapolated and scaled value.

   2. If the first condition is not satisfied and if the extrapolated value is positive, use the extrapolated value.

   3. If the first two conditions are not satisfied and if the scaled zero-torque fuel rate at the given engine speed is less than the fuel rate at the first load point, use the scaled value.

4. If none of the first three conditions are satisfied set the zero-torque fuel rate to 90% of the value at the lowest load point.*

II. Once the best value at each speed has been determined based on data for that engine speed alone, adjust the zero-torque values to ensure that the fuel rate increases as engine speed increases according to the procedure below. Start with the first engine speed above idle. Assume that the idle fuel rate is correct unless there is some indication that there is an error in this value. Repeat this process for each engine speed.

1. If the zero-torque fuel rate at a given engine speed is greater than the value at the next lower engine speed, accept the given value for fuel rate.

2. If the first condition is not satisfied adjust the zero-torque fuel rate at this engine speed as follows:

   a. If this is the last speed point compute the zero-torque fuel rate at this speed as the engine speed ratio (N_{last}/N_{last-1}) times the zero-torque fuel rate at the previous engine speed.

   b. If this is not the last speed point compute the average of the zero-torque fuel rate at the previous engine speed and the next highest engine speed. If this is greater than the zero-torque fuel rate at the previous engine speed use this average value.

   c. If conditions a and b are not true compute the zero-torque fuel rate at this speed as the engine speed ratio ($N_{current}/N_{previous}$) times the zero-torque fuel rate at the previous engine speed.

III. Steps I and II will provide zero-torque fuel rates at each engine speed that are positive, lower than the value at the first load point, and increasing with engine speed. The final behavior may be irregular, however. Use the values determined in steps I and II as the input to a regression analysis. Since engine friction power depends on engine speed as a cubic function, the starting point for the regression analysis should be a cubic equation with a zero intercept.

IV. Step III will usually produce the desired final result. Some further judgement may be used to fine-tune the final results. In particular, the regression analysis may produce a zero-torque fuel rate that is greater than the fuel rate at the first load point. Such values should be adjusted downward. This is usually done by replacing only the zero-torque fuel rates which are physically unrealistic by the values obtained from step II for the given

---

* The 90% number is arbitrary. Any other value (e.g. 80% or 95%) might be used.

engine speed. For some vehicles the extrapolated fuel rate at a given engine speed was very high. Under the "bootstrap" approach of step II such values would triger increases in the fuel rates at all higher engine speeds. These increased zero-troque fuel values could exceed those of the first torque point. In such cases it was necessary to reasign the best value for that engine speed (i.e. to return to step II) and redo the analysis. It is also possible to try to redo the regression analysis using a linear or quadratic fit with or without an intercept.

The decision rules outlined above in steps I to III have be automated in a Lotus 1-2-3 macro which constructs the zero and negative torque values for fuel rate and emissions from the most recent spread sheets supplied to Sierra by EPA. The results are displayed graphically to help the fine-tuning in step IV. This macro has not been used by anyone except its author and has only minimal documentation. It can be delivered to EPA with the understanding that it is somewhat less than a beta version of software.

Analysis of Improved Methods for Interpolating Sharp Emissions Changes

This additional study started from the preise that the major sharp changes in emissions are the increases in HC and CO emissions associated with enrichment of the fuel/air mixture. Improvements to the preliminary protocol must find ways to model this process.

Fuel enrichment is done mainly to increase engine power when the maximum engine flow is present at a given engine speed. By definition of the overall efficiency, η, the engine power can be expressed as follows:

$$P_{engine} = m_{air} \, (F/A) \, \eta \qquad [3.3]$$

As engine speed starts to increase the air flow increases, the fuel/air ratio remains constant and the efficiency increases due to reduced throttling losses. Near wide open throttle, when the air flow is near a maximum, the engine power can be increased by increasing the fuel/air ratio. Although this will decrease the efficiency, small increases in fuel/air ratio will increase the $(F/A)\eta$ product increasing the power output of the engine. Enrichment is also used to provide lower temperature operation at high loads. The actual enrichment pattern is dependent on the design decision about the need for such enrichment at various operations loads.

As a simplified approach assume that enrichment behavior is governed only by the only need to provide additional power when air flow is near a maximum and further assume that some characteristic air flow variable at which enrichment begins and/or ends can be determined. This approach starts with an examination of some model of enrichment behavior to determine an appropriate variable then examined the mapping data to see if such an approach would be fruitful.

The relation of the air flow rate to other engine variables is discussed in Chapter 4. Rearrangement of equation [4.4], gives the air flow rate as follows, where η_v is the volumetric efficiency.

$$m_{air} = \eta_v V_d N p_{in} / 2 R_{air} t_{in} \quad [3.4]$$

Equation [4.27] gives an empirical correlation of volumetric efficiency with the ratio of intake to exhaust pressures as,

$$\eta_v = C_1 - C_2 p_{ex} / p_{in} \quad [3.5]$$

In general, C_1 and C_2 may depend on engine speed. However, for an ideal cycle these constants are independent of engine speed and their speed dependence may be neglected for this analysis. Combining these two equations gives

$$m_{air} = V_d N C_1 p_{ex} / 2 R_{air} t_{in} - V_d N C_2 p_{in} / 2 R_{air} t_{in} \quad [3.6]$$

Assuming the dependence of inlet temperature, t_{in}, and exhaust pressure, p_{ex}, on engine speed can be neglected in this simple analysis. Dividing equation [3.6] by the engine speed gives the following result.

$$m_{air}/N = C_3 - C_4 p_{in} \quad [3.7]$$

where

$$C_3 = V_d C_1 / 2 R_{air} t_{in} \quad \text{and} \quad C_4 = V_d C_2 / 2 R_{air} t_{in} \quad [3.8]$$

Equation [3.8] suggested the following approach:

- Examine the mapping data to determine regions where enrichment can be well defined; call the air flow and manifold inlet pressure at this point $m_{air,enrich}$ and $p_{in,enrich}$, respectively.
- Find the air flow rates at these points from the mapping data on fuel flow rates and air/fuel ratio and compute $m_{air,enrich}/N$.
- See if any correlation exists between the value of $m_{air,enrich}/N$ for enrichment and the measured inlet manifold vacuum or pressure, p_{in}.
- Use this correlation to determine the enrichment points for engine speeds where this point is not clearly defined.
- Determine a relationship between emissions concentration and other characteristics of the enrichment point. Air/fuel ratio should be the main variable governing these concentrations for HC and CO. (For example it may be possible to find a relationship between pollutant mass fraction and air/fuel ratio.)
- Use the relation bewteen emissions concentration and engine variables to determine the emissions at the interpolated enrichment point. (For example if pollutant mass fraction were known as a function of air/fuel ratio, the correlated mass fraction could be scaled by the exhaust flow rate to get the mass emissions of the pollutant at the interpolation point.)

This was tried for three engines, particularly the Geo metro, for which a large data set is available. Two approaches were utilized. The first approach tried to develop a correlation for lean points just before enrichment and the first "rich" point to develop two correlation equations—one for the start, the other for the end of enrichment. This was not successful. The second approach defined the the enrichment point was arbitrarily defined as a boundary air/fuel ratio.

Various values were tried for this boundary air/fuel ratio. The most successful correlation was obtained by using linear interpolation, in each speed range where enrichment occurred, to find the values of fuel flow and intake vacuum for an air/fuel ratio of 13.5. The linear regression of $m_{air,enrch}/N$ with manifold vacuum for the three engines studied is shown in Figure 3.1. For two of the three engines there was a good correlation matching the predictions of equation [3.7]. the air flow per revolution, $m_{air,enrch}/N$ at a 13.5:1 air/fuel ratio, and intake vacuum at the same air/fuel ratio, it was not possible to develop a relation to determine how each of these quantities varied across speed ranges. Figure 3.2 shows that both of these variables generally increase with engine speed, but not in a predictable fashion.

Furthermore an examination of the pollutant mass fractions as a function of air/fuel ratio for these three engines did not show a good correlations. Figures 3.3 to 3.5 show that there is a reasonable correlation for CO, less of a correlation for HC and no correlation for NOx. These figures indicate that a simple process in which one interpolates to a certain air/fuel ratio to determine the enricument transition point should be possible for CO, may be done with some error for HC and cannot be done for NOx. However, the values of NOx in rich regions are low so that direct linear interpolation of the mapping data could be used.

Tentative Proposal for Interpolation of Enrichment Point

The results of the previous section are not conclusive and require additional confrimatory work. However, based on the results obtained so far the following procedure may be used to determine the enrichment point.

1. Use all data for the engine to deterine the best fit between HC and CO concentrations (mass fractions are the perferred approach, but parts per million can be used) and air/fuel ratio.

2. Determine the value of the air/fuel ratio for engine speeds where the enrichment transition is considered to be well defined.

3. Use the correlation found in step 1 to find the HC and CO mass fractions at this air fuel ratio.

4. For engine speeds where the transition is not well defined use linear interpolation in air/fuel ratios to determine the engine load and fuel flow rate at which the air/fuel ratio determined in step 2 occurs.

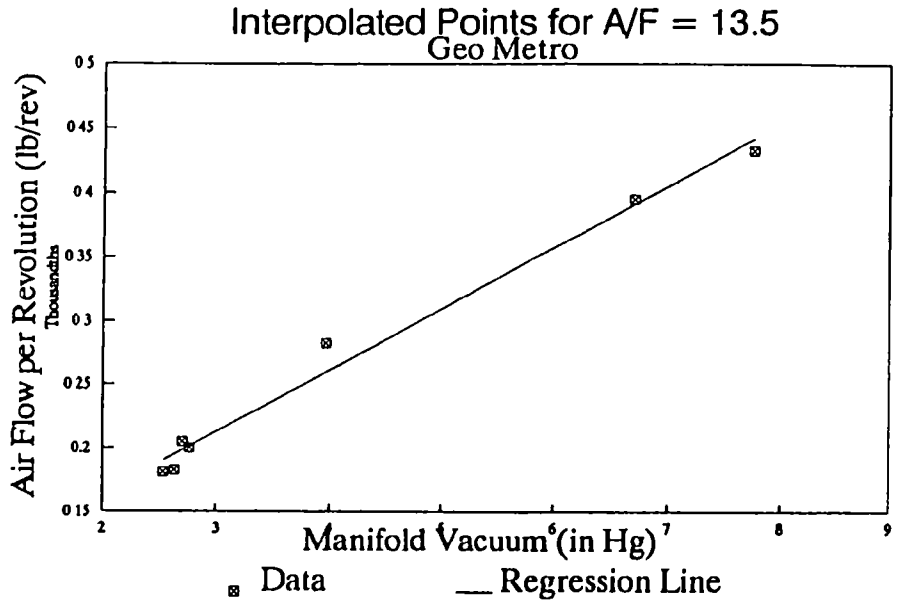

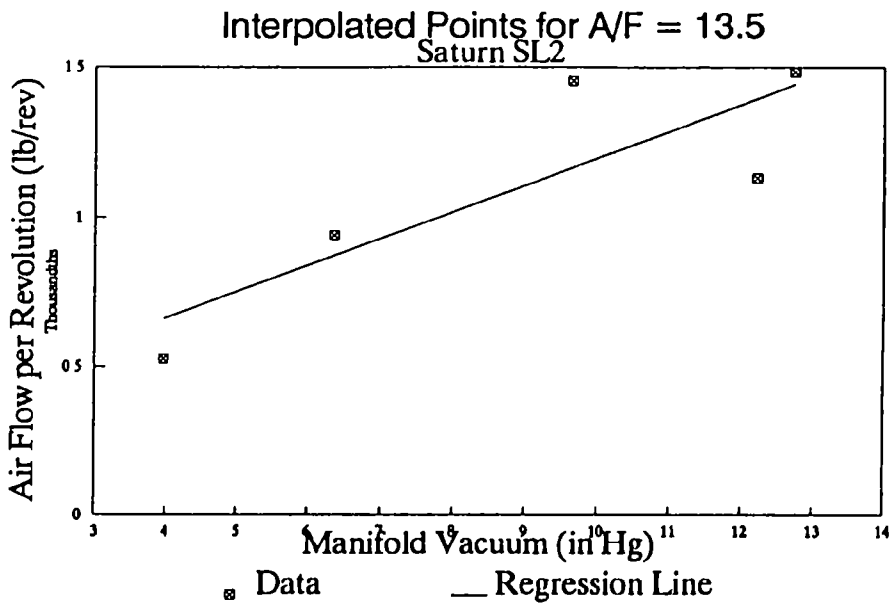

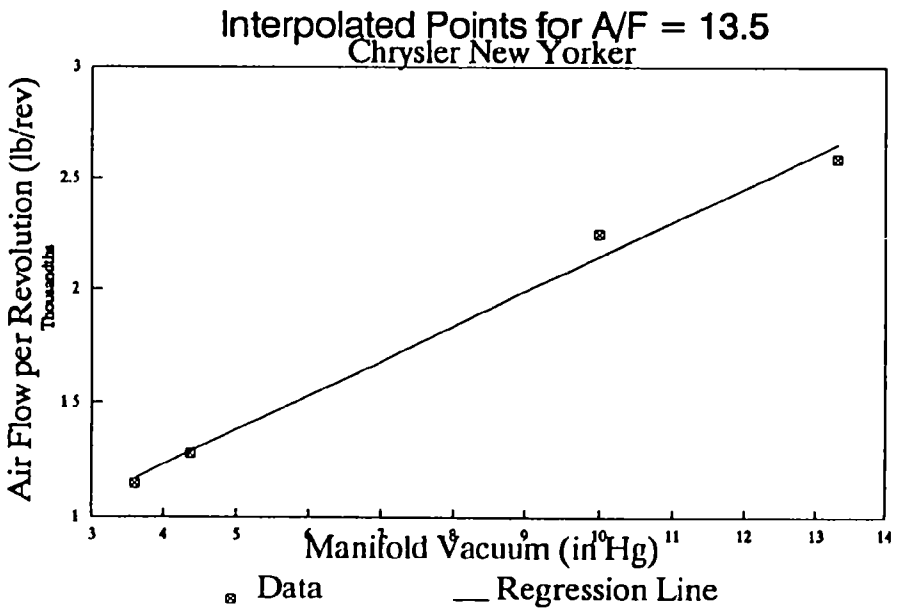

Figure 3.1

Correlation of Air Flow Per Revolution
With Manifold Vacuum at Interpolated Point of
13.5:1 Air/Fuel Ratio

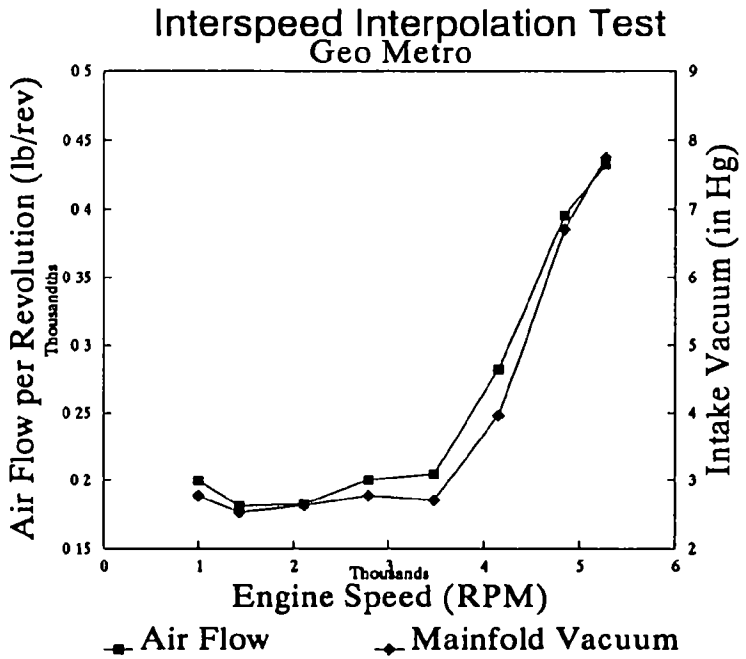

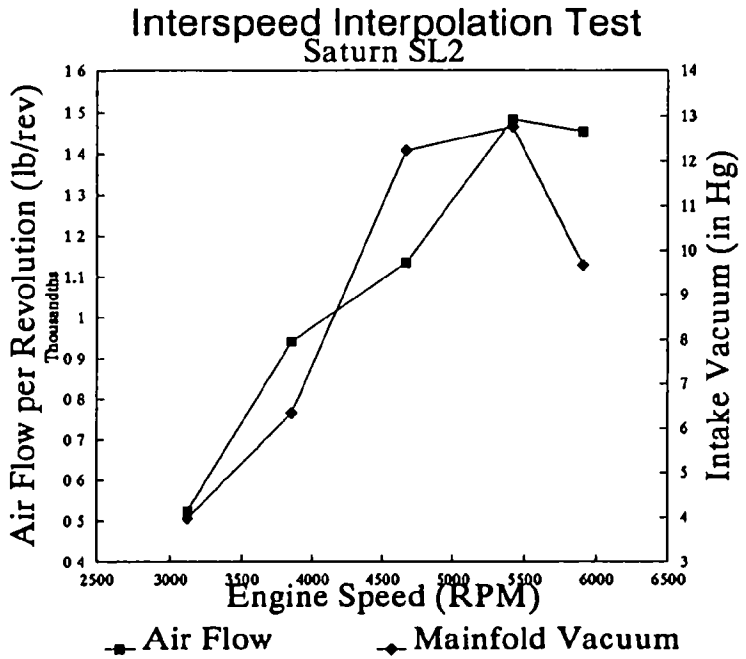

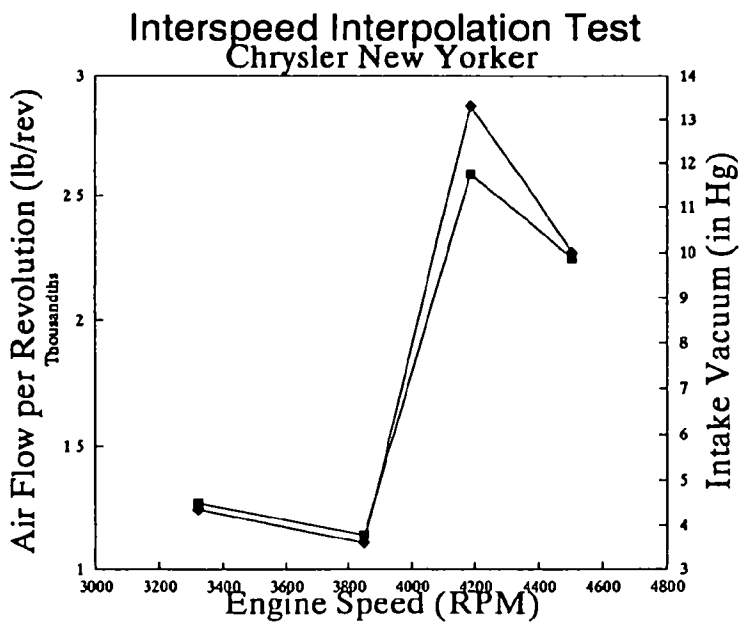

Figure 3.2

Variation in Air Flow Per Revolution and Manifold Vacuum at Interpolated Point with 13.5:1 Air/Fuel Ratio

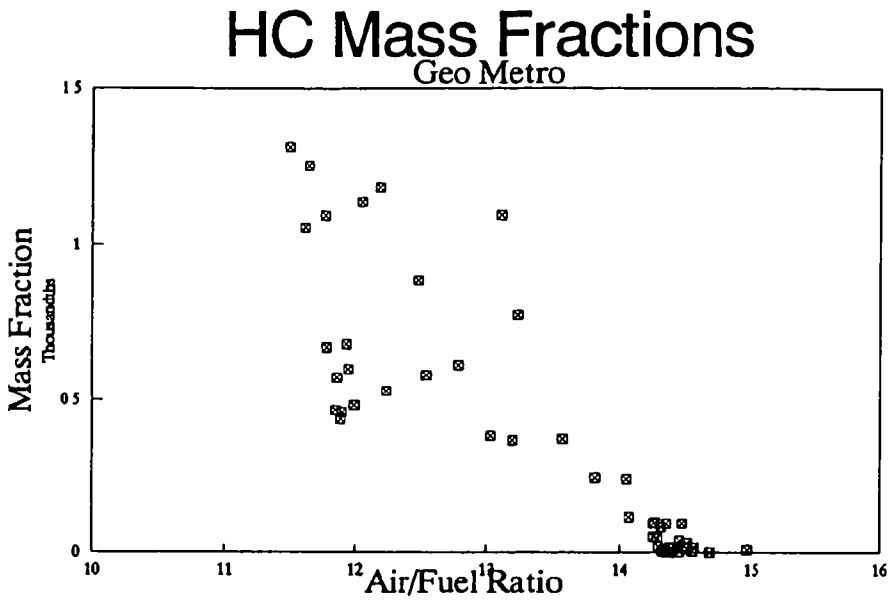

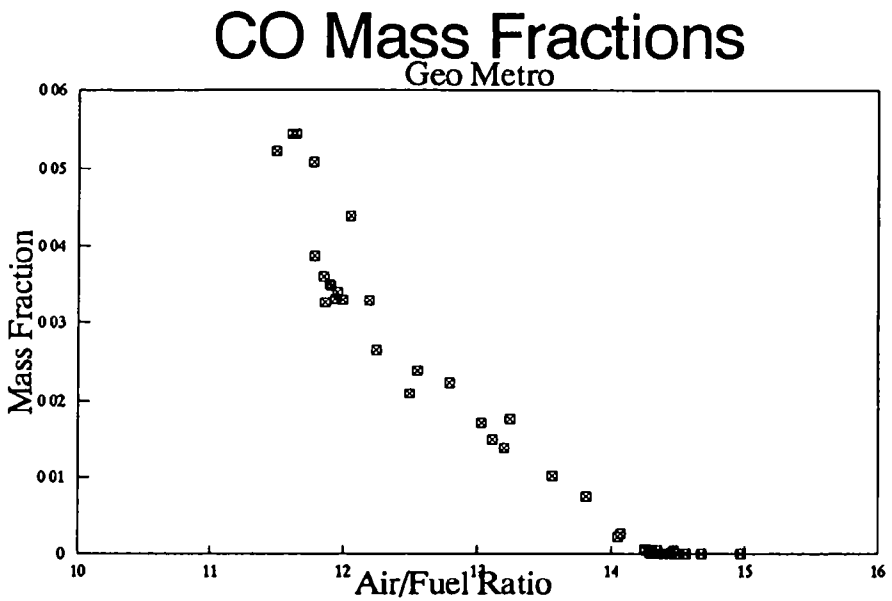

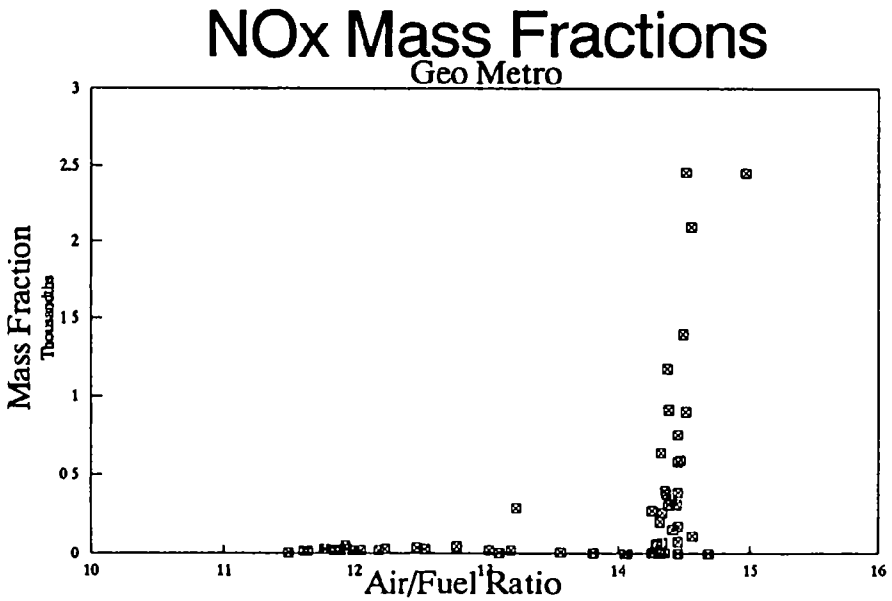

Figure 3.3

Pollutant Mass Fractions as a
Function of Air/Fuel Ratio for Geo Metro

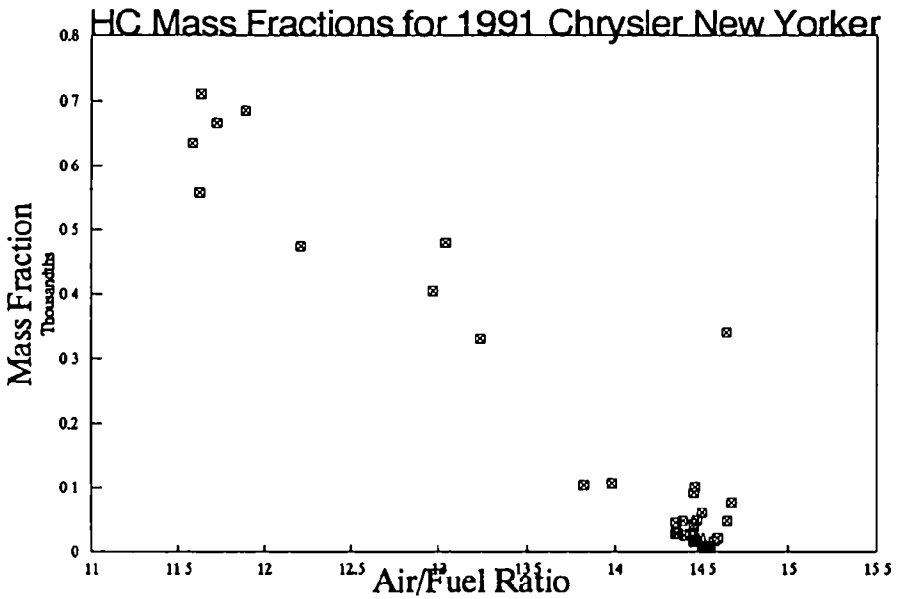

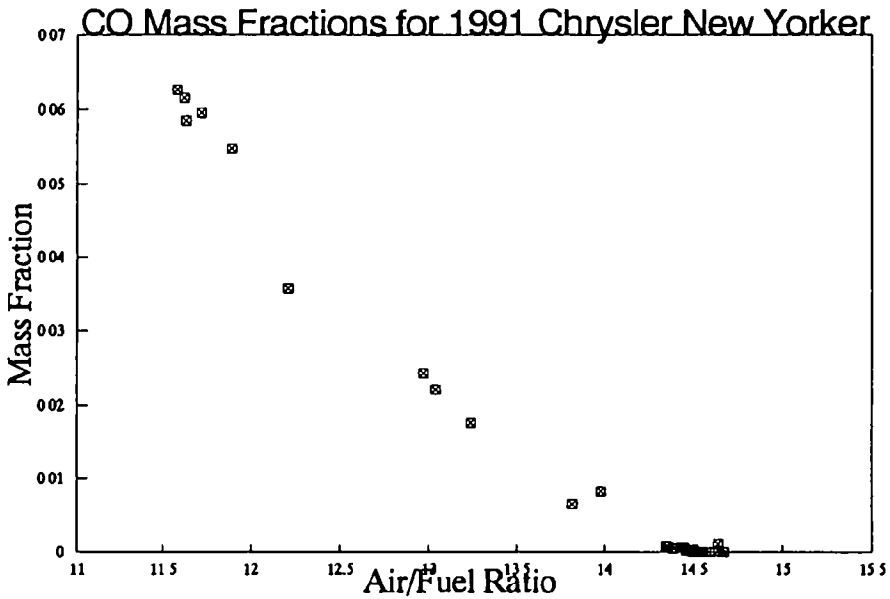

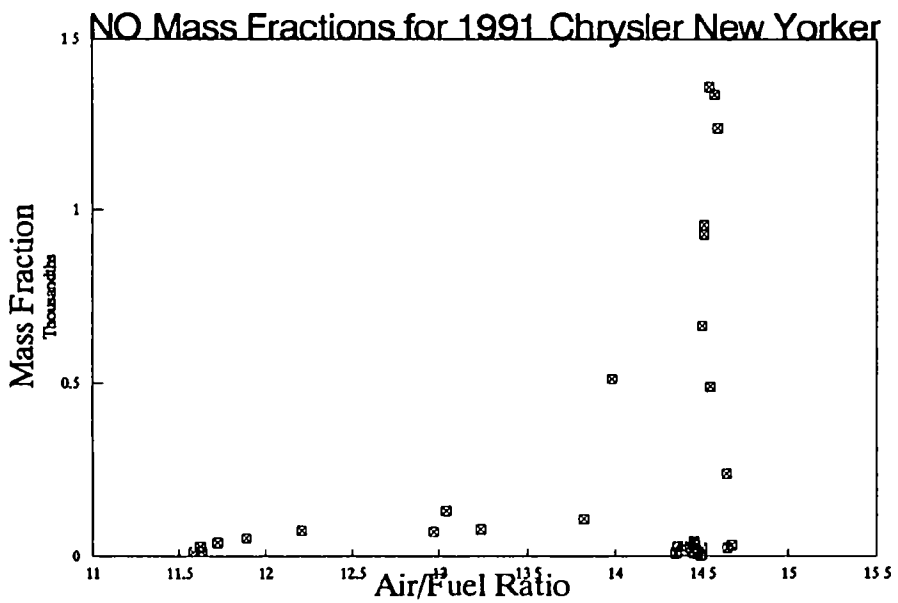

Figure 3.4

Pollutant Mass Fractions as a
Function of Air/Fuel Ratio for Chrysler New Yorker

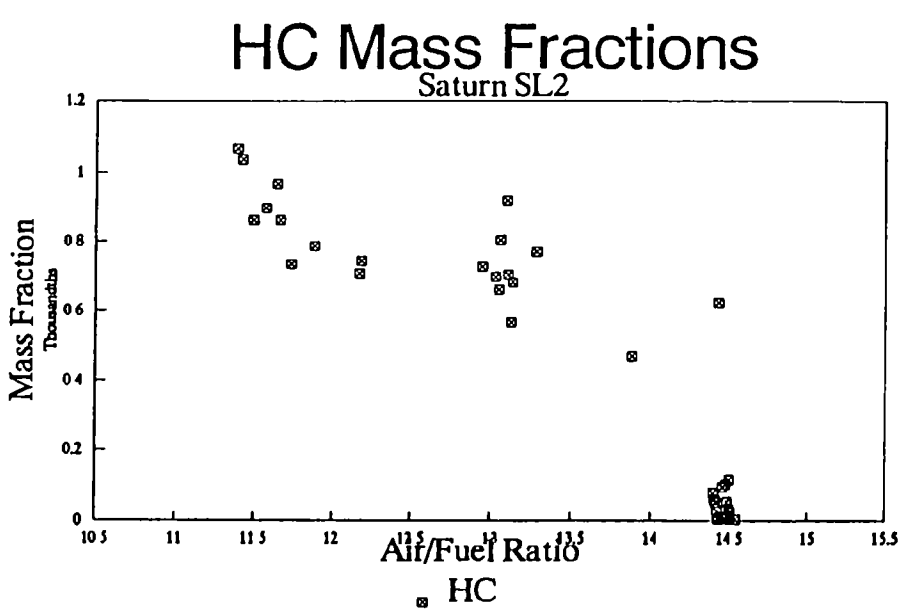

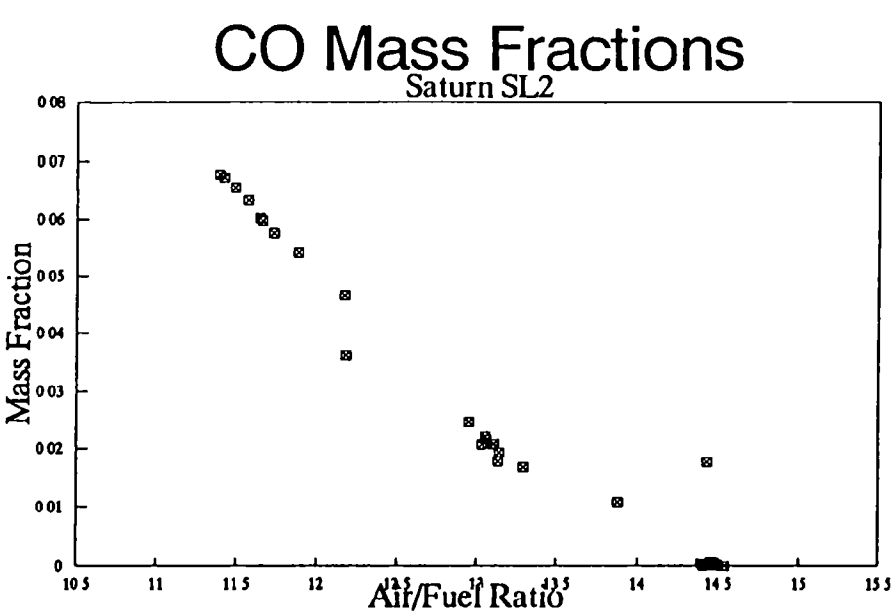

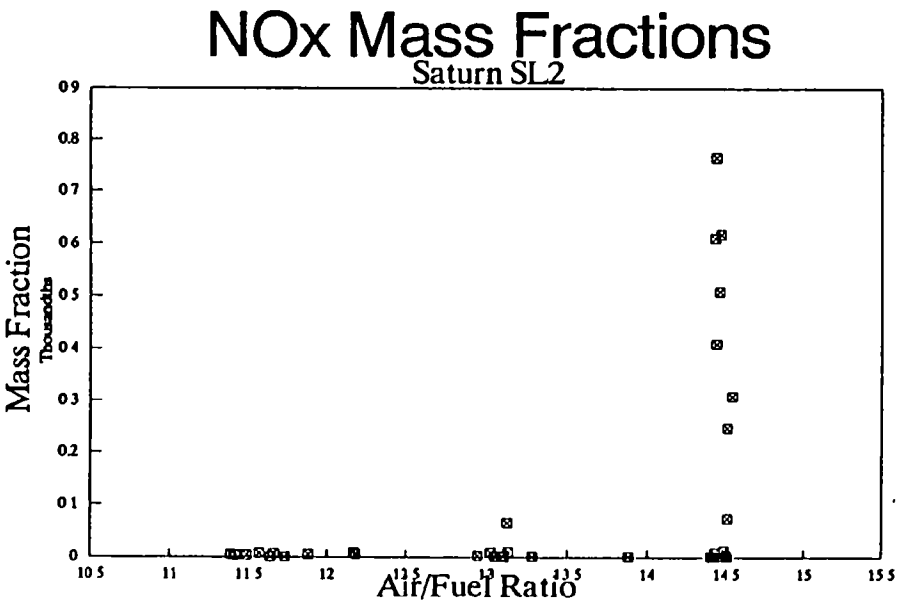

Figure 3.5

Pollutant Mass Fractions as a
Function of Air/Fuel Ratio for Saturn SL2

Although there was a reasonably successful correlation between

5. Create an interpolated point using the air/fuel ratio found in step 2, and the fuel flow rate found in step 4. Compute the mass rates of CO and HC at this point as m_{fuel} (1 + A/F) w_i, where w_i is the mass fraction of CO or HC found in step 3.

6. Use linear interpolation to find the NOx mass rate at the interpolation point.

7. Check the resulting pollutant emission rates to see that they are not out of line with neighboring points.

This procedure may be regarded as a formal way to implement the interpolation suggested in the perliminary procedure. More extensive study of this approach should be done to determine the limits of its applicability. For example, the use of all engine data to obtain the relation between air/fuel ratio and HC and CO emissions may be replaced by an examination of neighboring speed ranges only, if sufficient data are available.

Conclusions on Mapping Protocol

A preliminary protocol for determining a complete engine map from the data obtained by EPA in their engine mapping studies has been proposed.

The two main problems addressed are the determination of fuel and emissions rates at zero and negative torques and the refinement of the location of sharp increases in emissions.

Further study led to an improved procedure, which could be automated, for the determination of the emissions and fuel rates at zero and negative torques.

Further investigation of the sharp emissions change led to a tentative proposal for better defining this change.

4. CORRELATION BETWEEN INLET MANIFOLD PRESSURE AND BRAKE-MEAN EFFECTIVE PRESSURE

Introduction

This task involved two different subtasks. One was an examination of the (revised) engine mapping data obtained by EPA to determine the empirical relationships between brake mean effective pressure (BMEP) and intake manifold vacuum for these data; the other was an analytical study of the basic relationship between these two variables. Although each of these tasks is discussed separately below, these subtasks were done in parallel and the fairly consistent observation of a linear relationship between these variables motivated the analytical work to determine the fundamental basis for this empirical observation.

Examination of Engine Mapping Data

The data analysis for this task was done on the revised set of engine mapping data provided to Sierra by EPA. The operations on this revised engine mapping data are described below, followed by a discussion of the results of the analysis.

Analysis Procedures for Revised Data - The first step was to obtain a correspondence between the initial mapping data and the revised data set. The initial mapping data were provided to Sierra as a three-layer Lotus 1-2-3 spreadsheet. The revised data were a modified version of the third sheet of the original data set. Although this had the same format as the original data set, there was not a direct correspondence between the rows of the original and revised data sets because points had been removed or added in generating the revised data set.

The engine torques used in the EPA mapping data were found from measurements of dynamometer torque and calculations of the equivalent load on the engine. This was done by using a calculation procedure similar to the one used in the VEHSIM vehicle simulation program. In some cases where load measurement problems occurred, such as during excessive tire slip on the dynamometer, the torque was estimated by linear interpolation or extrapolation of BMEP and manifold pressure data. Part of EPA's interest in this task was to have Sierra determine the validity of this interpolation/extrapolation for the mapping data.

In order to do this, we generated a data set which included only points for which the torque was found by measurement (and appropriate calculation of the engine torque equivalent to the measured dynamometer

torque.) The following tasks were done by a series of Lotus macros and a spreadsheet template.

1. Copy the final three columns of the torque calculations from the initial engine mapping spreadsheet to allow a comparison between old and new data sets.

2. Copy the air/fuel ratio from the old data set to the revised data spreadsheet for use in subsequent calculations.

3. Compute the volumetric efficiencies for the engine mapping data to observe the behavior of this quantity which was shown to play a role in the relationship between BMEP and manifold pressure.

4. Create a series of named ranges for use in generating graphs and linear regression calculations of BMEP and manifold pressure.

5. Generate graphs, linear regression coefficients, and output for BMEP and manifold pressure at each engine speed.

The torque columns on the original data set were used to determine the data points for which the torque values were actually obtained from dynamometer measurements and VEHSIM-like calculations. The previous torque data had three final columns that showed the torque determined from the dynamometer measurements and the VEHSIM-like calculations, notations if any problems were observed with the measurements, and the value of torque actually used for the final results. Data points for which EPA's calculated torque value were not the same as the one used in EPA's final results were ignored in our analysis of the relation between BMEP and manifold pressure. These data points were already established by assuming a linear relationship between BMEP and manifold pressure and their use in any analysis of the relationship between these two variables would bias the analysis.

The air/fuel ratio was copied from the original data set so that the mass fraction of the exhaust emissions could be computed for our presentation of emissions data in the final report. It was also used to compute the volumetric efficiency as discussed in the next paragraph. After copying the air/fuel ratios and the final torque columns from the initial data set to the revised data set, it was necessary to edit these data to obtain the correct values for the revised data set.

The analysis in the next section shows that the volumetric efficiency is a key parameter in the relationship between manifold inlet pressure, P_{in}, and BMEP. Equation [4.7] provides the relationship between these variables as:

$$BMEP = \eta_v \, (F/A) \, P_{in} \, / \, (BSFC) \, R_{air} \, T_{in}$$

where η_v is the volumetric efficiency, F/A is the fuel/air ratio, BSFC is the brake specific fuel consumption, R_{air} is the gas constant for air and T_{in} is the inlet manifold temperature. This equation was rearranged as follows to compute the volumetric efficiency from the mapping data.

$$\eta_v = BMEP \, (A/F) \, BSFC \, R_{air} \, T_{in} \, / \, P_{in}$$

All data in this equation, except for the inlet manifold temperature, are available in the mapping data. The inlet manifold temperature was assumed to be 500 R for computing the volumetric efficiency. The volumetric efficiency increased with manifold pressure as expected. The only concern was that some data points have a volumetric efficiency greater than 100%. This might have been due to the assumption of a constant value of 500 R for the manifold inlet temperature. Although the computed engine torque is used to determine the BMEP and BSFC, it cancels when these two quantities are multiplied. Thus, any errors in the engine torque measurement/calculations would not affect this calculation. There may have been some errors in the other experimental quantities that are used to find the terms in this equation (fuel rate, air/fuel ratio, manifold inlet pressure, inlet speed). Absent such errors, the volumetric efficiencies that were greater than 100% would presumably be caused by the supercharging effect of pressure waves in the intake manifold runners.

The final set of BMEP and inlet manifold pressure used for this analysis was set up as named ranges in the spreadsheet. These named ranges were then used in plots and regression analyses of the data. This process retained all the data on the spreadsheet while using the appropriate subset for the analysis here.

Experimental Variation of BMEP with Inlet Manifold Pressure - A linear regression analysis of BMEP versus manifold pressure, at a given engine speed, was done for all engine mapping data. The full regression procedure, including the computation of the standard error, requires at least three data points for the regression. The data were fitted to the following equation:

$$BMEP = a + b\ p_m$$

The results for each vehicle and each engine speed are presented in the tables attached to this memo. The values in the tables include the number of data points available at the particular engine speed, the slope, b, and the intercept a. In addition, the standard error of the estimated BMEP values, $\sigma_{y|x}$, and the R^2, the square of the correlation coefficient, are listed. The values for R^2 show an almost perfect correlation for most of the engine speeds as summarized in the table below:

Total Number of Speed Correlations	214
Speed Correlations with $R^2 > .980$	182
Speed Correlations with $R^2 > .950$	207
Speed Correlations with $R^2 > .900$	212

The standard error for the predicted BMEP is correspondingly small. In only ten cases is this standard error greater than 7.0 psi. Two typical plots of experimental data points and the corresponding least squares line are shown in Figure 4.1. The data at 3200 RPM have an R^2 value of 0.9987 and a standard error of 1.3 psi in BMEP. This is an example of the best linear agreement. The data at 4060 RPM have an R^2 value of 0.95 and a standard error of 7.2 psi in BMEP. This is an example of the poorer agreement in some correlations.

Figure 4.1

Example of Linear Regression Fits

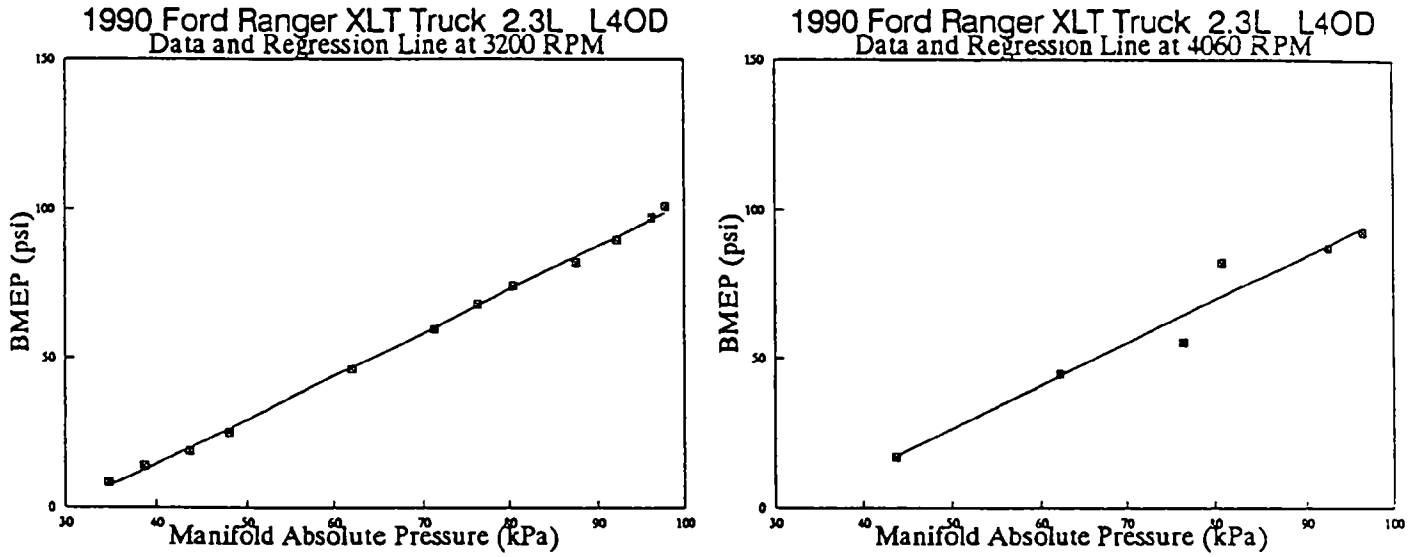

Although the observed correlations are very good, there is a need for caution in using data for extrapolation. Data for the Chrysler New Yorker at two different engine speeds were fitted using the full data set and a partial data set. The fitted line for the partial data set was then extrapolated to higher manifold pressures and the predicted results were compared to the experimental ones. These results, shown graphically in Figure 4.2, are an example of potential problems that can arise in extrapolation.

The regression lines for the full data set at the two engine speeds shown on these charts are as follows:

RPM = 2222 R^2 = 0.97 $\sigma_{y|x}$ = 8.8 psi N = 4

RPM = 3320 R^2 = 0.98 $\sigma_{y|x}$ = 6.4 psi N = 10

The partial fits, using the lower manifold pressure points only, have the following regression statistics.

RPM = 2222 R^2 = 0.99 $\sigma_{y|x}$ = 4.3 psi N = 3

RPM = 3320 R^2 = 0.98 $\sigma_{y|x}$ = 3.7 psi N = 6

Figure 4.2

Example of Extrapolation Error

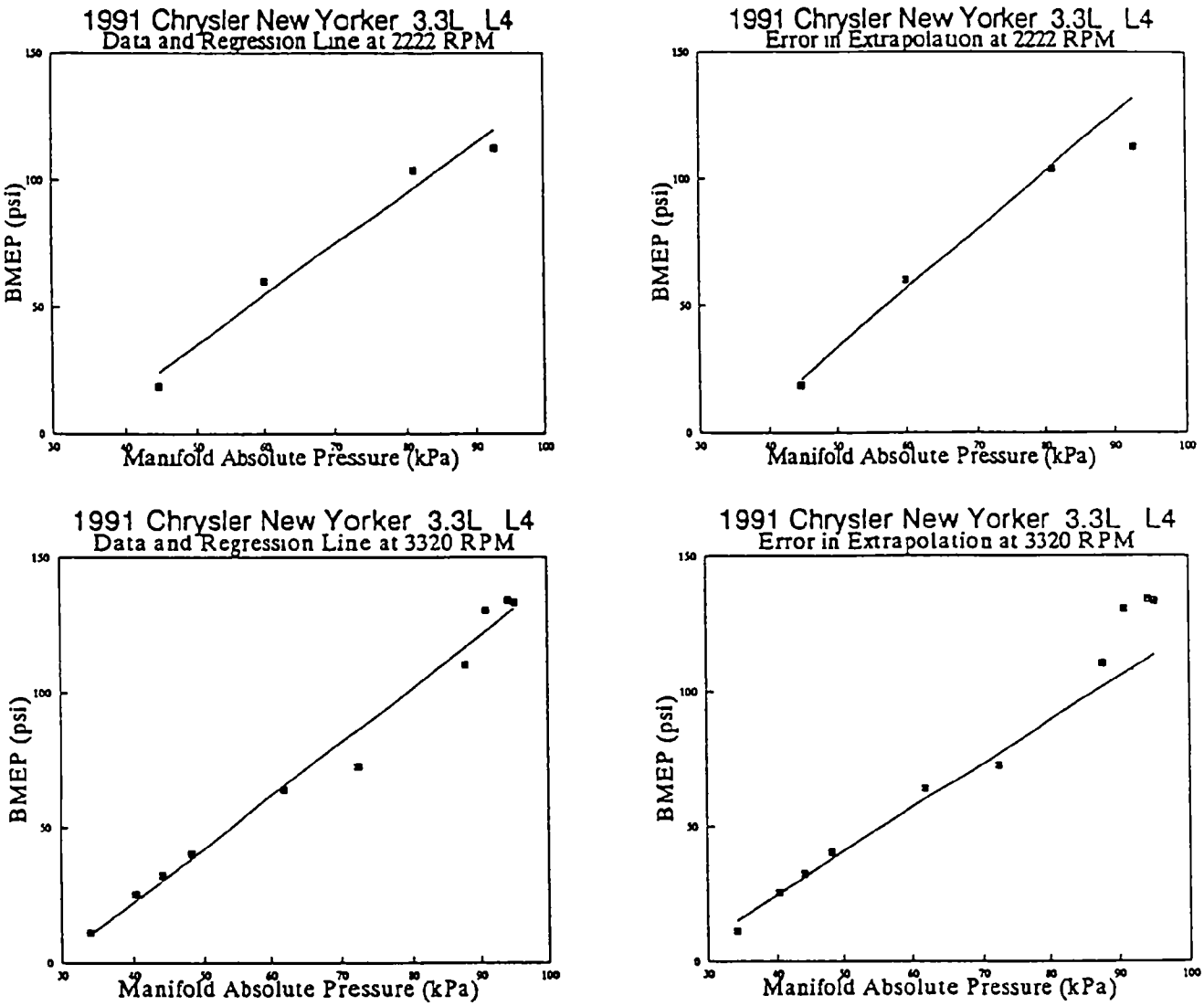

When the regression lines formed from a partial set of data at lower engine loads are extrapolated to find the BMEP values at high manifold pressures, the following errors occur: (1) at 2222 RPM, the BMEP is overpredicted by 15%; (2) at 3320 RPM, the four extrapolated points are underpredicted by 8%, 18%, 16%, and 15% as manifold pressure increases. The lines fitted to the partial data sets have a smaller standard error than those fitted to the complete data sets. The direction of the error is not consistent—the BMEP is overpredicted at one engine speed, underpredicted at another.

A review of the data for the empirical correlations of BMEP with manifold pressure shows a remarkable consistency. For almost all the engines and all engine speeds, the slope lies between 1.3 and 2.2 psi/kPa and the intercept lies between -20 and -80 psi. This range of values is consistent with the theoretical analysis in the next section

and the order of magnitude values computed there of 1.9 kPa/psi and -33 psi for the slope and intercept, respectively. Some exceptions to these observed ranges are noted below.

- The Volvo 740 at 2000 RPM has the poorest correlation (R^2 = 0.497) and standard error (23.4 psi). This is probably due to a bad data point that has a decrease in BMEP at the highest inlet manifold pressure.

- The Ford Escort at 4700 RPM, with only three data points, has a small slope.

- The Ford F250 has generally smaller slopes for all speed ranges. This truck has a 5.8 liter engine, the largest displacement in all of the engines tested.

- The Ford Ranger at 1630 RPM has a small slope. This line has only three data points.

- The GMC Sierra pickup, with a 5.0 liter displacement, has a small slope at all engine speeds.

- The Saab 9000 has slopes similar to other engines at the first four engine speeds, but the slopes are much higher at the five highest engine speeds.

EPA certification data for the four European cars (Saab, Volkswagen, Volvo and Mercedes) were reviewed to determine that only the Mercedes had exhaust gas recycle (EGR). EGR would be expected to increase the manifold pressure required per psi of BMEP; howeer, no difference in the relationship of BMEP to manifold pressure that could be attributed to EGR was observed for these vehicles.

Plots of all the data of BMEP versus inlet manifold pressure are included in Appendix B.

Analysis of The Theoretical Relationship Between BMEP and Intake Manifold Pressure

The starting point for this analysis was the use of the volumetric efficiency of the engine which can be related to the inlet manifold pressure, p_{in}. (For this study, the absolute pressure is a more convenient variable than the manifold vacuum.) The volumetric efficiency can be defined as follows:[29]

$$\eta_v = 2\, \dot{m}_{air} / \rho_{air,in}\, V_d\, N \qquad [4.1]$$

where

η_v = Volumetric Efficiency

$\dot{m}_{air}$ = Mass flow rate of air into the engine

$\rho_{air,in}$ = Density of air in the intake manifold

V_d = Displacement volume

N = Engine speed

This definition of volumetric efficiency, which uses the air density in the intake manifold, is a measure of the pumping performance of the inlet port and valve only. It is also possible to define the volumetric efficiency in terms of the intake (ambient) air density; in this case, the volumetric efficiency measures the efficiency of the entire intake system, including elements of the system (e.g., mass air flow sensor and air cleaner) that are upstream of the manifold.[30] The air density can be related to the pressure through the ideal gas law:

$$\rho_{air,in} = p_{air,in} / R_{air}\ t_{in} \qquad [4.2]$$

where

$p_{air,in}$ = Partial pressure of air in the intake manifold

R_{air} = Gas constant for air

t_{in} = Intake manifold temperature

Ignoring EGR, the mole fraction of air in the intake manifold is nearly one for typical gasolines and we can assume that the partial pressure of air in the intake manifold is essentially the same as the intake manifold pressure, p_{in}:

$$p_{air,in} = p_{in} \qquad [4.3]$$

With this substitution in the ideal gas equation, the volumetric efficiency equation becomes:

$$\eta_v = 2\ m_{air}\ R_{air}\ t_{in} / P_{in}\ V_d\ N \qquad [4.4]$$

The brake mean effective pressure (BMEP) is defined (for a four-stroke engine) as

$$BMEP = 2\ P_{engine} / V_d\ N \qquad [4.5]$$

The engine power, P_{engine}, can be replaced by the brake specific fuel consumption, (BSFC), and the fuel flow rate, m_{fuel}, giving

$$BMEP = 2\ m_{fuel} / (BSFC)\ V_d\ N \qquad [4.6]$$

If this equation is divided by equation [4.4] for volumetric efficiency, the relation between BMEP and intake pressure is obtained:

$$BMEP = \eta_v\ (m_{fuel}/m_{air})\ P_{in} / (BSFC)\ R_{air}\ t_{in} \qquad [4.7]$$

The basic relation between engine load, expressed as BMEP, and intake manifold pressure is thus related via the engine variables of volumetric efficiency, fuel/air ratio, BSFC, and inlet manifold temperature. Over

a range of speeds, the intake manifold temperature—expressed as an absolute temperature—will be essentially constant. Thus, it is the combination, η_v (F/A) / BSFC, that governs the relationship between the BMEP and the intake manifold pressure. The changes in each of these variables, for a given engine speed, is considered further below.

Studies of volumetric efficiency are usually directed at wide open throttle behavior where the air flow rate limits the engine performance. The behavior of volumetric efficiency under throttled conditions can be found, for an ideal cycle, from the equation[31]

$$\eta_v = (\gamma - 1)/\gamma + (r_c - p_{ex}/p_{in}) / \gamma(r_c - 1) \qquad [4.8]$$

where p_{ex} is the exhaust pressure, r_c is the compression ratio, and γ is the specific heat ratio. This ideal equation shows that the volumetric efficiency is one when the exhaust and intake pressures are equal; for throttled operation where p_{in}/p_{ex} is less than one, the volumetric efficiency decreases.

In actual engine operation, the volumetric efficiency depends on engine speed, inlet and exhaust temperatures, as well as the ratio of exhaust to inlet pressure. (It also depends on engine design variables such as compression ratio and valve sizes.) However, the main variable that represents the effect of part-throttle operation on volumetric efficiency is the exhaust/inlet pressure ratio.[32]

The volumetric efficiency will also be affected by the operation of exhaust gas recirculation (EGR). The exhaust gases that are recirculated at a given engine operating condition will reduce the amount of air flow available into the cylinder. However, Servati and De Losh[33] developed a correlation equation for volumetric efficiency for one Ford 4.9 liter engine which gave good agreement between predicted and measured results with no parameters to account for EGR operation. The effect of EGR probably entered their correlation through other parameters such as the intake/exhaust pressure ratio. Their correlation showed a linear dependence on this p_{ex}/p_{in} ratio.

It is also possible to make a slight revision to the above analysis to explicitly consider the effect of EGR on the volumetric efficiency. At wide open throttle operation, where there is no EGR, the only gases in the cylinder result from intake air/fuel and from residual gas. The volumetric efficiency should measure the pumping capacity of the engine for bringing in new cylinder gas. Thus, when EGR is present the definition of volumetric efficiency should be modified to be[34]

$$\eta_v' = 2 (m_{air} + m_{egr}) / \rho_{air,in} V_d N \qquad [4.9]$$

The difference between this equation and equation [4.1] depends on the definition of volumetric efficiency. With the original definition, two engines with the same intake system design would show different volumetric efficiencies, for the same mass flowing into the cylinder, if one engine used EGR and the other one didn't. With the modified definition, the two engines should show the same volumetric efficiency.

If the relative EGR rate, f_{egr}, is defined as

$$f_{egr} = m_{egr}/m_{air} \qquad [4.10]$$

the modified volumetric efficiency equation can be written as

$$\eta_v' = 2\, m_{air}\, (1 + f_{egr}) \,/\, \rho_{air,in}\, V_d\, N \qquad [4.11]$$

This is simply related to the previous definition of volumetric efficiency,

$$\eta_v' = (1 + f_{egr})\, \eta_v \qquad \text{or} \qquad \eta_v = \eta_v' \,/\, (1 + f_{egr}) \qquad [4.12]$$

For engines without EGR, f_{egr} is always zero and both definitions of volumetric efficiency are the same. For engines with EGR, the EGR fraction will decrease as load is increased until some point where the EGR is discontinued giving $f_{egr} = 0$. Thus, we expect that f_{egr} will decrease as load is increased.

If the modified volumetric efficiency relation in equation [4.12] is introduced into the BMEP/P_{in} relation in equation [4.7], the following result is obtained:

$$(BMEP) = \eta_v' \,(m_{fuel}/m_{air})\, P_{in} \,/\, [\, (1 + f_{egr}\,)\, (BSFC)\, R_{air}\, t_{in}] \qquad [4.13]$$

This displays the various factors that can affect the BMEP-P_{in} relationship. Because the modified definition of volumetric efficiency accounts for all new charge—except fuel—entering the cylinder, this variable may be expected to approximate more closely the observed behavior of volumetric efficiency with changes in load (*i.e.*, changes in manifold pressure) discussed above.

For further discussions of the analytical relationship between BMEP and inlet manifold pressure, it is convenient to define the ratio of these two variables as r_p and rewrite equation [4.7] as:

$$r_p = BMEP \,/\, p_{in} = \eta_v\, (F/A) \,/\, (BSFC)\, R_{air}\, t_{in} \qquad [4.14]$$

Alternatively, equation [4.13] can be rewritten to give

$$r_p = BMEP \,/\, p_{in} = \eta_v' \,(F/A) \,/\, [\, (1 + f_{egr}\,)\, (BSFC)\, R_{air}\, t_{in}] \qquad [4.15]$$

In the remaining analysis, we will use equation [4.14]. The modified definition of volumetric efficiency can be introduced by using equation [4.12] to obtain the relationship between η_v and η_v'.

Equation [4.14] contains the reciprocal brake-specific fuel consumption $(BSFC)^{-1} = P_{brake}/m_{fuel}$. In order to determine the dependence of this term on manifold inlet pressure, the brake power of the engine, P_{brake}, is

written as the gross (or indicated) engine power, P_{ind}, less the power due to rubbing friction, P_{rf}, and due to pump work,* $|P_{pump}|$:

$$P_{brake} = P_{ind} - P_{rf} - |P_{pump}| \qquad [4.16]$$

The reciprocal brake-specific fuel consumption then becomes:

$$(BSFC)^{-1} = (P_{ind} - P_{rf} - |P_{pump}|) / m_{fuel} \qquad [4.17]$$

The air/fuel ratio can be introduced into this equation giving

$$(BSFC)^{-1} = (A/F) (P_{ind} - P_{rf} - |P_{pump}|) / m_{air} \qquad [4.18]$$

This expression can be substituted into equation [4.14] for r_p to eliminate the BSFC term. Doing this and simplifying gives:

$$r_p = (\eta_v (F/A) / R_{air} t_{in}) \cdot ((A/F) (P_{ind} - P_{rf} - |P_{pump}|) / m_{air} \qquad [4.19]$$

$$r_p = [\eta_v (P_{ind} - P_{rf} - |P_{pump}|)] / [R_{air} t_{in} m_{air}] \qquad [4.20]$$

The terms $(P_{ind} - P_{rf}) / m_{air}$ represent the gross and friction power per unit mass of air charged. These quantities should be relatively independent of inlet pressure.** It will, however, depend on the engine speed. We can define a new quantity, $C_3(N)$, as follows.

$$C_3(N) = (P_{ind} - P_{rf}) / (m_{air} R_{air} t_{in}) \qquad [4.21]$$

This quantity should be only a weak function of intake pressure and, for this analysis, is assumed to be a function of engine speed only. Substituting this into equation [4.20] gives:

$$r_p = \eta_v C_3(N) - (\eta_v |P_{pump}|) / (R_{air} t_{in} m_{air}) \qquad [4.22]$$

The pumping power that appears in these equations will have a strong dependence on the inlet pressure. For an ideal cycle, the pumping work is given by the equation:

$$|P_{pump,ideal}| = (p_{ex} - p_{in}) V_d N / 2 \qquad [4.23]$$

This ideal cycle result will be substituted for $|P_{pump}|$ in the analysis here. This will be more nearly correct when the pumping work is small,

---

*The pumping power is written in absolute value signs to indicate that it is the positive value of this term that is intended here. Thermodynamic convention in cycle analysis would make the pump work a negative quantity.

**This statement is true for a fixed air/fuel ratio. For high output power, with richer fuel mixtures, the net power per mass of air will increase. Thus, any empirical results that are compared with this analysis would not be expected to agree for points where the engine has rich operation.

i.e., at high manifold pressure. When the manifold pressure is low and the pumping work is high, the error from introducing this ideal equation will increase. Substituting the ideal pump work for the pump work term in equation [4.22] gives the following result:

$$r_p = \eta_v\, C_3(N) - [\ \eta_v\ (p_{ex} - p_{in})\ V_d\ N\ ]\ /\ [\ 2\ R_{air}\ t_{in}\ m_{air}\ ] \qquad [4.24]$$

Rewriting the definition of volumetric efficiency from equation [4.11] as $\eta_v\ V_d\ N\ /\ (2\ m_{air}) = 1\ /\ \rho_{air,in}$ and substituting this result into equation [4.24] gives:

$$r_p = \eta_v\, C_3(N) - (p_{ex} - p_{in})\ /\ (\ \rho_{air,in}\ R_{air}\ t_{in}\ ) \qquad [4.25]$$

Applying the ideal gas law, $\rho_{air,in} = p_{in}\ /\ R_{air}\ t_{in}$, gives the following equation for r_p

$$r_p = \eta_v\, C_3(N) - (p_{ex}/p_{in} - 1) \qquad [4.26]$$

The discussion of volumetric efficiency given above noted that this efficiency depended linearly on the ratio of exhaust to intake pressure in both the ideal cycle analysis and in observed experimental data. This general result can be summarized by the following equation:

$$\eta_v = C_1(N) - C_2(N)\ p_{ex}/p_{in} \qquad [4.27]$$

Here $C_1(N)$ and $C_2(N)$ are regarded as empirical "constants", depending only on the engine speed. These empirical terms account for changes in volumetric efficiency caused by engine speed. Equation [4.27] is also consistent with equation [4.8] for the ideal cycle volumetric efficiency if we define:

$$C_1 = (\gamma - 1)/\gamma\ +\ r_c\ /\ \gamma(r_c - 1) \quad \text{and} \quad C_2 = 1\ /\ \gamma(r_c - 1) \qquad [4.28]$$

Substituting equation [4.27] for the volumetric efficiency into equation [4.26] and rearranging gives

$$r_p = [\ C_1(N) - C_2(N)\ p_{ex}/p_{in}\ ]\ C_3(N) - (p_{ex}/p_{in} - 1) \qquad [4.29]$$

$$r_p = [\ C_1(N)\ C_3(N) + 1\ ]$$

$$\quad - [\ C_2(N)\ C_3(N) + 1\ ]\ p_{ex}/p_{in} \qquad [4.30]$$

The dependence of r_p on p_{in} given in this equation has the simple form,

$$r_p(N) = \alpha(N)/p_{in} + \beta(N) \qquad [4.31]$$

if the following definitions are made,

$$\beta(N) = [\ C_1(N)\ C_3(N)\ /\ R_{air}\ t_{in}\ +\ 1\ ] \qquad [4.32]$$

and

$$\alpha(N) = \quad - [\ C_2(N)\ C_3(N)\ /\ R_{air}\ t_{in}\ +\ 1\ ]\ p_{ex} \qquad [4.33]$$

Substituting the definition of $r_p = BMEP/p_{in}$ into equation [4.31] gives the result that BMEP should have a linear dependence on p_{in} for the conditions assumed in this derivation.

$$BMEP = \alpha(N) + \beta(N)\ p_{in} \qquad [4.34]$$

There are three important conditions that limit the applicability of this equation:

- The engine pumping work is taken to be the pumping work for the ideal cycle. This will make equation [4.34] less accurate at lower manifold pressures where the pumping work becomes significant.

- The gross work per unit mass of air is assumed to depend only on the engine speed. This will make the equation less valid at higher manifold pressures when the air/fuel mixture is fuel-rich giving more power per mass of air.

- $\alpha(N)$ will depend on manifold pressure because it is proportional to the exhaust pressure. The exhaust pressure increases with inlet manifold pressure at a given engine speed. This variation increases at higher engine speeds. In one example, there was about a 25% increase in exhaust pressure at the highest engine speed as the intake pressure increased from 40 kPa to 100 kPa.[35]

Thus, the linear dependence of BMEP on manifold inlet pressure given in equation [4.33] can be expected to hold for moderate inlet pressures, but should be extrapolated to very high or very low inlet pressures with caution. Also, this derivation started from equation [4.14] which did not take explicit account of EGR in the definition of volumetric efficiency.

In order to account explicitly for EGR, equation [4.15] is used for the definition of r_p. Substituting equation [4.18] for $(BSFC)^{-1}$ into [4.15] and rearranging gives:

$$r_p = \{\ \eta_v'\ (F/A)\ /\ [\ (1 + f_{egr})\ R_{air}\ t_{in}]\ \}\ \cdot\ \{\ (A/F)\ (P_{ind} - P_{rf} - |P_{pump}|)\ /\ m_{air} \qquad [4.35]$$

$$r_p = \eta_v'\ (P_{ind} - P_{rf} - |P_{pump}|)\ /\ [(1 + f_{egr})\ R_{air}\ t_{in}\ m_{air}] \qquad [4.36]$$

In this case define $C_3'(N)$, analogous to the definition of $C_3(N)$ in equation [4.21],

$$C_3'(N) = (P_{ind} - P_{rf})\ /\ [m_{air}\ (1 + f_{egr})\ R_{air}\ t_{in}\ ] \qquad [4.37]$$

Here $C_3'(N)$ represents the gross power minus the rubbing friction power per unit mass of air plus recycled exhaust into the cylinder. This will change if the EGR fraction changes. Substituting this definition of $C_3'(N)$ and the definition of the ideal pumping power from equation [4.23] into equation [4.36] gives

$$r_p = \eta_v' \; C_3'(N)$$

$$- [\; \eta_v' \; (p_{ex} - p_m) \; V_d \; N \;] \; / \; [\; 2 \; (1 + f_{egr}) \; R_{air} \; t_{in} \; m_{air}] \qquad [4.38]$$

Rewriting the modified definition of volumetric efficiency from equation [4.11] as $\eta_v' \; V_d \; N \; / \; [2 \; (1 + f_{egr}) \; m_{air}] = 1 \; / \; \rho_{air,in}$ and substituting this result into equation [4.38] gives:

$$r_p = \eta_v' \; C_3'(N) - (p_{ex} - p_m) \; / \; (\; \rho_{air,in} \; R_{air} \; t_m \;) \qquad [4.39]$$

Applying the ideal gas law, $\rho_{air,in} = p_{in} \; / \; R_{air} \; t_{in}$, gives the following equation for r_p

$$r_p = \eta_v' \; C_3'(N) - (p_{ex} \; / \; p_m - 1) \qquad [4.40]$$

This equation is exactly the same as equation [4.26], except that the modified volumetric efficiency is used here. We assume that the dependence of this modified volumetric efficiency can be represented by an equation of the same form as equation [4.27], *i.e.*,

$$\eta_v' = C_1'(N) - C_2'(N) \; p_{ex}/p_m \qquad [4.41]$$

The substitution of equation [4.41] into equation [4.40] proceeds in exactly the same way as the previous derivation where equation [4.27] was substituted into equation [4.26].

$$r_p = [\; C_1'(N) - C_2'(N) \; p_{ex}/p_m \;] \; C_3'(N) - (p_{ex}/p_m - 1) \qquad [4.42]$$

$$r_p = [\; C_1'(N) \; C_3'(N) + 1 \;]$$

$$- [\; C_2'(N) \; C_3'(N) + 1 \;] \; p_{ex}/p_m \qquad [4.43]$$

The dependence of r_p on p_m given in this case has the simple form, as in the case where EGR was not considered:

$$r_p(N) = \alpha'(N)/p_m + \beta'(N) \qquad [4.44]$$

Here the following definitions are made,

$$\beta'(N) = [\; C_1'(N) \; C_3'(N) + 1 \;] \qquad [4.45]$$

and

$$\alpha'(N) = \quad - [\; C_2'(N) \; C_3'(N) \; + 1 \;] \; p_{ex} \qquad [4.46]$$

Substituting the definition of $r_p = BMEP/p_m$ into equation [4.44] gives the result that BMEP should have a linear dependence on p_m for the conditions assumed in this derivation.

$$BMEP = \alpha'(N) + \beta'(N) \; p_m \qquad [4.47]$$

There are four important conditions that limit the applicability of this equation:

- The EGR fraction is constant. If this is not the case, the collection of terms which involve C_3' will change and both $\alpha'(N)$ and $\beta'(N)$ will depend on the manifold pressure.

- The engine pumping work is taken to be the pumping work for the ideal cycle. This will make equation [4.34] less accurate at lower manifold pressures where the pumping work becomes significant.

- The gross work per unit mass of air is assumed to depend only on the engine speed. This will make the equation less valid at higher manifold pressures when the air/fuel mixture is fuel-rich giving more power per mass of air.

- $\alpha'(N)$ will depend on manifold pressure because it is proportional to the exhaust pressure. The exhaust pressure increases with inlet manifold pressure at a given engine speed. This variation increases at higher engine speeds.

Equations [4.34] and [4.47] for the case of no EGR and EGR, respectively, show that under given conditions we can expect a linear dependence of BMEP on intake manifold pressure. This has also been observed experimentally in the EPA engine mapping data discussed earlier. Although this analysis provides support for the use of linear interpolation, extrapolation to engine operation at high manifold pressures where enrichment takes place or to low manifold pressures where the pumping work is significant, are not justified by the results here. In addition, the use of linear interpolation in regions where EGR operation is taking place and the EGR fraction is changing is not justified by these results.

In order to compare the analysis of this section with the results of the previous section, an order of magnitude estimate of $\alpha(N)$ and $\beta(N)$ was carried out for the case of no EGR. The values of $C_1(N)$ and $C_2(N)$ were estimated from the ideal cycle values given in equation [4.28]. The effective value of the specific heat ratio, γ, was assumed to be 1.3 and the compression ratio, r_c, was assumed to be 9. This gives the following values for these dimensionless quantities:

$$C_1 \simeq 1 \qquad \text{and} \qquad C_2 \simeq 0.1$$

Equation [4.21] is used to compute $C_3(N) = (P_{ind} - P_{rf}) / (m_{air}\, R_{air}\, t_{in})$. This was estimated by using the gas constant for air as 0.06655 BTU/lb-R and assuming the inlet temperature was 500 R. The term $(P_{ind} - P_{rf}) / m_{air}$ was estimated by assuming (1) a 15:1 ratio for m_{air}/m_{fuel}, (2) that $(P_{ind} - P_{rf})$ is about 30% of the fuel energy $m_{fuel}\, Q_c$, and (3) the heat of combustion of the fuel is 20,000 BTU/lb. This gives the dimensionless value of C_3 as

$$C_3 \simeq 12$$

When the values of C_1, C_2, and C_3 are substituted into equations [4.32] and [4.33] for $\beta(N)$ and $\alpha(N)$, with an assumed exhaust pressure of 15 psi (absolute), the following values are obtained:

$\alpha \simeq -33$ psi and $\beta \simeq 13$ [dimensionless]
or $\beta \simeq 1.9$ psi/kPa

These values are the same order of magnitude as the linear regression constants obtained when the BMEP was fit to the manifold pressure.

Conclusions from this Task

The measured correlation between BMEP and inlet manifold pressure is quite good for almost all of the engines and speed ranges considered.

An analysis of the expected behavior of BMEP and inlet manifold pressure, at a given engine speed, shows that a linear relationship between these two variables can be expected under certain conditions.

The experimentally observed regression coefficients in the equation BMEP = a + b P_m have the same order of magnitude as predicted from the analysis in all cases except one.

Extrapolation of an experimental linear relationship between BMEP and inlet manifold pressure has been shown to produce errors in experimental data and violated the conditions used to derive an analytical linear relationship between these two variables.

The analytical results do not provide any useful guidance on a non-linear extrapolation approach. Although linear extrapolation should be used with caution, it is the most reasonable approach to use in the absence of any data.

5. LIST OF SYMBOLS

a	Empirical constant in equation for fuel energy rate (kJ/rev).
a'	Empirical constant (= a/V_d — kJ/liter-revolution)
b	Empirical constant in equation for fuel energy rate (dimensionless).
A/F	Air/Fuel ratio
BMEP	Brake-mean effective pressure (psi)
BSFC	Brake-specific fuel consumption (lb_m/HP-hr)
f_{egr}	Ratio of EGR flow to total of air plus EGR flows
m	Mass flow rate (lb/sec or kg/sec)
m_{air}	Mass flow rate of air.
m_{fuel}	Mass flow rate of fuel.
m_i	Mass flow rate of i^{th} pollutant species.
$M_{exhaust}$	Molecular weight of exhaust.
M_i	Molecular weight of i^{th} pollutant species.
N	Engine speed (RPM)
p	Pressure (psi or kPa)
P_{engine}	Engine brake power output (HP or kW)
P_{fuel}	Fuel energy rate (= $m_{fuel}\ Q_c$ — HP or kW)
$P_{friction}$	Power required to overcome all friction (HP or kW)
P_{ind}	Indicated or gross power (HP or kW)
P_{pump}	Pump work (HP or kW)
P_{rf}	Total friction power minus pump work (HP or kW)
ppm_i	Parts per million (by volume) for species i.
R_{air}	Gas constant for air

r_c Compression ratio

r_p Ratio of BEMP to manifold inlet pressure

T Torque ($ft-lb_f$)

t_{in} Temperature of intake manifold (R)

V_d Engine displacement volume (in^3 or liters)

w_i Weight fraction of i^{th} pollutant species

$\alpha(N)$ Constant in linear equation between BMEP and p_m (psi)

$\beta(N)$ Coefficient of p_m in equation for BMEP (dimensionless or psi/kPa)

γ Ideal gas specific heat ratio (dimensionless)

η Overall engine efficiency

η_v Volumetric efficiency

η_v' Modified volumetric efficiency for explicit consideration of EGR

ρ_{air} Air density (lb/ft^3 or kg/m^3)

6. REFERENCES

1. Feng An, *Automobile Fuel Economy and Traffic Congestion*, Phd Dissertation, University of Michigan, 1991. (Subsequently referred do as An, Dissertation.)

2. Marc Ross and Feng An, "The Use of Fuel by Spark Ignition Engines," Draft for Review from Applied Physics Department, University of Michigan, May 18, 1992.

3. An, Dissertation, p. 47.

4. Ross and An, *op. cit.*, p. 7.

5. An, Dissertation, p. 38.

6. Ross and An, *op. cit.*, p. 5.

7. An, Dissertation, p. 84.

8. Bosch, *Automotive Handbook* (1st English edition), 1976, pp.218-223.

9. An, Dissertation, p. 75.

10. An, Dissertation, p. 83.

11. Heywood, *Internal Combustion Engine Fundamentals*, McGraw-Hill, 1988, p. 719

12. An, Dissertation, p. 32.

13. Russell W. Zub, "A Computer Porgram (VEHSIM) for Vehicle Fuel Economy and Performance Simulation (Automobiles and Light Trucks)," Report DOT-HS-806-037, U. S. Department of Transportation, Transportation Systems Center, Cambridge, MA, October, 1981.

14. An, Dissertation, p. 36.

15. An, Dissertation, p. 116.

16. Heywood, *op. cit.*, Chapter 14.

17. J. I. Ramos, *Internal Combustion Modeling*, Hemisphere, 1989.

18. *Engine Combustion Analysis: New Approaches*, P-156, Society of Automotive Engineers, February, 1985. This is somewhat dated, but provides a good introduction to the field.

19. A. A. Amsden, P. J. O'Rourke, and T. D. Butler, "KIVA-II: A Computer Program for Chemically Reactive Flows with Sprays," Los Alamos National Laboratory, Report LA-11560-MS, May 1989.

20. H. C. Watson, *et al.*, "Predicting Fuel Consumption and Emissions—Transferring Chassis Dynamometer Results to Real Driving Conditions, SAE Paper 830435, Detroit, February 28, March 4, 1983.

21. H. C. Watson, *et al.*, "In-use Vehicle Survey of Fuel Consumption and Emissions on Dynamometer and Road," SAE Paper 850524, 1985.

22. Yoshihary Hori, Mizuho Fukada, and Yoichi Kobayashi, "Computer Simulation of Vehicle Fuel Economy and Performance," *SAE Transactions*, v. 95, pp. 2.652-2.665, 1986. (Paper Number 860364)

23. Mikio Matsumoto, *et al.*, "Improvement of Lambda Control Based on an Exhaust Emission Simulation Model that Takes into Account Fuel Transportation in the Intake Manifold," SAE PAper 900612, Detroit Michigan, February 26-March 2, 1990.

24. Thomas C. Austin, Thomas R. Carlson, and John M. Lee, "Estimating the Effect of Driving Pattern on Exhuast Emissions Using a Vehicle Simulation Model," Prepared for EPA, Certification Division, Office of Mobile Source Air Pollution Control, October 1990.

25. Thomas C. Austin, Thomas R. Carlson, and John M. Lee, "Development of an Improved Computer Simulation of Vehicle Emissions During Cold Start and Warm-Up Operation," Sierra Research, Inc. report for EPA Certification Division, Work Assignment 1-02 under Contract 68-C9-0053, September 30, 1991.

26. David S. K. Chen, Edward J. Bissett, Se H. Oh, and David L. Van Ostrom, "A Three-Dimensional Model for the Analysis of Transient Thermal and Conversion Characteristics of Monolithic Converters," SAE Paper 880282, Detroit, February 29-March 4, 1988.

27. Heywood, *op. cit.*, Chapter 11.

28. Golden Software, Inc., *SURFER® Reference Manual*, P. O. Box 111, Golden, CO 80402.

29. 29.

30. *ibid.*

31. C. F. Taylor and E. S. Taylor, *The Internal Combustion Engine*, International Textbook Company, 1961, p. 238.

32. Taylor and Taylor, *op. cit.*, pp. 243-244 provide a dimensional analysis to show that the effect of inlet and exhaust pressure

enter the functional equation for volumetric efficiency only through the p_{ex}/p_{in} ratio.

33. H. B. Servati and R. G. DeLosh, "A Regression Model for Volumetric Efficiency," Paper 860328 at SAE International Congress, Detroit, MI, February 24–28, 1986.

34. This is similar to a definition of volumetric efficiency which accounts for both the intake charge and the residual gases given in the text, ***Internal Combustion Engines***, by Benson and Porter (Cited in Kimon Roussopoulos, "A Convenient Technique for Determining Comparative Volumetric Efficiency," SAE Paper 900352 at International Congress, Detroit, February 26–March 2, 1990.)

35. Heywood, *op. cit.*, p. 214.

APPENDIX A

ENGINE EMISSION MAPS

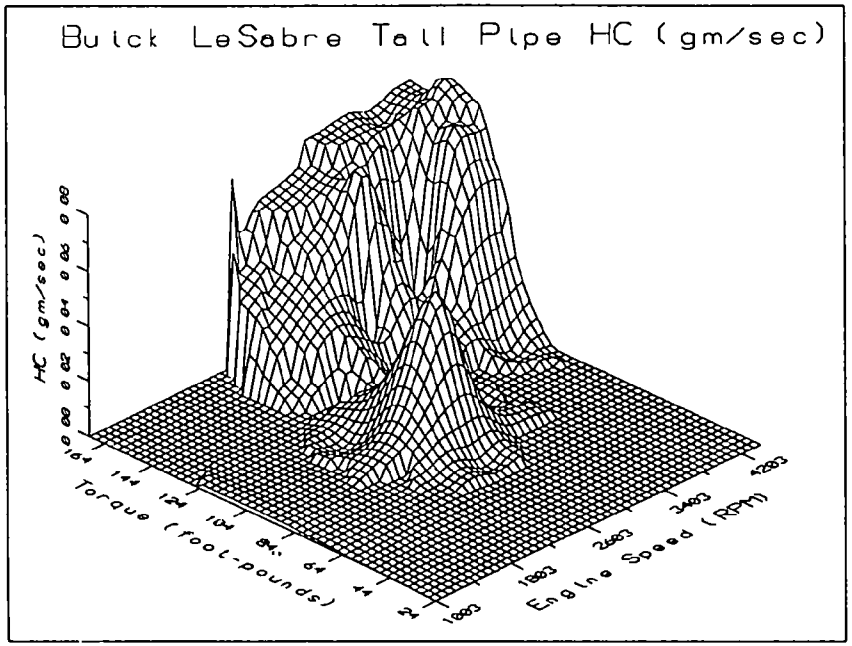

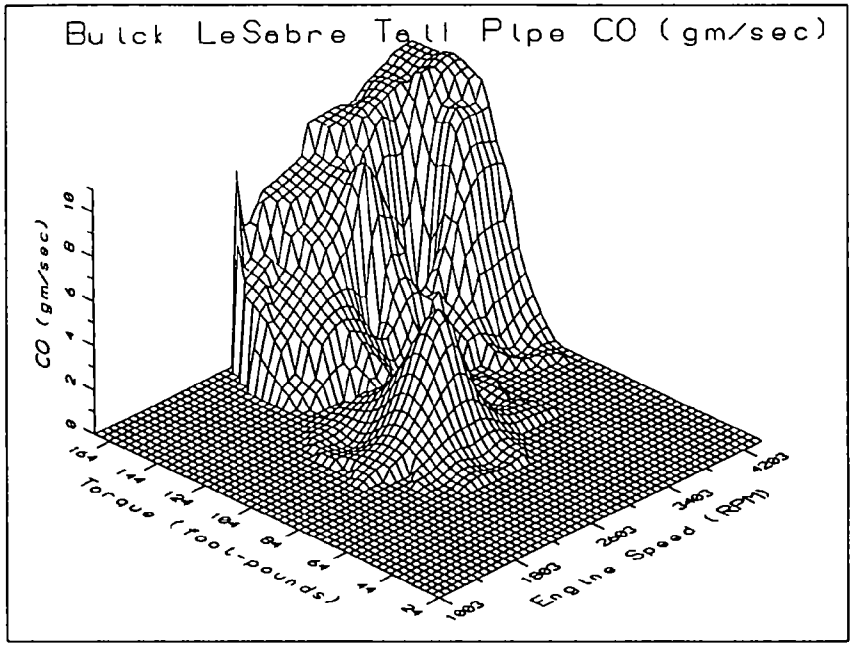

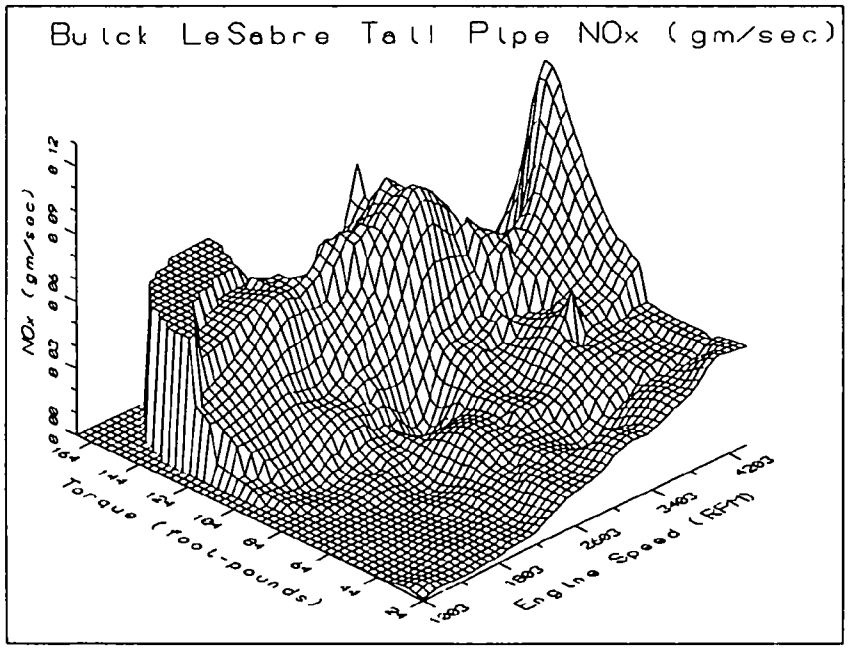

Surface Plots of Emissions for
1990 Buick LeSabre 3.0L L4OD

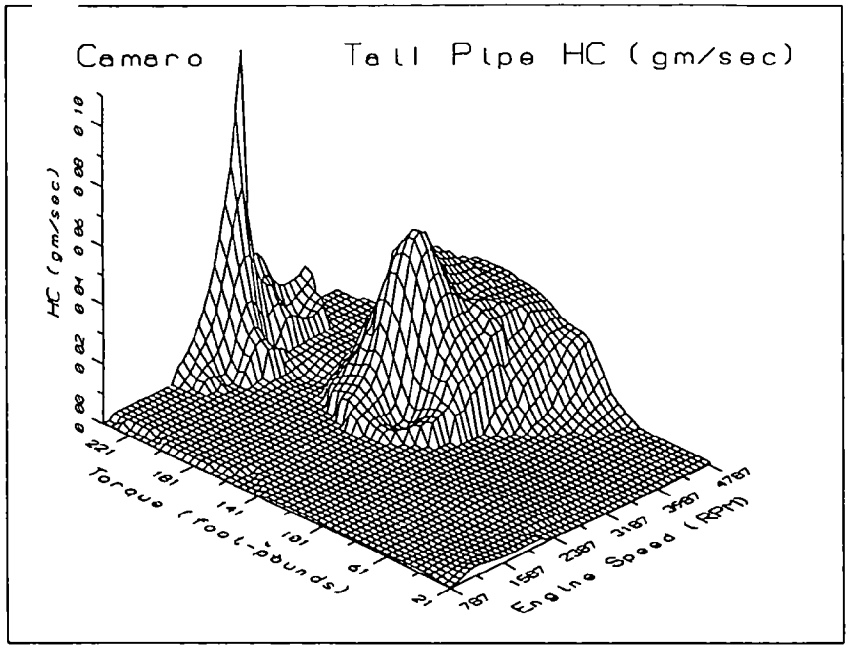

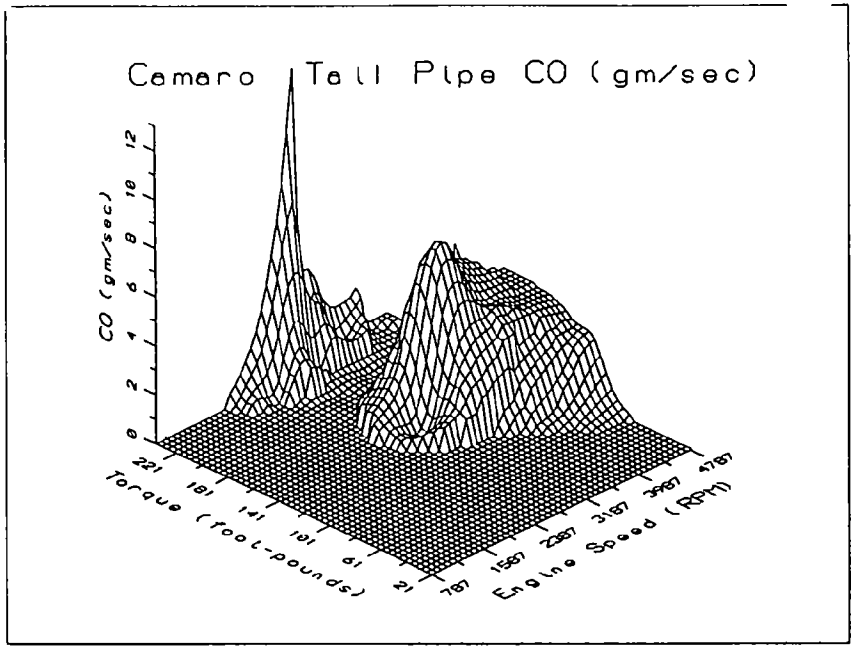

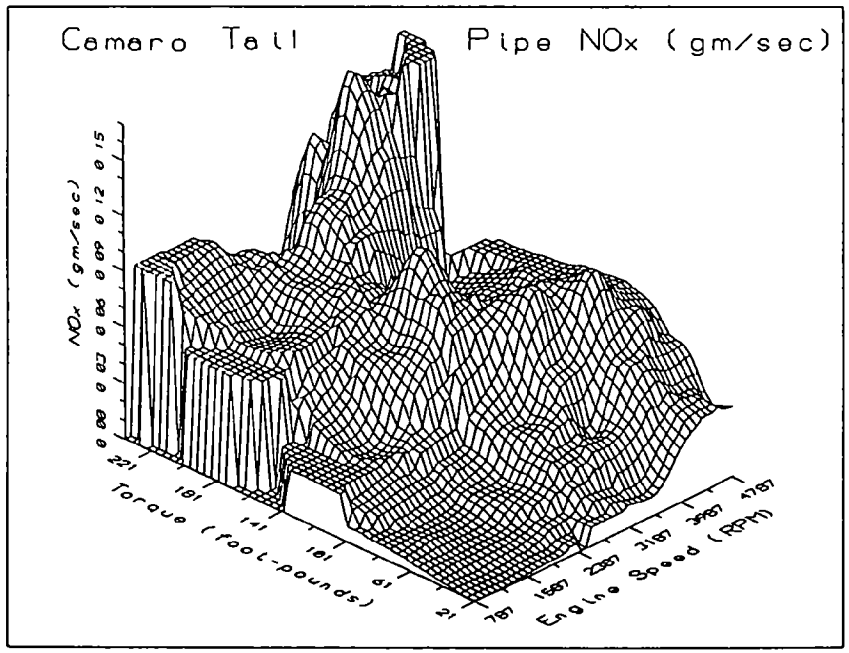

Surface Plots of Emissions for
1991 Chevrolet Camaro 5.7L L4OD

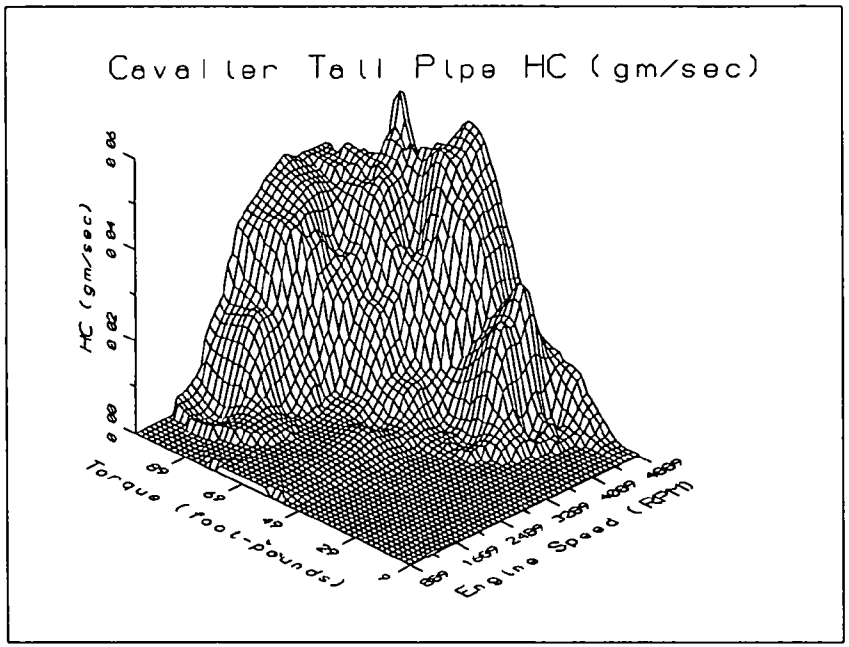

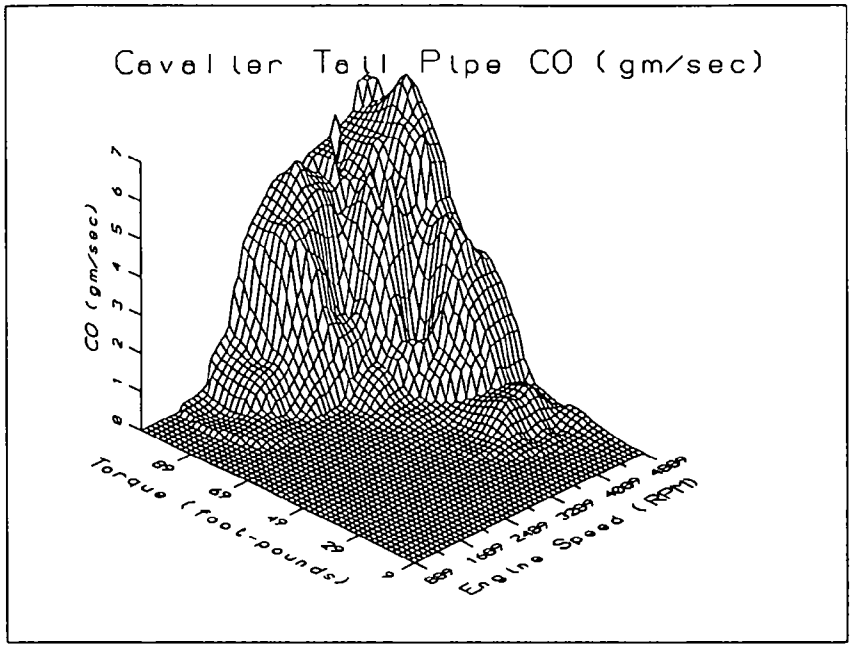

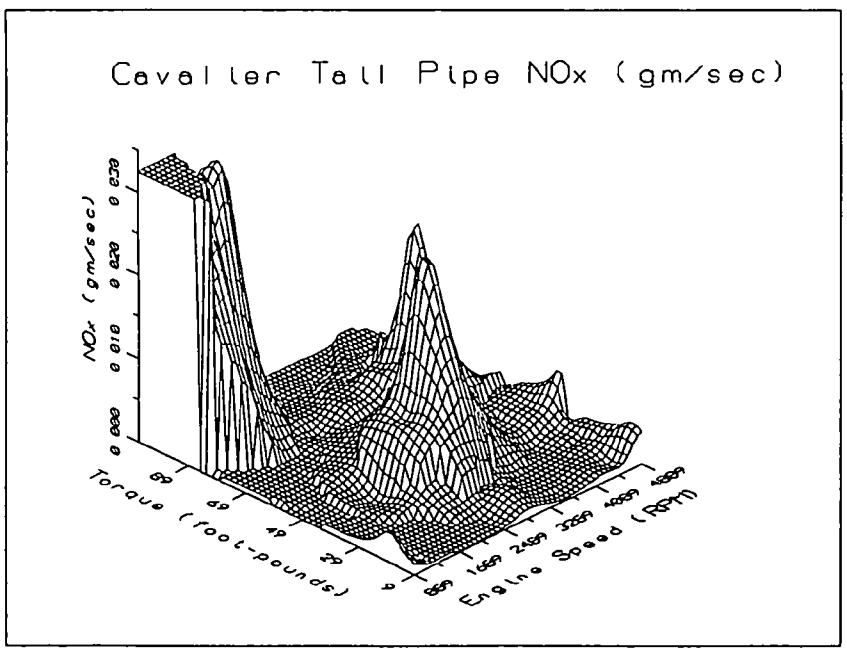

Surface Plots of Emissions for
1990 Chevrolet Cavalier 2.2L L3

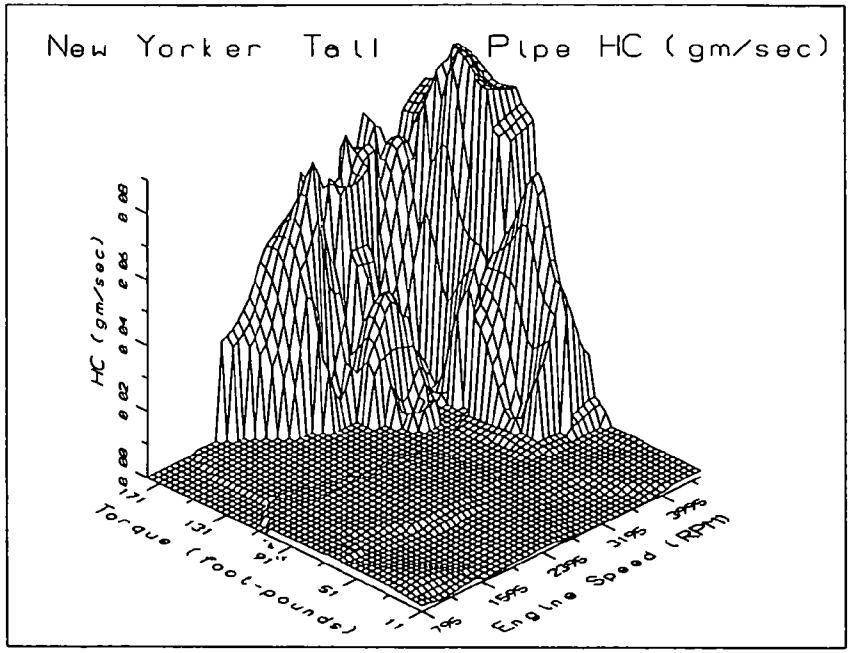

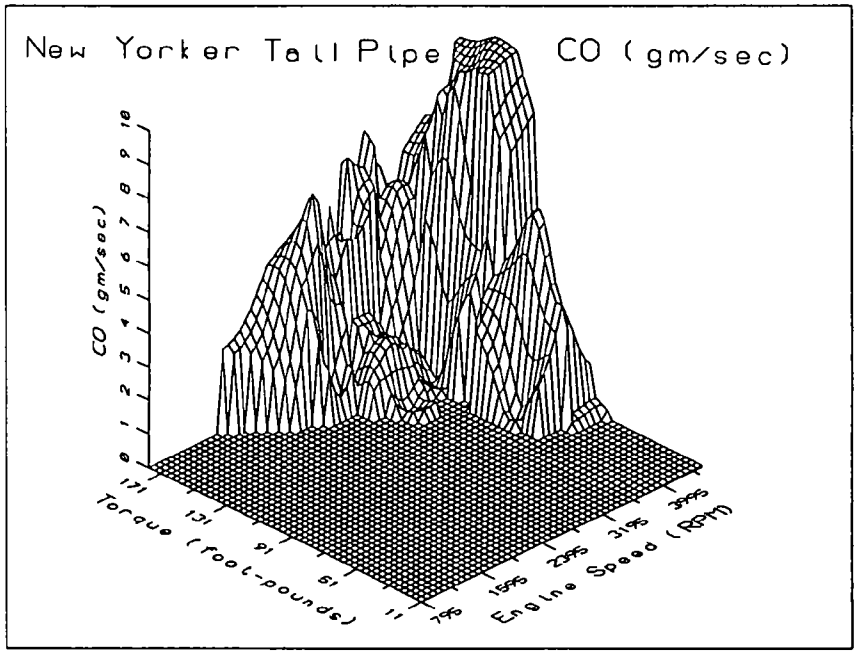

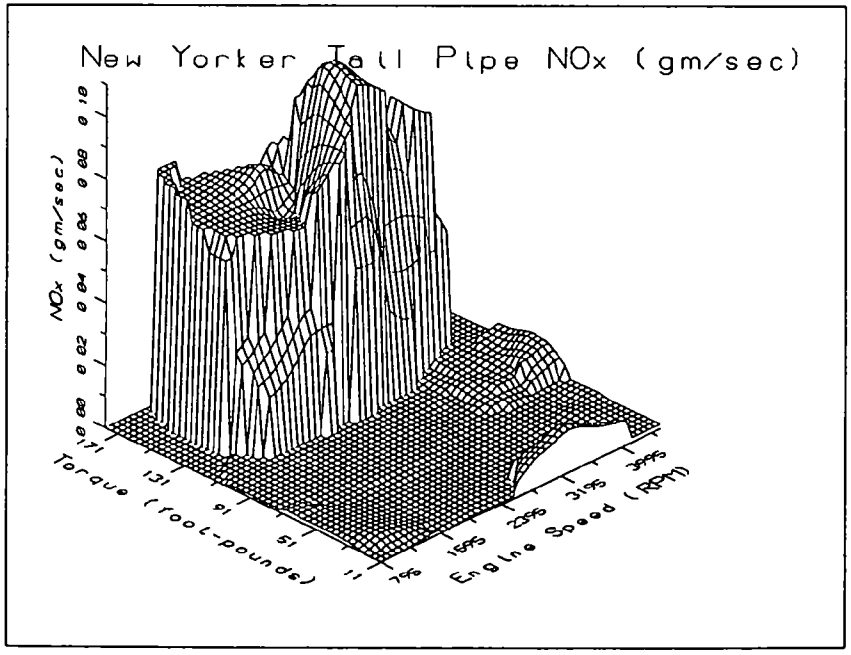

Surface Plots of Emissions for
1991 Chrysler New Yorker 3.3L L4

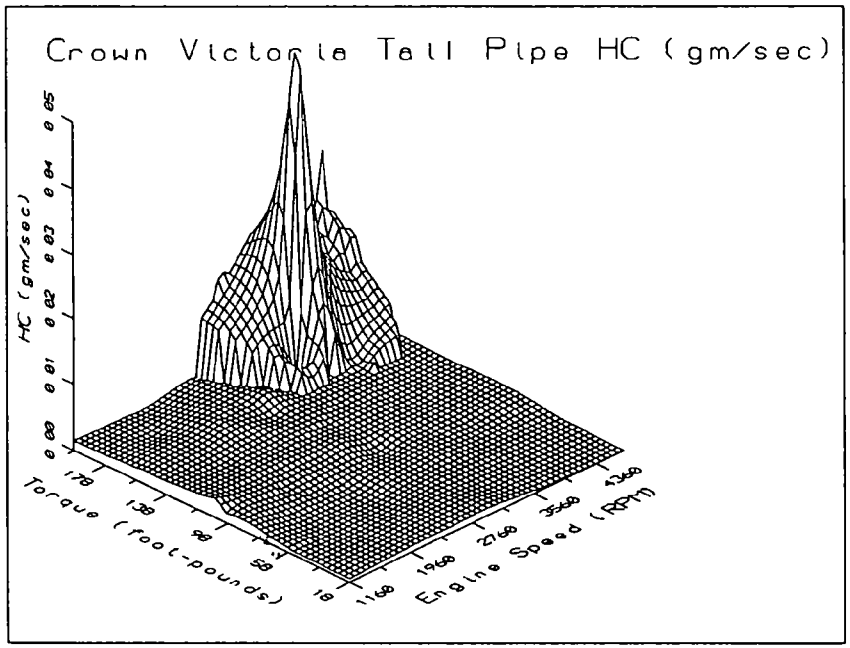

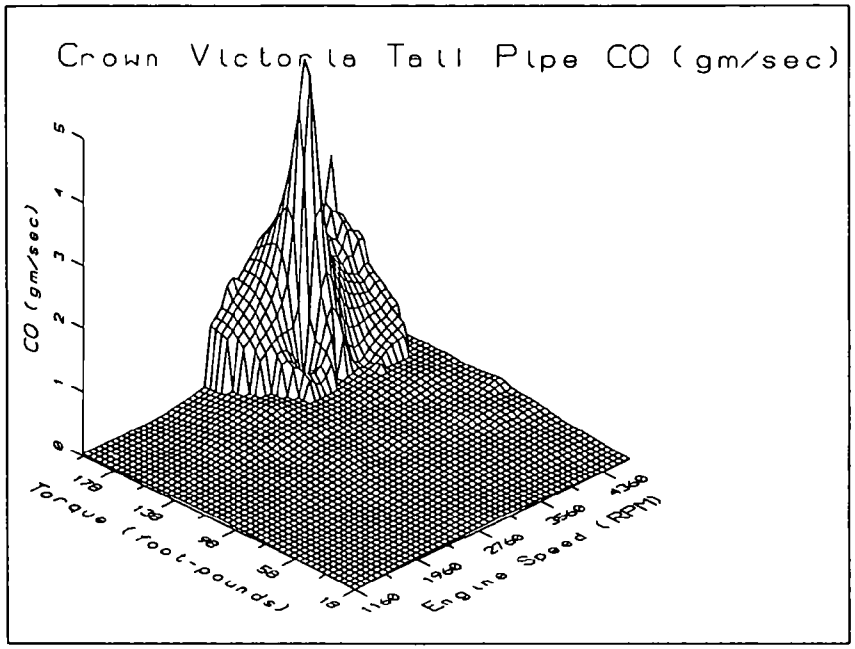

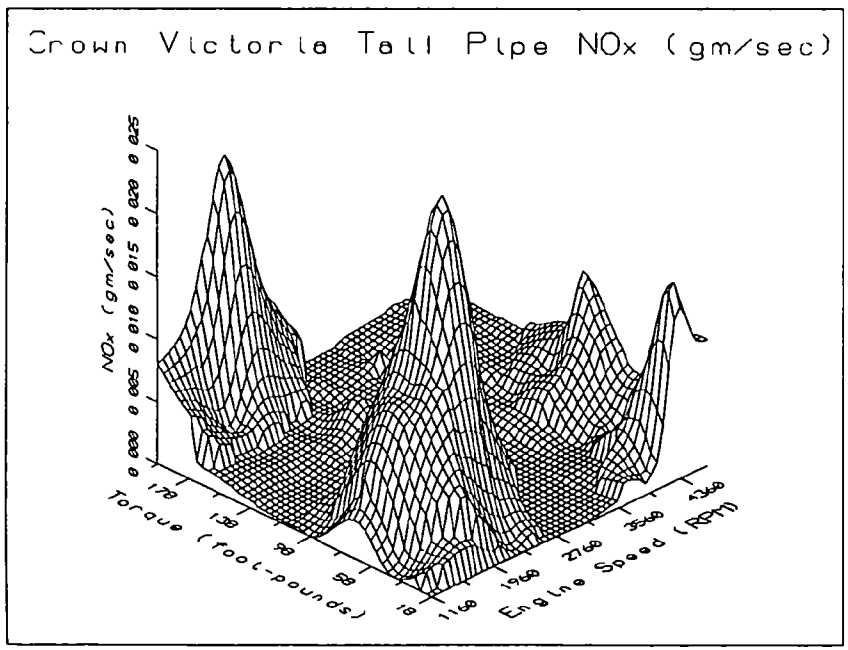

Surface Plots of Emissions for
1992 Ford Crown Victoria 4.6L L4AEOD

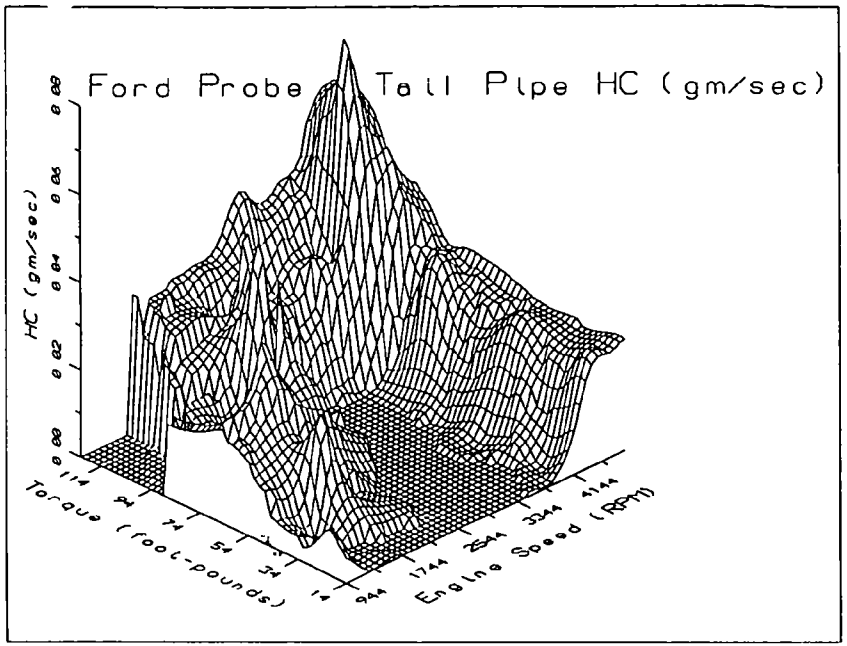

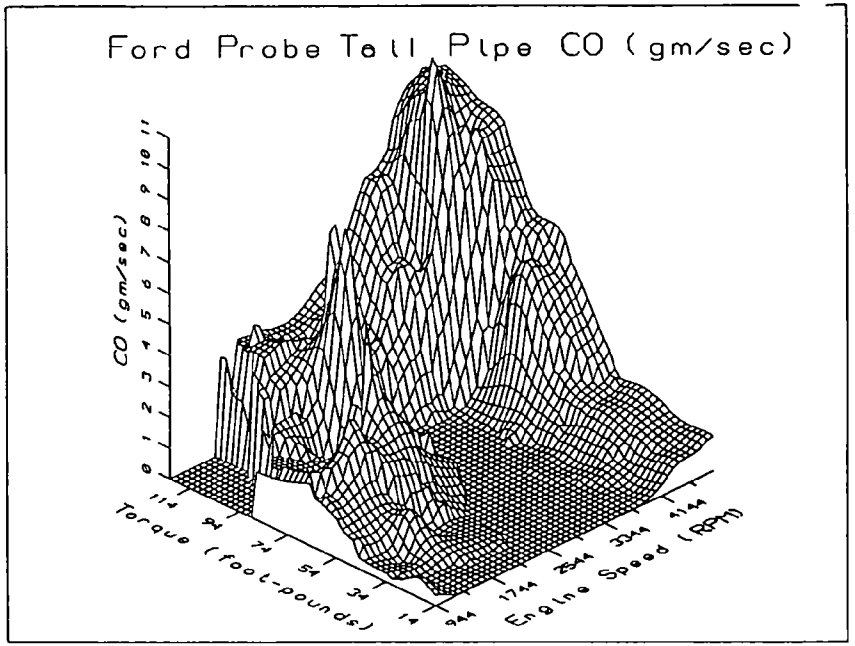

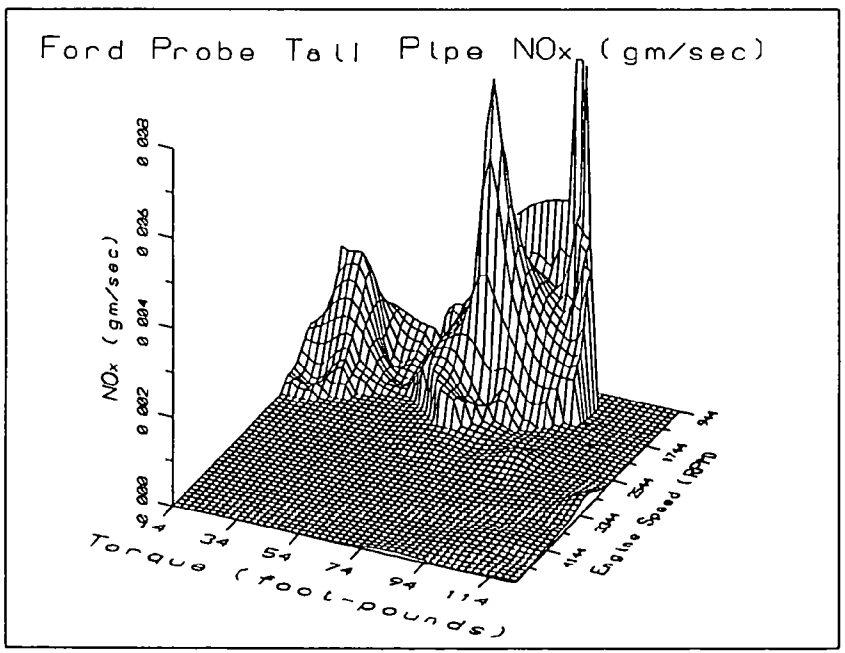

Surface Plots of Emissions for
1991 Ford Probe 2.2L L4AEOD

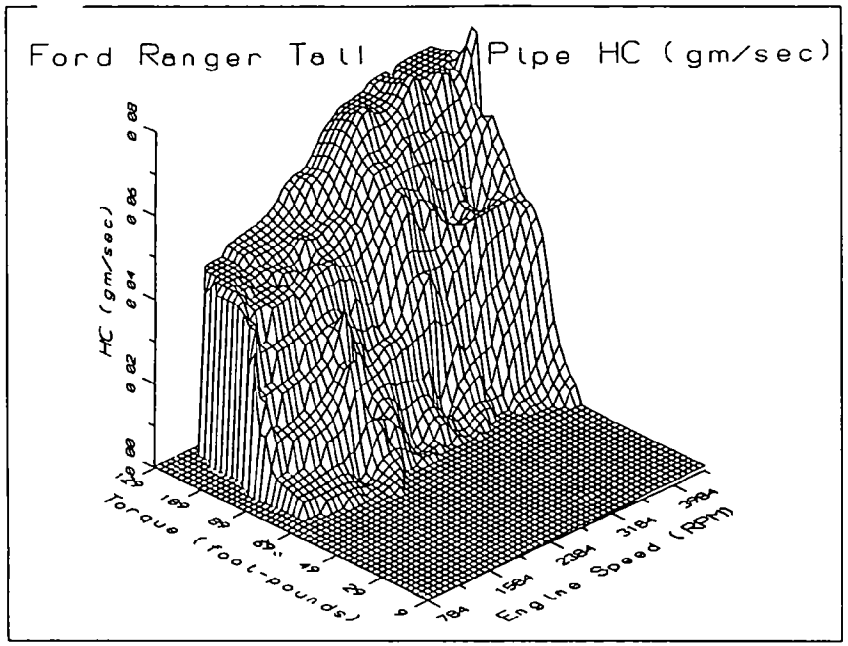

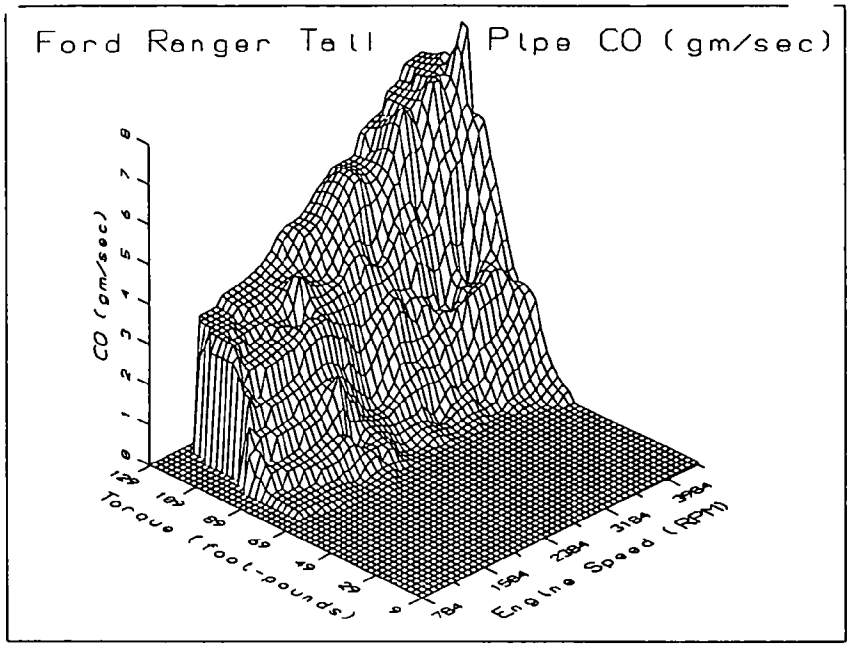

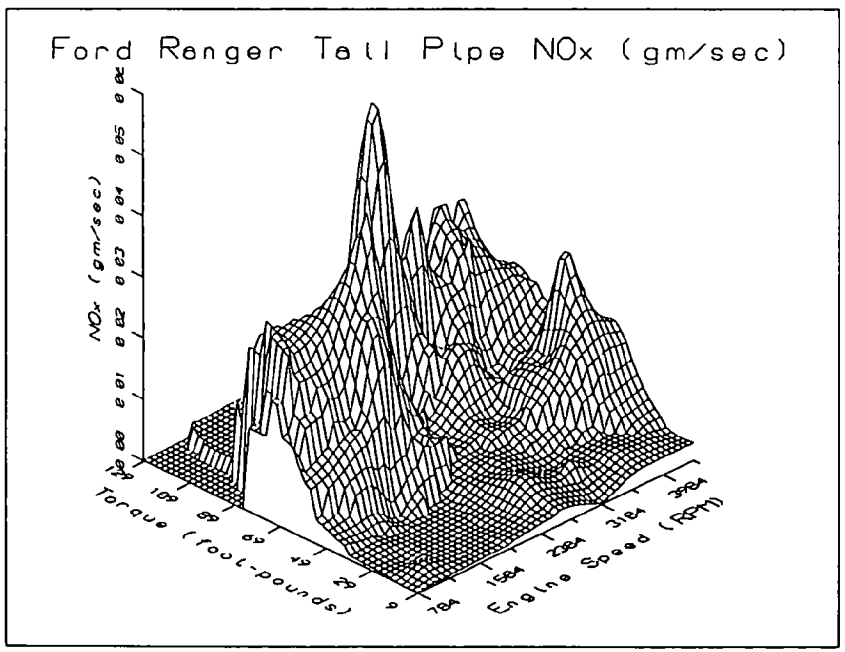

Surface Plots of Emissions for
1990 Ford Ranger 2.3L L4OD

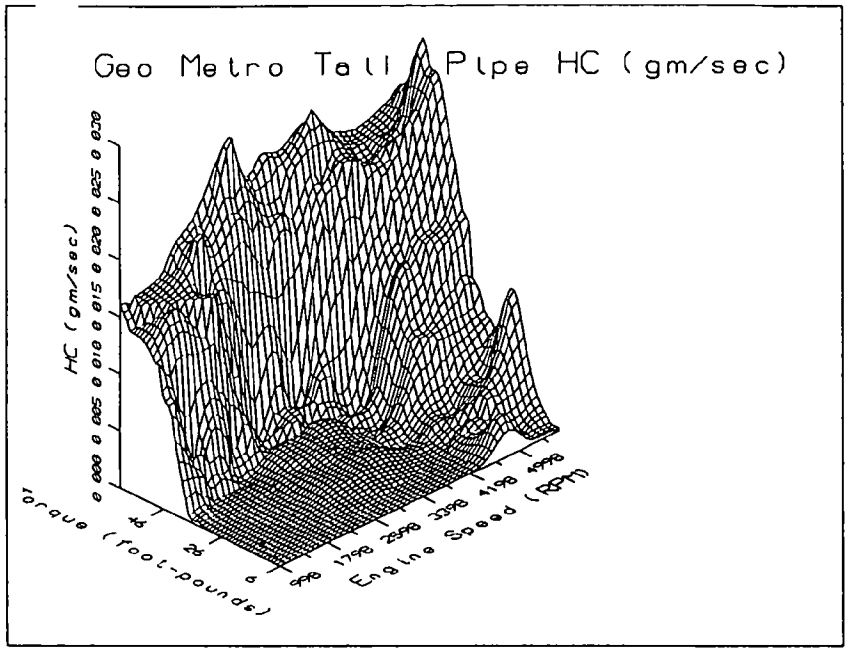

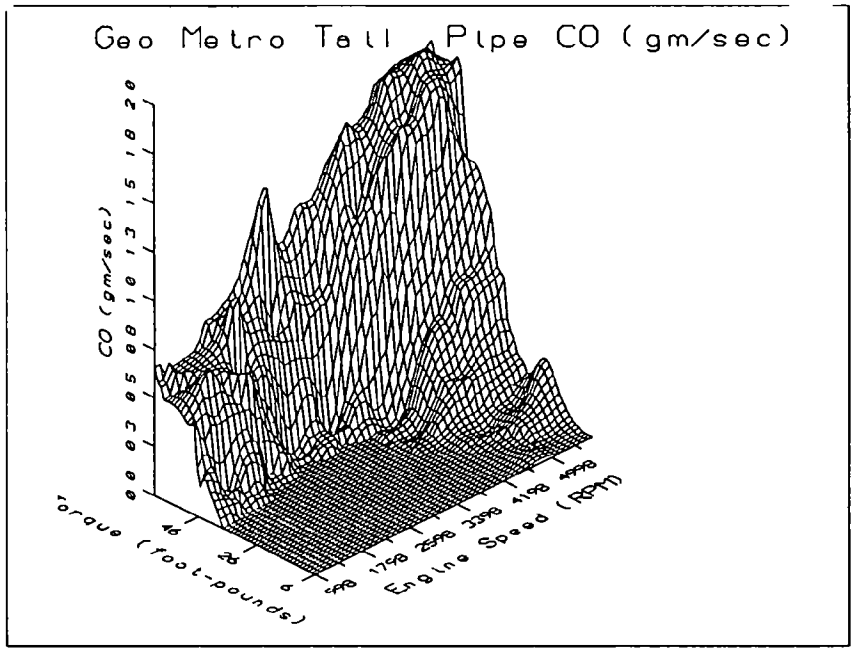

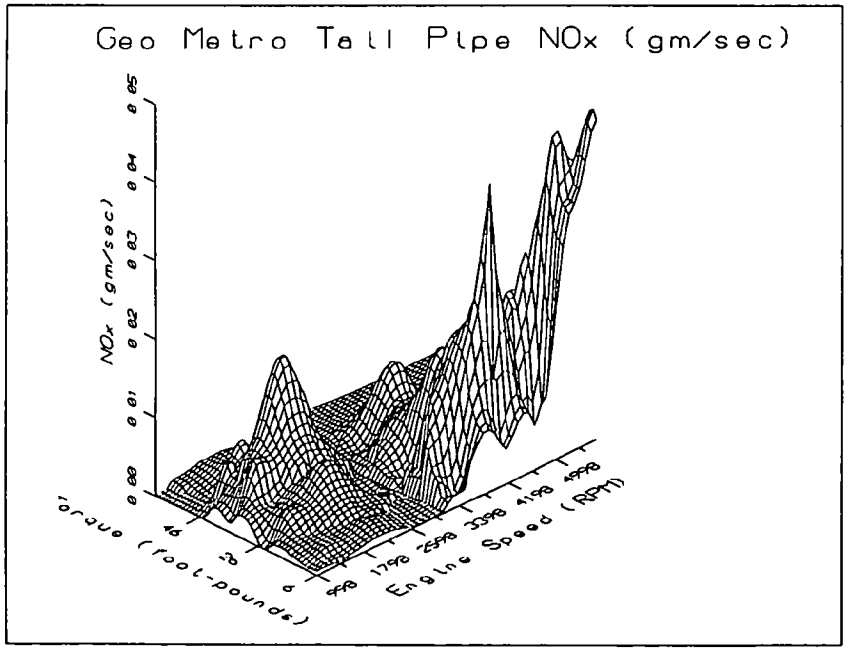

Surface Plots of Emissions for
1992 Geo Metro 1.0L M5OD

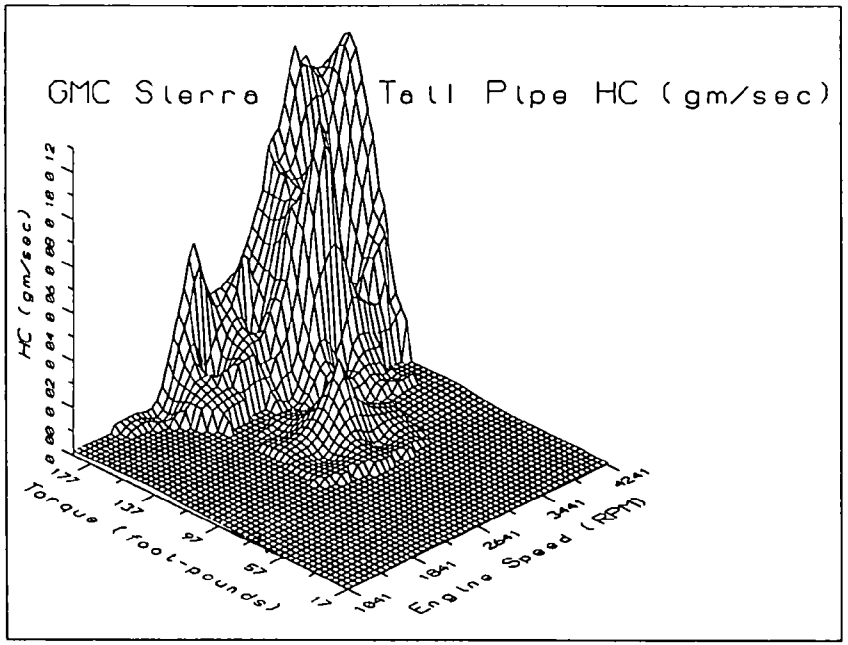

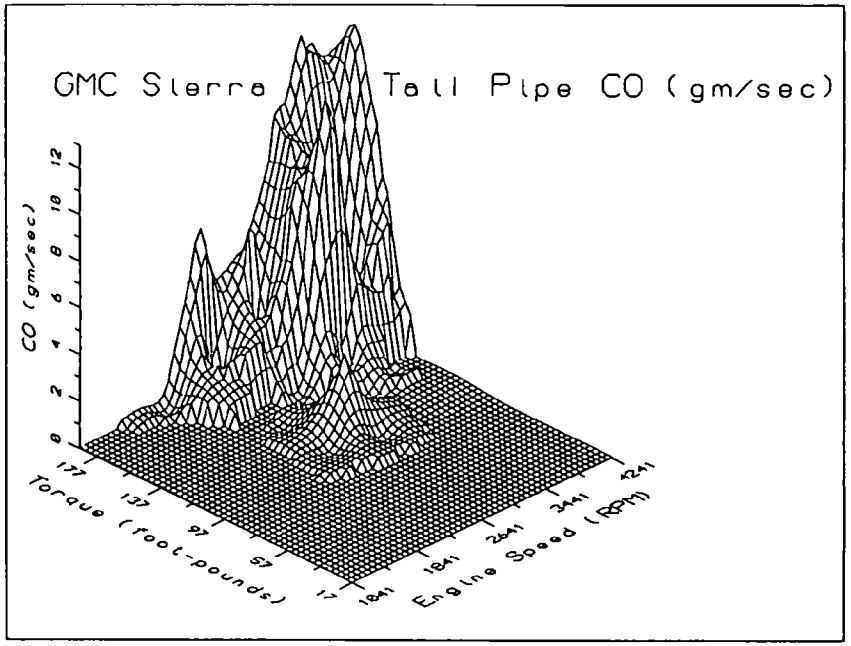

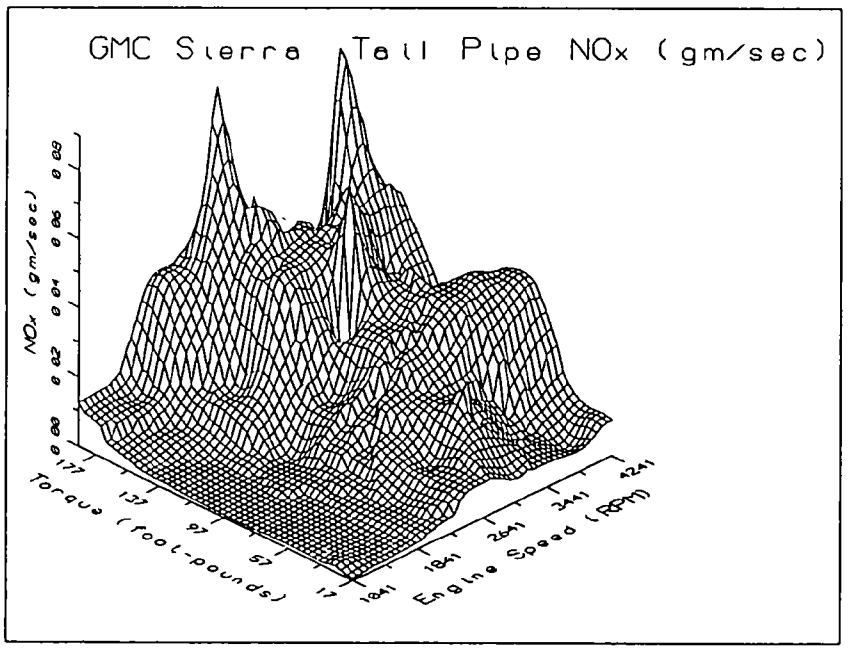

Surface Plots of Emissions for 1990 GMC Sierra 5.0L L4OD

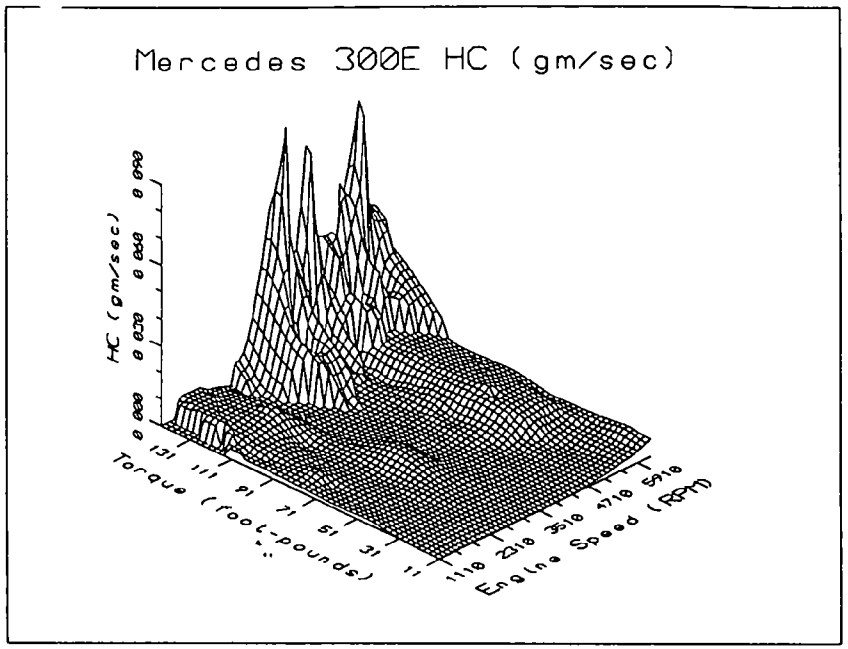

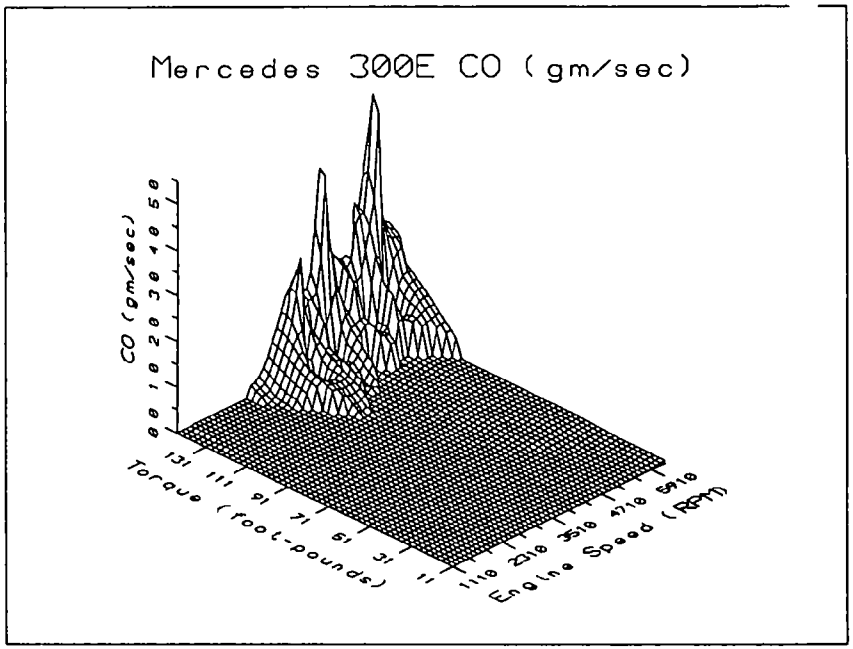

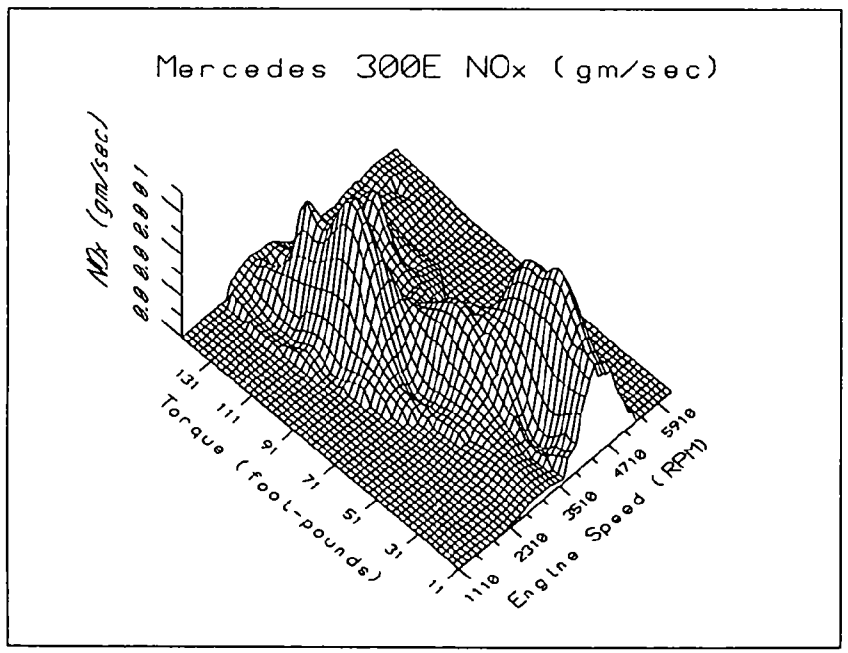

Surface Plots of Emissions for
1992 Mercedes Benz 300E 3.0L A4

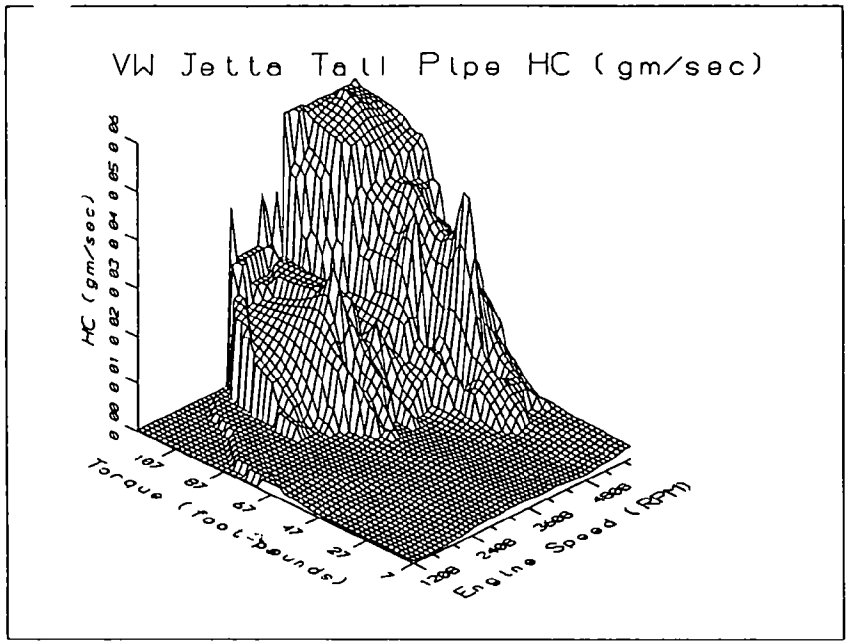

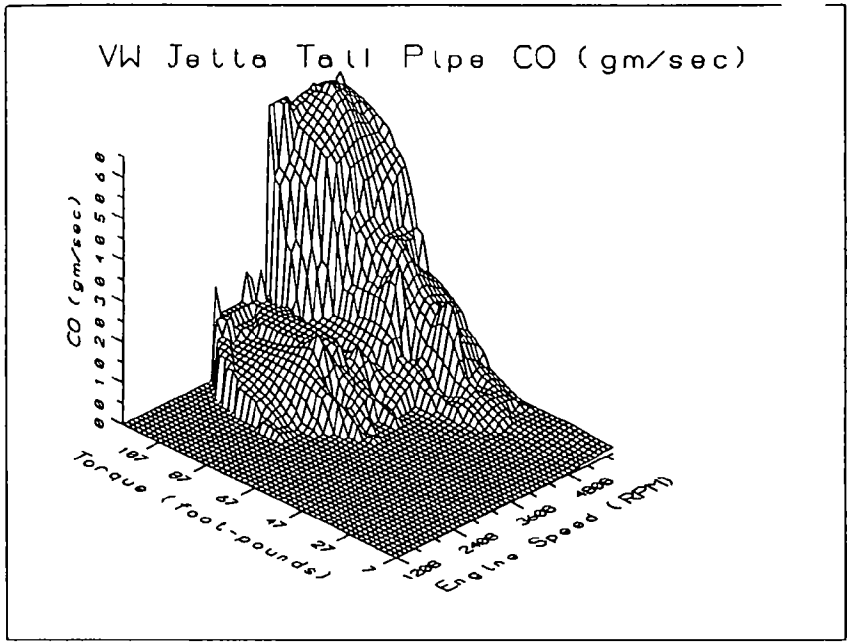

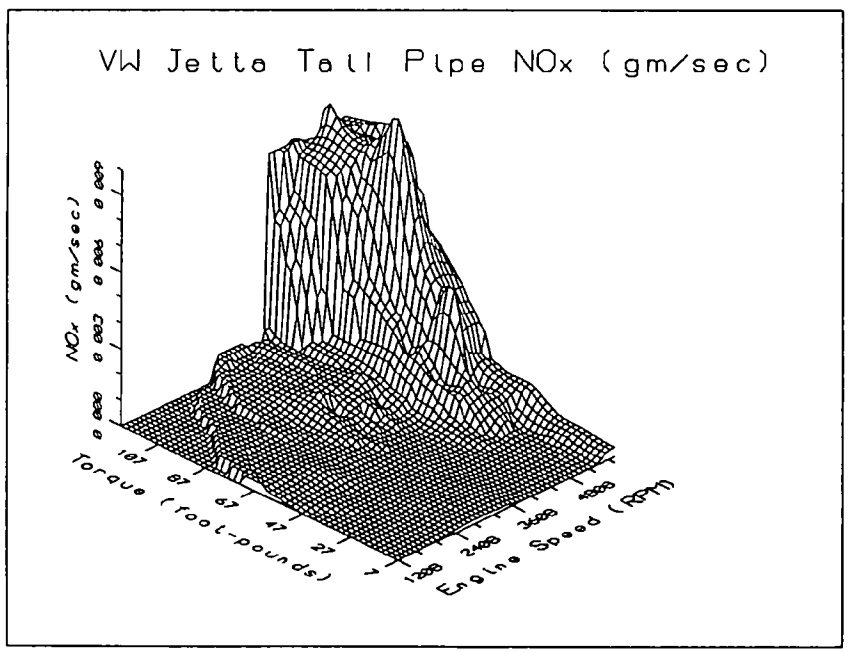

Surface Plots of Emissions for
1991 Volkswagen Jetta 1.8L A3

APPENDIX B

REGRESSION ANALYSIS TABLES AND CHARTS:

CORRELATION BETWEEN BRAKE-MEAN EFFECTIVE PRESSURE AND INLET MANIFOLD PRESSURE

The following set of tables shows the linear regression coefficients (slope and intercept) as well as the correlation coefficient squared (R^2) and the standard error in the estimated BMEP ($\sigma_{y|x}$). The data are shown for each engine at each speed for which three or more data points are available to obtain the correlation.

Following the tables, a plot of the experimental variation of BMEP with inlet manifold pressure is shown for each engine.

1990 PONTIAC 6000
4 DR SEDAN 3.1 L L4OD
VIN: 1G2AF54T2L6211503

RPM	Slope psi / kPa	Intercept psi	R^2	$\sigma_{y\|x}$	No of Data Points
1370	1.468	-43.20	0.9983	0.3281	3
2030	1.682	-44.08	0.9725	7.5744	4
2680	1.757	-50.85	0.9977	1.6765	5
3325	1.860	-53.53	0.9807	6.5840	5
3950	1.718	-41.27	0.9844	5.4083	9
4600	1.337	-33.45	0.9979	1.2071	4
5000	1.367	-38.63	0.9999	0.4177	3
5420	1.348	-42.54	0.9983	1.4944	3

1991 VOLVO 740
4 DR SEDAN 2.3 L L4OD
VIN: YV1FA8845M2514833

RPM	Slope psi / kPa	Intercept psi	R^2	$\sigma_{y\|x}$	No of Data Points
1360	2.924	-96.80	0.9755	2.9552	4
2000	0.952	-4.86	0.4974	23.4387	4
2630	1.717	-41.70	0.9960	2.7103	5
3260	1.717	-54.24	0.9507	9.9048	5
3950	1.495	-41.42	0.9840	3.5075	6
4540	1.471	-49.45	0.9769	4.9086	4
4900	1.670	-70.65	0.9925	2.8170	4
5350	1.546	-65.71	0.9949	1.7535	4

1990 CHEV CAVALIER
4 DR WAGON 2.2 L L3
VIN: 1G1JC84G91J187781

RPM	Slope psi / kPa	Intercept psi	R^2	$\sigma_{y\|x}$	No of Data Points
1240	2.303	-80.05	0.9983	0.6287	3
1810	1.790	-61.60	0.9869	5.5093	4
2400	1.821	-62.46	0.9982	2.1389	4
2975	1.687	-51.65	0.9982	1.6402	5
3550	1.912	-67.96	0.9976	1.8470	9
4140	1.692	-56.01	0.9888	3.9043	7
4500	1.770	-62.52	0.9968	2.3156	6
4880	1.828	-69.18	0.9980	1.7814	5

1991 FORD F150
4x2 PCKUP 4.9 L L4AEOD
VIN: 1FTEF15Y4MLA82098

RPM	Slope psi / kPa	Intercept psi	R^2	$\sigma_{y\|x}$	No of Data Points
1190	1.537	-55.93	0.9497	9.2199	4
1760	1.624	-56.69	0.9828	5.6242	3
2325	1.655	-56.10	0.9932	3.3850	11
2930	1.289	-43.30	0.9910	3.2246	3
3180	1.691	-67.63	0.9813	5.6080	5

1991 FORD ESCORT LX
2 DR HTCHBCK 1.9 L L4AEOD
VIN: 1FAPP14J7MW137707

RPM	Slope psi / kPa	Intercept psi	R^2	$\sigma_{y\|x}$	No of Data Points
1270	1.535	-35.82	0.9748	5.6275	4
1870	1.371	-21.30	0.9819	4.0176	5
2475	1.395	-27.25	0.9726	6.1244	4
3093	1.828	-47.83	0.9980	2.1162	4
3700	1.741	-37.48	0.9905	4.2203	7
4320	1.717	-43.63	0.9367	11.7374	4
4700	0.951	-8.87	0.9826	3.3514	3
5100	1.320	-29.60	0.9471	6.5325	3

1990 FORD F250
4x2 PCKUP 5.8 L L4AEOD
VIN: 1FTEF25H9LLA85776

RPM	Slope psi / kPa	Intercept psi	R^2	$\sigma_{y\|x}$	No of Data Points
1110	1.267	-44.22	0.9745	3.8692	5
1560	1.118	-32.97	0.9091	9.3799	3
2070	1.073	-31.19	0.9999	0.2522	5
2550	0.989	-24.34	0.9978	1.2008	3
3060	1.273	-35.80	0.9968	1.3965	7
3570	Only two data points at this RPM				
3860	Only two data points at this RPM				
4180	Only two data points at this RPM				

1991 FORD PROBE GL
2 DR HATCH 2.2 L L4AEOD
VIN: 1ZVPT20C2M5163427

RPM	Slope psi / kPa	Intercept psi	R^2	$\sigma_{y\|x}$	No of Data Points
1325	1.118	-26.05	0.9470	3.0065	4
1950	1.609	-49.02	0.9951	2.9665	3
2580	2.186	-84.00	0.9904	4.9519	6
3215	2.266	-88.94	0.9860	6.0707	6
3840	2.438	-103.68	0.9855	3.7762	9
4500	2.089	-73.53	0.9951	4.0959	4
4875	2.182	-84.50	0.9981	2.3745	4

1990 FORD RANGER XLT
4x2 REG CAB 2.3 L L4OD
VIN: 1FTCR10A9LUA34064

RPM	Slope psi / kPa	Intercept psi	R^2	$\sigma_{y\|x}$	No of Data Points
1125	1.475	-41.92	0.9697	2.1258	4
1630	0.551	0.27	0.9753	1.4098	3
2150	1.331	-36.73	0.9969	1.9450	3
2675	1.508	-45.97	0.9826	4.5010	6
3200	1.466	-44.09	0.9987	1.2997	12
3750	1.467	-46.59	0.9650	6.2710	6
4060	1.461	-46.87	0.9519	7.2385	6
4395	1.503	-50.76	0.9997	0.6547	5

1991 NISSAN SENTRA
2 DR SEDAN 1.6 L M5OD
VIN: 1N4EB32A9MC727980

RPM	Slope psi / kPa	Intercept psi	R^2	$\sigma_{y\|x}$	No of Data Points
2210	1.809	-50.98	0.9977	2.2714	5
2930	1.902	-55.43	0.9974	2.2287	6
3640	1.934	-48.87	0.9990	1.4243	6
4340	1.772	-34.86	0.9897	4.5973	11
5080	1.480	-18.31	0.9534	8.1272	6
5520	1.706	-32.31	0.9815	5.8557	6
5980	1.935	-50.11	0.9920	4.3450	6

1990 NISSAN PICKUP
KING CAB 2.4 L M5OD
VIN: 1N4EB32A9MC727980

RPM	Slope psi / kPa	Intercept psi	R^2	$\sigma_{y\|x}$	No of Data Points
920	1.532	-40.08	0.9925	3.9713	6
1300	1.644	-39.67	0.9979	1.8780	10
1915	1.769	-45.79	0.9986	1.6934	5
2530	1.894	-54.38	0.9973	2.3034	6
3150	1.760	-43.44	0.9969	2.1935	6
3775	1.760	-40.64	0.9957	2.9413	11
4400	1.855	-44.59	0.9966	2.8161	4
4780	1.759	-42.10	0.9938	3.4846	5
5175	1.649	-35.91	0.9821	4.8551	6

1992 GEO METRO
3 DR HATCH 1.0 L M5OD
VIN: 2C1MR24C4N6704201

RPM	Slope psi / kPa	Intercept psi	R^2	$\sigma_{y\|x}$	No of Data Points
998	1.721	-51.62	0.9929	3.7926	5
1425	1.837	-55.99	0.9932	3.7934	11
2109	2.054	-64.75	0.9924	4.1925	6
2793	2.390	-88.71	0.9942	4.2127	6
3477	2.379	-85.39	0.9969	3.0603	6
4161	2.223	-72.56	0.9995	1.1713	10
4845	2.243	-77.50	0.9998	0.6594	6
5273	2.233	-80.99	0.9996	1.1838	6
5700	2.224	-87.30	0.9991	1.9639	4

1991 TOYOTA MR2 TURBO
3 DR LFTBK 2.0 L M5
VIN: JT25W22NXM0015597

RPM	Slope psi / kPa	Intercept psi	R^2	$\sigma_{y\|x}$	No of Data Points
1040	1.497	-39.12	0.9918	3.6765	6
1500	1.561	-43.96	0.9944	4.0131	9
2200	1.355	-16.74	0.9919	3.0831	4
2950	1.415	-21.72	0.9637	7.0640	4
3675	1.516	-34.90	0.9947	3.7655	8
4350	1.500	-32.52	0.9965	2.9419	17
5090	1.559	-35.59	0.9992	1.6817	3
5550	Only two data points at this RPM				
6000	1.369	-35.08	0.9896	3.6185	4

1991 CHRY NEW YORK
4 DR SEDAN 3.3 L L4
VIN: 1C3X466R9MD260

RPM	Slope psi / kPa	Intercept psi	R^2	$\sigma_{y\|x}$	No of Data Points
1116	Only two data points at this RPM				
1665	Only two data points at this RPM				
2222	1.982	-64.08	0.9722	8.8408	4
2775	1.759	-46.23	0.9973	2.3446	5
3320	1.980	-56.98	0.9845	6.3687	10
3850	1.958	-52.32	0.9958	4.3713	3
4180	2.141	-61.48	0.9961	1.8408	3
4510	1.944	-55.66	0.9993	1.0263	4

1991 DODGE SHADOW
4 DR HATCH 2.5 L L3
VIN: 1B3XP48D8MN638550

RPM	Slope psi / kPa	Intercept psi	R^2	$\sigma_{y\|x}$	No of Data Points
1425	1.593	-44.64	0.9970	1.0160	5
2110	1.468	-38.10	0.9961	2.4126	4
2770	1.431	-36.88	0.9983	1.3315	6
3450	1.484	-40.95	0.9985	1.3288	6
4130	1.562	-47.58	0.9995	0.7723	10
4850	1.553	-51.72	0.9984	1.3190	5
5230	1.497	-51.63	0.9989	1.0564	5
5700	1.380	-51.23	0.9981	1.4116	4

1991 SATURN SL2
4 DR SEDAN 1.9 L L4AEOD
VIN: 1G8ZK5471MZ102666

RPM	Slope psi / kPa	Intercept psi	R^2	$\sigma_{y\|x}$	No of Data Points
1610	1.263	-26.34	0.9770	1.9119	4
2350	1.576	-38.90	0.8317	16.7249	5
3120	1.860	-51.31	0.9843	5.5225	5
3880	1.925	-56.41	0.9962	3.1070	5
4650	2.075	-59.39	0.9899	4.9678	10
5400	2.084	-60.34	0.9898	5.3358	5
5850	2.154	-70.17	0.9944	4.0372	5
6250	2.111	-76.66	0.9900	5.2961	5

1990 GMC SIERRA
2 DR PKUP 5.0 L L4OD
VIN: 1GTDC14H9LE506190

RPM	Slope psi / kPa	Intercept psi	R^2	$\sigma_{y\|x}$	No of Data Points
1135	0.286	-8.10	0.9767	0.9566	8
1550	0.444	-11.44	0.9113	3.6949	3
2050	0.521	-13.38	0.9855	1.6500	4
2550	0.618	-14.67	0.9840	2.0322	4
3050	0.713	-16.73	0.9901	1.7521	10
3550	0.871	-25.38	0.9784	3.1084	7
3880	1.166	-41.09	0.9873	3.2288	5
4200	1.220	-45.05	0.9658	6.0115	4

1991 GMC SONOMA
4x2 PKUP 2.8 L M5OD
VIN: 1GTCS14R7MO534382

RPM	Slope psi / kPa	Intercept psi	R^2	$\sigma_{y\|x}$	No of Data Points
825	1.513	-60.47	0.9997	0.6805	5
1200	1.770	-78.63	0.9354	8.8373	8
1750	1.559	-57.49	0.9931	3.4145	5
2350	1.645	-61.93	0.9954	2.7203	6
2900	1.706	-66.13	0.9992	1.2391	5
3520	1.698	-67.00	0.9957	2.5584	8
4050	1.648	-64.00	0.9696	7.4549	5
4440	1.728	-71.45	0.9866	4.5258	6
4800	1.636	-64.71	0.9847	4.4507	6

1991 GMC SONOMA
EXT CAB PICKUP 4.3 L L4OD
VIN: 1GTCS19Z3MO517197

RPM	Slope psi / kPa	Intercept psi	R^2	$\sigma_{y\|x}$	No of Data Points
1120	1.271	-34.59	0.9884	2.8669	4
1620	1.255	-23.59	0.9718	5.7191	3
2150	1.670	-44.29	0.9987	1.6226	3
2670	1.485	-36.20	0.9986	1.4456	3
3200	1.556	-40.88	0.9966	1.9423	8
3740	1.533	-41.76	0.9930	3.4380	4
4050	1.329	-37.17	0.9799	5.0412	4
4400	1.050	-32.42	0.9660	5.1522	3

1990 TOYOTA 4RUNNER
4x4 5 DR 3.0 L L4AEOD
VIN: JT3VN39W5L0017546

RPM	Slope psi / kPa	Intercept psi	R^2	$\sigma_{y\|x}$	No of Data Points
1373	1.5782	-42.45	0.9638	2.0135	4
1900	1.4674	-39.45	0.9964	2.2949	3
2750	2.0727	-80.73	0.9975	2.6542	5
3531	2.5664	-104.17	0.9888	6.9969	4
3811	2.5293	-96.27	0.9952	4.0659	6
4488	Not enough data				
5042	1.7127	-57.83	0.9973	1.8199	4
5246	1.6153	-54.93	0.9668	5.0528	5

1992 MERCEDES-BENZ 300E
4 DR SEDAN 2.6 L A4
VIN: WDBEA26D61B235485

RPM	Slope psi / kPa	Intercept psi	R^2	$\sigma_{y\|x}$	No of Data Points
1124	Not enoug				
1570	1.4917	-42.82	0.9959	1.9910	6
2316	1.8152	-55.54	0.9960	3.0047	4
3049	1.8337	-51.71	0.9980	2.1544	4
3800	1.9816	-59.65	1.0000	0.2629	4
4549	2.0011	-56.20	0.9997	0.9325	4
5306	2.0776	-62.77	0.9996	1.1114	4
5747	2.1152	-68.98	0.9994	1.3488	5
6209	2.0723	-72.83	0.9998	0.7304	4

1991 SAAB 9000
5 DR HTBK 2.3 L M5
VIN: Y53CK55B2M1001898

RPM	Slope psi / kPa	Intercept psi	R^2	$\sigma_{y\|x}$	No of Data Points
945	1.6862	-58.74	0.9970	2.3406	5
1245	1.7343	-55.27	0.9839	5.4520	11
1633	1.8737	-54.12	0.9962	3.0022	5
2283	1.8303	-54.40	0.9880	5.1884	5
2848	2.6397	-120.63	0.9971	3.6163	4
3684	2.7514	-120.97	0.9889	6.1903	6
4318	2.7967	-126.86	0.9973	3.3598	6
4634	2.7595	-128.22	0.9963	3.6155	5
5230	2.4666	-114.52	0.9954	3.1623	5

1991 HONDA ACCORD
4 DR SEDAN 2.2 L L4OD
VIN: 1HGCB7654MAI36491

RPM	Slope psi / kPa	Intercept psi	R^2	$\sigma_{y\|x}$	No of Data Points
1298	1.0333	-25.73	0.9990	0.2471	4
1924	Not enough data				
2535	1.9755	-63.06	0.9921	4.4093	5
3153	1.9668	-54.19	0.9934	3.5966	6
3774	2.0026	-49.36	0.9983	2.1712	10
4384	2.2204	-57.93	0.9994	1.3205	4
4762	2.1692	-55.46	1.0000	0.0346	3
5200	1.7502	-40.67	0.9894	4.7829	4

1991 CHEV CAMARO
2 DR LIFT 5.7 L L4OD
VIN: 1G1FP2381ML190343

RPM	Slope psi / kPa	Intercept psi	R^2	$\sigma_{y\|x}$	No of Data Points
1214	1.7879	-58.73	0.9997	0.1995	4
1690	Not enough data				
2328	1.3404	-28.49	0.9921	3.1110	3
2938	Not enough data				
3524	2.0270	-56.14	0.9972	0.8375	4
4099	2.1565	-69.25	1.0000	0.0994	3
4454	2.2258	-77.76	1.0000	0.0162	3
4814	1.9590	-70.17	0.9979	0.9979	3

1991 DODGE CRVN
MINIVAN 3.0 L L3
VIN: 2B4GK4530MR273404

RPM	Slope psi / kPa	Intercept psi	R^2	$\sigma_{y\|x}$	No of Data Points
1234	Not enough data				
1822	Not enough data				
2401	1.5682	-26.76	0.9935	3.2571	3
2961	1.8760	-47.07	0.9987	1.6699	5
3498	1.9380	-49.15	0.9982	1.8538	9
4136	1.9435	-47.97	0.9999	0.3774	3
4517	1.7642	-42.11	0.9904	3.4674	4
4868	1.9602	-59.18	0.9989	1.3830	5

1992 FORD CRWN VIC
4 DR SEDAN 4.6 L L4AEOD
VIN: 2FACP74W4NX113934

RPM	Slope psi / kPa	Intercept psi	R^2	$\sigma_{y\|x}$	No of Data Points
1172	1.1529	-31.85	0.9213	7.3386	3
1734	1.5579	-57.53	0.9970	1.6976	4
2297	1.4955	-52.76	0.9999	0.4429	4
2822	1.5146	-53.76	0.9510	7.7331	4
3408	Not enough data				
3971	1.5597	-62.21	0.9914	3.5891	4
4313	1.3511	-53.61	0.9984	1.2045	3
4675	1.1065	-42.53	0.9603	4.9154	4

1991 PONTIAC GRAN PRIX
4 DR SEDAN 2.3 L Q4 L3
VIN: 1G2WH54D8MF271439

RPM	Slope psi / kPa	Intercept psi	R^2	$\sigma_{y\|x}$	No of Data Points
1486	2.2641	-81.21	0.9744	3.1371	3
2224	1.6392	-50.28	0.9970	2.3677	3
2921	1.7096	-50.41	0.9981	1.9610	4
3629	1.8697	-61.34	0.9990	1.4007	4
4349	1.8050	-53.16	0.9924	3.2701	9
5067	2.1261	-66.75	0.9936	3.4897	4
5517	2.0666	-65.54	0.9994	1.0034	4
5928	1.9196	-62.25	0.9906	4.8184	4

1992 DODGE DAKOTA
4x2 PKUP 5.2 L L4OD
VIN: 1B7GL23Y5NS502694

RPM	Slope psi / kPa	Intercept psi	R^2	$\sigma_{y\|x}$	No of Data Points
1096	1.6109	-57.55	0.9904	0.9042	3
1629	1.2771	-39.58	0.9632	6.0561	3
2157	Not enough data				
2698	1.2587	-37.96	0.9907	3.7830	3
3204	1.6185	-52.81	0.9986	0.7117	5
3735	1.5731	-39.25	0.9997	0.7216	3
4066	Not enough data				
4409	1.6141	-44.47	0.9819	5.6106	3

1991 VW JETTA
4 DR CUSTOM 1.8 L A3
VIN: 3VWRA21G3MM027141

RPM	Slope psi / kPa	Intercept psi	R^2	$\sigma_{y\|x}$	No of Data Points
1399	1.9135	-61.09	0.9959	0.7015	3
2127	1.5077	-38.80	0.9865	4.6277	3
2811	1.7588	-51.83	0.9991	1.4060	4
3495	1.7518	-52.18	0.9977	2.2361	4
4173	1.7073	-49.42	0.9955	2.8140	11
4861	1.7403	-56.42	0.9997	0.7431	5
5290	1.7503	-62.79	1.0000	0.2008	3
5687	1.6182	-67.80	0.9995	0.7498	3

1990 BUICK LESABRE
4 DR SEDAN 3.8 L L4OD
VIN: 1G4HP54C2LH473366

RPM	Slope psi / kPa	Intercept psi	R^2	$\sigma_{y\|x}$	No of Data Points
1094	1.2508	-31.83	0.9862	0.9632	3
1645	Not enough data				
2175	1.3963	-39.18	0.9930	2.8663	4
2734	1.3510	-35.80	0.9975	1.8686	3
3232	1.3777	-36.35	0.9968	1.5018	3
3745	1.7514	-58.49	0.9948	3.8782	4
4098	1.7598	-62.11	0.9910	3.5505	6
4401	Not enough data				

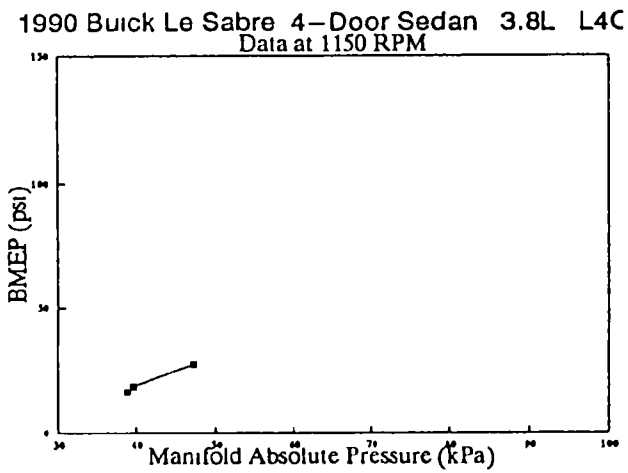
1990 Buick Le Sabre 4-Door Sedan 3.8L L4C
Data at 1150 RPM
BMEP (psi)
Manifold Absolute Pressure (kPa)

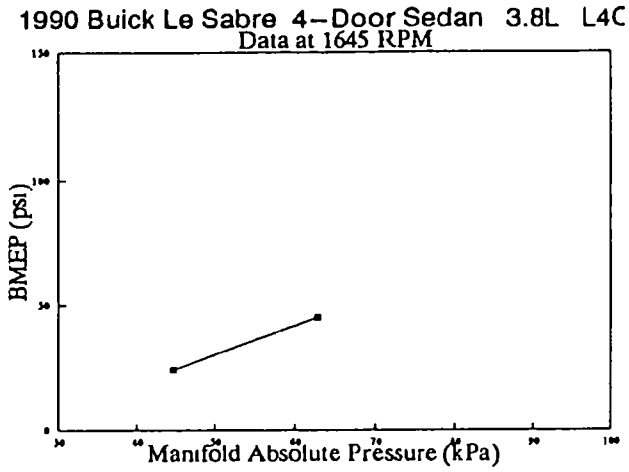
1990 Buick Le Sabre 4-Door Sedan 3.8L L4C
Data at 1645 RPM
BMEP (psi)
Manifold Absolute Pressure (kPa)

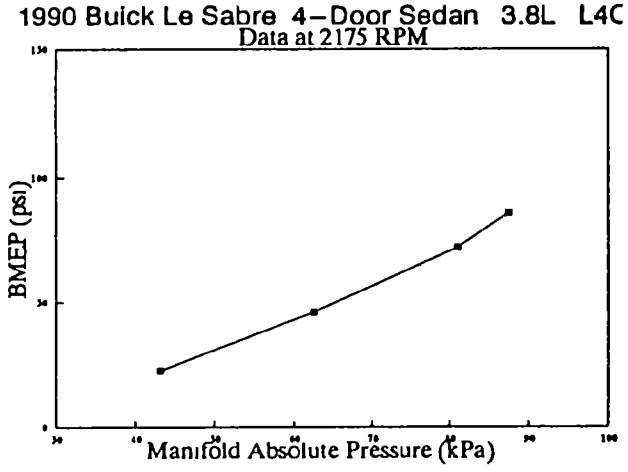
1990 Buick Le Sabre 4-Door Sedan 3.8L L4C
Data at 2175 RPM
BMEP (psi)
Manifold Absolute Pressure (kPa)

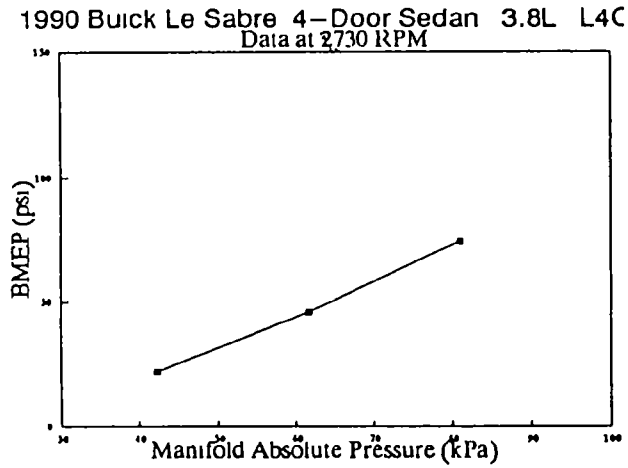
1990 Buick Le Sabre 4-Door Sedan 3.8L L4C
Data at 2730 RPM
BMEP (psi)
Manifold Absolute Pressure (kPa)

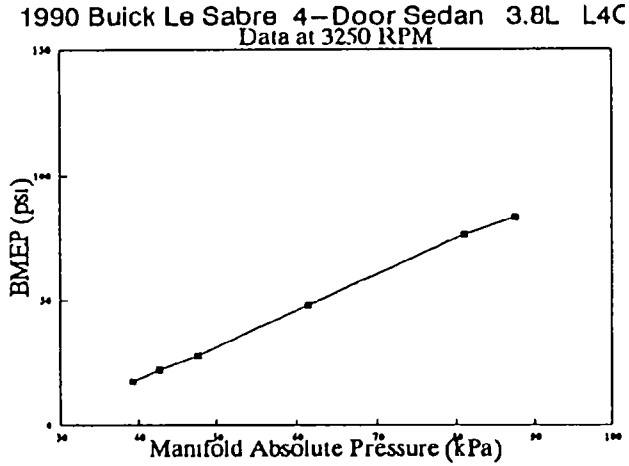
1990 Buick Le Sabre 4-Door Sedan 3.8L L4C
Data at 3250 RPM
BMEP (psi)
Manifold Absolute Pressure (kPa)

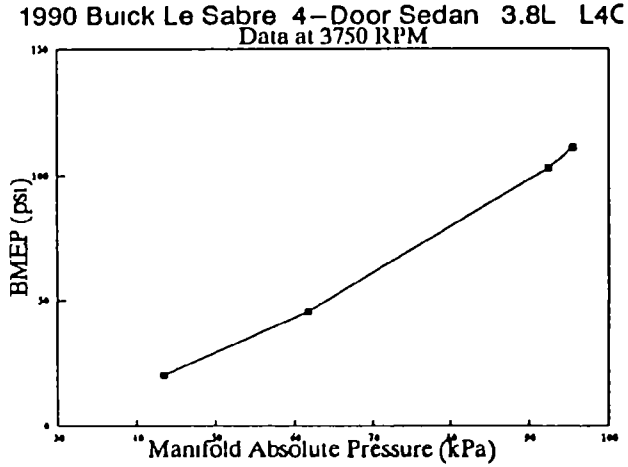
1990 Buick Le Sabre 4-Door Sedan 3.8L L4C
Data at 3750 RPM
BMEP (psi)
Manifold Absolute Pressure (kPa)

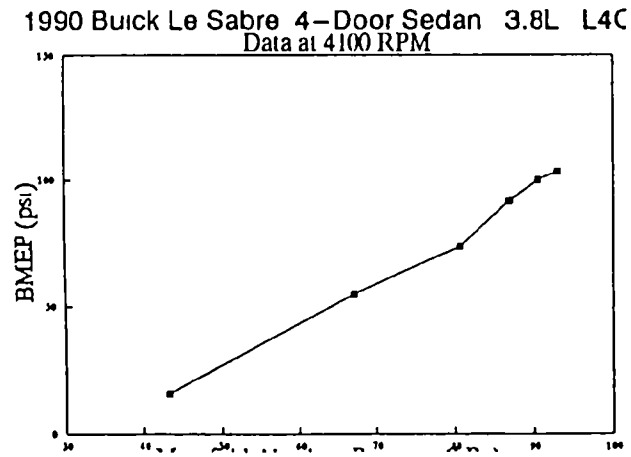
1990 Buick Le Sabre 4-Door Sedan 3.8L L4C
Data at 4100 RPM
BMEP (psi)

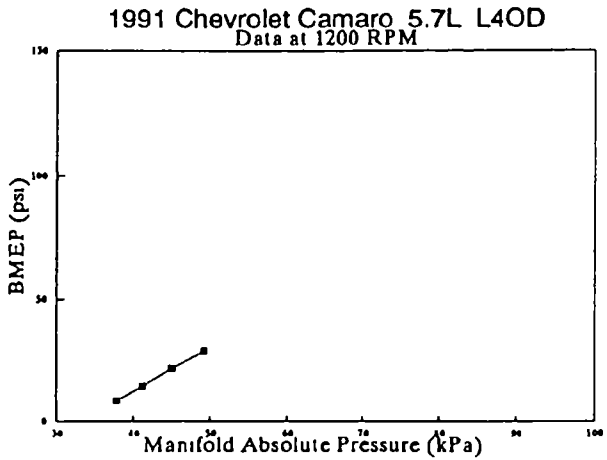
1991 Chevrolet Camaro 5.7L L4OD
Data at 1200 RPM
BMEP (psi)
Manifold Absolute Pressure (kPa)

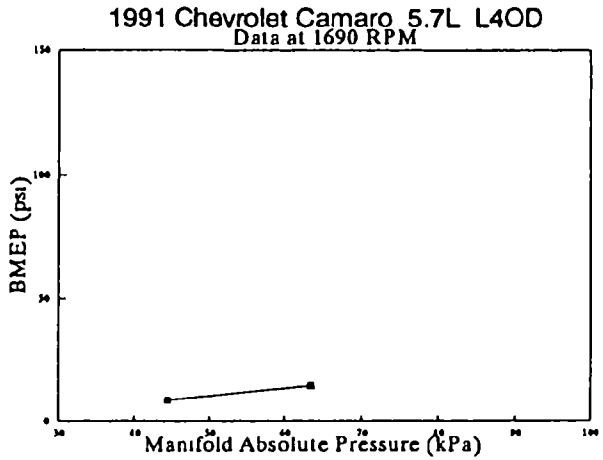
1991 Chevrolet Camaro 5.7L L4OD
Data at 1690 RPM
BMEP (psi)
Manifold Absolute Pressure (kPa)

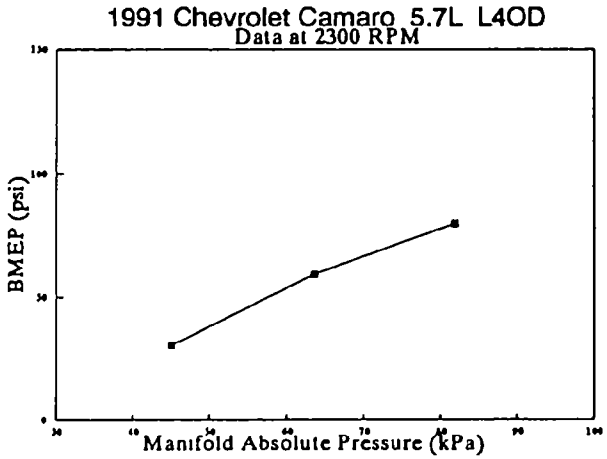
1991 Chevrolet Camaro 5.7L L4OD
Data at 2300 RPM
BMEP (psi)
Manifold Absolute Pressure (kPa)

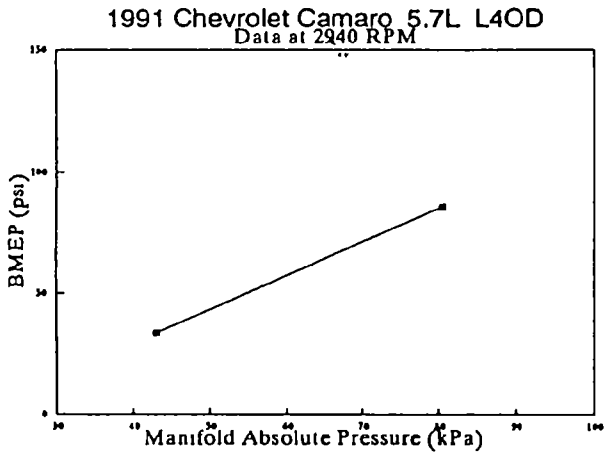
1991 Chevrolet Camaro 5.7L L4OD
Data at 2940 RPM
BMEP (psi)
Manifold Absolute Pressure (kPa)

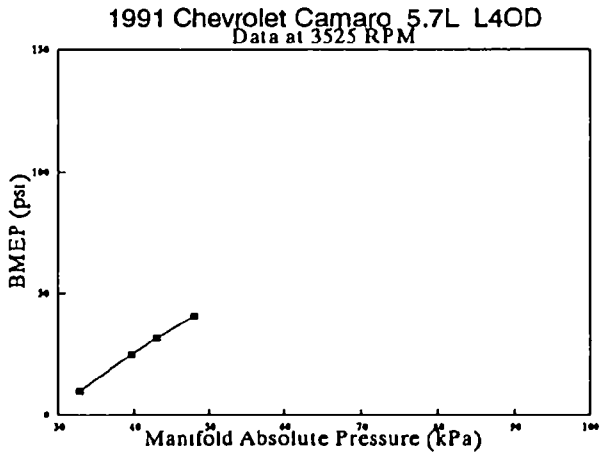
1991 Chevrolet Camaro 5.7L L4OD
Data at 3525 RPM
BMEP (psi)
Manifold Absolute Pressure (kPa)

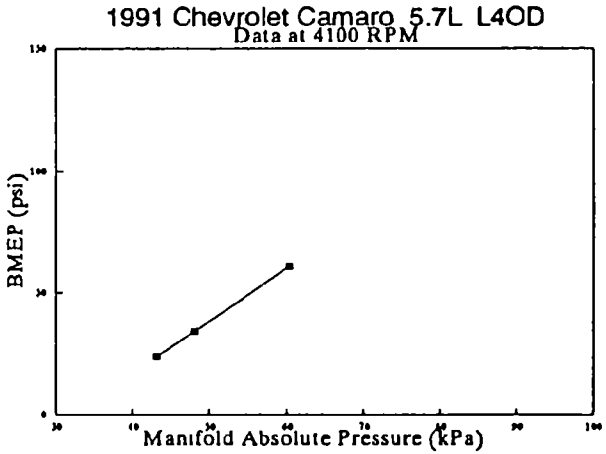
1991 Chevrolet Camaro 5.7L L4OD
Data at 4100 RPM
BMEP (psi)
Manifold Absolute Pressure (kPa)

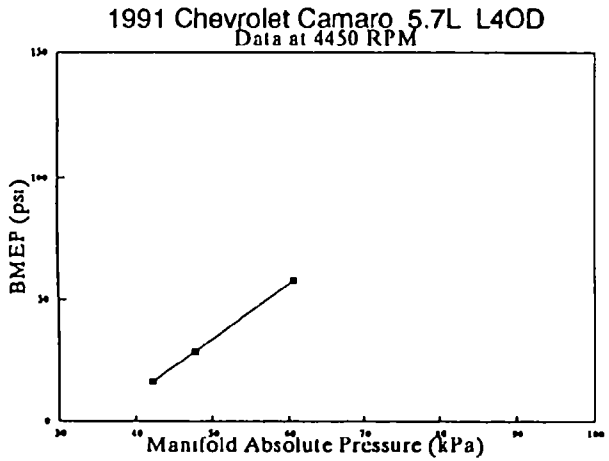
1991 Chevrolet Camaro 5.7L L4OD
Data at 4450 RPM
BMEP (psi)
Manifold Absolute Pressure (kPa)

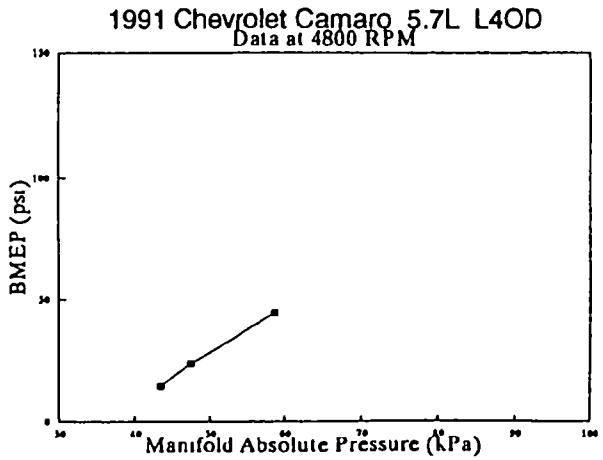
1991 Chevrolet Camaro 5.7L L4OD
Data at 4800 RPM
BMEP (psi)
Manifold Absolute Pressure (kPa)

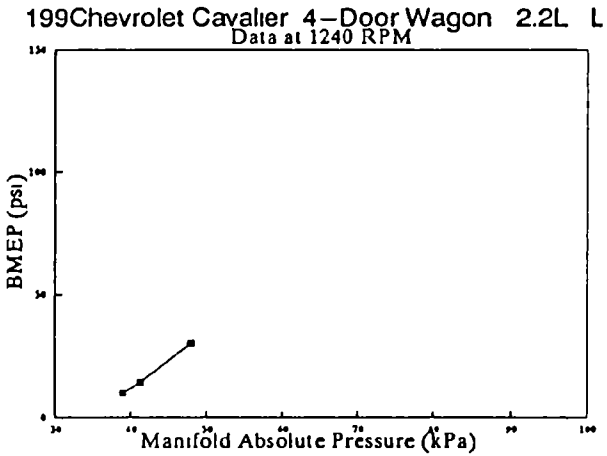
199Chevrolet Cavalier 4-Door Wagon 2.2L L
Data at 1240 RPM
BMEP (psi)
Manifold Absolute Pressure (kPa)

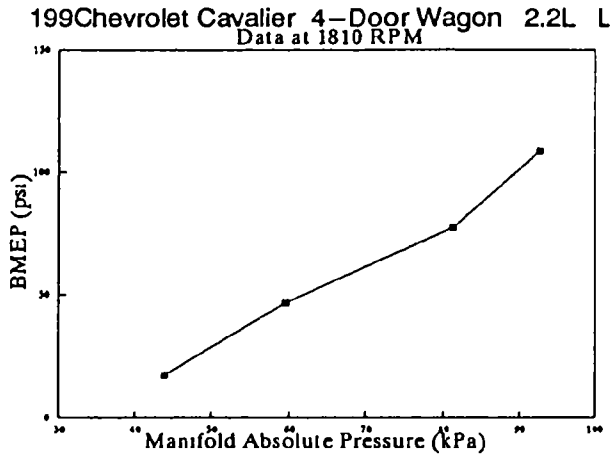
199Chevrolet Cavalier 4-Door Wagon 2.2L L
Data at 1810 RPM
BMEP (psi)
Manifold Absolute Pressure (kPa)

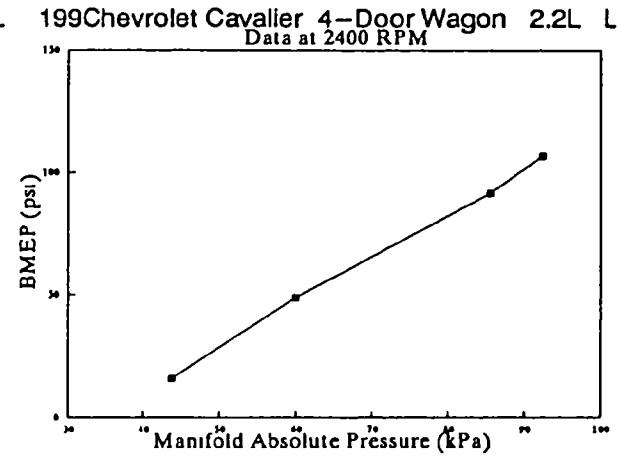
199Chevrolet Cavalier 4-Door Wagon 2.2L L
Data at 2400 RPM
BMEP (psi)
Manifold Absolute Pressure (kPa)

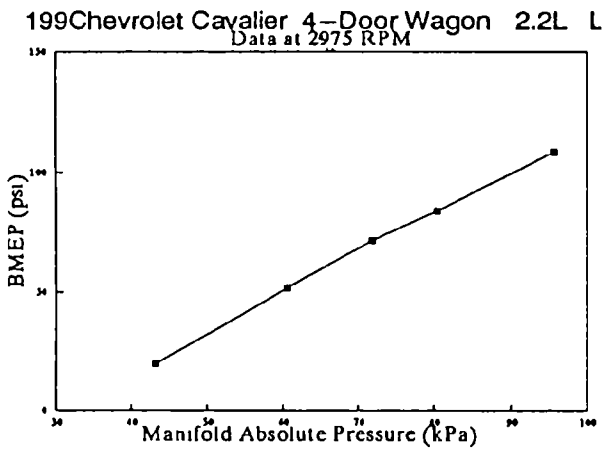
199Chevrolet Cavalier 4-Door Wagon 2.2L L
Data at 2975 RPM
BMEP (psi)
Manifold Absolute Pressure (kPa)

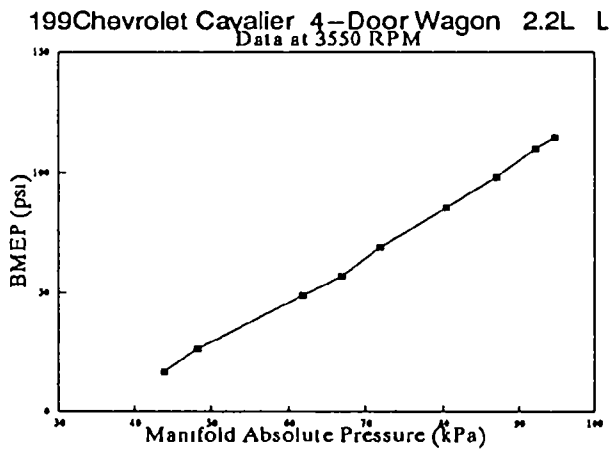
199Chevrolet Cavalier 4-Door Wagon 2.2L L
Data at 3550 RPM
BMEP (psi)
Manifold Absolute Pressure (kPa)

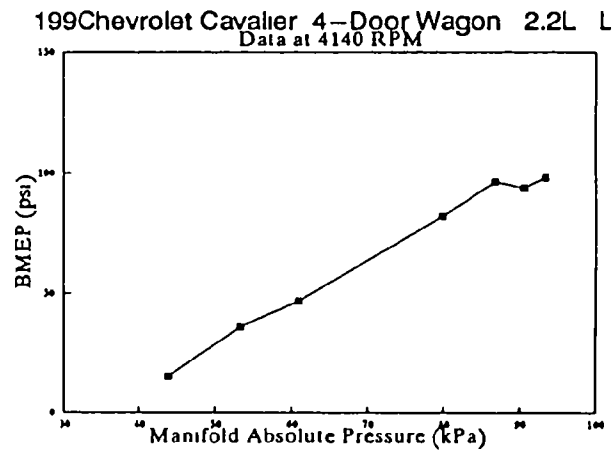
199Chevrolet Cavalier 4-Door Wagon 2.2L L
Data at 4140 RPM
BMEP (psi)
Manifold Absolute Pressure (kPa)

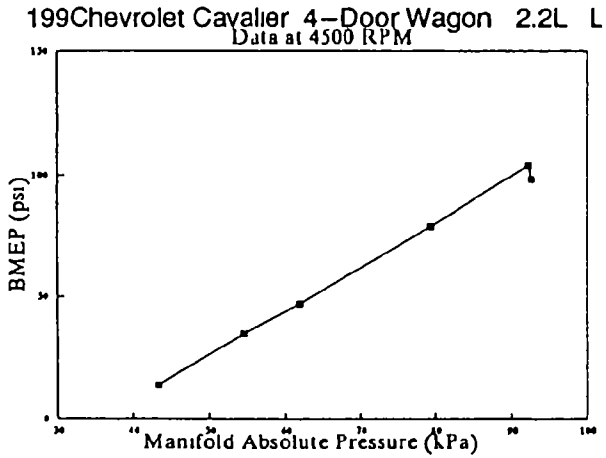
199Chevrolet Cavalier 4-Door Wagon 2.2L L
Data at 4500 RPM
BMEP (psi)
Manifold Absolute Pressure (kPa)

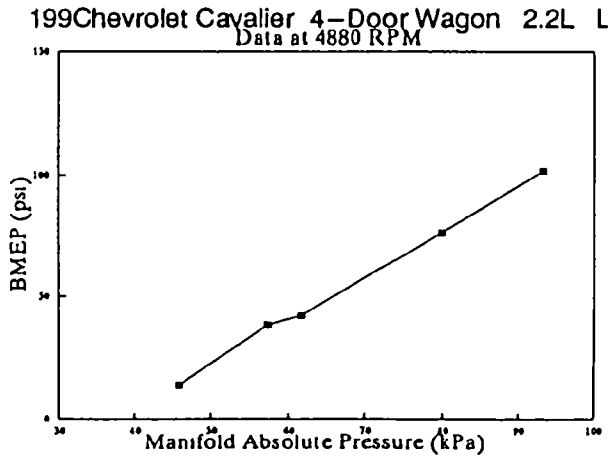
199Chevrolet Cavalier 4-Door Wagon 2.2L L
Data at 4880 RPM
BMEP (psi)
Manifold Absolute Pressure (kPa)

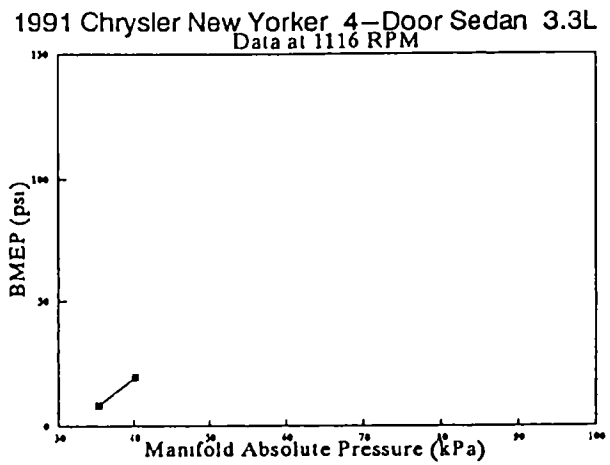
1991 Chrysler New Yorker 4-Door Sedan 3.3L
Data at 1116 RPM
BMEP (psi)
Manifold Absolute Pressure (kPa)

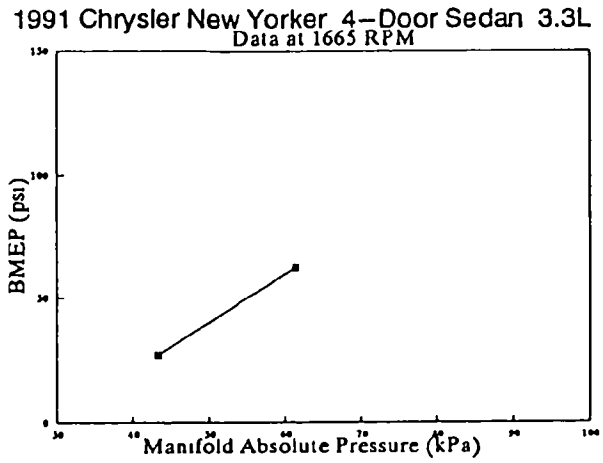
1991 Chrysler New Yorker 4-Door Sedan 3.3L
Data at 1665 RPM
BMEP (psi)
Manifold Absolute Pressure (kPa)

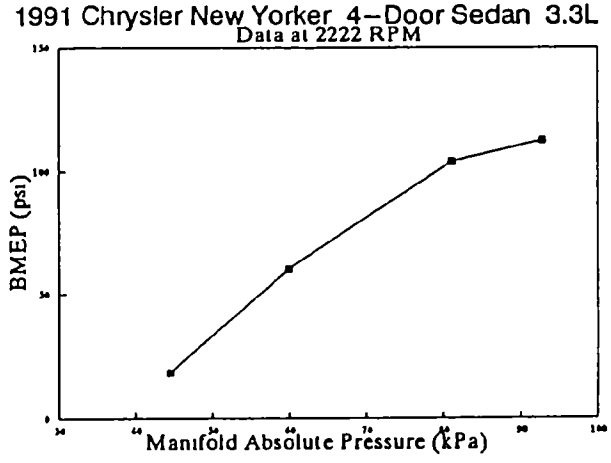
1991 Chrysler New Yorker 4-Door Sedan 3.3L
Data at 2222 RPM
BMEP (psi)
Manifold Absolute Pressure (kPa)

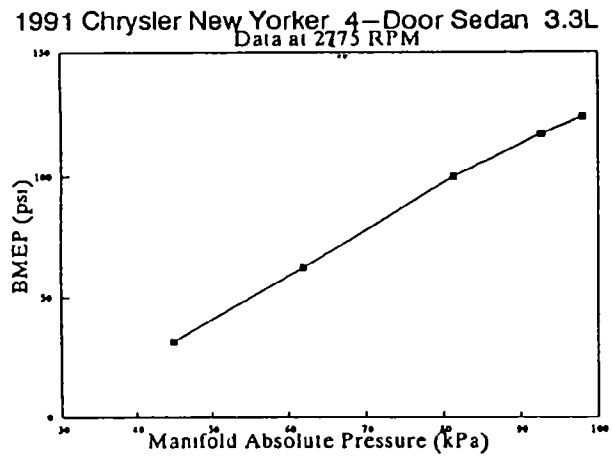
1991 Chrysler New Yorker 4-Door Sedan 3.3L
Data at 2775 RPM
BMEP (psi)
Manifold Absolute Pressure (kPa)

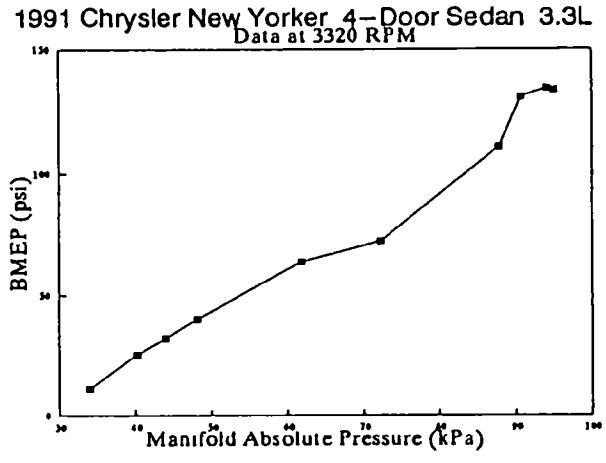
1991 Chrysler New Yorker 4-Door Sedan 3.3L
Data at 3320 RPM
BMEP (psi)
Manifold Absolute Pressure (kPa)

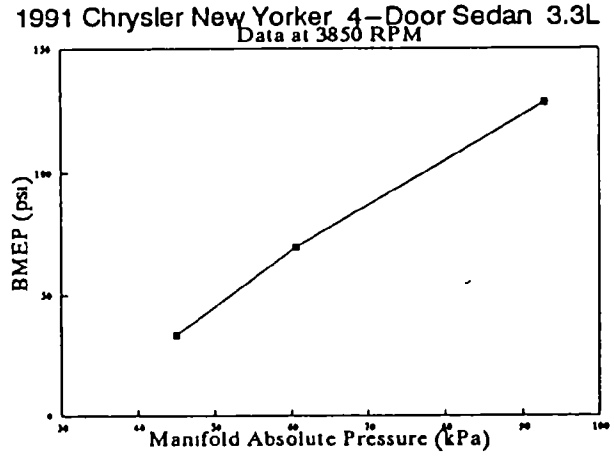
1991 Chrysler New Yorker 4-Door Sedan 3.3L
Data at 3850 RPM
BMEP (psi)
Manifold Absolute Pressure (kPa)

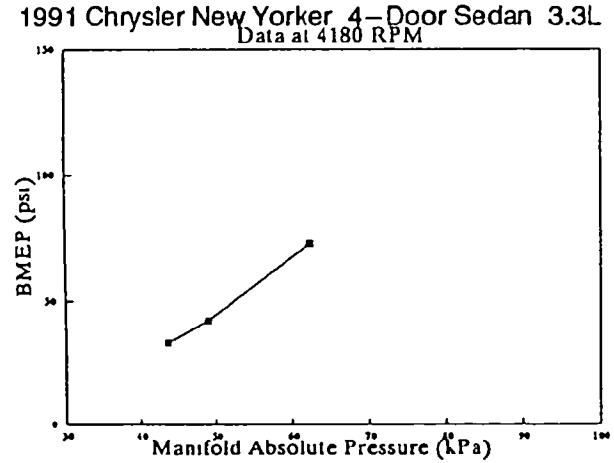
1991 Chrysler New Yorker 4-Door Sedan 3.3L
Data at 4180 RPM
BMEP (psi)
Manifold Absolute Pressure (kPa)

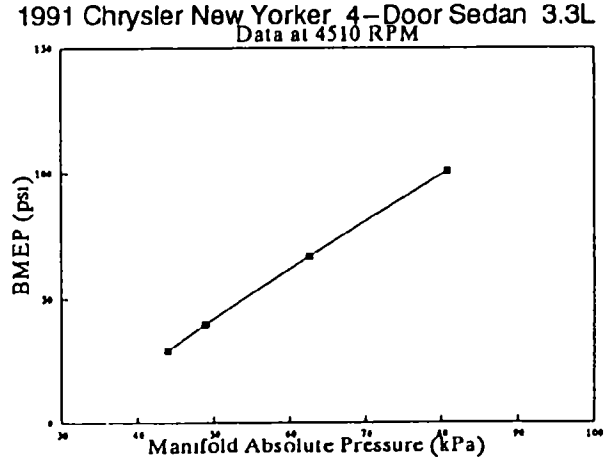
1991 Chrysler New Yorker 4-Door Sedan 3.3L
Data at 4510 RPM
BMEP (psi)
Manifold Absolute Pressure (kPa)

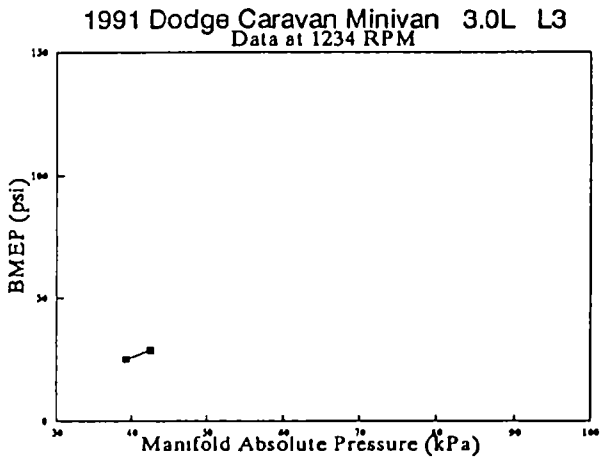
1991 Dodge Caravan Minivan 3.0L L3
Data at 1234 RPM
BMEP (psi)
Manifold Absolute Pressure (kPa)

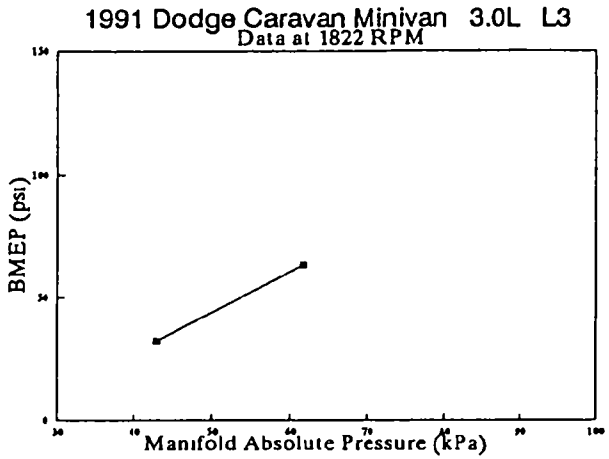
1991 Dodge Caravan Minivan 3.0L L3
Data at 1822 RPM
BMEP (psi)
Manifold Absolute Pressure (kPa)

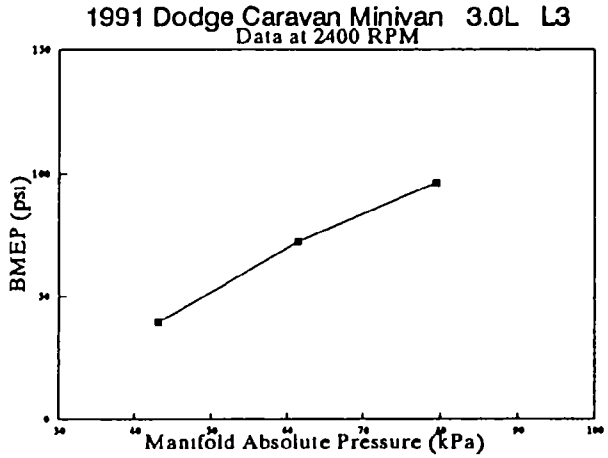
1991 Dodge Caravan Minivan 3.0L L3
Data at 2400 RPM
BMEP (psi)
Manifold Absolute Pressure (kPa)

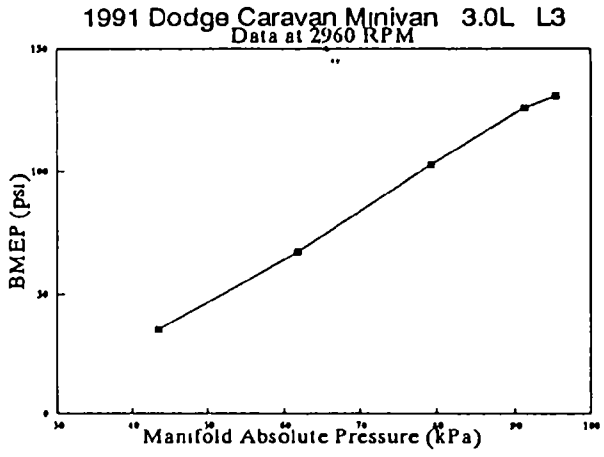
1991 Dodge Caravan Minivan 3.0L L3
Data at 2960 RPM
BMEP (psi)
Manifold Absolute Pressure (kPa)

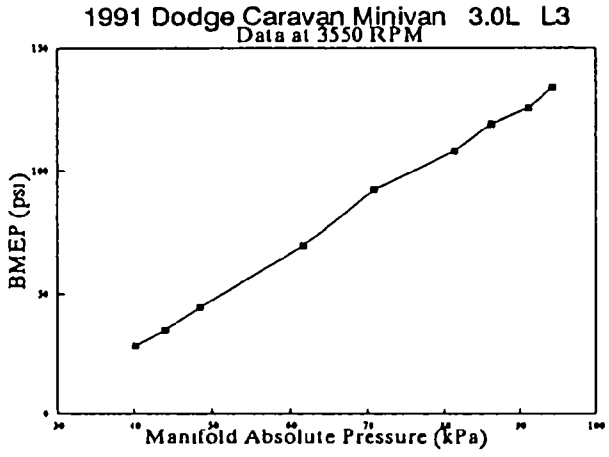
1991 Dodge Caravan Minivan 3.0L L3
Data at 3550 RPM
BMEP (psi)
Manifold Absolute Pressure (kPa)

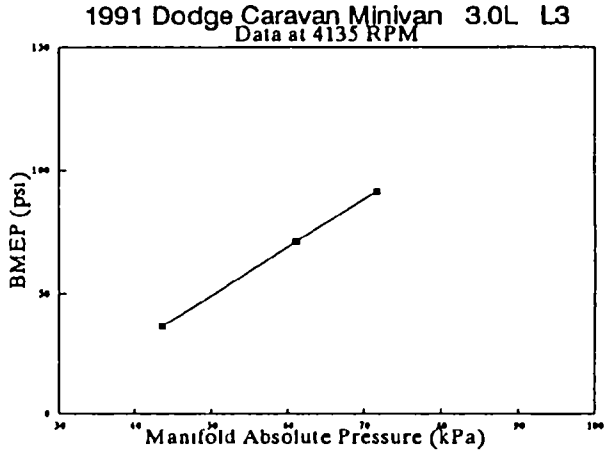
1991 Dodge Caravan Minivan 3.0L L3
Data at 4135 RPM
BMEP (psi)
Manifold Absolute Pressure (kPa)

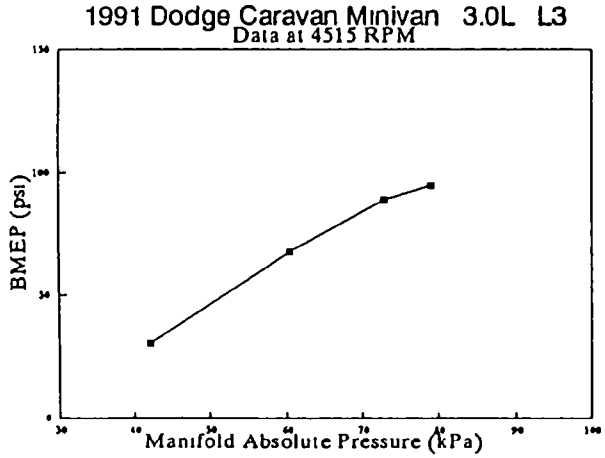
1991 Dodge Caravan Minivan 3.0L L3
Data at 4515 RPM
BMEP (psi)
Manifold Absolute Pressure (kPa)

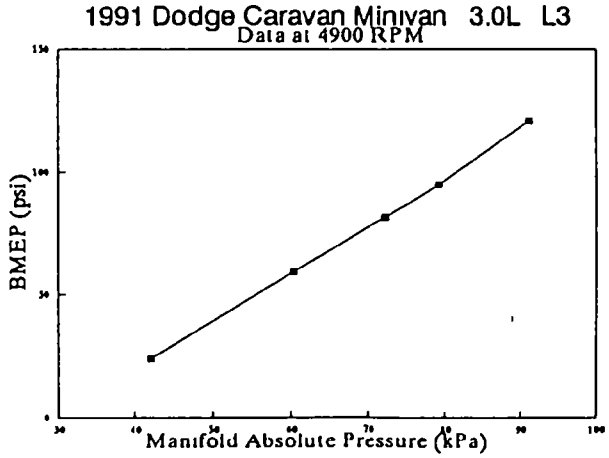
1991 Dodge Caravan Minivan 3.0L L3
Data at 4900 RPM
BMEP (psi)
Manifold Absolute Pressure (kPa)

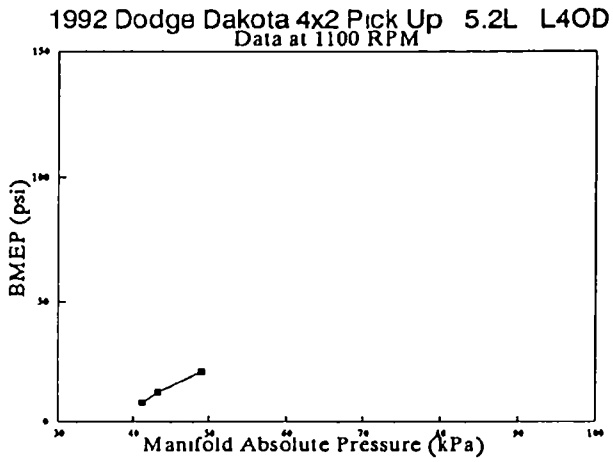
1992 Dodge Dakota 4x2 Pick Up 5.2L L4OD
Data at 1100 RPM
BMEP (psi)
Manifold Absolute Pressure (kPa)

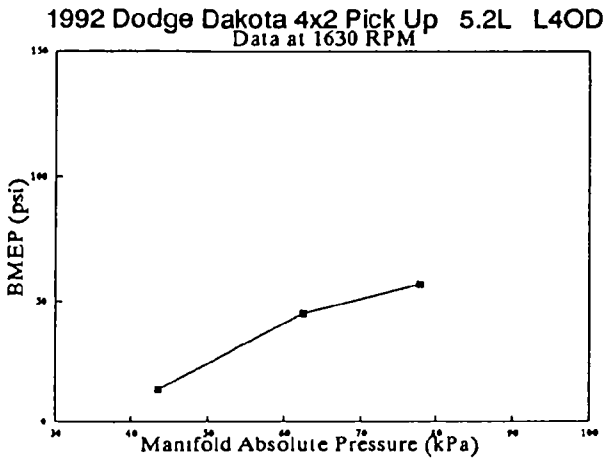
1992 Dodge Dakota 4x2 Pick Up 5.2L L4OD
Data at 1630 RPM
BMEP (psi)
Manifold Absolute Pressure (kPa)

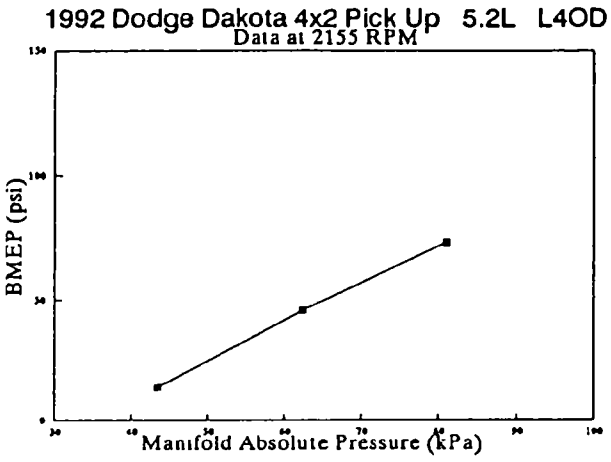
1992 Dodge Dakota 4x2 Pick Up 5.2L L4OD
Data at 2155 RPM
BMEP (psi)
Manifold Absolute Pressure (kPa)

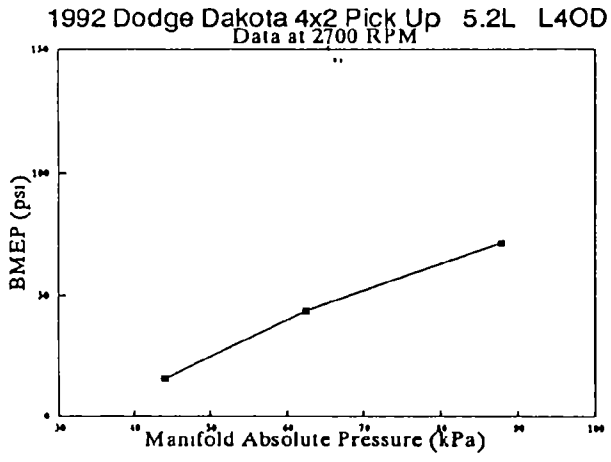
1992 Dodge Dakota 4x2 Pick Up 5.2L L4OD
Data at 2700 RPM
BMEP (psi)
Manifold Absolute Pressure (kPa)

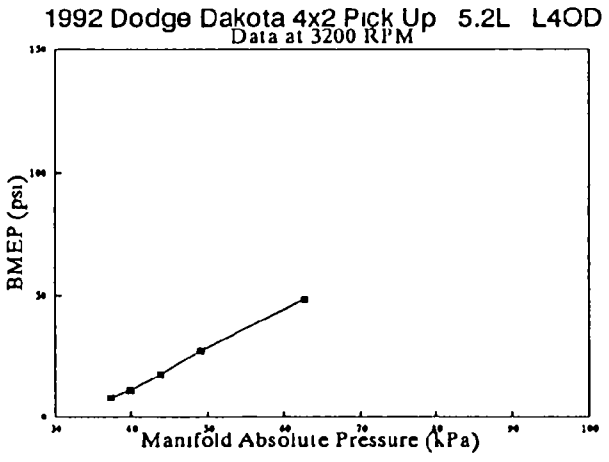
1992 Dodge Dakota 4x2 Pick Up 5.2L L4OD
Data at 3200 RPM
BMEP (psi)
Manifold Absolute Pressure (kPa)

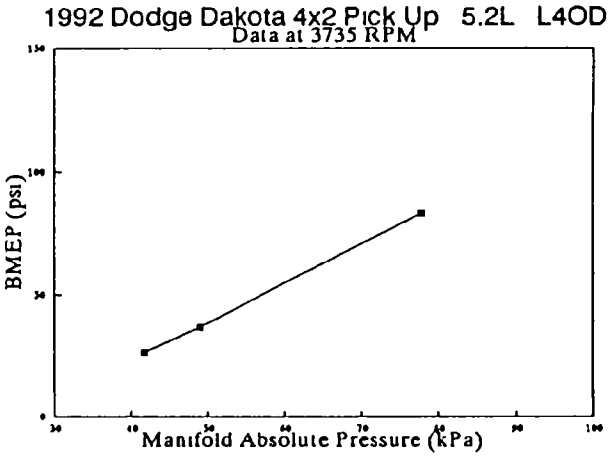
1992 Dodge Dakota 4x2 Pick Up 5.2L L4OD
Data at 3735 RPM
BMEP (psi)
Manifold Absolute Pressure (kPa)

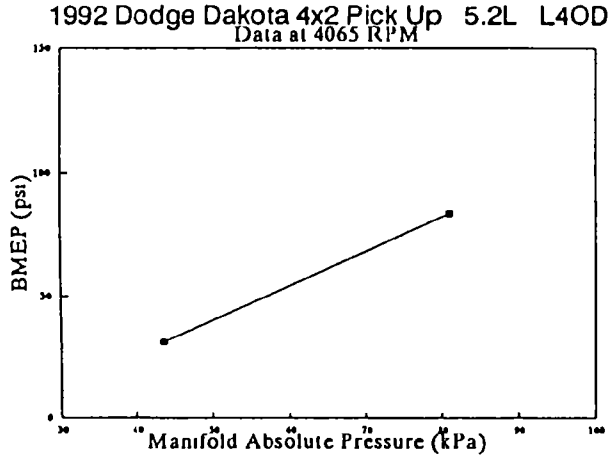
1992 Dodge Dakota 4x2 Pick Up 5.2L L4OD
Data at 4065 RPM
BMEP (psi)
Manifold Absolute Pressure (kPa)

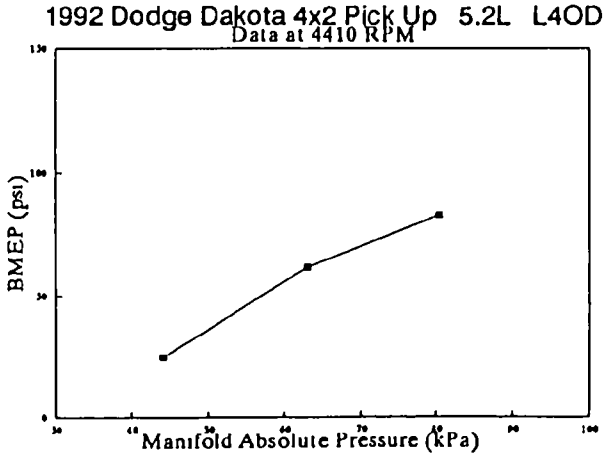
1992 Dodge Dakota 4x2 Pick Up 5.2L L4OD
Data at 4410 RPM
BMEP (psi)
Manifold Absolute Pressure (kPa)

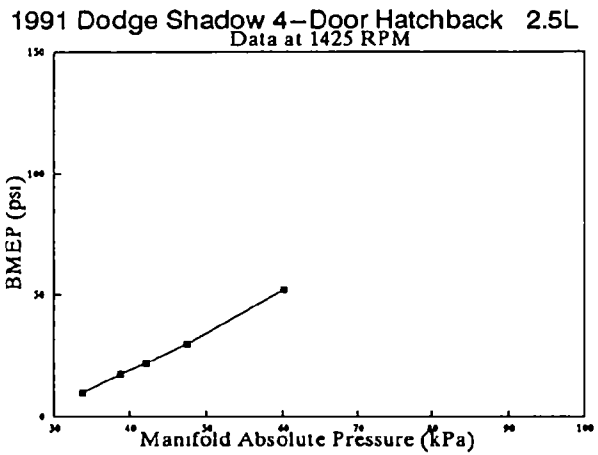
1991 Dodge Shadow 4-Door Hatchback 2.5L
Data at 1425 RPM
BMEP (psi)
Manifold Absolute Pressure (kPa)

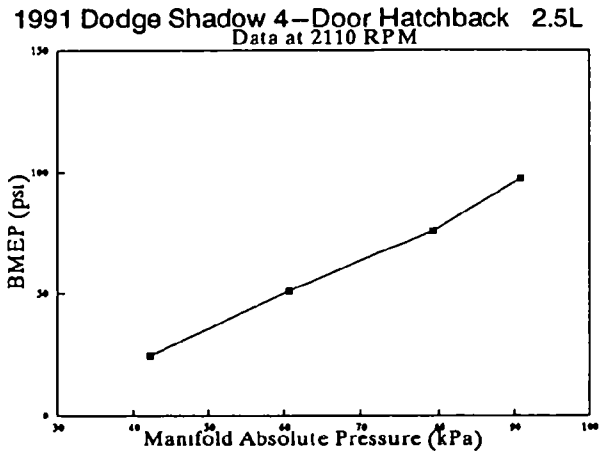
1991 Dodge Shadow 4-Door Hatchback 2.5L
Data at 2110 RPM
BMEP (psi)
Manifold Absolute Pressure (kPa)

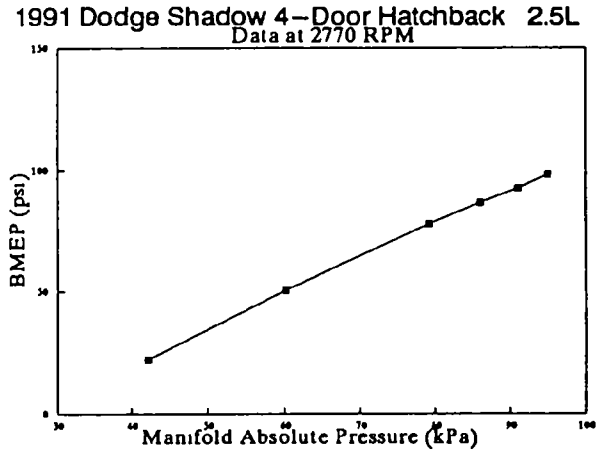
1991 Dodge Shadow 4-Door Hatchback 2.5L
Data at 2770 RPM
BMEP (psi)
Manifold Absolute Pressure (kPa)

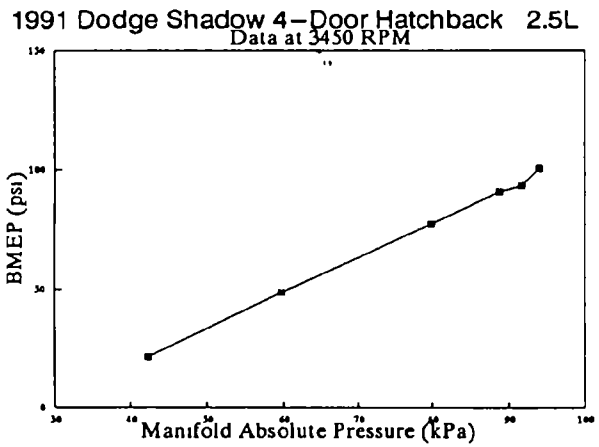
1991 Dodge Shadow 4-Door Hatchback 2.5L
Data at 3450 RPM
BMEP (psi)
Manifold Absolute Pressure (kPa)

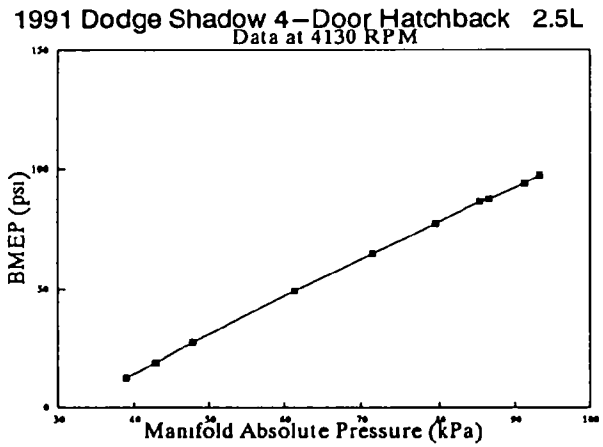
1991 Dodge Shadow 4-Door Hatchback 2.5L
Data at 4130 RPM
BMEP (psi)
Manifold Absolute Pressure (kPa)

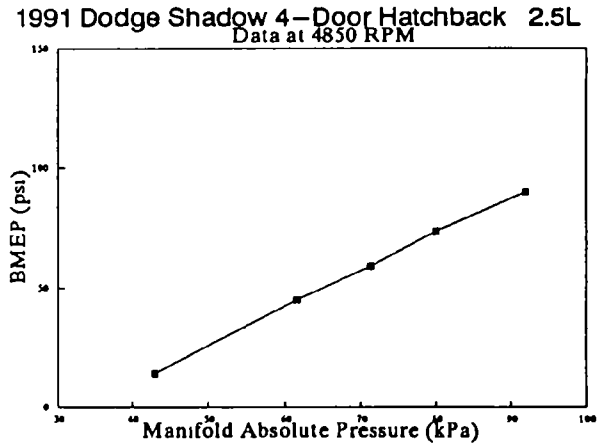
1991 Dodge Shadow 4-Door Hatchback 2.5L
Data at 4850 RPM
BMEP (psi)
Manifold Absolute Pressure (kPa)

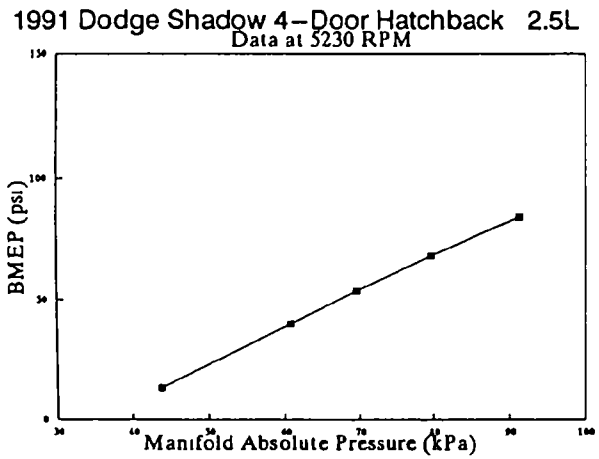
1991 Dodge Shadow 4-Door Hatchback 2.5L
Data at 5230 RPM
BMEP (psi)
Manifold Absolute Pressure (kPa)

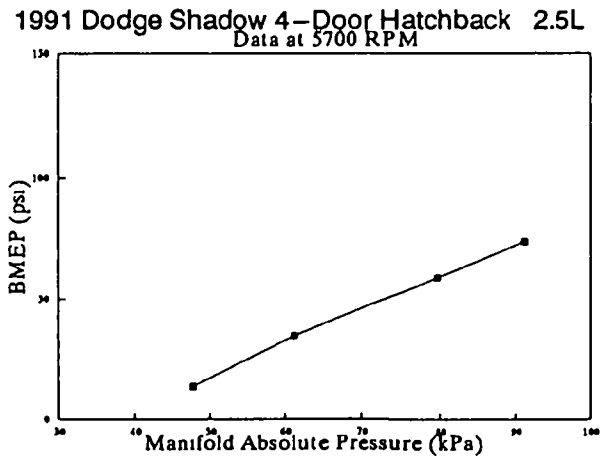
1991 Dodge Shadow 4-Door Hatchback 2.5L
Data at 5700 RPM
BMEP (psi)
Manifold Absolute Pressure (kPa)

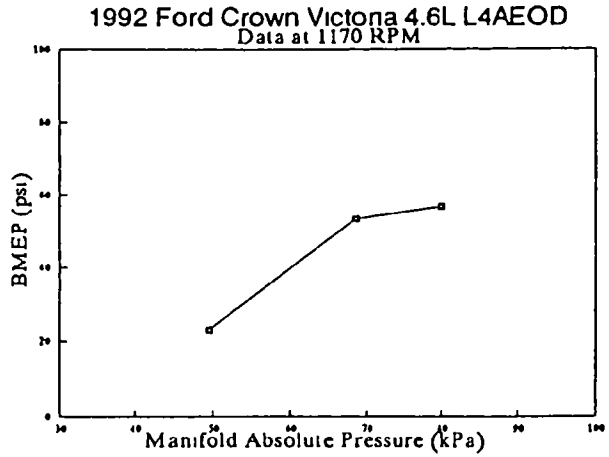

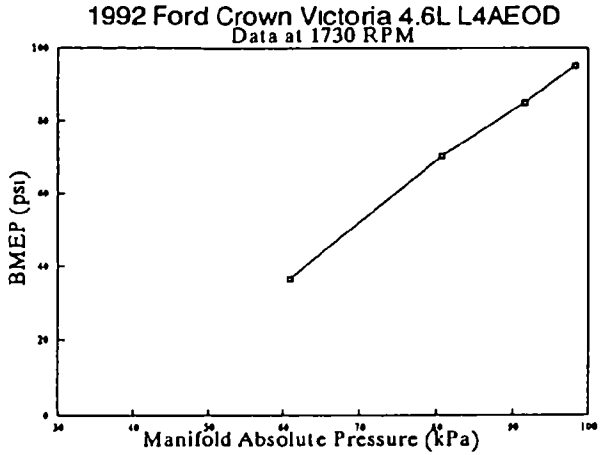

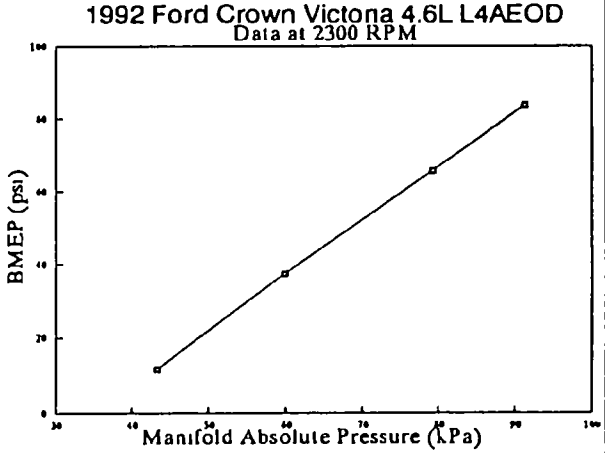

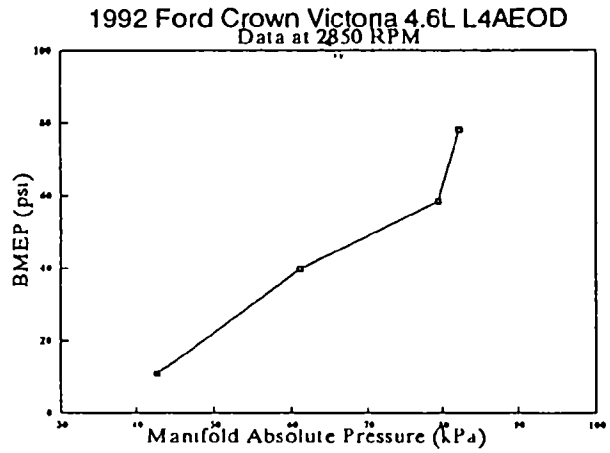

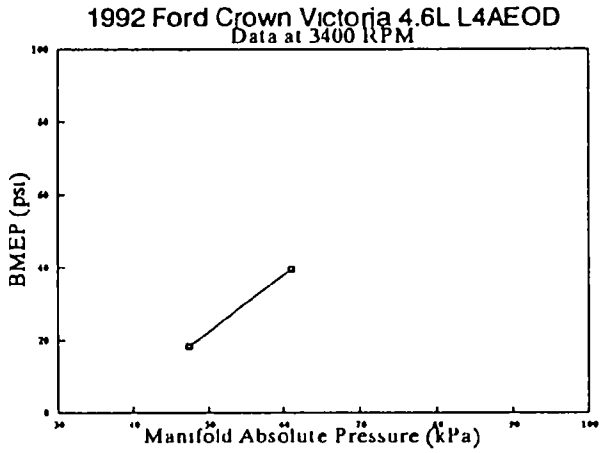

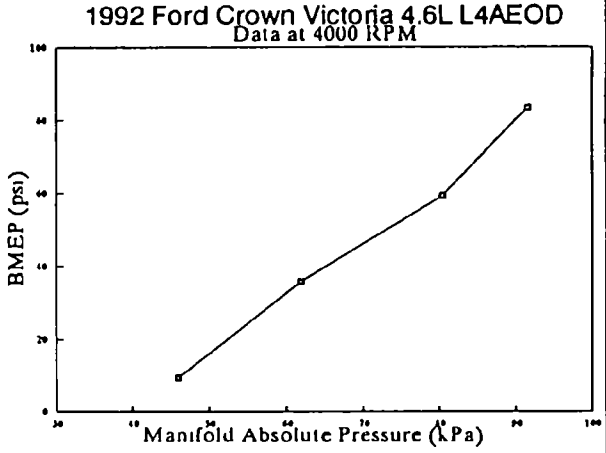

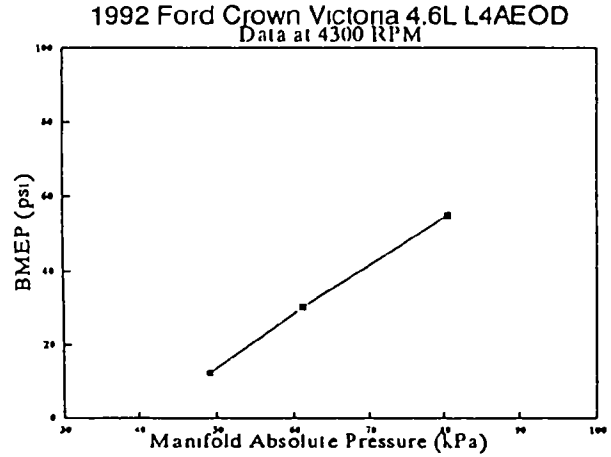

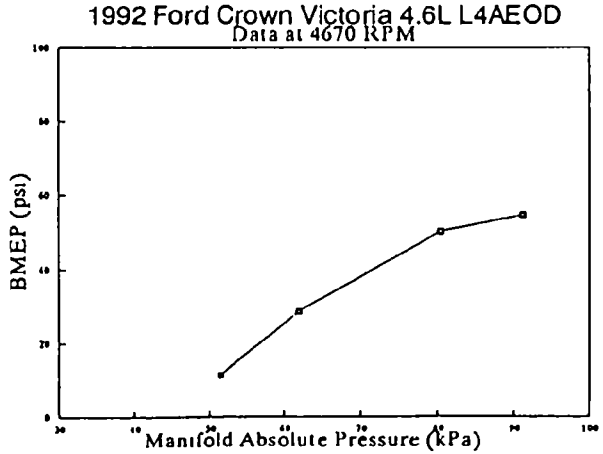

Corrected engine mapping data.
Only points whose BMEP values
are calculated from measured dyno
torques are included

991 Ford Escort LX 2-Door Hatchback 1.9L L4/991 Ford Escort LX 2-Door Hatchback 1.9L L4/991 Ford Escort LX 2-Door Hatchback 1.9L L4/

Data at 1270 RPM

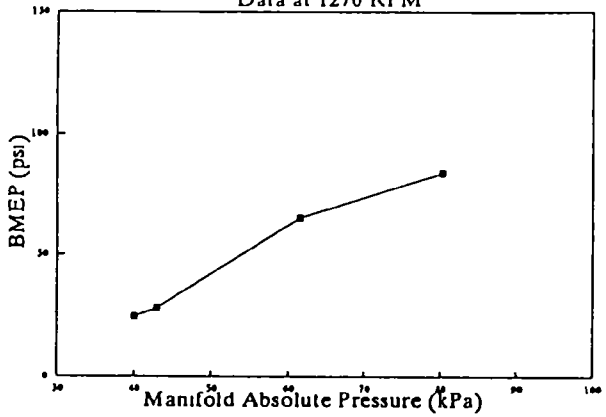

Data at 1870 RPM

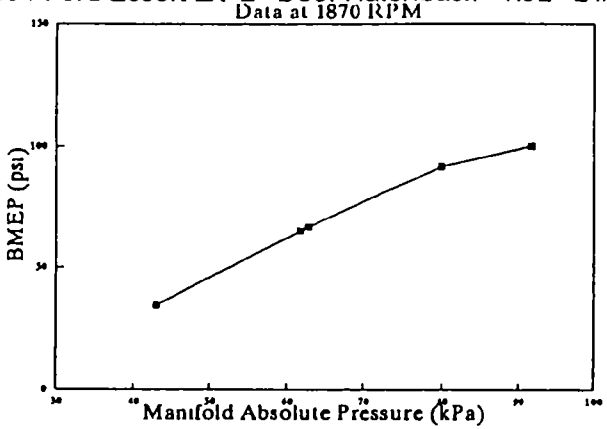

Data at 2475 RPM

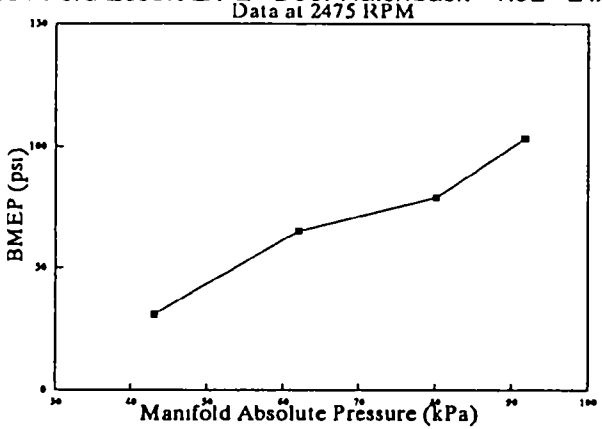

991 Ford Escort LX 2-Door Hatchback 1.9L L4/991 Ford Escort LX 2-Door Hatchback 1.9L L4/991 Ford Escort LX 2-Door Hatchback 1.9L L4/

Data at 3090 RPM

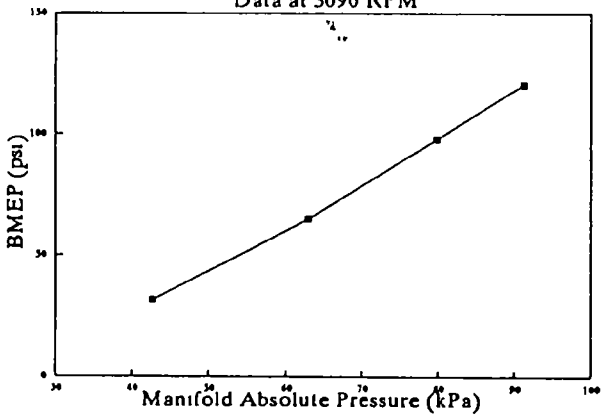

Data at 3700 RPM

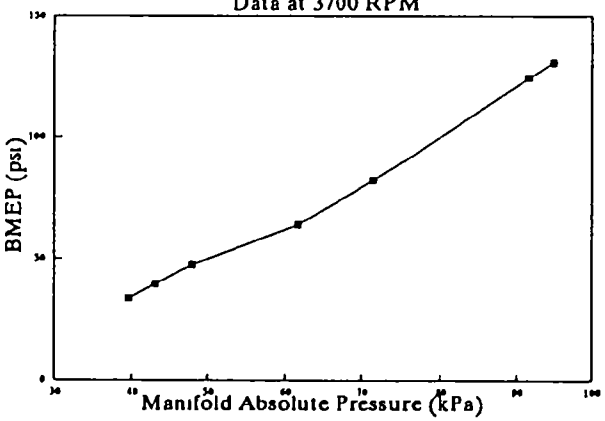

Data at 4320 RPM

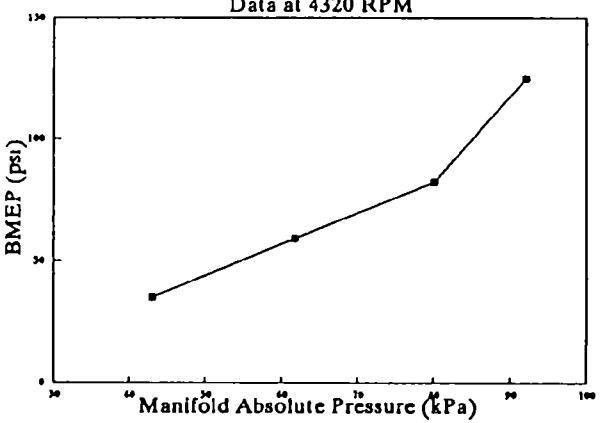

991 Ford Escort LX 2-Door Hatchback 1.9L L4/991 Ford Escort LX 2-Door Hatchback 1.9L L4/

Data at 4700 RPM

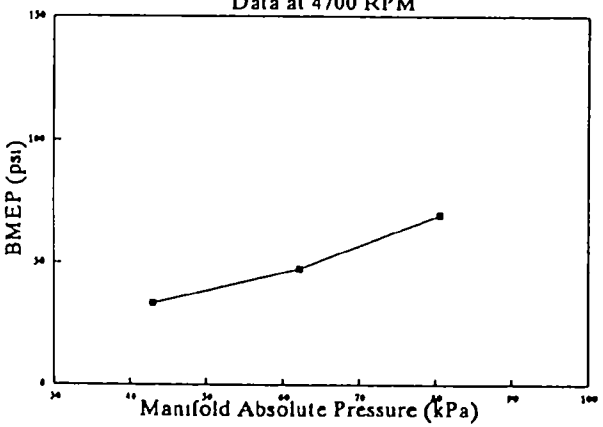

Data at 5100 RPM

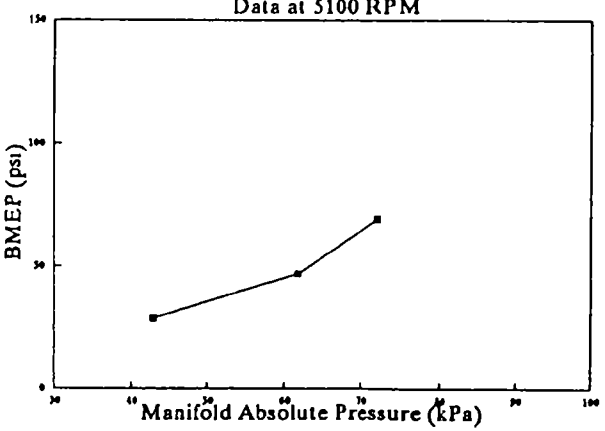

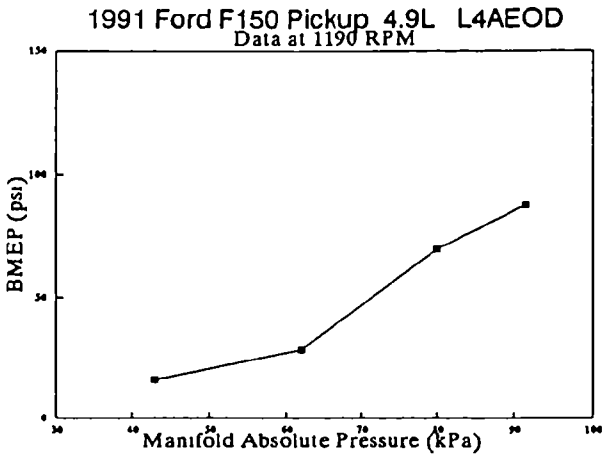
1991 Ford F150 Pickup 4.9L L4AEOD
Data at 1190 RPM
BMEP (psi)
Manifold Absolute Pressure (kPa)

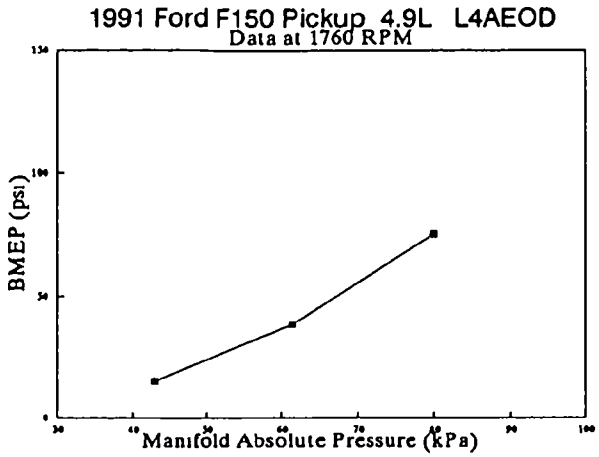
1991 Ford F150 Pickup 4.9L L4AEOD
Data at 1760 RPM
BMEP (psi)
Manifold Absolute Pressure (kPa)

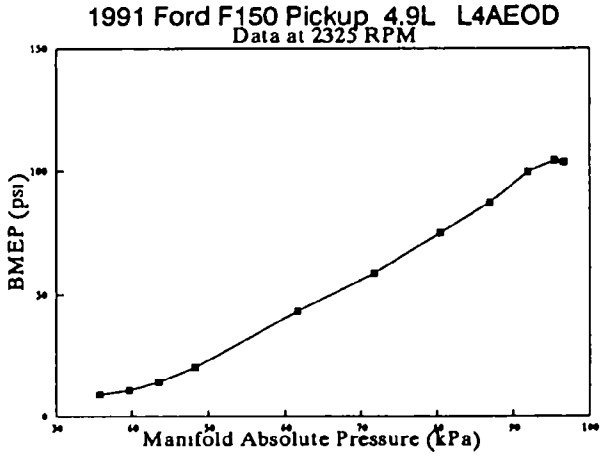
1991 Ford F150 Pickup 4.9L L4AEOD
Data at 2325 RPM
BMEP (psi)
Manifold Absolute Pressure (kPa)

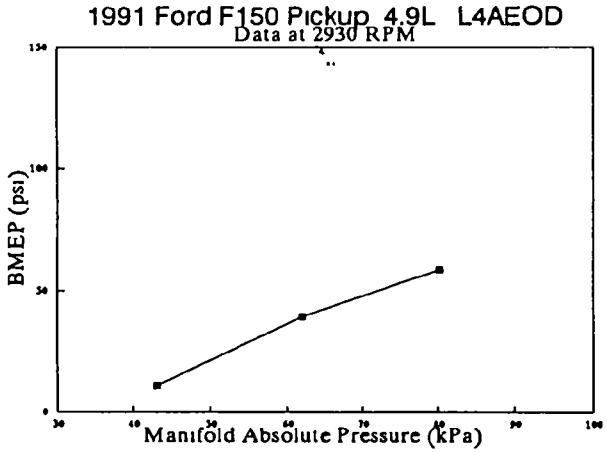
1991 Ford F150 Pickup 4.9L L4AEOD
Data at 2930 RPM
BMEP (psi)
Manifold Absolute Pressure (kPa)

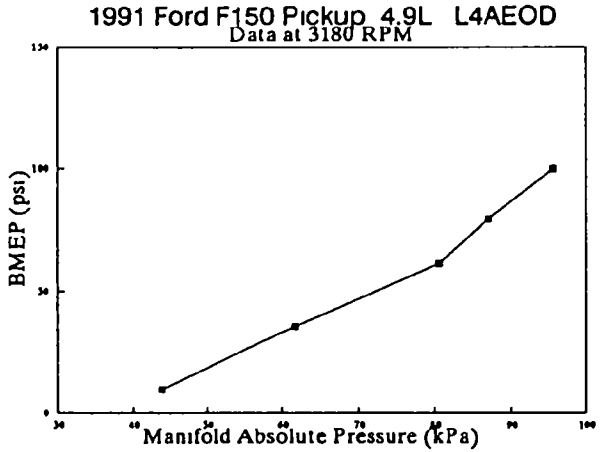
1991 Ford F150 Pickup 4.9L L4AEOD
Data at 3180 RPM
BMEP (psi)
Manifold Absolute Pressure (kPa)

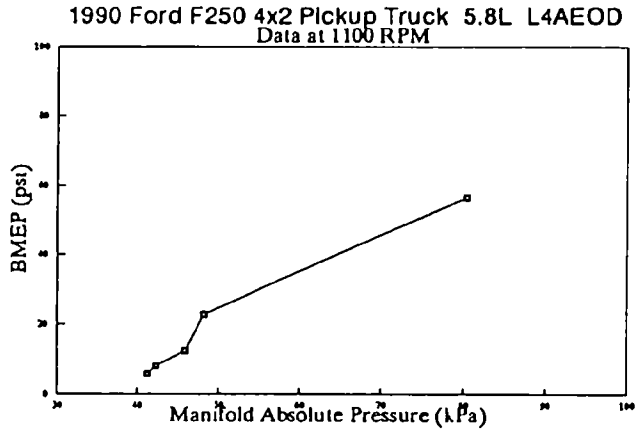
1990 Ford F250 4x2 Pickup Truck 5.8L L4AEOD
Data at 1100 RPM
BMEP (psi)
Manifold Absolute Pressure (kPa)

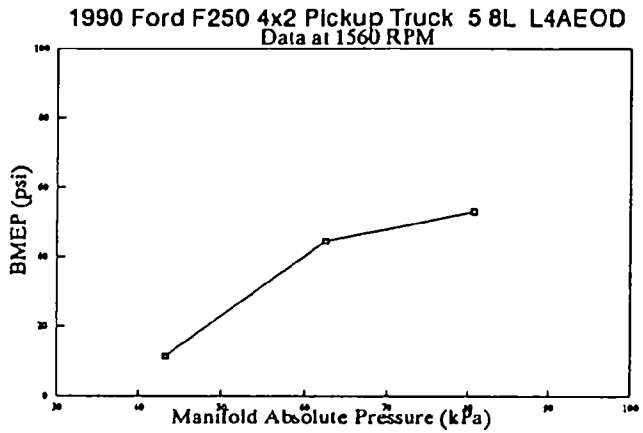
1990 Ford F250 4x2 Pickup Truck 5 8L L4AEOD
Data at 1560 RPM
BMEP (psi)
Manifold Absolute Pressure (kPa)

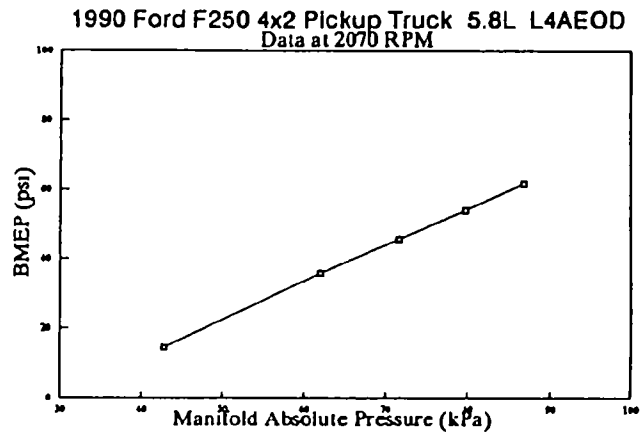
1990 Ford F250 4x2 Pickup Truck 5.8L L4AEOD
Data at 2070 RPM
BMEP (psi)
Manifold Absolute Pressure (kPa)

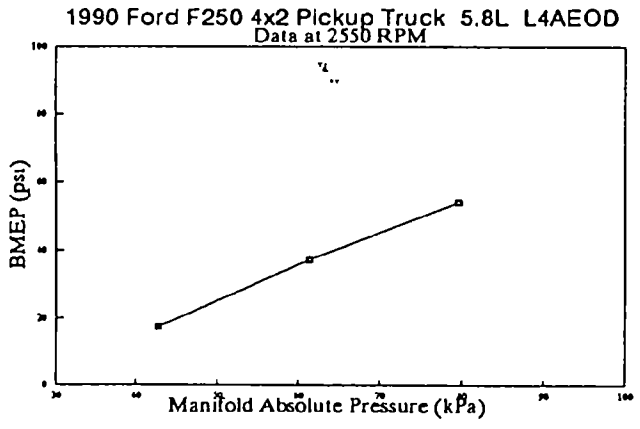
1990 Ford F250 4x2 Pickup Truck 5.8L L4AEOD
Data at 2550 RPM
BMEP (psi)
Manifold Absolute Pressure (kPa)

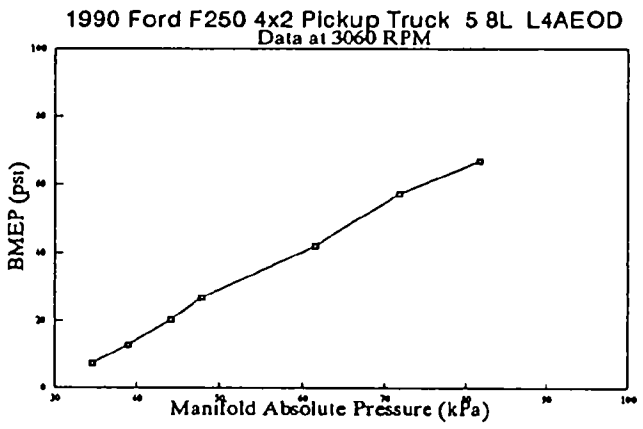
1990 Ford F250 4x2 Pickup Truck 5 8L L4AEOD
Data at 3060 RPM
BMEP (psi)
Manifold Absolute Pressure (kPa)

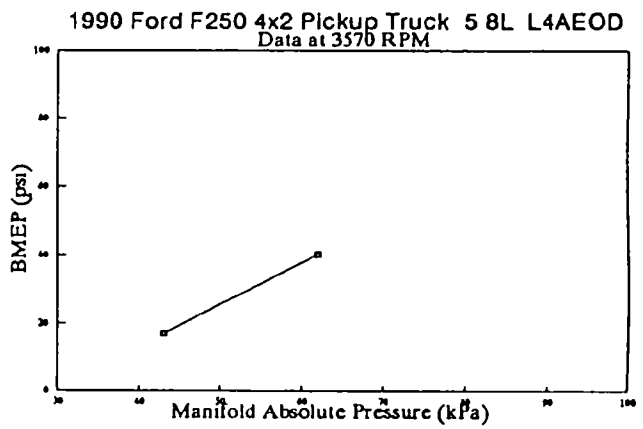
1990 Ford F250 4x2 Pickup Truck 5 8L L4AEOD
Data at 3570 RPM
BMEP (psi)
Manifold Absolute Pressure (kPa)

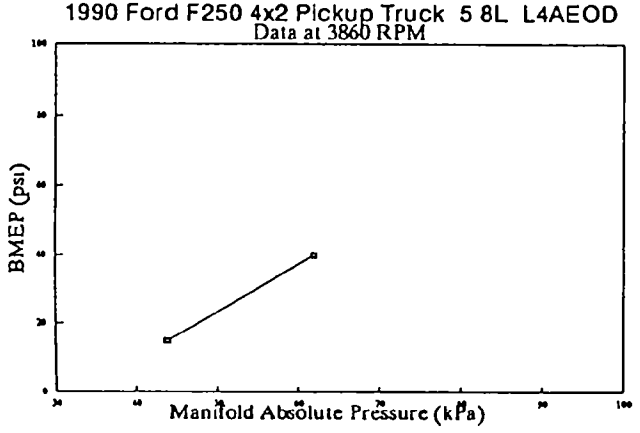
1990 Ford F250 4x2 Pickup Truck 5 8L L4AEOD
Data at 3860 RPM
BMEP (psi)
Manifold Absolute Pressure (kPa)

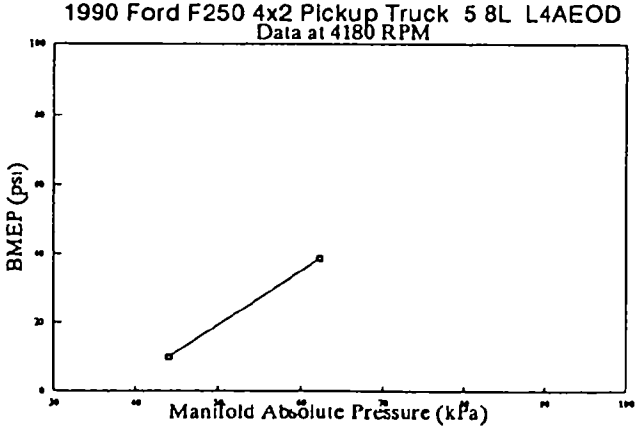
1990 Ford F250 4x2 Pickup Truck 5 8L L4AEOD
Data at 4180 RPM
BMEP (psi)
Manifold Absolute Pressure (kPa)

991 Ford Probe GL 2-Door Hatchback 2.2L L4/991 Ford Probe GL 2-Door Hatchback 2.2L L4/991 Ford Probe GL 2-Door Hatchback 2.2L L4/

Data at 1325 RPM

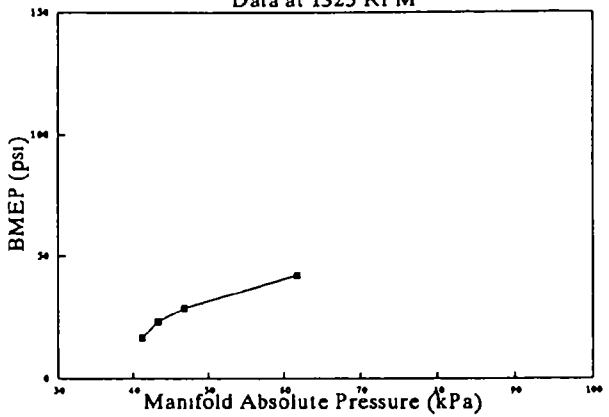

Data at 1950 RPM

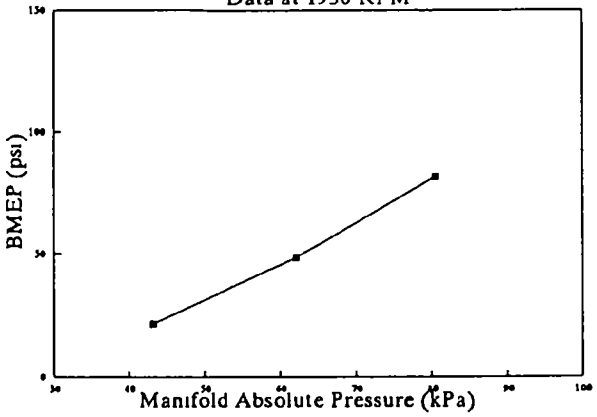

Data at 2580 RPM

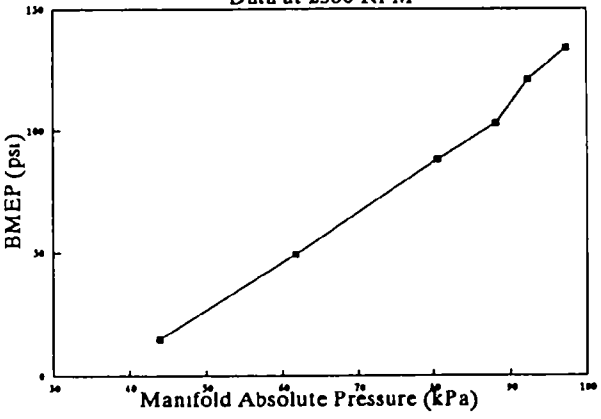

991 Ford Probe GL 2-Door Hatchback 2.2L L4/991 Ford Probe GL 2-Door Hatchback 2.2L L4/991 Ford Probe GL 2-Door Hatchback 2.2L L4/

Data at 3215 RPM

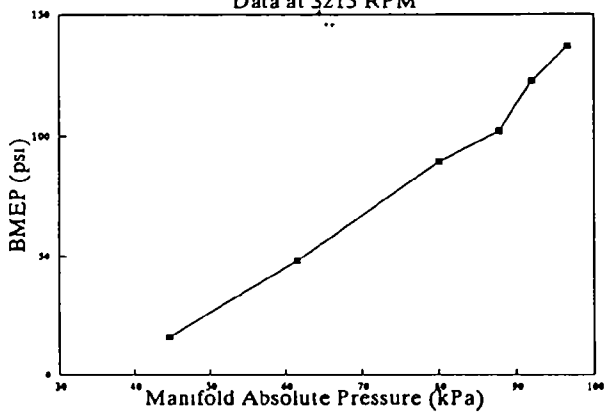

Data at 3840 RPM

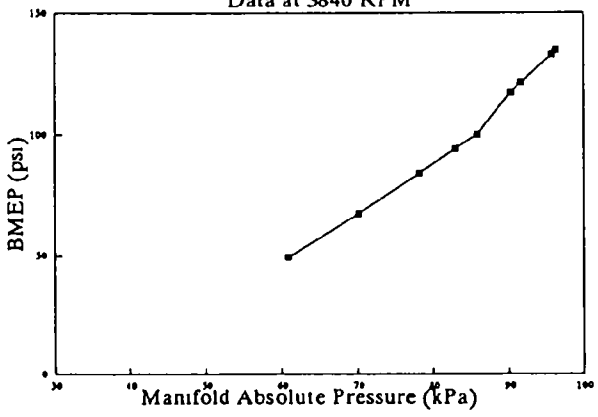

Data at 4500 RPM

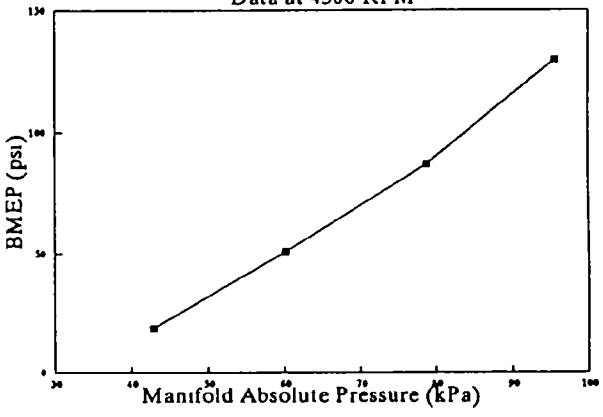

991 Ford Probe GL 2-Door Hatchback 2.2L L4/

Data at 4875 RPM

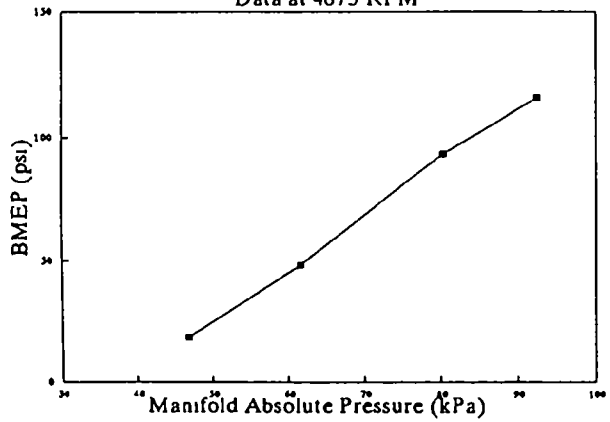

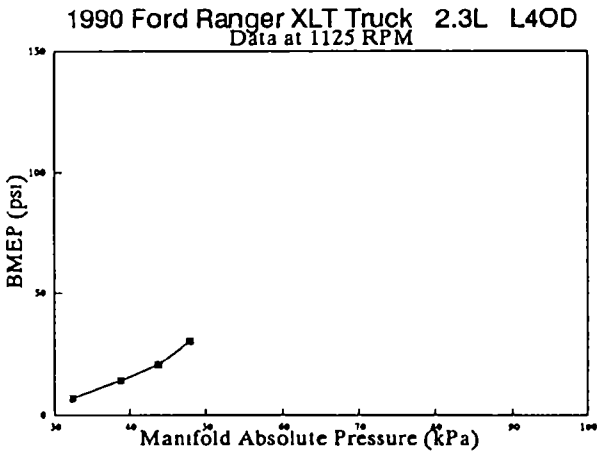
1990 Ford Ranger XLT Truck 2.3L L4OD
Data at 1125 RPM
BMEP (psi)
Manifold Absolute Pressure (kPa)

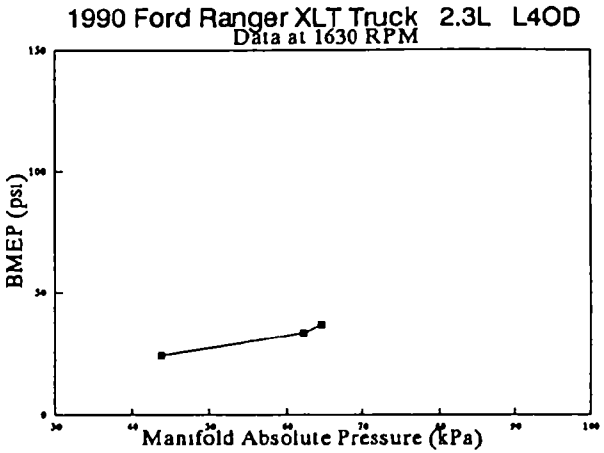
1990 Ford Ranger XLT Truck 2.3L L4OD
Data at 1630 RPM
BMEP (psi)
Manifold Absolute Pressure (kPa)

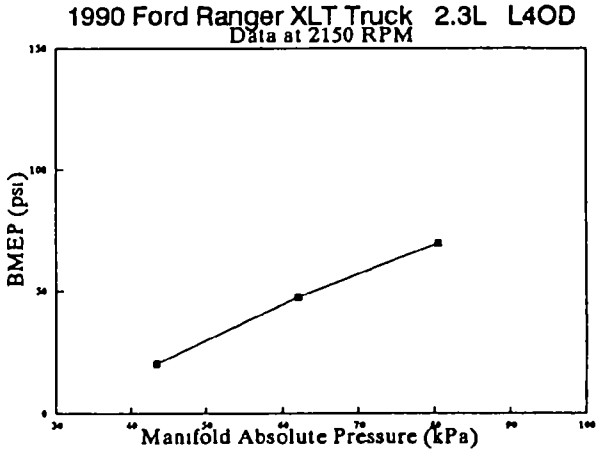
1990 Ford Ranger XLT Truck 2.3L L4OD
Data at 2150 RPM
BMEP (psi)
Manifold Absolute Pressure (kPa)

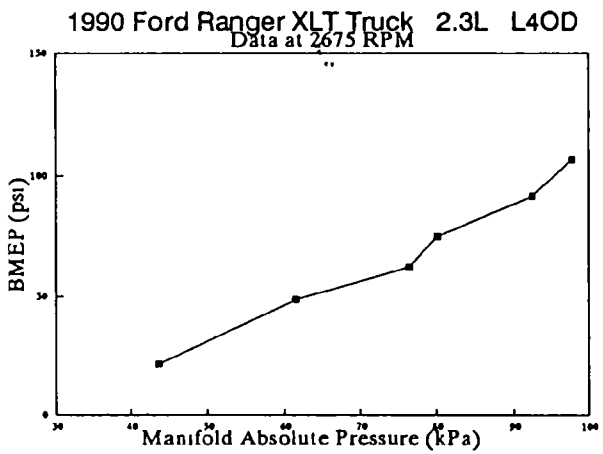
1990 Ford Ranger XLT Truck 2.3L L4OD
Data at 2675 RPM
BMEP (psi)
Manifold Absolute Pressure (kPa)

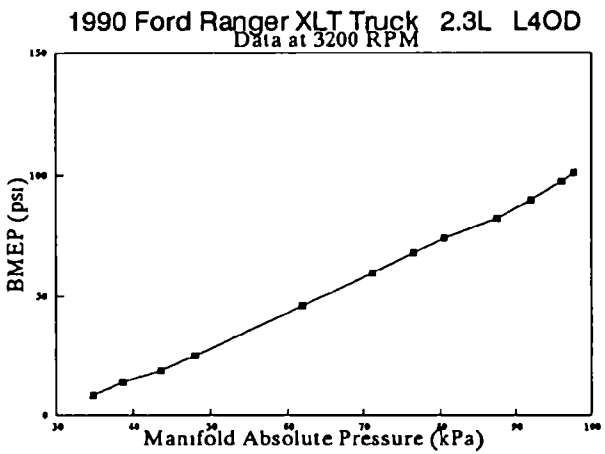
1990 Ford Ranger XLT Truck 2.3L L4OD
Data at 3200 RPM
BMEP (psi)
Manifold Absolute Pressure (kPa)

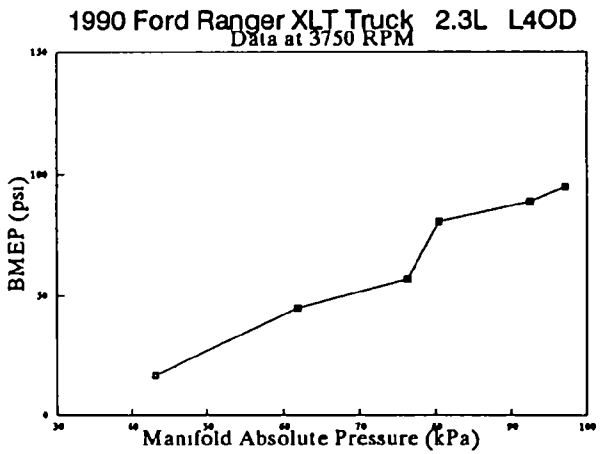
1990 Ford Ranger XLT Truck 2.3L L4OD
Data at 3750 RPM
BMEP (psi)
Manifold Absolute Pressure (kPa)

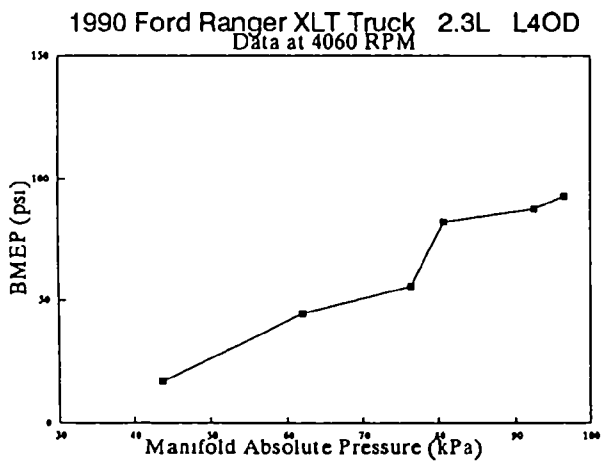
1990 Ford Ranger XLT Truck 2.3L L4OD
Data at 4060 RPM
BMEP (psi)
Manifold Absolute Pressure (kPa)

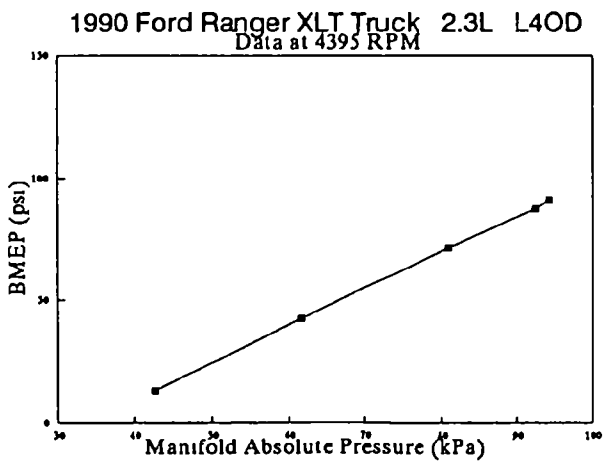
1990 Ford Ranger XLT Truck 2.3L L4OD
Data at 4395 RPM
BMEP (psi)
Manifold Absolute Pressure (kPa)

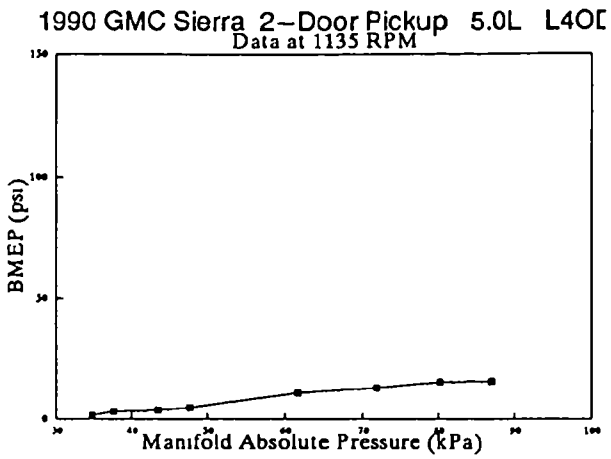
1990 GMC Sierra 2-Door Pickup 5.0L L4OE
Data at 1135 RPM
BMEP (psi)
Manifold Absolute Pressure (kPa)

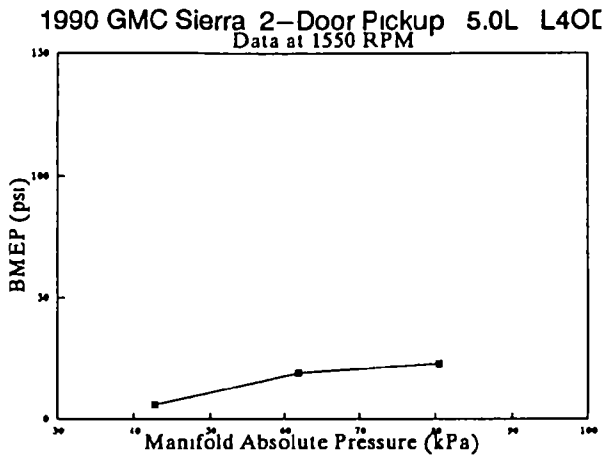
1990 GMC Sierra 2-Door Pickup 5.0L L4OE
Data at 1550 RPM
BMEP (psi)
Manifold Absolute Pressure (kPa)

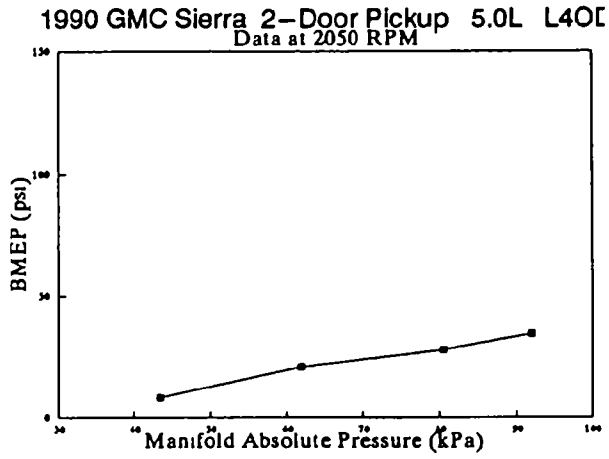
1990 GMC Sierra 2-Door Pickup 5.0L L4OE
Data at 2050 RPM
BMEP (psi)
Manifold Absolute Pressure (kPa)

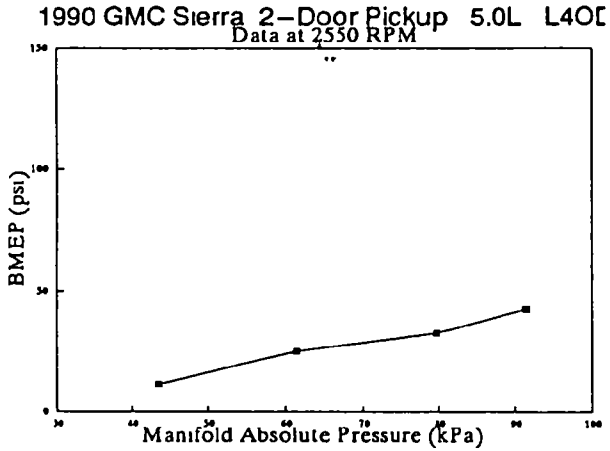
1990 GMC Sierra 2-Door Pickup 5.0L L4OE
Data at 2550 RPM
BMEP (psi)
Manifold Absolute Pressure (kPa)

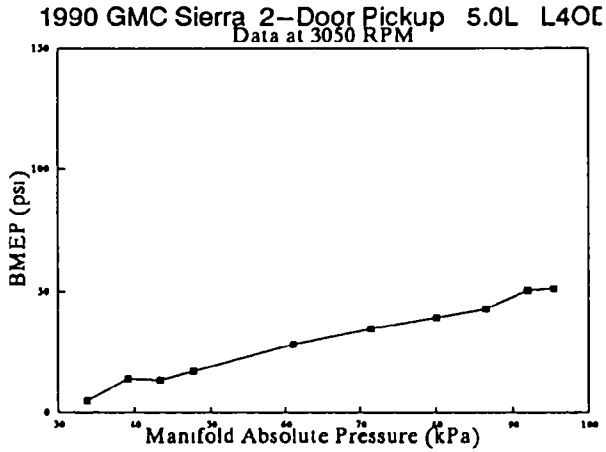
1990 GMC Sierra 2-Door Pickup 5.0L L4OE
Data at 3050 RPM
BMEP (psi)
Manifold Absolute Pressure (kPa)

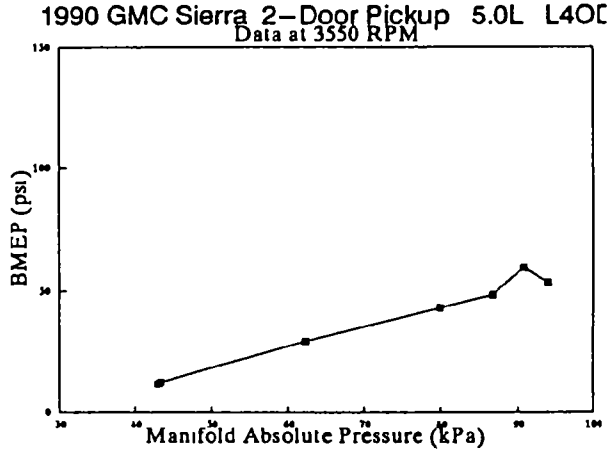
1990 GMC Sierra 2-Door Pickup 5.0L L4OE
Data at 3550 RPM
BMEP (psi)
Manifold Absolute Pressure (kPa)

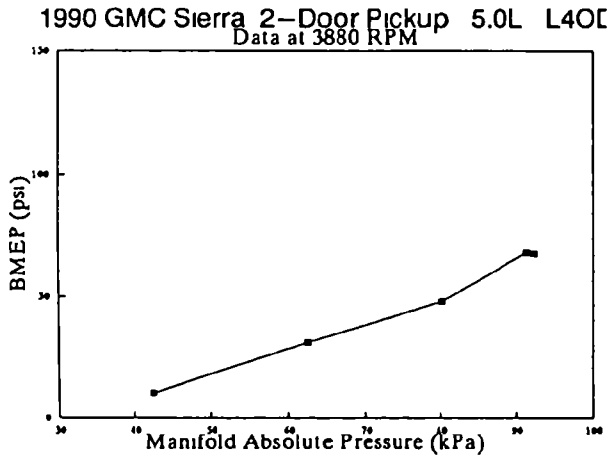
1990 GMC Sierra 2-Door Pickup 5.0L L4OE
Data at 3880 RPM
BMEP (psi)
Manifold Absolute Pressure (kPa)

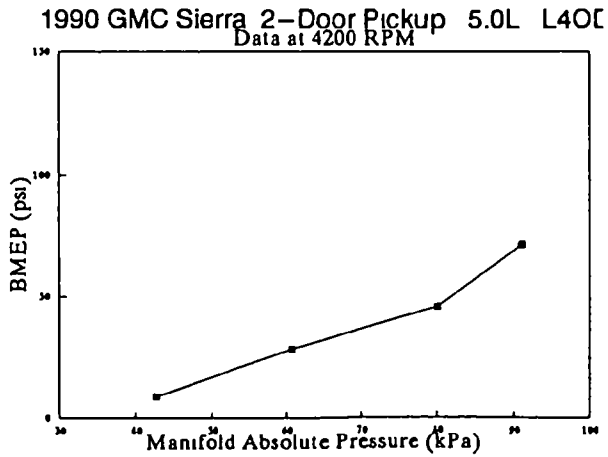
1990 GMC Sierra 2-Door Pickup 5.0L L4OE
Data at 4200 RPM
BMEP (psi)
Manifold Absolute Pressure (kPa)

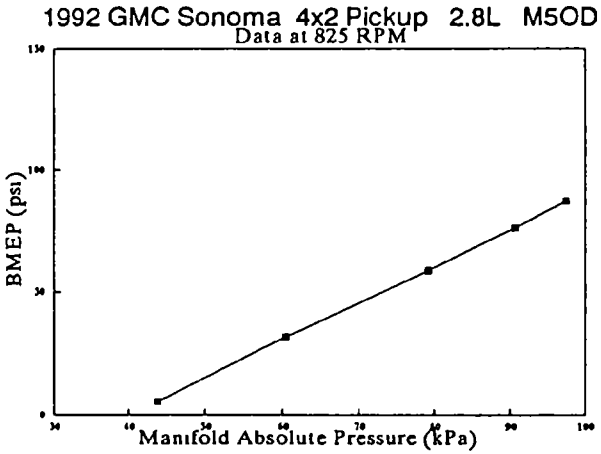
1992 GMC Sonoma 4x2 Pickup 2.8L M5OD
Data at 825 RPM
BMEP (psi)
Manifold Absolute Pressure (kPa)

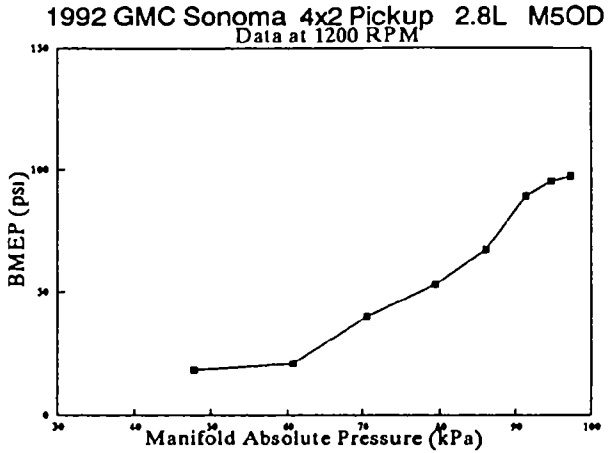
1992 GMC Sonoma 4x2 Pickup 2.8L M5OD
Data at 1200 RPM
BMEP (psi)
Manifold Absolute Pressure (kPa)

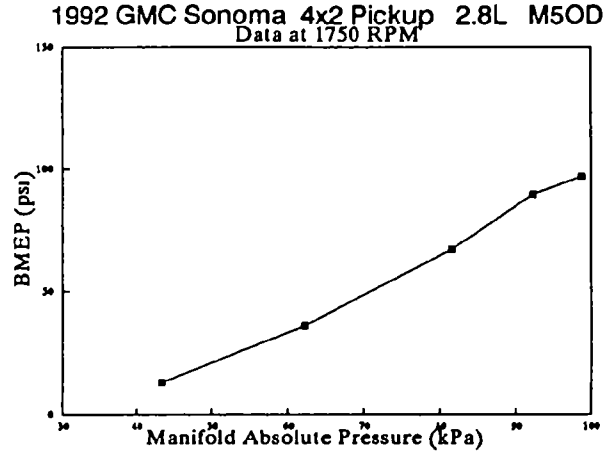
1992 GMC Sonoma 4x2 Pickup 2.8L M5OD
Data at 1750 RPM
BMEP (psi)
Manifold Absolute Pressure (kPa)

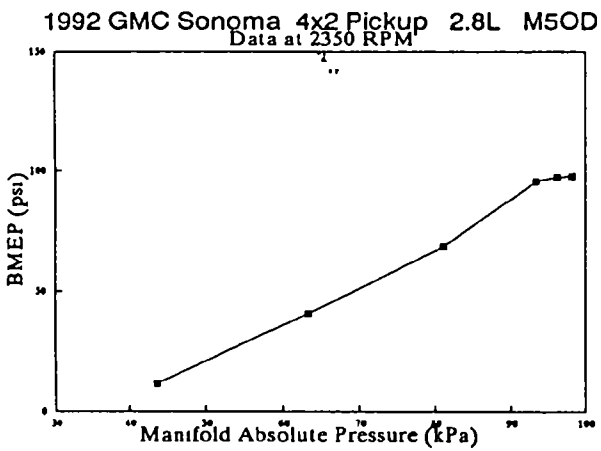
1992 GMC Sonoma 4x2 Pickup 2.8L M5OD
Data at 2350 RPM
BMEP (psi)
Manifold Absolute Pressure (kPa)

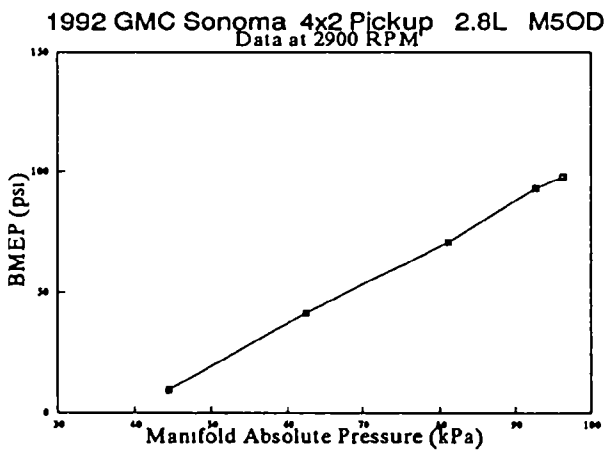
1992 GMC Sonoma 4x2 Pickup 2.8L M5OD
Data at 2900 RPM
BMEP (psi)
Manifold Absolute Pressure (kPa)

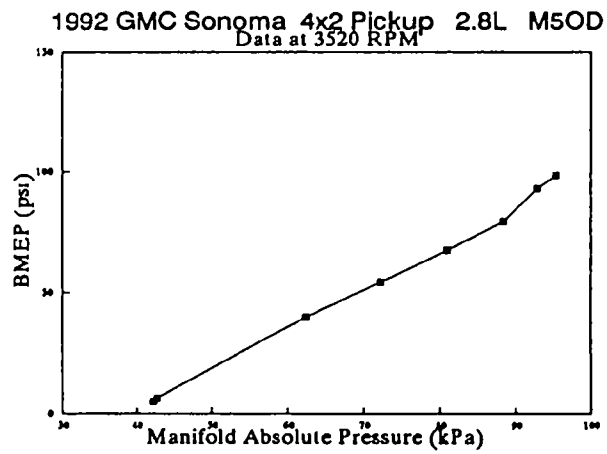
1992 GMC Sonoma 4x2 Pickup 2.8L M5OD
Data at 3520 RPM
BMEP (psi)
Manifold Absolute Pressure (kPa)

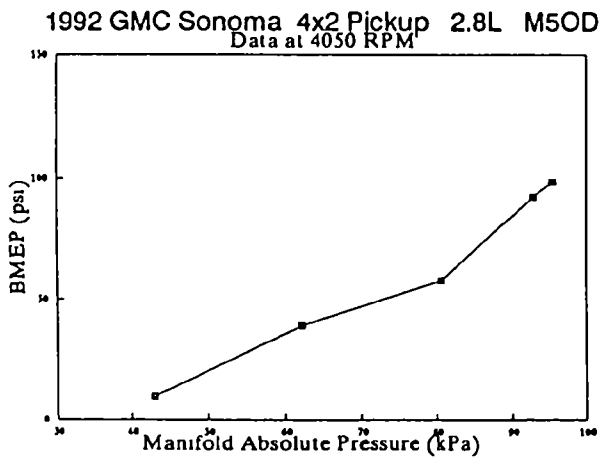
1992 GMC Sonoma 4x2 Pickup 2.8L M5OD
Data at 4050 RPM
BMEP (psi)
Manifold Absolute Pressure (kPa)

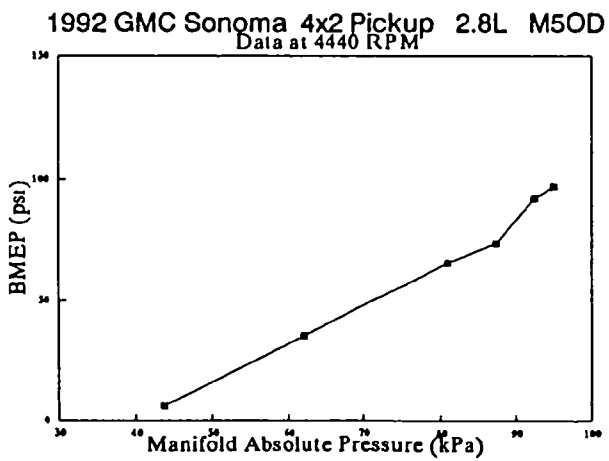
1992 GMC Sonoma 4x2 Pickup 2.8L M5OD
Data at 4440 RPM
BMEP (psi)
Manifold Absolute Pressure (kPa)

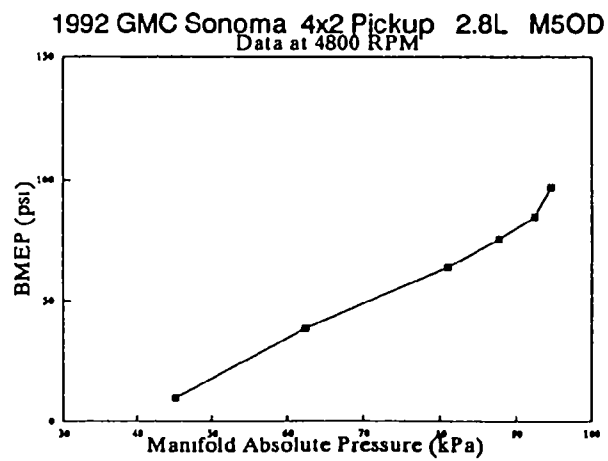
1992 GMC Sonoma 4x2 Pickup 2.8L M5OD
Data at 4800 RPM
BMEP (psi)
Manifold Absolute Pressure (kPa)

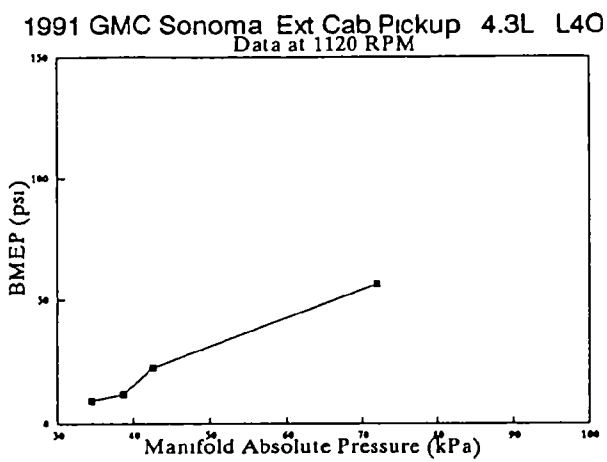
1991 GMC Sonoma Ext Cab Pickup 4.3L L4O
Data at 1120 RPM
BMEP (psi)
Manifold Absolute Pressure (kPa)

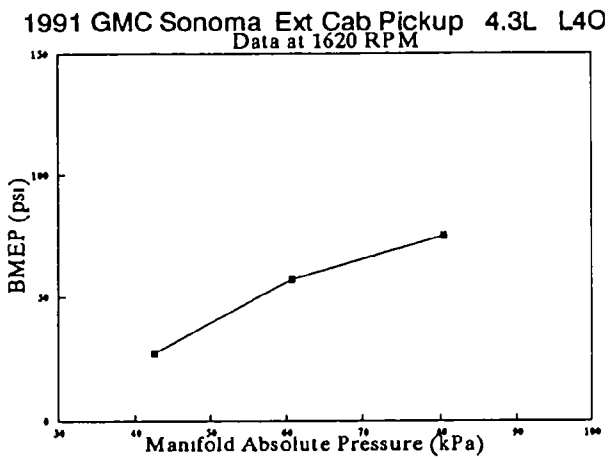
1991 GMC Sonoma Ext Cab Pickup 4.3L L4O
Data at 1620 RPM
BMEP (psi)
Manifold Absolute Pressure (kPa)

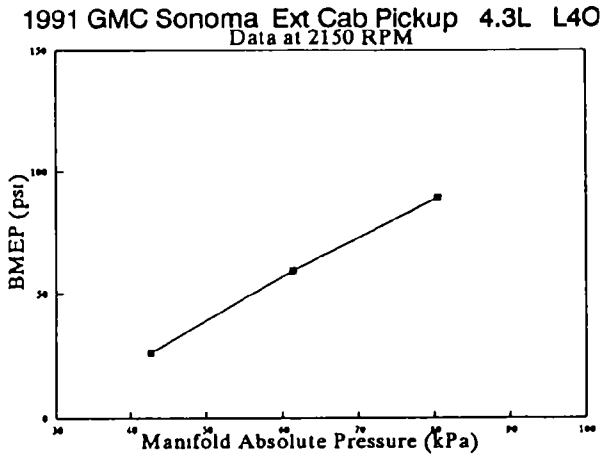
1991 GMC Sonoma Ext Cab Pickup 4.3L L4O
Data at 2150 RPM
BMEP (psi)
Manifold Absolute Pressure (kPa)

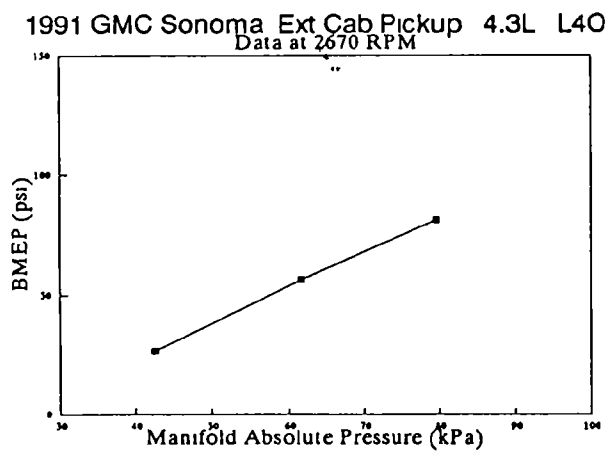
1991 GMC Sonoma Ext Cab Pickup 4.3L L4O
Data at 2670 RPM
BMEP (psi)
Manifold Absolute Pressure (kPa)

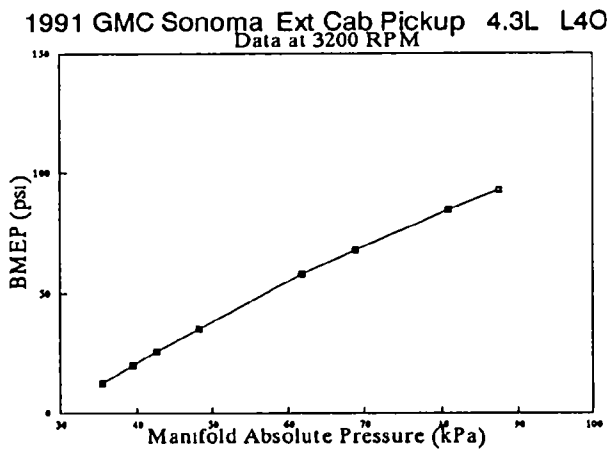
1991 GMC Sonoma Ext Cab Pickup 4.3L L4O
Data at 3200 RPM
BMEP (psi)
Manifold Absolute Pressure (kPa)

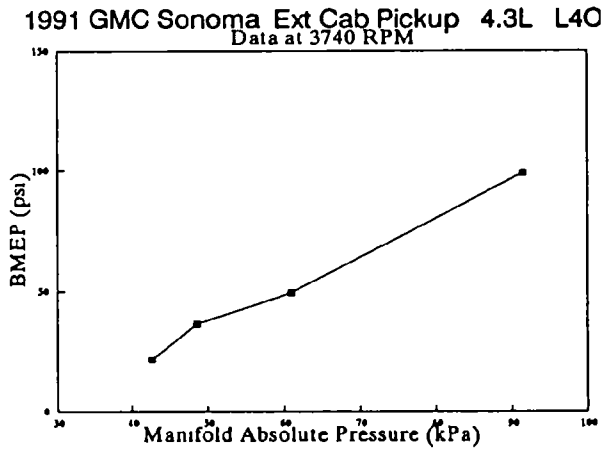
1991 GMC Sonoma Ext Cab Pickup 4.3L L4O
Data at 3740 RPM
BMEP (psi)
Manifold Absolute Pressure (kPa)

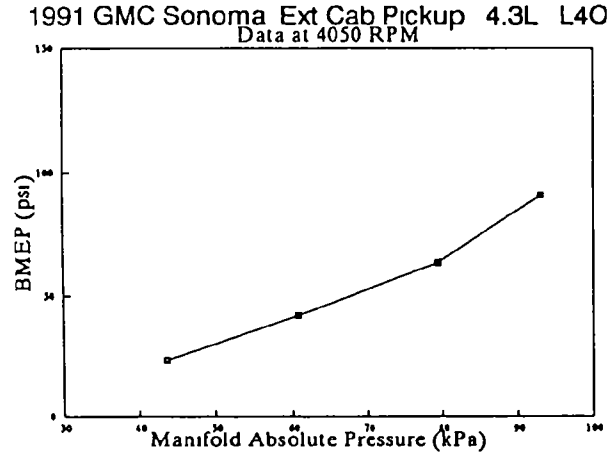
1991 GMC Sonoma Ext Cab Pickup 4.3L L4O
Data at 4050 RPM
BMEP (psi)
Manifold Absolute Pressure (kPa)

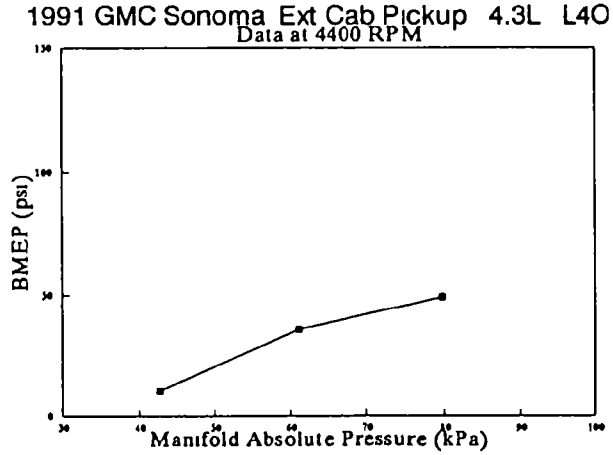
1991 GMC Sonoma Ext Cab Pickup 4.3L L4O
Data at 4400 RPM
BMEP (psi)
Manifold Absolute Pressure (kPa)

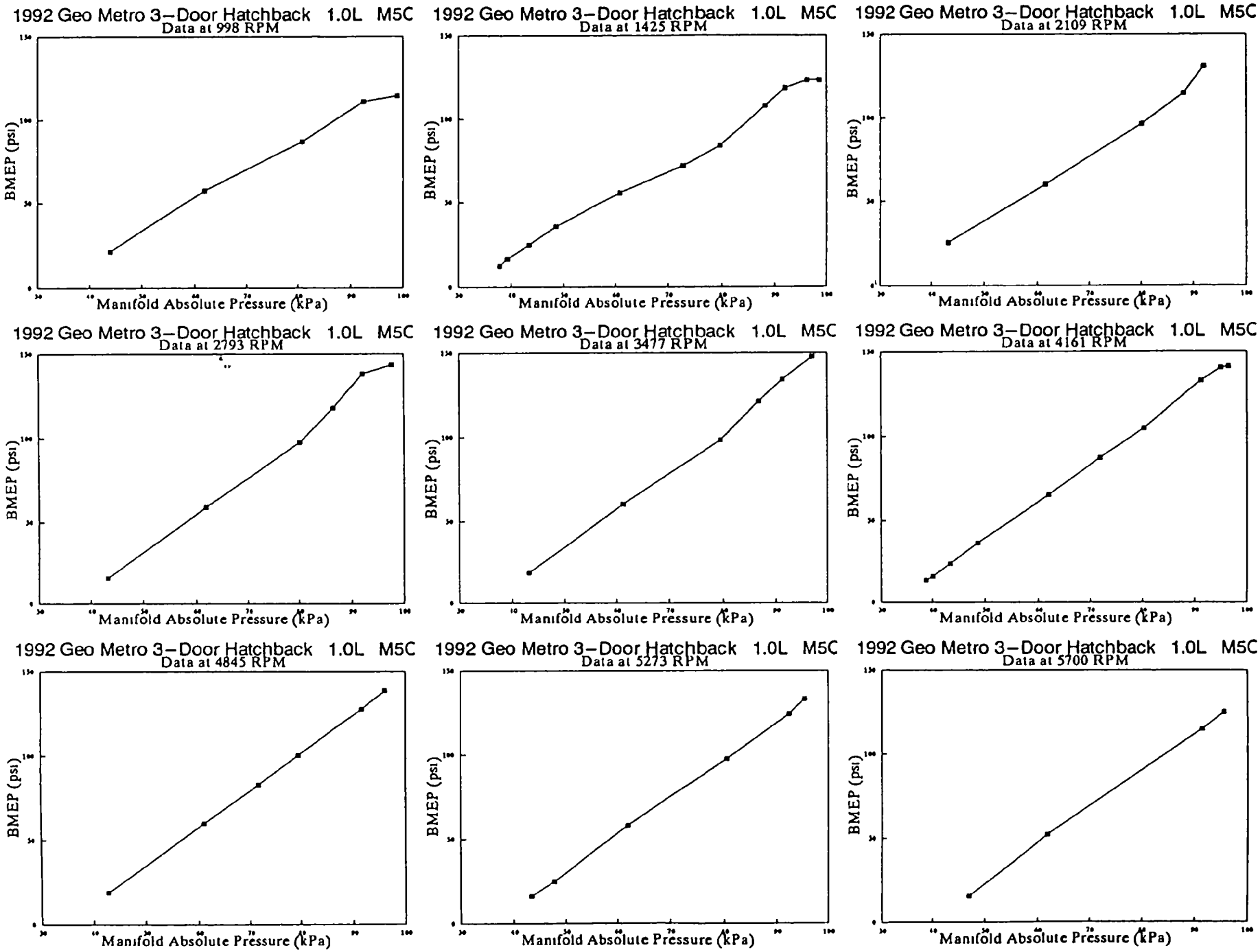
1992 Geo Metro 3–Door Hatchback 1.0L M5C
Data at 998 RPM
1992 Geo Metro 3–Door Hatchback 1.0L M5C
Data at 1425 RPM
1992 Geo Metro 3–Door Hatchback 1.0L M5C
Data at 2109 RPM
1992 Geo Metro 3–Door Hatchback 1.0L M5C
Data at 2793 RPM
1992 Geo Metro 3–Door Hatchback 1.0L M5C
Data at 3477 RPM
1992 Geo Metro 3–Door Hatchback 1.0L M5C
Data at 4161 RPM
1992 Geo Metro 3–Door Hatchback 1.0L M5C
Data at 4845 RPM
1992 Geo Metro 3–Door Hatchback 1.0L M5C
Data at 5273 RPM
1992 Geo Metro 3–Door Hatchback 1.0L M5C
Data at 5700 RPM
BMEP (psi)
Manifold Absolute Pressure (kPa)

1991 Honda Accord 2.2L L4(

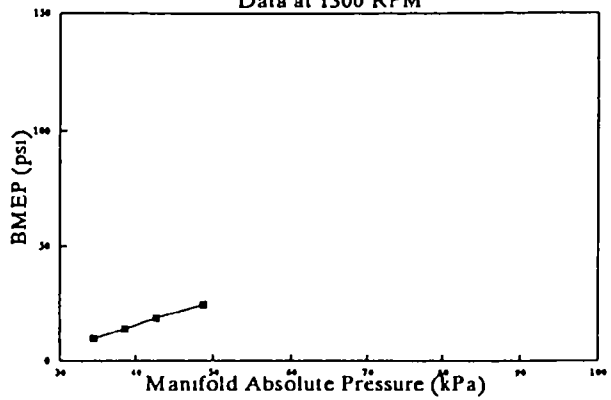

1991 Honda Accord 2.2L L4(

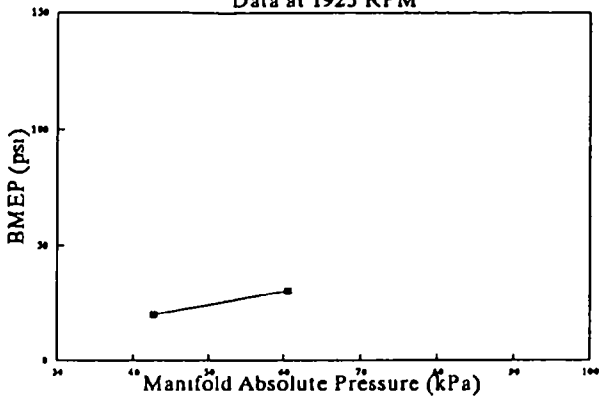

1991 Honda Accord 2.2L L4(

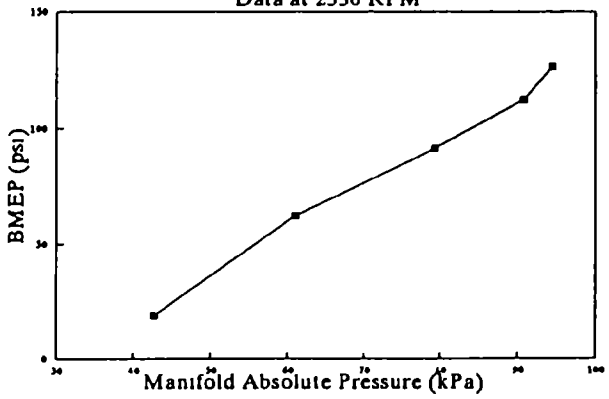

1991 Honda Accord 2.2L L4(

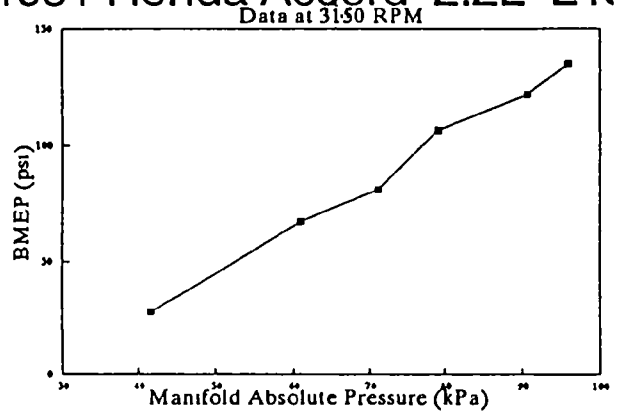

1991 Honda Accord 2.2L L4(

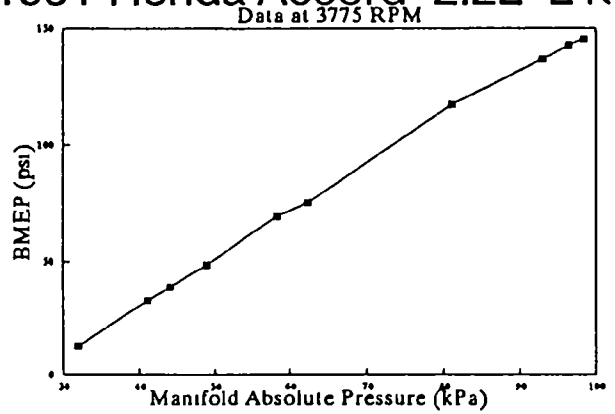

1991 Honda Accord 2.2L L4(

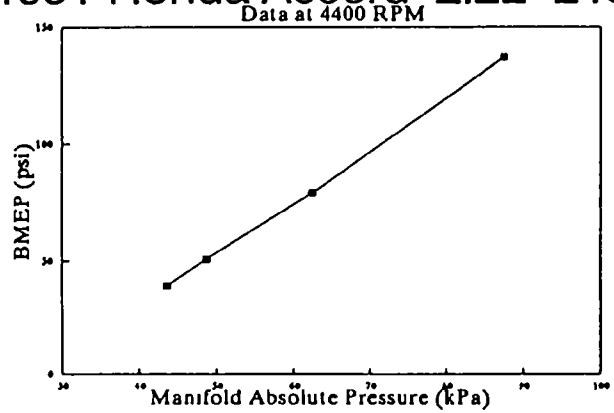

1991 Honda Accord 2.2L L4(

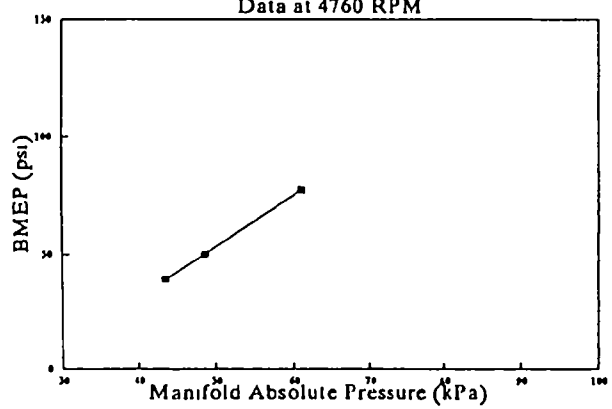

1991 Honda Accord 2.2L L4(

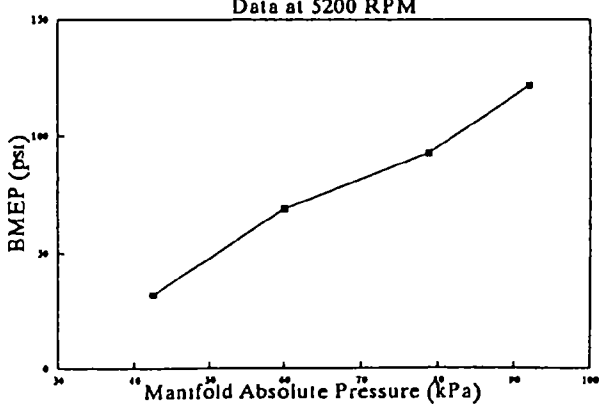

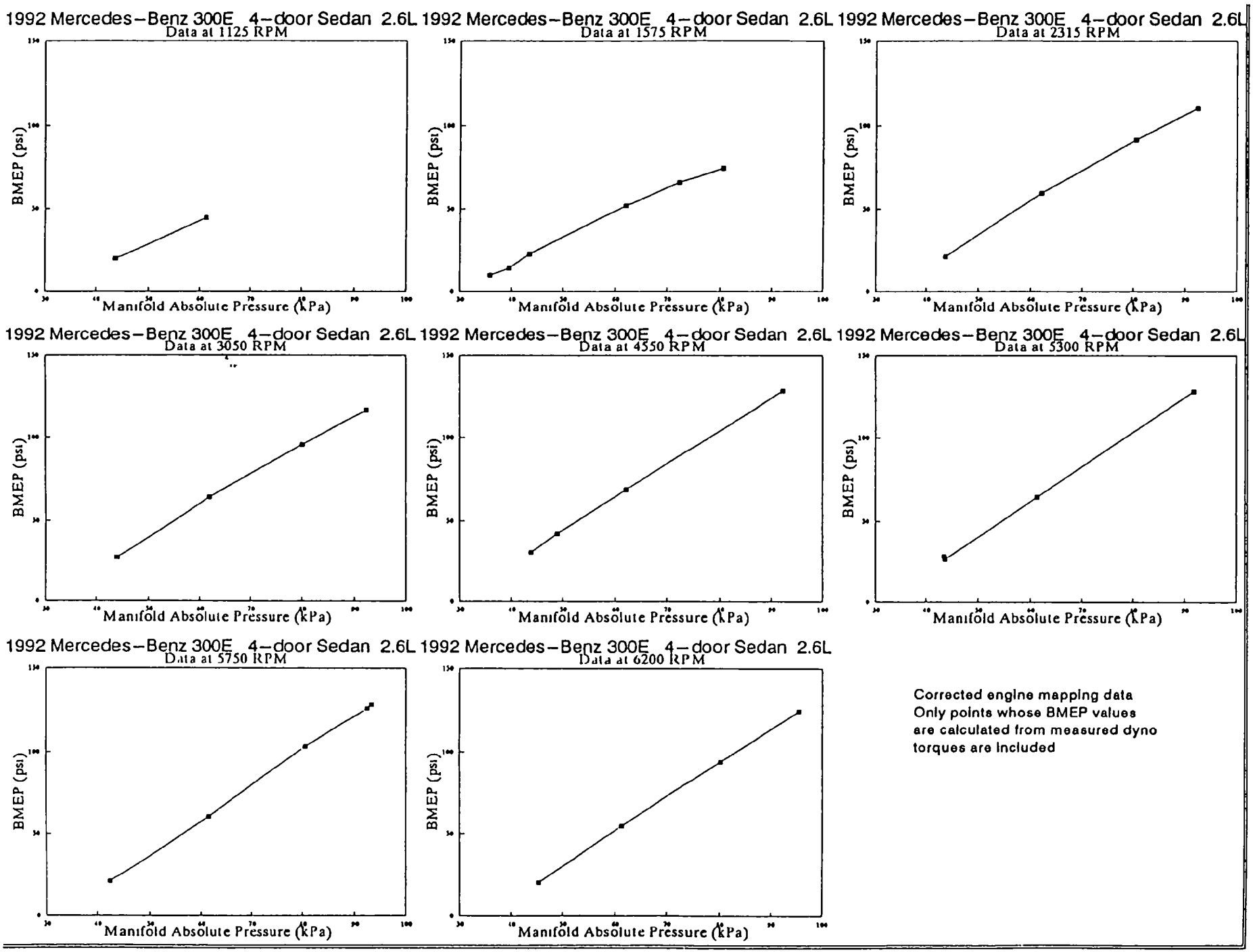
1992 Mercedes-Benz 300E 4-door Sedan 2.6L
Data at 1125 RPM
1992 Mercedes-Benz 300E 4-door Sedan 2.6L
Data at 1575 RPM
1992 Mercedes-Benz 300E 4-door Sedan 2.6L
Data at 2315 RPM
1992 Mercedes-Benz 300E 4-door Sedan 2.6L
Data at 3050 RPM
1992 Mercedes-Benz 300E 4-door Sedan 2.6L
Data at 4550 RPM
1992 Mercedes-Benz 300E 4-door Sedan 2.6L
Data at 5300 RPM
1992 Mercedes-Benz 300E 4-door Sedan 2.6L
Data at 5750 RPM
1992 Mercedes-Benz 300E 4-door Sedan 2.6L
Data at 6200 RPM
BMEP (psi)
Manifold Absolute Pressure (kPa)
Corrected engine mapping data
Only points whose BMEP values
are calculated from measured dyno
torques are included

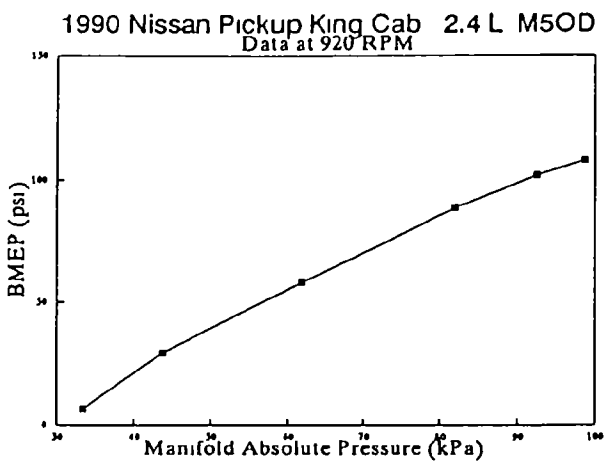
1990 Nissan Pickup King Cab 2.4 L M5OD
Data at 920 RPM
BMEP (psi)
Manifold Absolute Pressure (kPa)

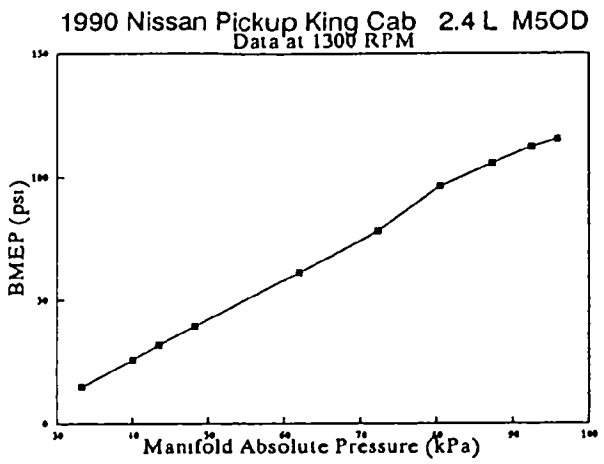
1990 Nissan Pickup King Cab 2.4 L M5OD
Data at 1300 RPM
BMEP (psi)
Manifold Absolute Pressure (kPa)

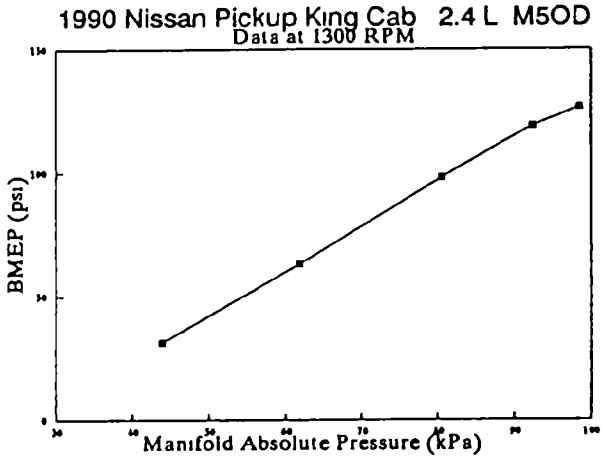
1990 Nissan Pickup King Cab 2.4 L M5OD
Data at 1300 RPM
BMEP (psi)
Manifold Absolute Pressure (kPa)

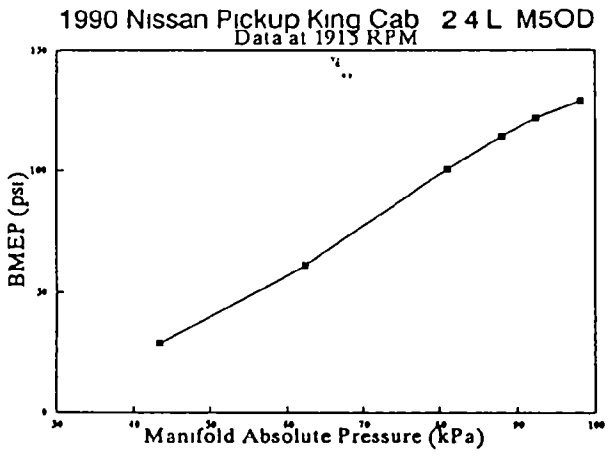
1990 Nissan Pickup King Cab 2 4 L M5OD
Data at 1915 RPM
BMEP (psi)
Manifold Absolute Pressure (kPa)

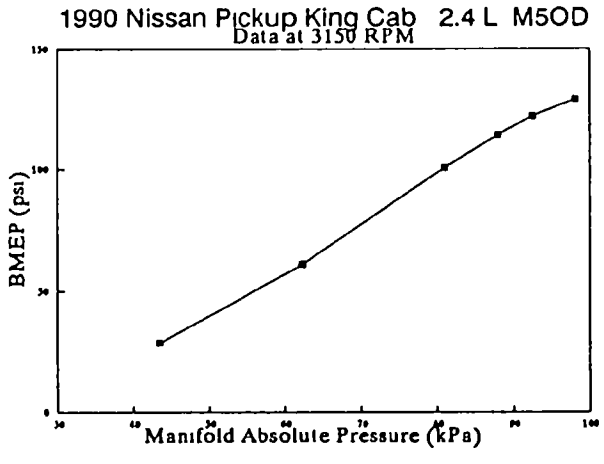
1990 Nissan Pickup King Cab 2.4 L M5OD
Data at 3150 RPM
BMEP (psi)
Manifold Absolute Pressure (kPa)

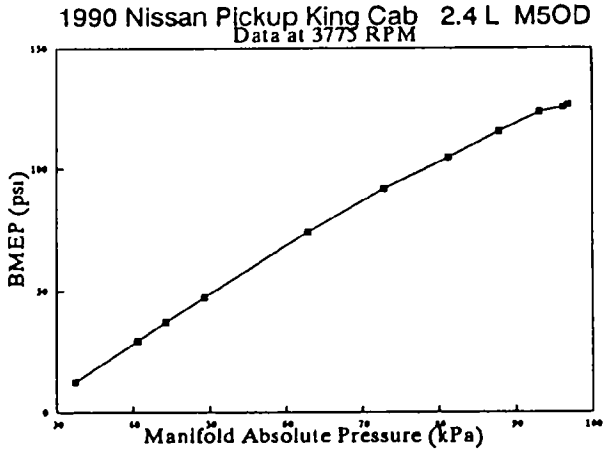
1990 Nissan Pickup King Cab 2.4 L M5OD
Data at 3775 RPM
BMEP (psi)
Manifold Absolute Pressure (kPa)

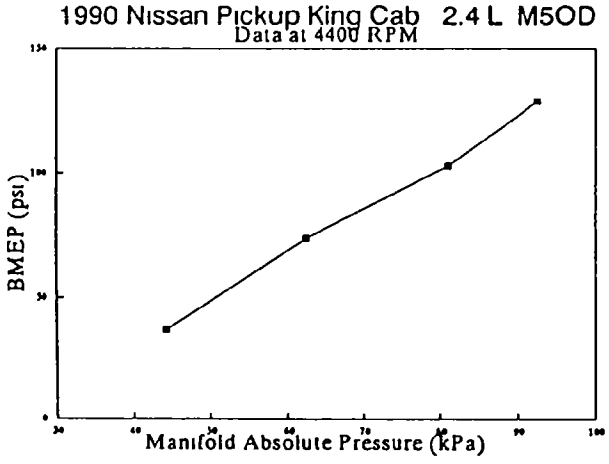
1990 Nissan Pickup King Cab 2.4 L M5OD
Data at 4400 RPM
BMEP (psi)
Manifold Absolute Pressure (kPa)

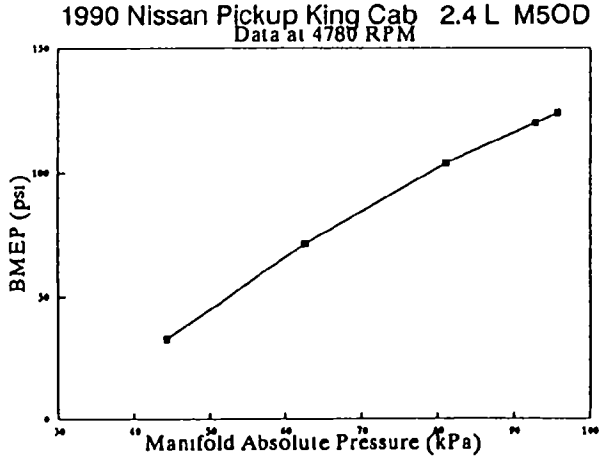
1990 Nissan Pickup King Cab 2.4 L M5OD
Data at 4780 RPM
BMEP (psi)
Manifold Absolute Pressure (kPa)

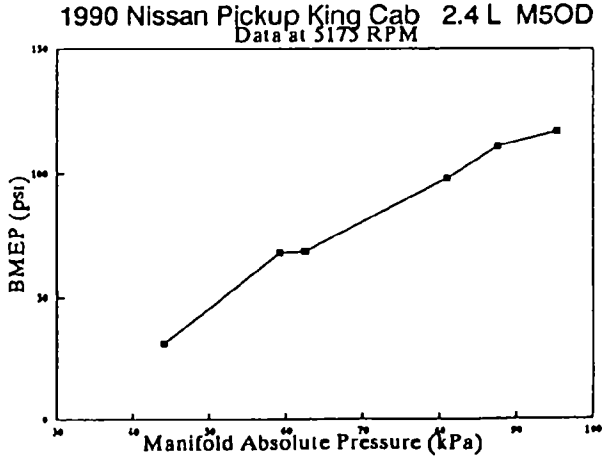
1990 Nissan Pickup King Cab 2.4 L M5OD
Data at 5175 RPM
BMEP (psi)
Manifold Absolute Pressure (kPa)

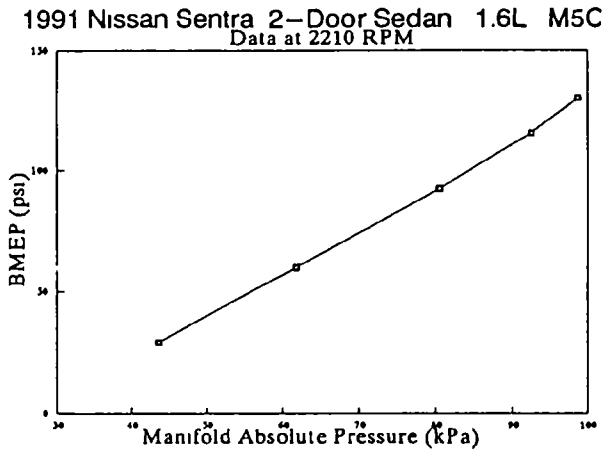
1991 Nissan Sentra 2-Door Sedan 1.6L M5C
Data at 2210 RPM
BMEP (psi)
Manifold Absolute Pressure (kPa)

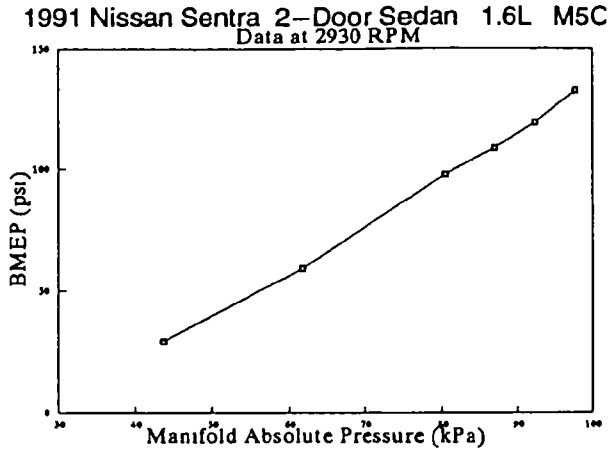
1991 Nissan Sentra 2-Door Sedan 1.6L M5C
Data at 2930 RPM
BMEP (psi)
Manifold Absolute Pressure (kPa)

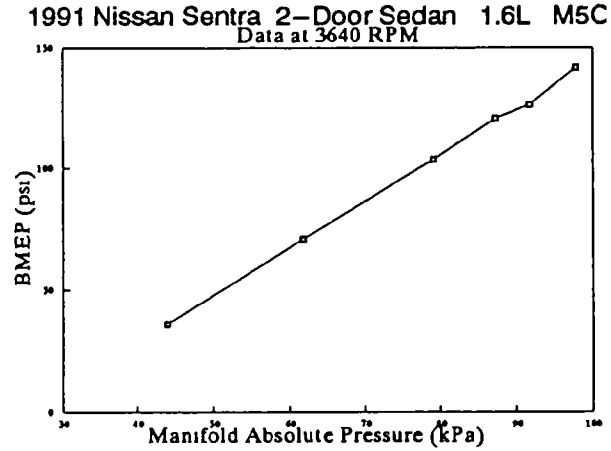
1991 Nissan Sentra 2-Door Sedan 1.6L M5C
Data at 3640 RPM
BMEP (psi)
Manifold Absolute Pressure (kPa)

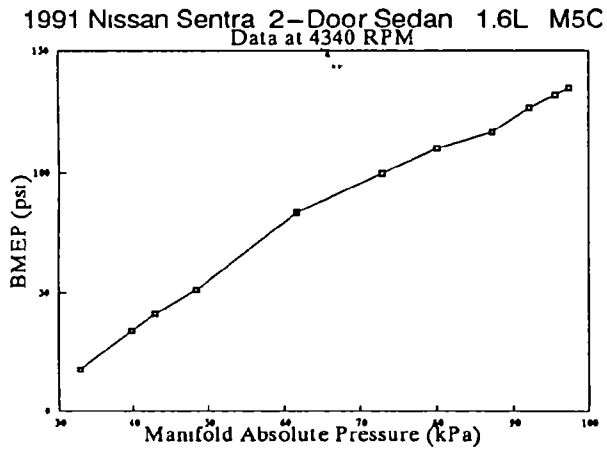
1991 Nissan Sentra 2-Door Sedan 1.6L M5C
Data at 4340 RPM
BMEP (psi)
Manifold Absolute Pressure (kPa)

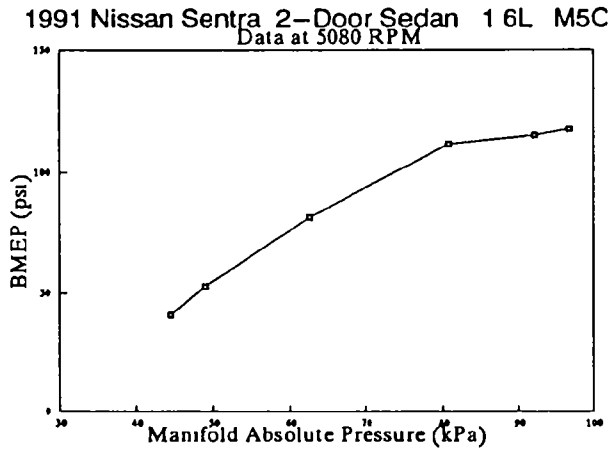
1991 Nissan Sentra 2-Door Sedan 1 6L M5C
Data at 5080 RPM
BMEP (psi)
Manifold Absolute Pressure (kPa)

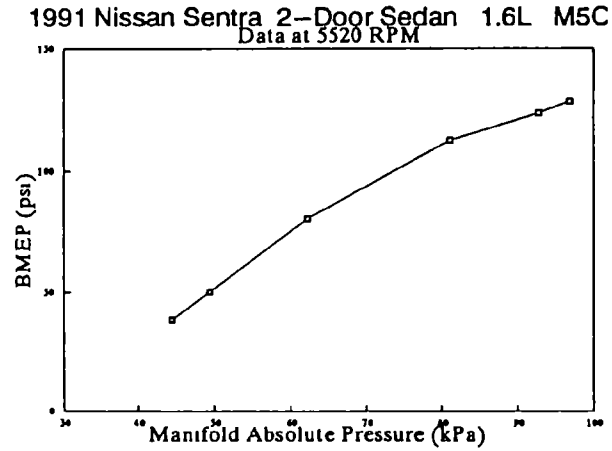
1991 Nissan Sentra 2-Door Sedan 1.6L M5C
Data at 5520 RPM
BMEP (psi)
Manifold Absolute Pressure (kPa)

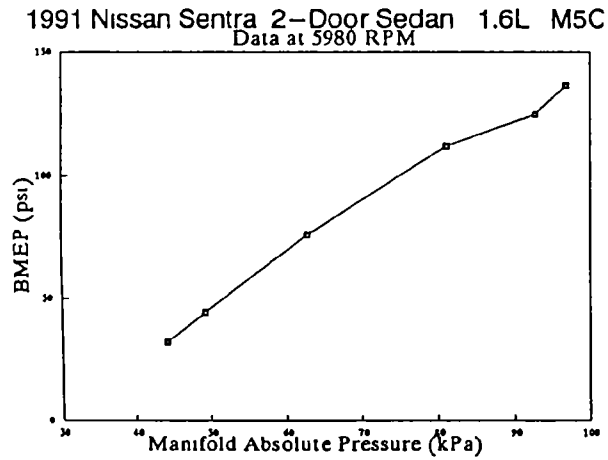
1991 Nissan Sentra 2-Door Sedan 1.6L M5C
Data at 5980 RPM
BMEP (psi)
Manifold Absolute Pressure (kPa)

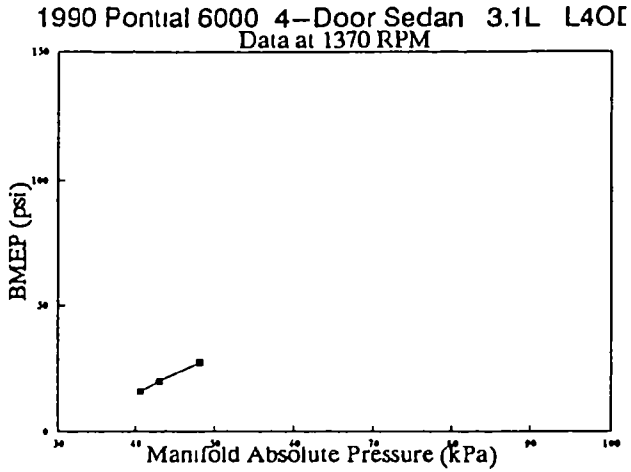
1990 Pontial 6000 4-Door Sedan 3.1L L4OI
Data at 1370 RPM
BMEP (psi)
Manifold Absolute Pressure (kPa)

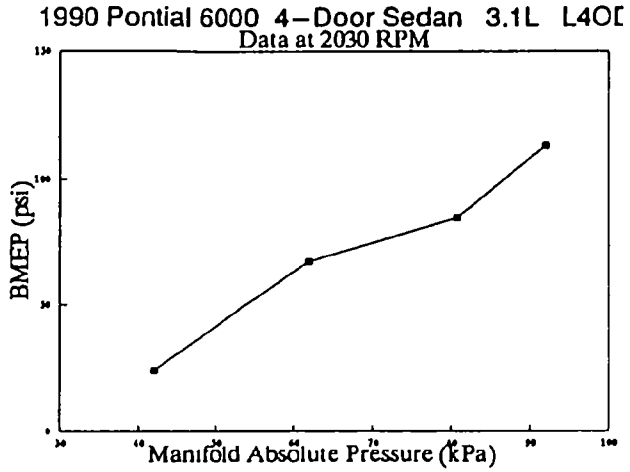
1990 Pontial 6000 4-Door Sedan 3.1L L4OI
Data at 2030 RPM
BMEP (psi)
Manifold Absolute Pressure (kPa)

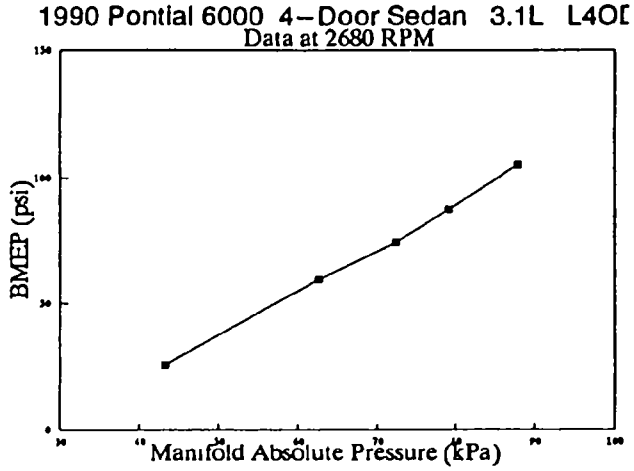
1990 Pontial 6000 4-Door Sedan 3.1L L4OI
Data at 2680 RPM
BMEP (psi)
Manifold Absolute Pressure (kPa)

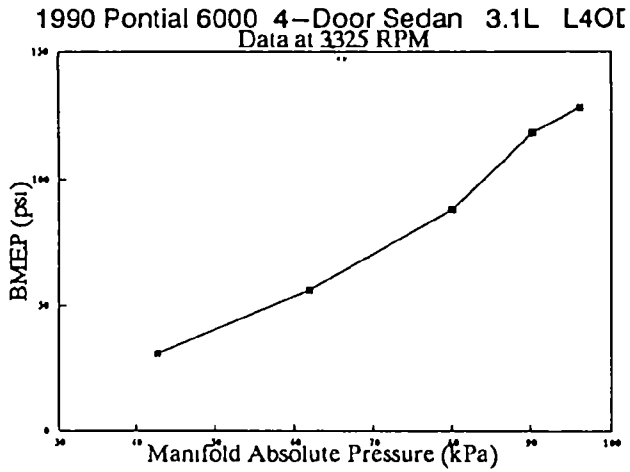
1990 Pontial 6000 4-Door Sedan 3.1L L4OI
Data at 3325 RPM
BMEP (psi)
Manifold Absolute Pressure (kPa)

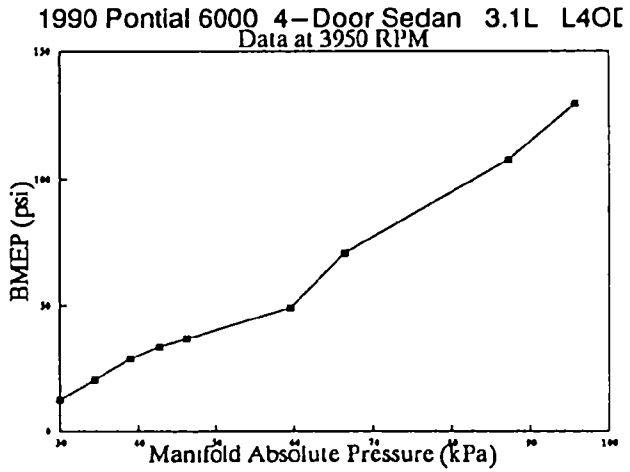
1990 Pontial 6000 4-Door Sedan 3.1L L4OI
Data at 3950 RPM
BMEP (psi)
Manifold Absolute Pressure (kPa)

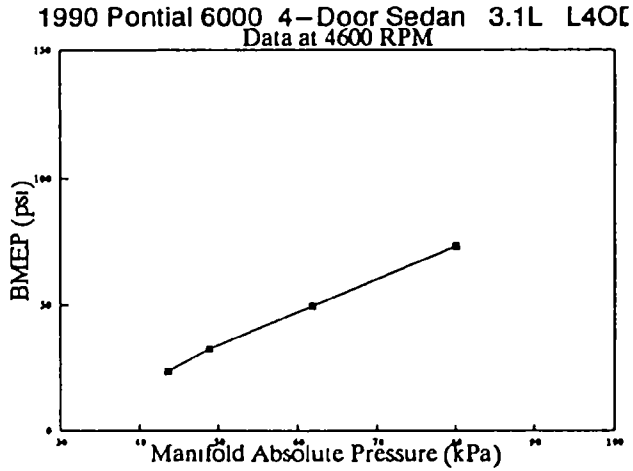
1990 Pontial 6000 4-Door Sedan 3.1L L4OI
Data at 4600 RPM
BMEP (psi)
Manifold Absolute Pressure (kPa)

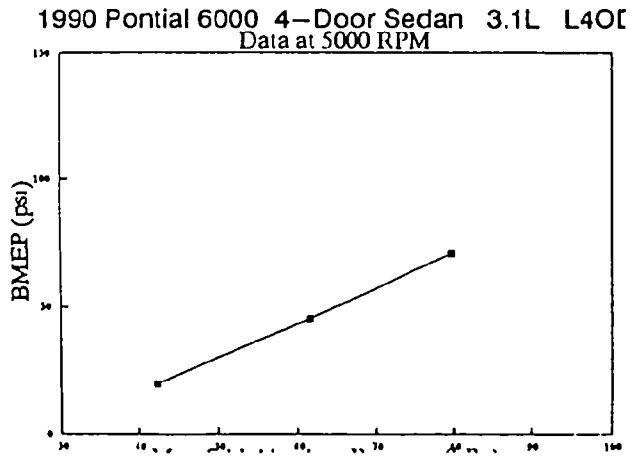
1990 Pontial 6000 4-Door Sedan 3.1L L4OI
Data at 5000 RPM
BMEP (psi)

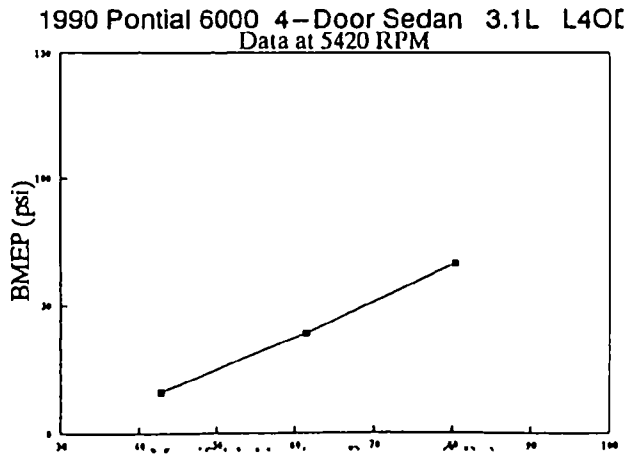
1990 Pontial 6000 4-Door Sedan 3.1L L4OI
Data at 5420 RPM
BMEP (psi)

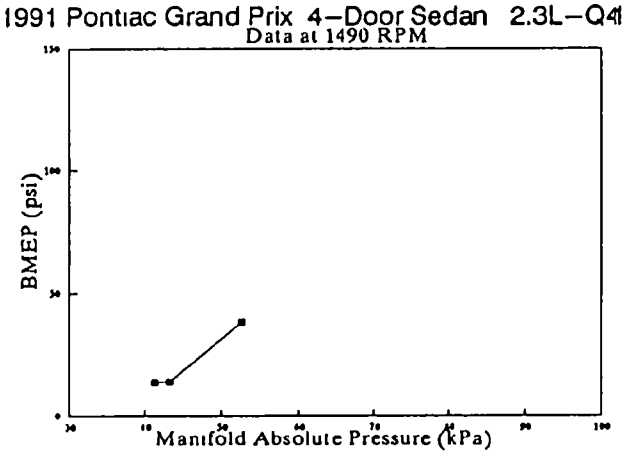
1991 Pontiac Grand Prix 4-Door Sedan 2.3L-Q4
Data at 1490 RPM
BMEP (psi)
Manifold Absolute Pressure (kPa)

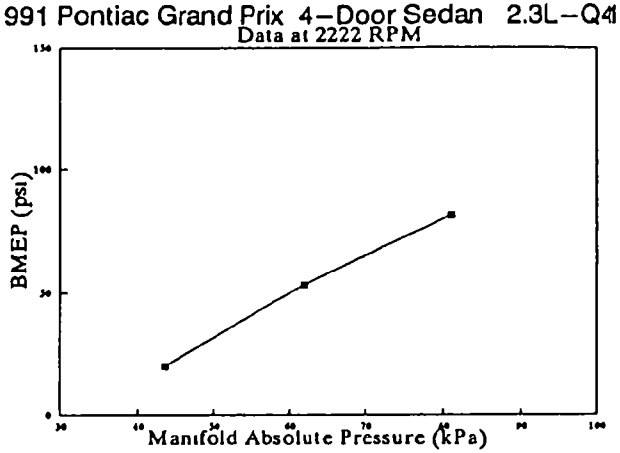
1991 Pontiac Grand Prix 4-Door Sedan 2.3L-Q4
Data at 2222 RPM
BMEP (psi)
Manifold Absolute Pressure (kPa)

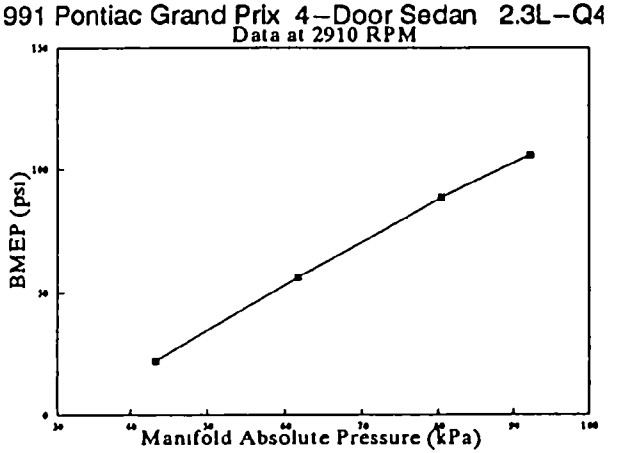
1991 Pontiac Grand Prix 4-Door Sedan 2.3L-Q4
Data at 2910 RPM
BMEP (psi)
Manifold Absolute Pressure (kPa)

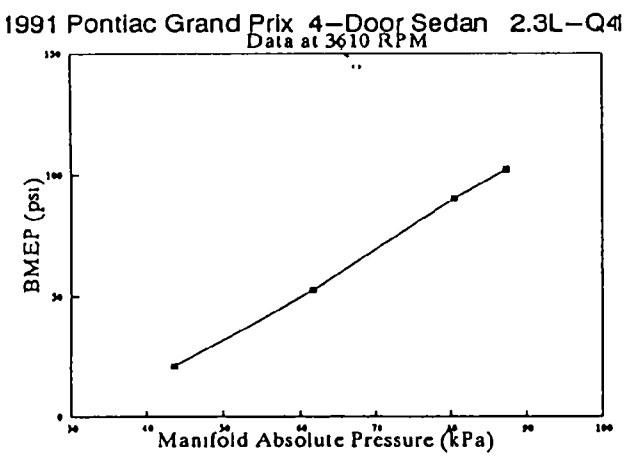
1991 Pontiac Grand Prix 4-Door Sedan 2.3L-Q4
Data at 3610 RPM
BMEP (psi)
Manifold Absolute Pressure (kPa)

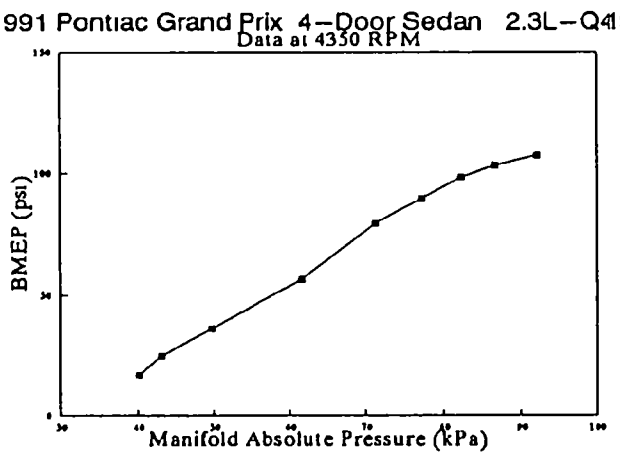
1991 Pontiac Grand Prix 4-Door Sedan 2.3L-Q4
Data at 4350 RPM
BMEP (psi)
Manifold Absolute Pressure (kPa)

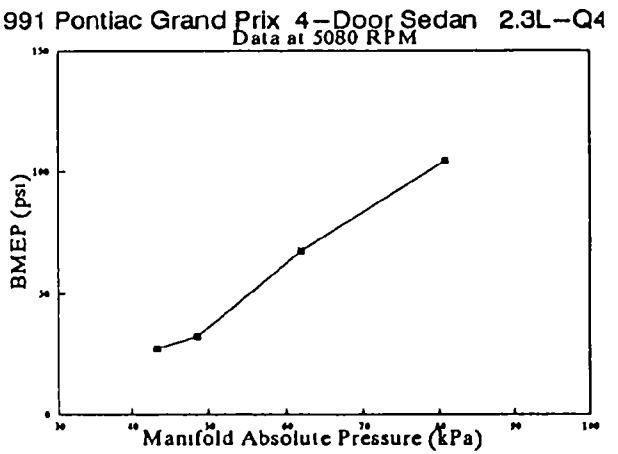
1991 Pontiac Grand Prix 4-Door Sedan 2.3L-Q4
Data at 5080 RPM
BMEP (psi)
Manifold Absolute Pressure (kPa)

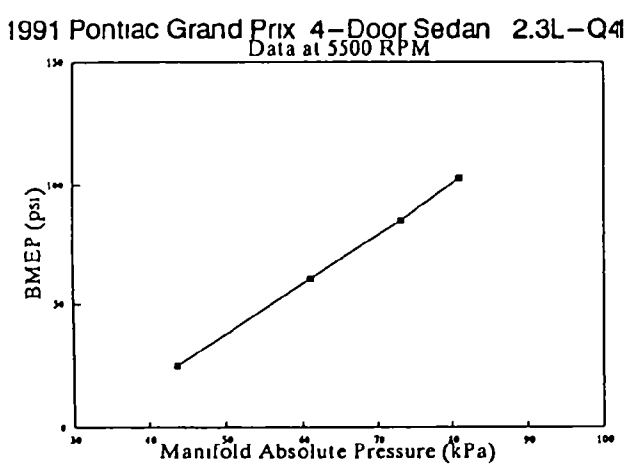
1991 Pontiac Grand Prix 4-Door Sedan 2.3L-Q4
Data at 5500 RPM
BMEP (psi)
Manifold Absolute Pressure (kPa)

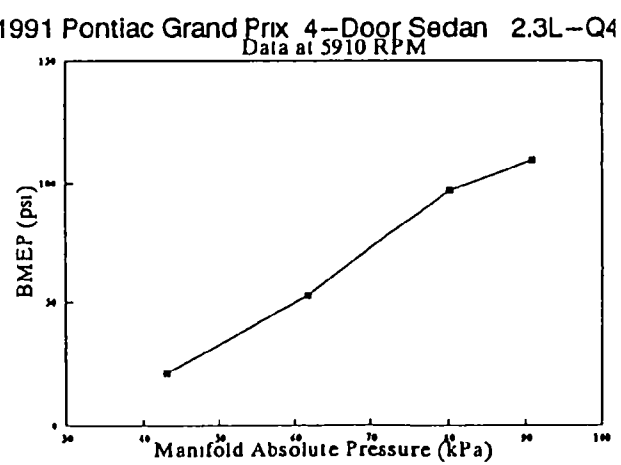
1991 Pontiac Grand Prix 4-Door Sedan 2.3L-Q4
Data at 5910 RPM
BMEP (psi)
Manifold Absolute Pressure (kPa)

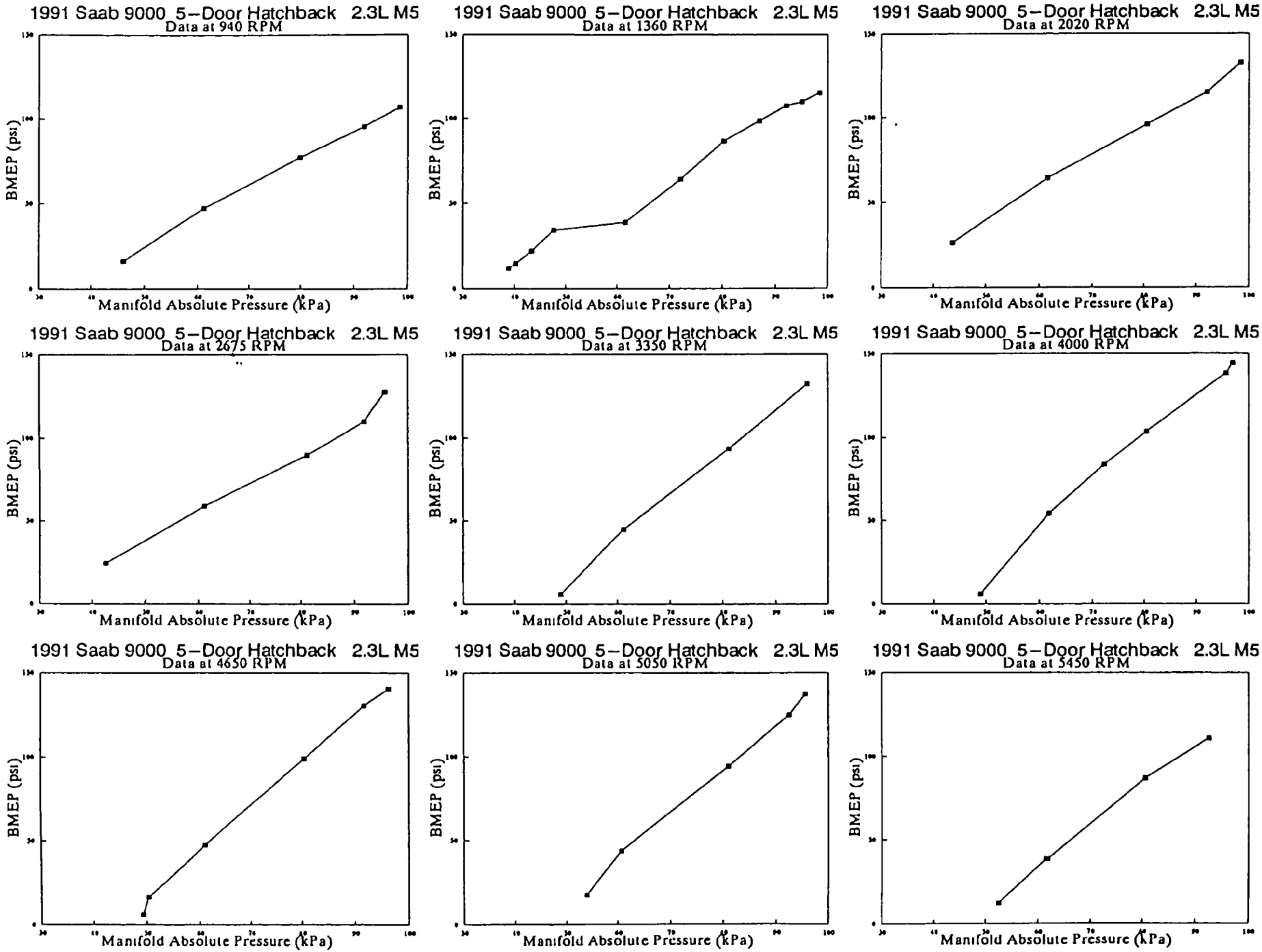
1991 Saab 9000 5-Door Hatchback 2.3L M5
Data at 940 RPM
1991 Saab 9000 5-Door Hatchback 2.3L M5
Data at 1360 RPM
1991 Saab 9000 5-Door Hatchback 2.3L M5
Data at 2020 RPM
1991 Saab 9000 5-Door Hatchback 2.3L M5
Data at 2675 RPM
1991 Saab 9000 5-Door Hatchback 2.3L M5
Data at 3350 RPM
1991 Saab 9000 5-Door Hatchback 2.3L M5
Data at 4000 RPM
1991 Saab 9000 5-Door Hatchback 2.3L M5
Data at 4650 RPM
1991 Saab 9000 5-Door Hatchback 2.3L M5
Data at 5050 RPM
1991 Saab 9000 5-Door Hatchback 2.3L M5
Data at 5450 RPM
BMEP (psi)
Manifold Absolute Pressure (kPa)

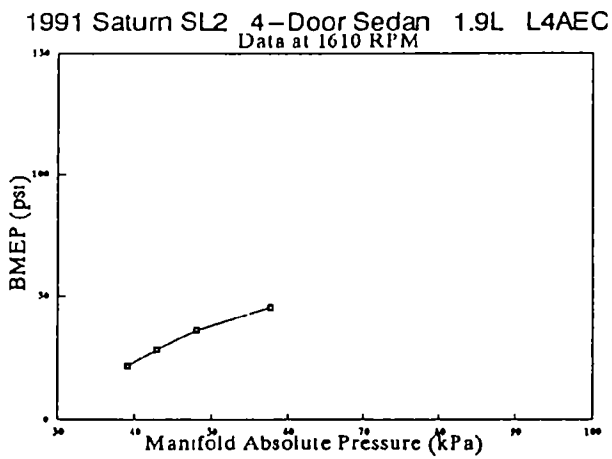
1991 Saturn SL2 4-Door Sedan 1.9L L4AEC
Data at 1610 RPM
BMEP (psi)
Manifold Absolute Pressure (kPa)

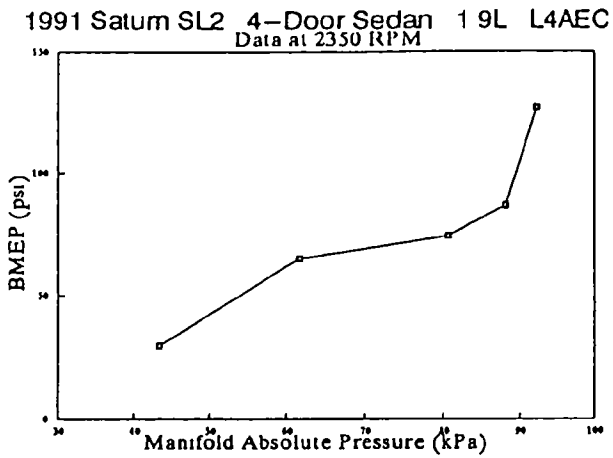
1991 Saturn SL2 4-Door Sedan 1.9L L4AEC
Data at 2350 RPM
BMEP (psi)
Manifold Absolute Pressure (kPa)

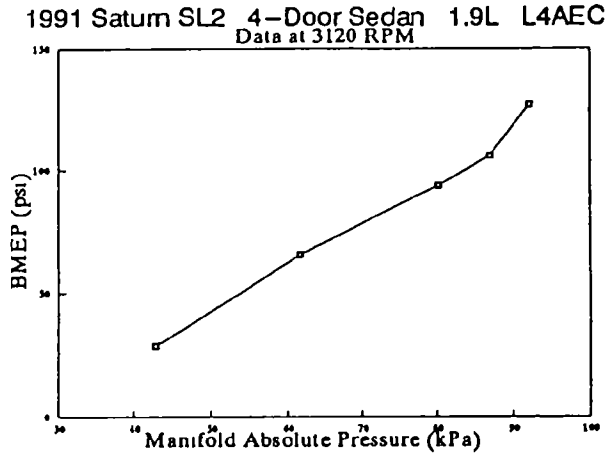
1991 Saturn SL2 4-Door Sedan 1.9L L4AEC
Data at 3120 RPM
BMEP (psi)
Manifold Absolute Pressure (kPa)

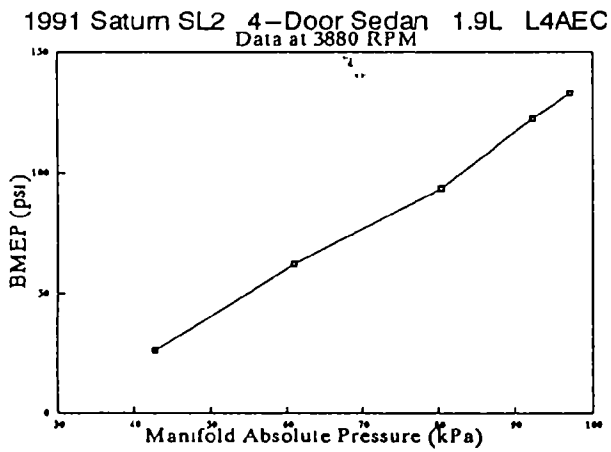
1991 Saturn SL2 4-Door Sedan 1.9L L4AEC
Data at 3880 RPM
BMEP (psi)
Manifold Absolute Pressure (kPa)

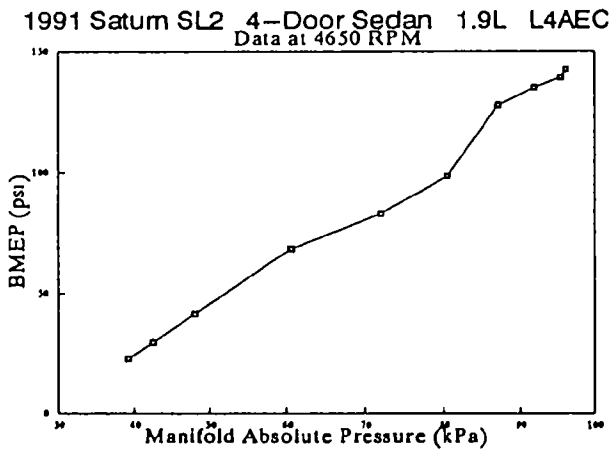
1991 Saturn SL2 4-Door Sedan 1.9L L4AEC
Data at 4650 RPM
BMEP (psi)
Manifold Absolute Pressure (kPa)

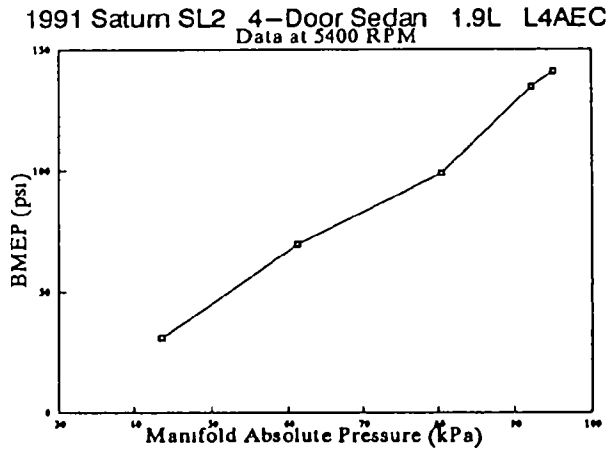
1991 Saturn SL2 4-Door Sedan 1.9L L4AEC
Data at 5400 RPM
BMEP (psi)
Manifold Absolute Pressure (kPa)

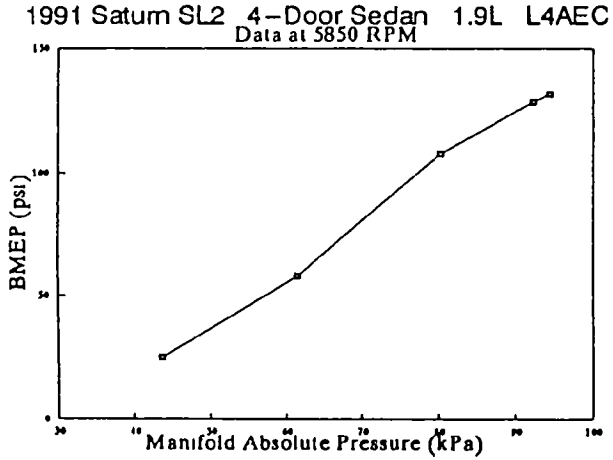
1991 Saturn SL2 4-Door Sedan 1.9L L4AEC
Data at 5850 RPM
BMEP (psi)
Manifold Absolute Pressure (kPa)

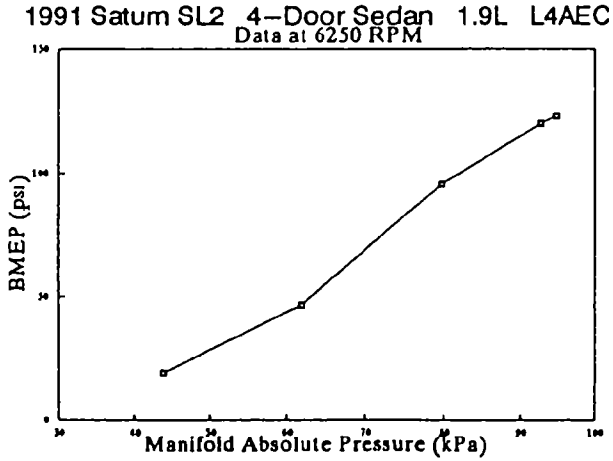
1991 Saturn SL2 4-Door Sedan 1.9L L4AEC
Data at 6250 RPM
BMEP (psi)
Manifold Absolute Pressure (kPa)

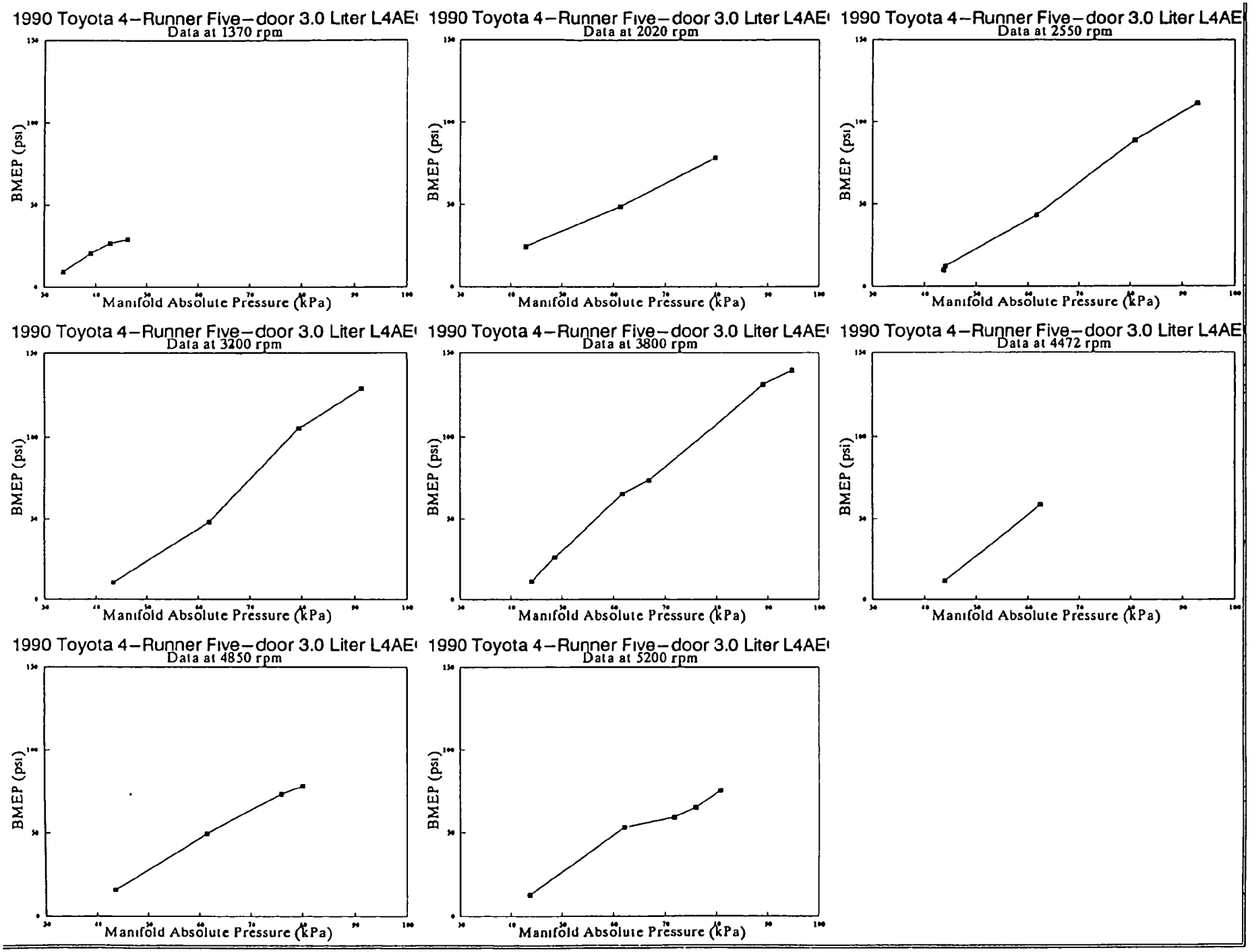
1990 Toyota 4-Runner Five-door 3.0 Liter L4AE
Data at 1370 rpm
1990 Toyota 4-Runner Five-door 3.0 Liter L4AE
Data at 2020 rpm
1990 Toyota 4-Runner Five-door 3.0 Liter L4AE
Data at 2550 rpm
1990 Toyota 4-Runner Five-door 3.0 Liter L4AE
Data at 3200 rpm
1990 Toyota 4-Runner Five-door 3.0 Liter L4AE
Data at 3800 rpm
1990 Toyota 4-Runner Five-door 3.0 Liter L4AE
Data at 4472 rpm
1990 Toyota 4-Runner Five-door 3.0 Liter L4AE
Data at 4850 rpm
1990 Toyota 4-Runner Five-door 3.0 Liter L4AE
Data at 5200 rpm
BMEP (psi)
Manifold Absolute Pressure (kPa)

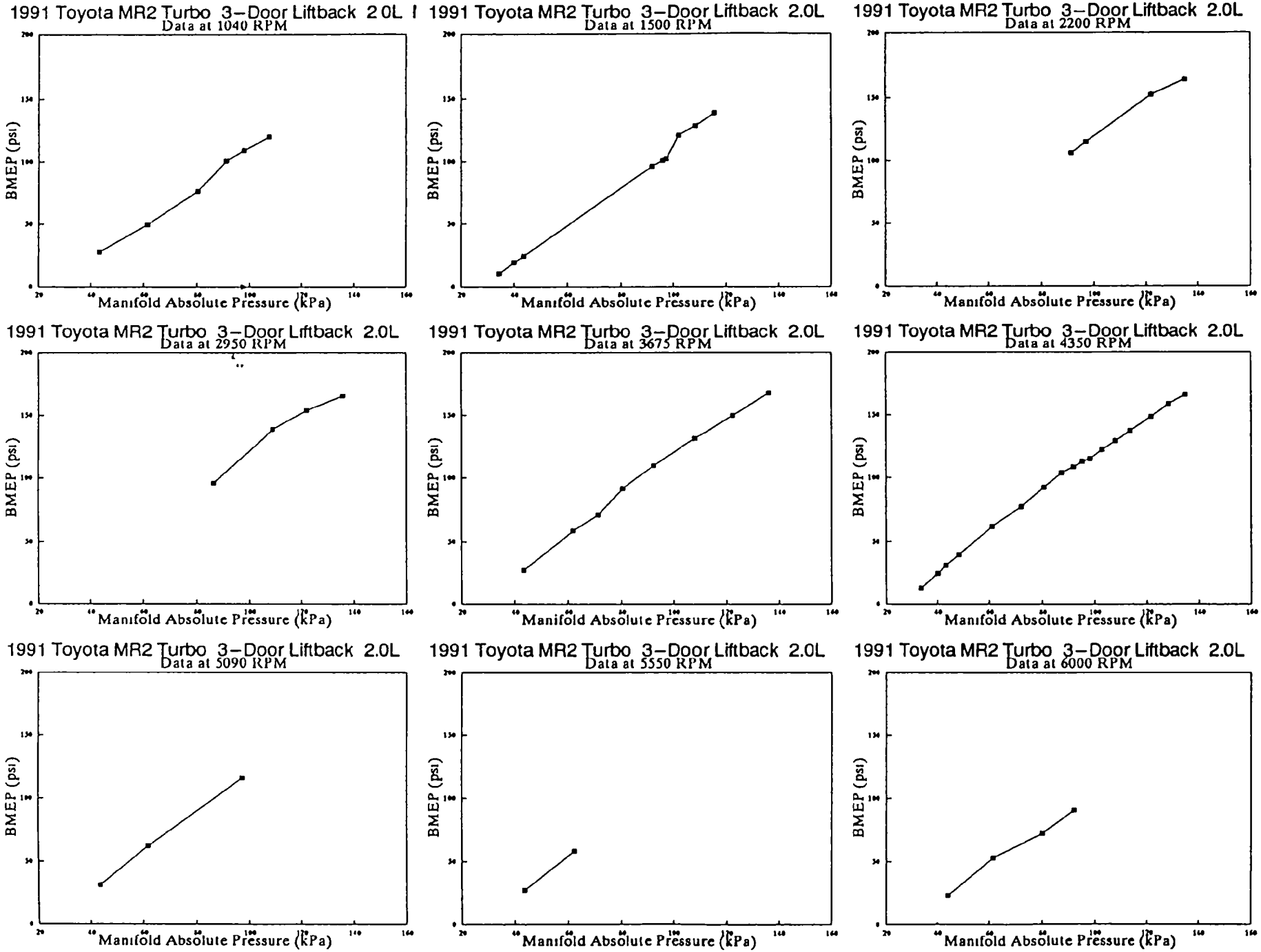
1991 Toyota MR2 Turbo 3-Door Liftback 2.0L
Data at 1040 RPM
1991 Toyota MR2 Turbo 3-Door Liftback 2.0L
Data at 1500 RPM
1991 Toyota MR2 Turbo 3-Door Liftback 2.0L
Data at 2200 RPM
1991 Toyota MR2 Turbo 3-Door Liftback 2.0L
Data at 2950 RPM
1991 Toyota MR2 Turbo 3-Door Liftback 2.0L
Data at 3675 RPM
1991 Toyota MR2 Turbo 3-Door Liftback 2.0L
Data at 4350 RPM
1991 Toyota MR2 Turbo 3-Door Liftback 2.0L
Data at 5090 RPM
1991 Toyota MR2 Turbo 3-Door Liftback 2.0L
Data at 5550 RPM
1991 Toyota MR2 Turbo 3-Door Liftback 2.0L
Data at 6000 RPM
BMEP (psi)
Manifold Absolute Pressure (kPa)

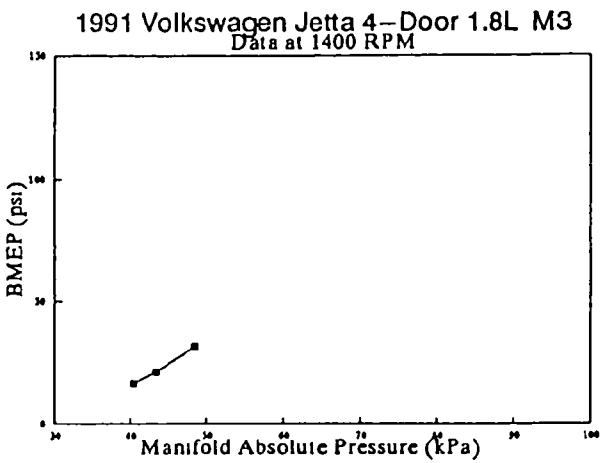
1991 Volkswagen Jetta 4-Door 1.8L M3
Data at 1400 RPM
BMEP (psi)
Manifold Absolute Pressure (kPa)

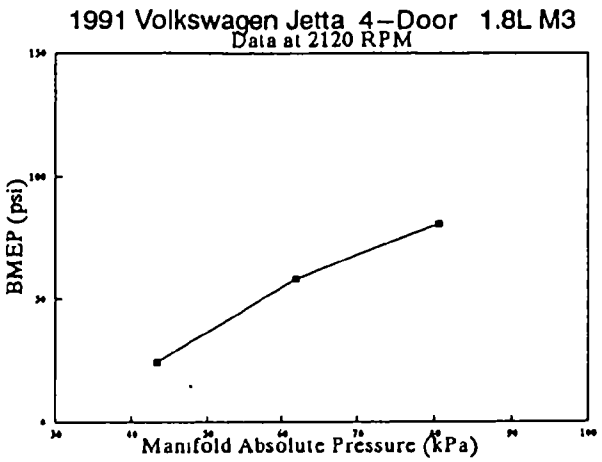
1991 Volkswagen Jetta 4-Door 1.8L M3
Data at 2120 RPM
BMEP (psi)
Manifold Absolute Pressure (kPa)

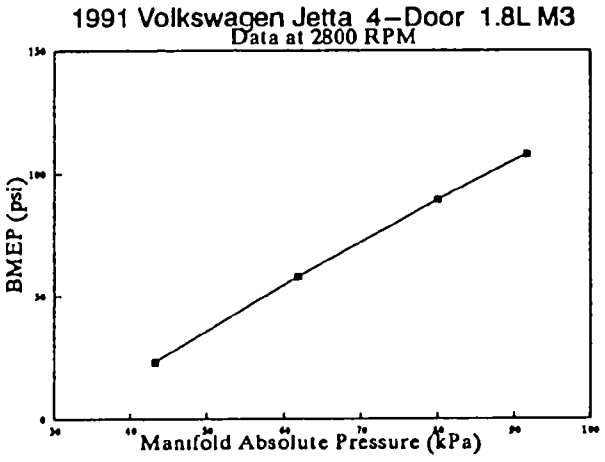
1991 Volkswagen Jetta 4-Door 1.8L M3
Data at 2800 RPM
BMEP (psi)
Manifold Absolute Pressure (kPa)

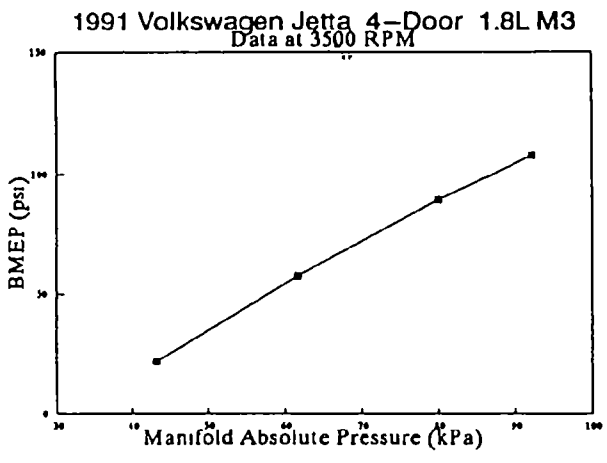
1991 Volkswagen Jetta 4-Door 1.8L M3
Data at 3500 RPM
BMEP (psi)
Manifold Absolute Pressure (kPa)

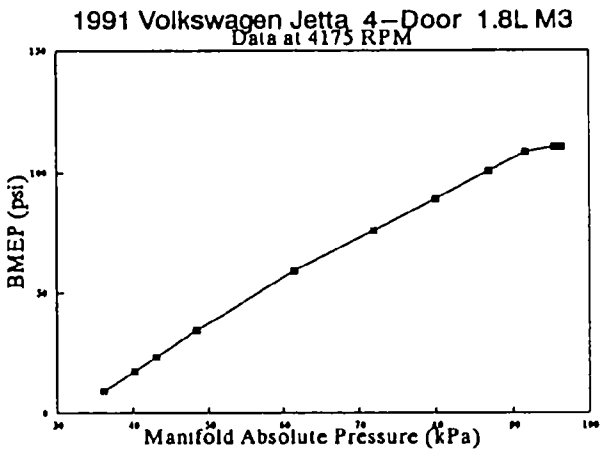
1991 Volkswagen Jetta 4-Door 1.8L M3
Data at 4175 RPM
BMEP (psi)
Manifold Absolute Pressure (kPa)

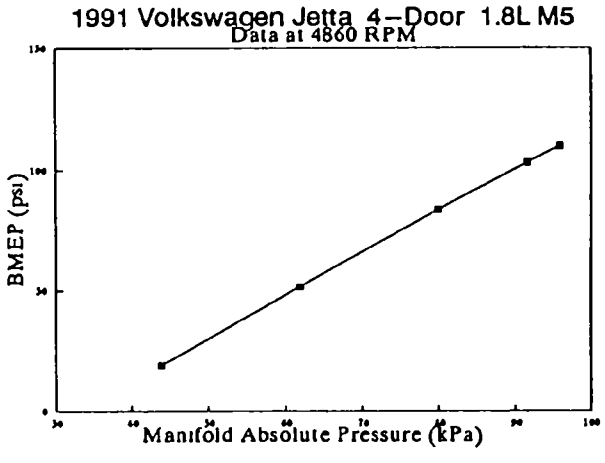
1991 Volkswagen Jetta 4-Door 1.8L M5
Data at 4860 RPM
BMEP (psi)
Manifold Absolute Pressure (kPa)

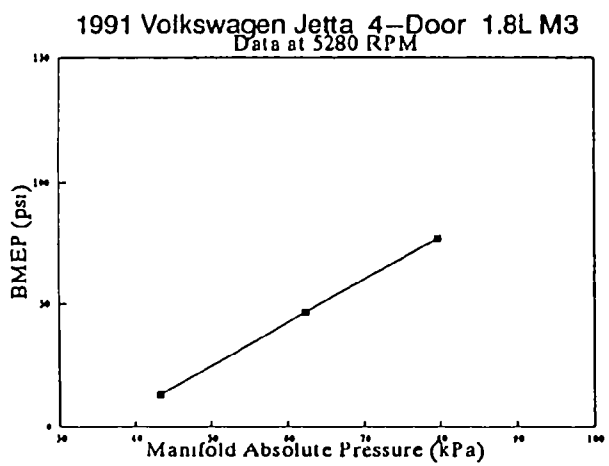
1991 Volkswagen Jetta 4-Door 1.8L M3
Data at 5280 RPM
BMEP (psi)
Manifold Absolute Pressure (kPa)

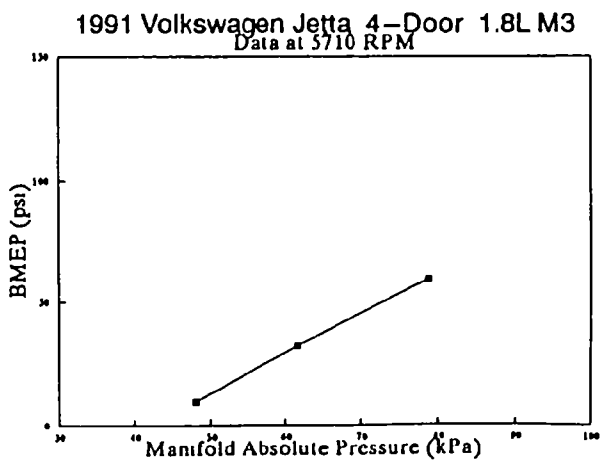
1991 Volkswagen Jetta 4-Door 1.8L M3
Data at 5710 RPM
BMEP (psi)
Manifold Absolute Pressure (kPa)

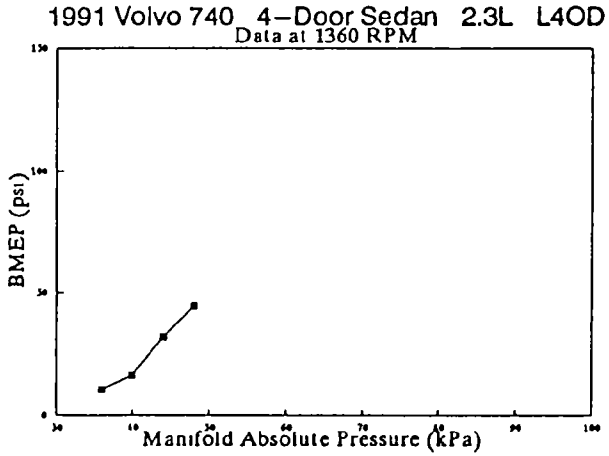
1991 Volvo 740 4-Door Sedan 2.3L L4OD
Data at 1360 RPM
BMEP (psi)
Manifold Absolute Pressure (kPa)

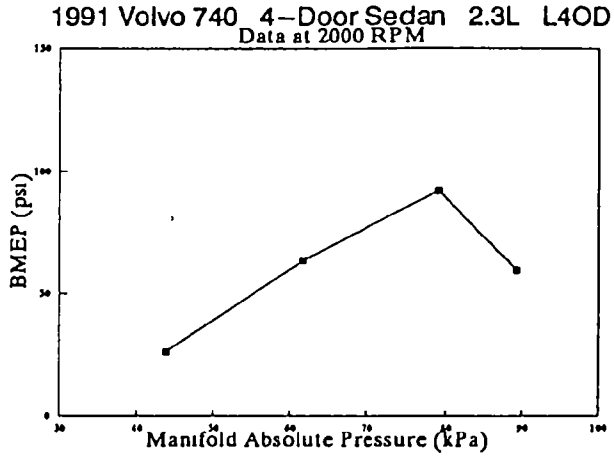
1991 Volvo 740 4-Door Sedan 2.3L L4OD
Data at 2000 RPM
BMEP (psi)
Manifold Absolute Pressure (kPa)

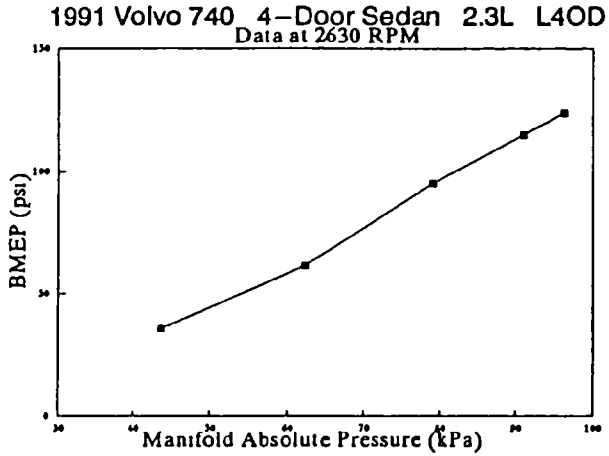
1991 Volvo 740 4-Door Sedan 2.3L L4OD
Data at 2630 RPM
BMEP (psi)
Manifold Absolute Pressure (kPa)

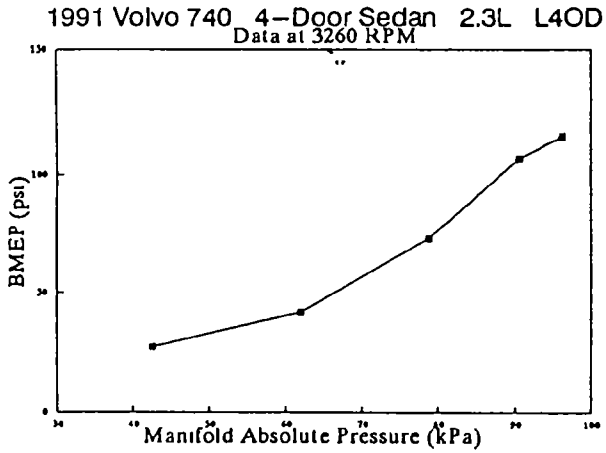
1991 Volvo 740 4-Door Sedan 2.3L L4OD
Data at 3260 RPM
BMEP (psi)
Manifold Absolute Pressure (kPa)

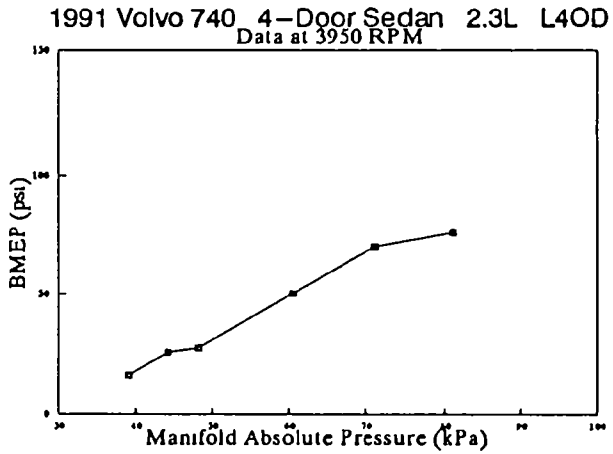
1991 Volvo 740 4-Door Sedan 2.3L L4OD
Data at 3950 RPM
BMEP (psi)
Manifold Absolute Pressure (kPa)

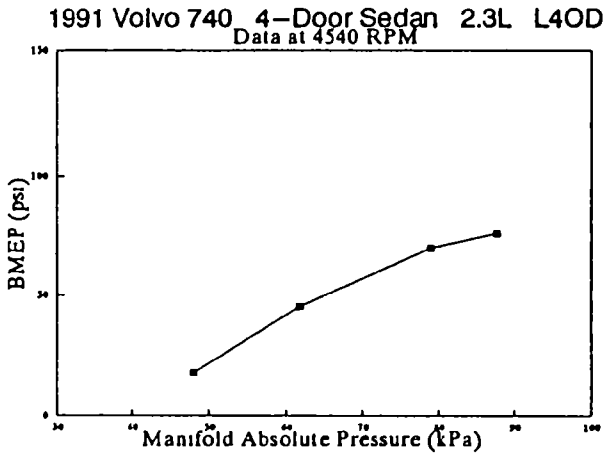
1991 Volvo 740 4-Door Sedan 2.3L L4OD
Data at 4540 RPM
BMEP (psi)
Manifold Absolute Pressure (kPa)

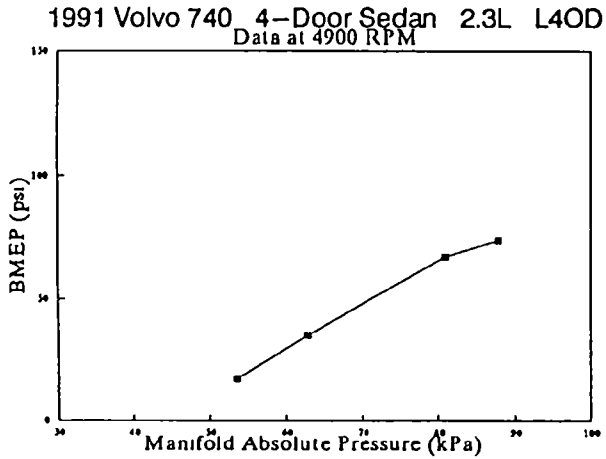
1991 Volvo 740 4-Door Sedan 2.3L L4OD
Data at 4900 RPM
BMEP (psi)
Manifold Absolute Pressure (kPa)

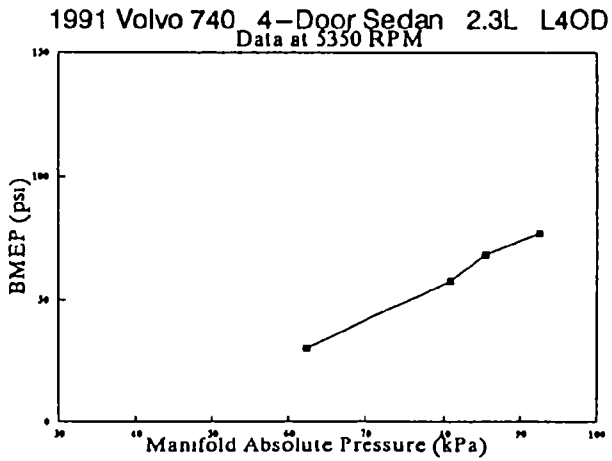
1991 Volvo 740 4-Door Sedan 2.3L L4OD
Data at 5350 RPM
BMEP (psi)
Manifold Absolute Pressure (kPa)